Neural Plasticity

Stress Induced Neuroplasticity and Mental Disorders 2020

Lead Guest Editor: Fushun Wang
Guest Editors: Fang Pan, Lee Shapiro, and Jason H. Huang

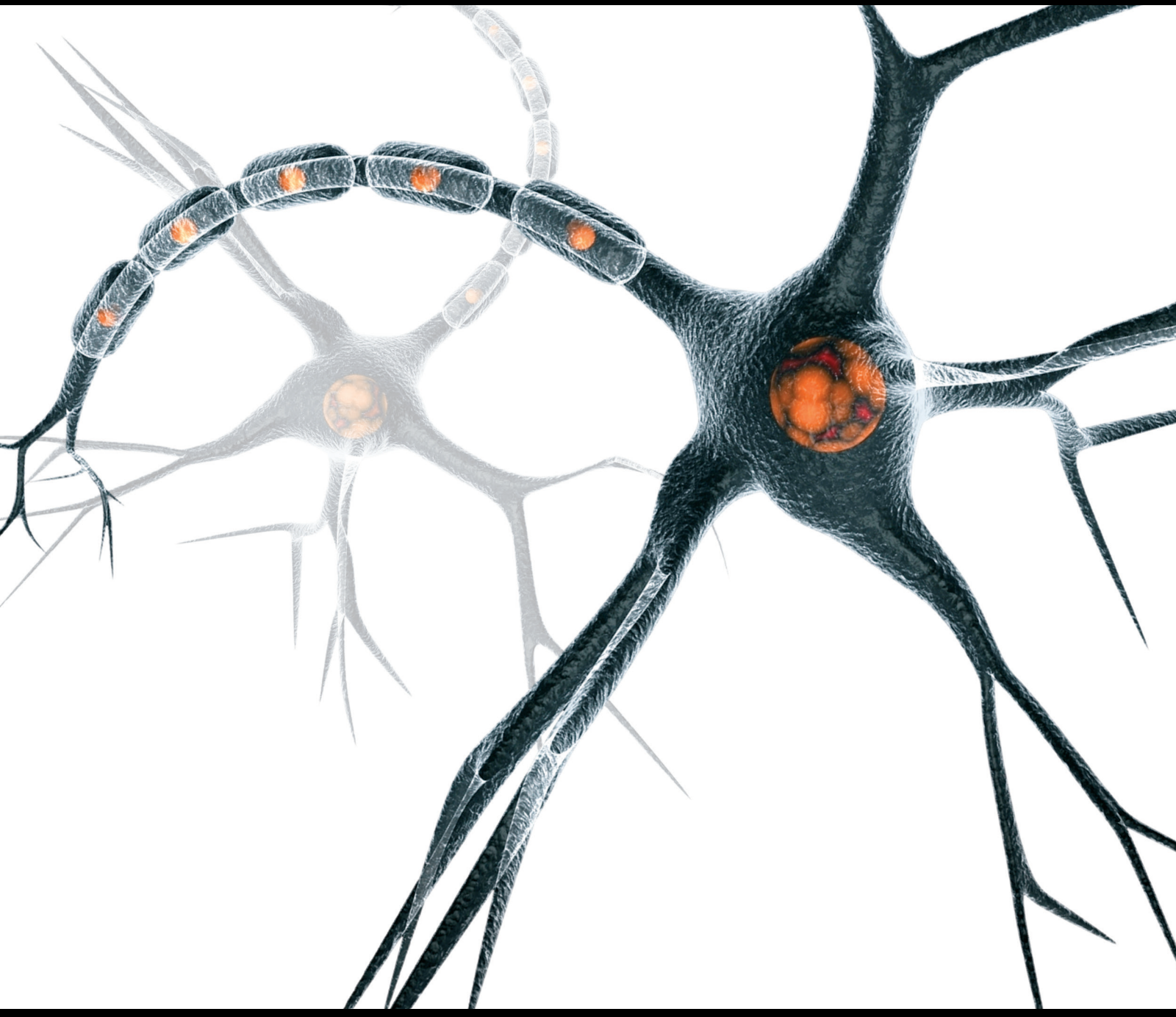

Stress Induced Neuroplasticity and Mental Disorders 2020

Neural Plasticity

Stress Induced Neuroplasticity and Mental Disorders 2020

Lead Guest Editor: Fushun Wang
Guest Editors: Fang Pan, Lee Shapiro, and Jason H. Huang

Contents

Biases of Happy Faces in Face Classification Processing of Depression in Chinese Patients
Yuying Tong, Gang Zhao, Jinbo Zhao, Nianxiang Xie, Dong Han, Bowen Yang, Qi Liu, Hailian Sun, and Yanjie Yang
Research Article (8 pages), Article ID 7235734, Volume 2020 (2020)

Neuroprotective Effects of the Sonic Hedgehog Signaling Pathway in Ischemic Injury through Promotion of Synaptic and Neuronal Health
Sen Yin, Xuemei Bai, Danqing Xin, Tingting Li, Xili Chu, Hongfei Ke, Min Han, Wenqiang Chen, Xingang Li, and Zhen Wang
Research Article (11 pages), Article ID 8815195, Volume 2020 (2020)

GABAergic System in Stress: Implications of GABAergic Neuron Subpopulations and the Gut-Vagus-Brain Pathway
Xueqin Hou, Cuiping Rong, Fugang Wang, Xiaoqian Liu, Yi Sun, and Han-Ting Zhang
Review Article (11 pages), Article ID 8858415, Volume 2020 (2020)

Hindawi
Neural Plasticity
Volume 2021, Article ID 9762592, 2 pages
https://doi.org/10.1155/2021/9762592

Corrigendum

Corrigendum to "Neuroprotective Effects of the Sonic Hedgehog Signaling Pathway in Ischemic Injury through Promotion of Synaptic and Neuronal Health"

Sen Yin,[1,2] Xuemei Bai,[2] Danqing Xin,[2] Tingting Li,[2] Xili Chu,[2] Hongfei Ke,[2] Min Han,[2] Wenqiang Chen,[1] Xingang Li,[1] and Zhen Wang[2]

[1]*Qilu Hospital, Cheeloo College of Medicine, Shandong University, Jinan, Shandong, China*
[2]*Department of Physiology, School of Basic Medical Sciences, Cheeloo College of Medicine, Shandong University, Jinan, Shandong 250012, China*

Correspondence should be addressed to Xingang Li; lixg@sdu.edu.cn and Zhen Wang; wangzhen@sdu.edu.cn

Received 5 May 2021; Accepted 5 May 2021; Published 26 May 2021

In the article titled "Neuroprotective Effects of the Sonic Hedgehog Signaling Pathway in Ischemic Injury through Promotion of Synaptic and Neuronal Health" [1], the authors have identified that in Figure 4, the incorrect images were provided due to an error during the preparation of the manuscript. The authors confirm that this error does not affect the results of the article and the corrected Figure 4 is shown below.

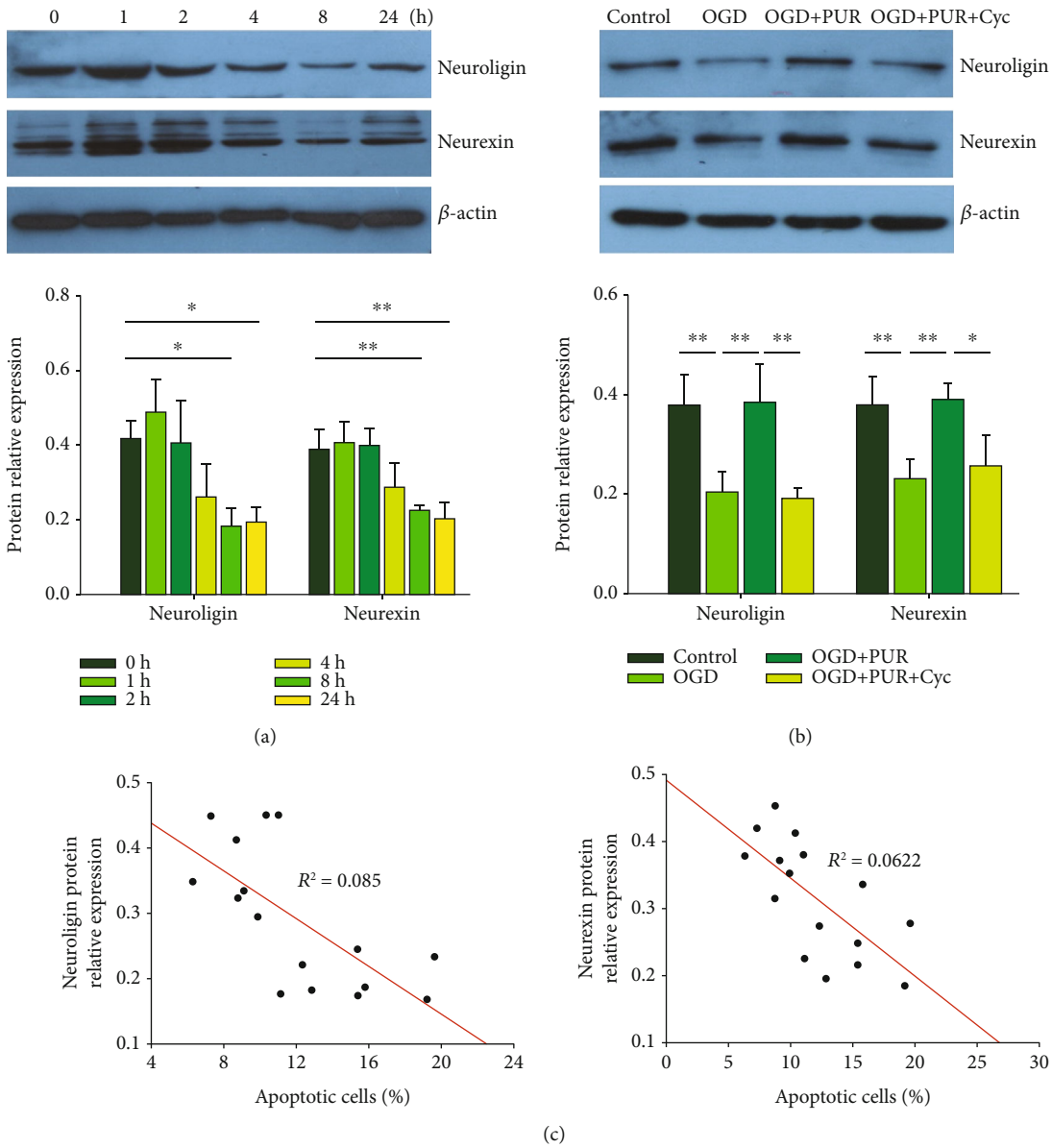

Figure 4: PUR activation of Shh on OGD-induced neuroligin and neurexin: (a) protein levels of neuroligin and neurexin at 1, 2, 4, 8, and 24 h after OGD as determined by Western blot ($N = 3$/group); (b) protein levels of neuroligin and neurexin at 24 h after OGD as determined by Western blot ($N = 4$/group); (c) Pearson correlation coefficients obtained between neuroligin/neurexin expressions and apoptosis following PUR treatment. Values represent the mean ± SD; $^{*}p < 0.05$ and $^{**}p < 0.01$ according to ANOVA with the Dunnett test in (a) and Tukey's post hoc comparisons in (b).

References

[1] S. Yin, X. Bai, D. Xin et al., "Neuroprotective Effects of the Sonic Hedgehog Signaling Pathway in Ischemic Injury through Promotion of Synaptic and Neuronal Health," *Neural Plasticity*, vol. 2020, Article ID 8815195, 11 pages, 2020.

Hindawi
Neural Plasticity
Volume 2021, Article ID 8529613, 10 pages
https://doi.org/10.1155/2021/8529613

Research Article

Acute Stress and Gender Effects in Sensory Gating of the Auditory Evoked Potential in Healthy Subjects

Zengyou Xin,[1,2] **Simeng Gu**,[3,4] **Wei Wang**,[5] **Yi Lei**,[3,6] **and Hong Li**[3,6]

[1]*School of Education Science, Minnan Normal University, Zhangzhou, Fujian 363000, China*
[2]*Brain and Cognitive Neuroscience Research Center, Liaoning Normal University, Dalian, Liaoning 116029, China*
[3]*Institute of Brain and Psychological Sciences, Sichuan Normal University, Chengdu, Sichuan 610060, China*
[4]*Department Medical Psychology, Jiangsu University Medical School, Zhenjiang, Jiangsu 210023, China*
[5]*Department of Neurosurgery, University of Rochester Medical Center, Rochester, New York 14643, USA*
[6]*Center for Language and Brain, Shenzhen Institute of Neuroscience, Shenzhen Key Laboratory of Affective and Social Cognitive Science, School of Psychology, Shenzhen University, Shenzhen, 518060 Guangdong, China*

Correspondence should be addressed to Yi Lei; leiyi821@vip.sina.com

Received 20 March 2020; Revised 11 February 2021; Accepted 22 February 2021; Published 13 March 2021

Academic Editor: Fang Pan

Sensory gating is a neurophysiological measure of inhibition that is characterized by a reduction in the P_{50}, N_{100}, and P_{200} event-related potentials to a repeated identical stimulus. It was proposed that abnormal sensory gating is involved in the neural pathological basis of some severe mental disorders. Since then, the prevailing application of sensory gating measures has been in the study of neuropathology associated with schizophrenia and so on. However, sensory gating is not only trait-like but can be also state-like, and measures of sensory gating seemed to be affected by several factors in healthy subjects. The objective of this work was to clarify the roles of acute stress and gender in sensory gating. Data showed acute stress impaired inhibition of P_{50} to the second click in the paired-click paradigm without effects on sensory registration leading to worse P_{50} sensory gating and disrupted attention allocation reflected by attenuated P_{200} responses than control condition, without gender effects. As for N_{100} and P_{200} gating, women showed slightly better than men without effects of acute stress. Data also showed slightly larger N_{100} amplitudes across clicks and significant larger P_{200} amplitude to the first click for women, suggesting that women might be more alert than men.

1. Introduction

Acute stress is a stereotypical and multimodal response to a present or imminent challenge overcharging an organism [1] and causes the release of many stress hormones and neuromodulators (e.g., [2]), which can change cellular properties of large-scale neuronal populations throughout the brain [3]. The common stress induction paradigms in laboratory include cold water pressing (also called cold pressor stress (CPS); e.g., [4]) and the Trier Social Stress Test (TSST; [5]). Sensory gating is the ability of the central nervous system to filter incoming stimuli and protect a person from being flooded with irrelevant information (e.g., [6]). It is typically measured by using a paired-click paradigm. In such a paradigm, the event-related potential P_{50} is measured during the presentation of two identical clicks with an interstimulus interval (ISI) of 500 ms and a typical interpair interval (IPI) no less than 8 s [7]. The attenuation of the P_{50} amplitude to the second click (S_2), relative to that of the first click (S_1), is the operational definition of gating inhibition (i.e., gating or sensory gating; [8, 9]). The difference and the ratio between these P_{50} responses are the means to quantitatively assess gating mechanisms (e.g., [9–11]).

Freedman and colleagues initially demonstrated that schizophrenic patients and their family members fail to exhibit typical P_{50} response inhibition to S_2 during a paired-click paradigm (e.g., [8, 12]). Since then, sensory gating has been one of the foci of psychopathological researches on schizophrenia. Because of the highly replicable results across studies on schizophrenia (e.g., [13–16]) and the findings that filtering deficits also occur in unaffected family members [17, 18], P_{50} filtering has been investigated as a

Table 1: Summary of studies investigating auditory sensory gating concerning gender difference and acute stress effects.

Study	Subjects	Stress and recording timing	Components	Findings
Franks et al. [19]	22f, 21m	No acute stress	P_{50}	Women showed less suppression of the P_{50} than men in a mixed sample of manic and normal subjects
Freedman et al. [8, 20]	73f, 90m	No acute stress	P_{50}	Women had a higher P_{50} amplitude to S_1 than men across all age groups, without gender differences in P_{50} ratios
Hetrick et al. [10]	30f, 30m	No acute stress	P_{50}, N_{100}, P_{200}	Women had higher P_{50} and N_{100} amplitudes to S_2 and worse gating for P_{50} and N_{100} without gender effects at P_{200}
Rasco et al. [21]	25f, 25m	No acute stress	P_{50}	No gender differences in P_{50} amplitudes, latencies, and sensory gating across all age groups
Clementz et al. [22]	15f, 25m	No acute stress	P_{50}, N_{100}	No gender differences in P_{50} and N_{100} amplitudes, latencies, and sensory gating
Brinkman et al. [6]	67f, 45m	No acute stress	P_{50}	No gender differences of P_{50} latency, amplitude, and inhibition across all age groups
Fuerst et al. [23]	38f, 29m	No acute stress	P_{50}, N_{100}, P_{200}	Men scored higher than women in P_{50}, N_{100}, or P_{200} amplitude to S_1 and in all gating differences
Lijffijt et al. [24]	34f, 26m	No acute stress	P_{50}, N_{100}, P_{200}	No gender effects in P_{50}, N_{100}, or P_{200} amplitudes and sensory gating
Thomas et al. [25]	21f, 13m	No acute stress	P_{50}	No gender effects in P_{50} amplitudes and P_{50} gating ratios
Johnson and Adler [26]	2f, 8m	Immediately after 2 min CPS	P_{50}	S_2 P_{50} amplitude increased, and the gating ratio also increased, after exposure to CPS
White et al. [27]	7f, 6m	During mental arithmetic stressor	P_{50}	P_{50} gating was reduced, due to a reduction of S_1 P_{50} amplitude, relative to nonstress task
Yee et al. [28]	9f, 11m	During mental arithmetic stressor	P_{50}	Stressor disrupted P50 sensory gating without differential effects on P_{50} amplitudes to S_1 and S_2
*Ermutlu et al. [29]	7f, 8m	During 5 min CPS	P_{50}, N_{100}	CPS impaired P_{50} sensory gating without effect on N_{100} gating (deviant/standard)
Woods et al. [11]	21f, 9m	Immediately after 50 s CPS	P_{50}	S_1 P_{50} amplitude decreased, without effect on P_{50} gating ratio, after exposure to CPS
Atchley [30]	20f, 10m	Immediately after 2 min CPS	P_{50}	P_{50} gating ratios increased after CPS
White et al. [12]	13f, 16m	During mental arithmetic stressor	P_{50}, N_{100}	S_1 P_{50} was reduced for women, whereas men showed reductions for both clicks, and women showed disrupted P_{50} N_{100} gating whereas men only disrupted N_{100} gating, during stress compared to baseline

*Using oddball paradigm; f: female; m: male; CPS: cold pressor stress.

candidate potential endophenotype for schizophrenia. Additionally, in psychopathological studies, there also have been concerns on N_{100} and P_{200} sensory gating, which were assessed using event-related potential N_{100} and P_{200}, respectively. However, as for normative data regarding the characteristics of sensory gating, up till now, relatively limited studies using healthy volunteers have targeted gender and acute stress, respectively, and have reported inconsistent outcomes (see Table 1).

According to previous studies focusing on gender difference, three studies supported less P_{50} sensory gating for women [10, 19, 23], and six of the limited documents support no gender difference in P_{50} sensory gating. The similarly inconsistent findings on the P_{50} amplitudes for S_1 or S_2 were reported between genders. As for the influences of acute stress, although adverse P_{50} sensory gating effects were reported in almost all studies (except for Woods et al. [11]), there were inconsistent findings on the P_{50} response to the two clicks after acute stress intervention. As for auditory evoked potential components other than P_{50}, as shown in Table 1, the results of N_{100} and P_{200} seemed even more inconsistent.

To date, except for a single study, no attempt has been made to investigate the gender difference in the effects of acute stress on sensory gating. During an oral mental arithmetic stressor task, sensory gating ratios were measured to the paired-click paradigm, and women showed disrupted P_{50} and N_{100} gating whereas men exhibited only disrupted N_{100} gating [12]. Although White et al. reported valuable information, several limitations have to be noted. The first is the protocol used to induce acute stress. According to White et al. [12], P_{50} data were recorded while mental arithmetic was performing, in which the experimental effect was

inevitably contaminated by the concurrent working memory task; however, P_{50} sensory gating was not a complete automatic and preattentive process; it involved top-down modulations and could be influenced by attention manipulation [16, 31, 32]. Furthermore, the muscle artifacts of oral mental arithmetic cannot be ignored. The second is the different interpair intervals (10-14 s for some subjects, while 7-10 s for others), which may deeply affect the P_{50} response (e.g., [7]), because the sensory gating data were derived from two different studies [27, 28]. The third is numbers of epochs averaged (80 trials for data from White and Yee [27], 60 trials from Yee and White [28]), and the fourth is limited sample size (13 women and 16 men), in addition to some differences in experimental procedures.

Thus, the main objective of this study was to further investigate possible gender differences in the sensory gating after exposure to stressful treatment or control condition. It has been reported that the fluctuation of sex steroid hormone during menstrual cycles affects the performance of working memory [33], proponent response inhibition [34], arousal state [35], and fear conditioning and inhibition [36] in healthy women. Thus, only women during their midluteal phase were included to control the potential effects of menstrual cycle. A body of literature suggests the major neural sources of P_{50} suppression involves the hippocampus and prefrontal cortex (e.g., [9, 37, 38]), where stress hormone receptors are abundant and stress exerts effects on cognitive processes (e.g., [3, 39, 40]). Therefore, sensory gating under acute stress would therefore be expected to be impaired. Additionally, it has been supposed that two processes contribute to the gating deficit, i.e., a reduced sensory registration (S_1 amplitude reduction) and a reduced ability to inhibit the repeated auditory stimulation (lack of reduction of S_2 amplitude; e.g., [41–43]). Sensory registration and suppression may be differentially affected by acute stress and may show gender difference meanwhile. Thus, another aim of this study is to determine which one plays a big role in the gender and acute stress effects. Given that fewer studies using paired-click paradigm focused on N_{100} and P_{200} gating, an exploratory investigation was also made in the current study.

2. Method

2.1. Participants. Forty-three healthy university students (25 males, 18 females) were included in the study. One female subject dropped out, data of a male subject was incomplete because of technical failure, and another female was excluded because of failure to obtain reliable P_{50} response in CPS experimental session. Thus, data were from 24 men (ranged in age from 20 to 23 years, mean = 21.3, SD = 0.86) and 16 women (for N_{100} and P_{200} data; ranged from 19 to 23; mean = 20.76, SD = 0.97). Statistical results of 16 women other than P_{50} data would not be present in the paper because there was no significant difference from 17-woman sample that were included in the analyses. Only women during their midluteal phase (with regular menstrual cycles, days 16 to 24) were included to control possible gender and ovarian cycle effects on adrenocortical reactivity [44, 45]. Participants were asked to refrain from caffeine, alcohol, tea, and smoking within 6 h before the experimental sessions. The volunteers were recruited by announcements and received financial compensation. The study was approved by the Ethics Committee of the Minnan Normal University. All participants were naive to the purpose of the study and gave their written informed consent prior to their inclusion in the study.

2.2. Procedure. After a participant's arrival, he or she was allowed to rest briefly, and then, preexperimental saliva sample (to measure cortisol level) was taken, and systolic blood pressure (SBP), diastolic blood pressure (DBP), and heart rate (HR) were recorded at the same time to evaluate participant's physical baseline. Then, participants filled out the Positive and Negative Affect Schedule (PANAS; [46]), Beck Depression Inventory-Second Edition (BDI-II; [47]), and Anxiety Inventory [48]. Data of Trait Anxiety Inventory was collected during their first experimental session. Then, participants were exposed to either the CPS treatment or the warm water (control) treatment (adapted from) [4]. Immediately after treatment, all subjects had a rest, and then SBP, DBP, and HR were measured at about 4 min after CPS or control procedures. Then, subjects were engaged in the experimental task, and meanwhile, EEG data was collected. Further, saliva samples were taken immediately after the task (about 15 min after treatment). The method of salivary cortisol measurement was described in Yang et al. [49]. All salivary samples were stored at -40°C, and analyses were completed within about one month.

This experiment was conducted by adopting a within-subjects design, in which CPS and control procedures were, respectively, applied by an interval of at least 24 h, and treatment order was counterbalanced. Subjects were instructed to submerge their hands and wrists in cold water (6° to 9°C) for 5 min for CPS session while in warm water (35° to 38°C) during control session (adapted from [4]). To avoid any influence of the circadian profiles of adrenocortical reactivity and cognitive ability, CPS or control procedures were conducted in the same time period of the experiment day and the other experimental procedures were the very same.

2.3. Stimuli and EEG Recording and Analysis

2.3.1. Auditory Stimulation. About 5 min after treatment, paired clicks of 2000 Hz, 95 dB SPL tones, and 4 ms in duration were delivered via headphones with 50 dB SPL background white noise. The sound intensity was measured at the subject's ear by a sound meter. All 60 paired clicks were separated by a 500 ms interval, and interpair interval was random ranged from 7.5 to 10 s in order to allow brain activity to return to baseline (e.g., [6, 7]).

2.3.2. EEG Recording. Participants were seated in a comfortable chair in an electromagnetically shielded room, wearing headphones, and instructed to sit comfortably and still, close their eyes, relax, and listen to clicks. All subjects were monitored for signs of drowsiness by visual observation and EEG monitoring because P_{50} component is sleep-state dependent (e.g., [11]). Brain electrical activity was recorded at F_z, C_z, P_z, F_3, F_4, C_3, C_4, O_1, and O_2 sites using Ag/AgCl electrodes mounted on an elastic cap (Brain Product, München,

Germany), with references on FC_z, and a ground electrode on the medial frontal aspect. Vertical electrooculograms (EOGs) were recorded supra- and infraorbitally at the left eye. The horizontal EOG was recorded from the left versus right orbital rim. The EEG and EOG were amplified using a 0.05 to 100 Hz bandpass and were continuously digitized at 1000 Hz/channel during online recording. All interelectrode impedances were maintained below 5 kΩ.

2.3.3. EEG Analysis. Offline, the data were referenced to the average of the left and right mastoids, digitally filtered at 10–50 Hz for P_{50} and 1–30 Hz for N_{100} and P_{200}, a 50 Hz notch filter and both a roll-off of 24 dB/octave, segmented (−100 to 200 ms for P_{50}; −100 to 400 ms for N_{100} and P_{200}), and baseline-corrected (100 ms). Trials containing artifacts (activity in any channel exceeded 75 μV) were removed from further analyses. Totally, 75–100% of the epochs (45–60 trials) were included in the N_{100} and P_{200} analyses and 77-100% (46-60 trials) for P_{50}. There is no statistical difference in number of epochs of each condition.

After averaging, according to the procedures of former studies (e.g., [11, 12, 16, 27, 38]), latencies and amplitudes of the P_{30}, N_{40}, P_{50}, N_{100}, and P_{200} at C_z were analyzed on the basis of automatic peak detection in combination with a visual inspection according to the waveforms drawn using Excel 2007. The P_{50} component was defined as the most positive response between 45 and 90 ms poststimulus preceded by a P_{30} wave in a 15–45 ms range. The N_{100} and P_{200} component was defined as a prominent negative-positive complex (N_{100}: 80–180 ms, P_{200}: 120–250 ms). P_{50} amplitude was normally measured relative to the N_{40} (defined as the most negative response between P_{30} and P_{50} latencies; if no identifiable P_{30}, then between 30 ms and P_{50} latency). If no identifiable N_{40} happened under any condition, all P_{50} amplitudes of this subject were measured relative to the prestimulus baseline, and this solution was also used in case of negative P_{50} gating ratios. N_{100} and P_{200} amplitudes were measured relative to the prestimulus baseline. As for components of S_2, they were additionally determined by reference to the S_1 component latencies (i.e., ±15 ms away from latency of S_1 P_{50} for S_2 P_{50}, ±30 ms for S_2 N_{100} and ±35 ms for S_2 P_{200}). When no amplitude was identifiable for S_1, the subject's response was excluded from further analysis (one case for P_{50}). If this was the case for S_2, it was interpreted as maximum suppression and the amplitude was set to zero in accordance [50]. Gating indices were calculated as gating ratio ($S_2/S_1 \times 100$) as well as gating difference ($S_1 - S_2$).

3. Results

3.1. Mood, Trait Anxiety, and Physiological Measurements. Results of trait anxiety test demonstrated no difference between males ($M = 40.5$, SD = 4.7) and females ($M = 40.8$, SD = 4.9, $p = 0.85$). To evaluate potential differences in baseline mood variables (positive and negative affect, state anxiety, and depression), mixed measure ANOVAs were conducted with treatment (CPS vs. control) as a within-subjects factor and gender as a between-subjects factor. The ANOVA showed no main effects of gender ($p = 0.86$, 0.29, 0.48, and 0.59, respectively), treatment ($p = 0.44$, 0.64, 0.24, and 0.77, respectively), and no interactions ($p = 0.99$, 0.22, 0.22, and 0.88, respectively) (Table 2). Mixed measure ANOVAs were also conducted on cardiovascular and cortisol reactivity with two within-subjects factors: treatment (CPS vs. control) and timing (baseline and after treatment) and gender as another factor to evaluate the effect of experimental manipulation. The results showed significant main effects of treatment in HR [$F(1, 39) = 14.13$, $p = 0.001$, $\eta 2\,\mathrm{p} = 0.27$], DBP [$F(1, 39) = 16.30$, $p < 0.001$, $\eta 2\,\mathrm{p} = 0.30$], SBP [$F(1, 39) = 11.25$, $p = 0.002$, $\eta 2\,\mathrm{p} = 0.22$], and cortisol concentrations [$F(1, 39) = 7.09$, $p = 0.011$, $\eta 2\,\mathrm{p} = 0.15$] and significant main effects of gender. Specifically, data showed significantly higher HR ($p = 0.026$) and cortisol concentrations ($p = 0.024$) for females, while higher DBP ($p = 0.051$) and SBP ($p < 0.001$) for males. The results also showed significant interactions of treatment × timing to DBP [$F(1, 39) = 7.50$, $p = 0.009$, $\eta 2\,\mathrm{p} = 0.16$], SBP [$F(1, 39) = 6.02$, $p = 0.019$, $\eta 2\,\mathrm{p} = 0.13$], and cortisol [$F(1, 39) = 13.0$, $p = 0.001$, $\eta 2\,\mathrm{p} = 0.25$]. Further analysis showed no difference of blood pressures between baseline and after-treatment data during control session while in CPS session there were significantly higher after-treatment DBP ($p < 0.001$), SBP ($p = 0.002$), and cortisol concentrations ($p = 0.001$), relative to baseline data.

3.2. P_{50} Latencies, Amplitudes, and Sensory Gating. The grand averaged auditory evoked potentials for both genders, during two experimental sessions, are presented in Figure 1, and descriptive results on P_{50} measures can be found in Table 3. P_{50} amplitudes and latencies to peak were evaluated by performing separate 2 (gender) × 2 (stimuli: S_1 vs. S_2) × 2 (treatment: CPS vs. control) mixed measure ANOVAs. The ANOVA showed the P_{50} latencies did not show any main effects and interactions (all $p > 0.14$). However, the P_{50} amplitudes showed a significant main effect of stimuli [$F(1, 38) = 25.29$, $p < 0.001$, $\eta 2\,\mathrm{p} = 0.40$] and a significant interaction of stimuli × treatment [$F(1, 38) = 17.18$, $p < 0.001$, $\eta 2\,\mathrm{p} = 0.31$], but no main effect of gender or other interactions. Further analysis showed P_{50} amplitude to S_2 during CPS experimental session was significantly larger than that to S_2 during control session ($p = 0.01$), while there is no difference for P_{50} amplitude to S_1 between two sessions. Additionally, P_{50} amplitude to S_1 was significantly larger than that to S_2 for both sessions ($p = 0.037$ for CPS and $p < 0.001$ for control).

P_{50} gating ratios and gating difference were evaluated by performing 2 (gender) × 2 (treatment) mixed measure ANOVAs. The results showed no gender main effect ($p = 0.79$) and interaction ($p = 0.85$), but a significant main effect of treatment [$F(1, 38) = 9.72$, $p = 0.003$, $\eta 2\,\mathrm{p} = 0.20$] for gating ratios. As for gating difference, the same results were obtained, which showed a better gating function after control procedures than that of CPS [$F(1, 38) = 17.18$, $p < 0.001$, $\eta 2\,\mathrm{p} = 0.31$], without gender effect ($p = 0.77$) and interaction ($p = 0.93$).

3.3. N_{100} Latencies, Amplitudes, and Sensory Gating. The grand averaged potentials are presented in Figure 2, and

Table 2: Preexperiment mood and physiological measurements before and after control or CPS treatment.

	Gender	Positive affect	Negative affect	State anxiety	Depression	Baseline HR	HR after 4 min
CON (M, SD)	Male	29.3 (8.3)	16.1 (5.1)	35.9 (8.4)	6.9 (6.2)	69 (13)	66 (16)
	Female	28.9 (8.0)	18.6 (5.3)	35.2 (8.8)	7.9 (6.5)	75 (8)	73 (11)
CPS (M, SD)	Male	30.0 (6.8)	16.7 (4.6)	36.0 (7.4)	7.3 (5.4)	62 (11)	61 (9)
	Female	29.6 (7.8)	17.3 (5.4)	33.0 (9.4)	8.1 (4.9)	70 (9)	67 (10)
	Gender	Baseline DBP	DBP after 4 min	Baseline SBP	SBP after 4 min	Baseline CORT	CORT after 15 min
CON (M, SD)	Male	63 (6)	63 (5)	112 (9)	111 (9)	5.0 (1.6)	5.0 (1.5)
	Female	62 (6)	61 (4)	101 (10)	100 (7)	6.2 (2.1)	6.1 (2.0)
CPS (M, SD)	Male	67 (6)	69 (7)	115 (7)	116 (7)	5.8 (1.5)	6.1 (1.7)
	Female	62 (5)	66 (5)	101 (7)	105 (7)	6.6 (1.8)	7.3 (2.3)

Values represent means (M) and standard deviations (SD); CON: control condition; CPS: cold pressor stress; HR: heart rate (beats per minute); DBP: diastolic blood pressure (mmHg); SBP: systolic blood pressure (mmHg); CORT: cortisol (nmol/L).

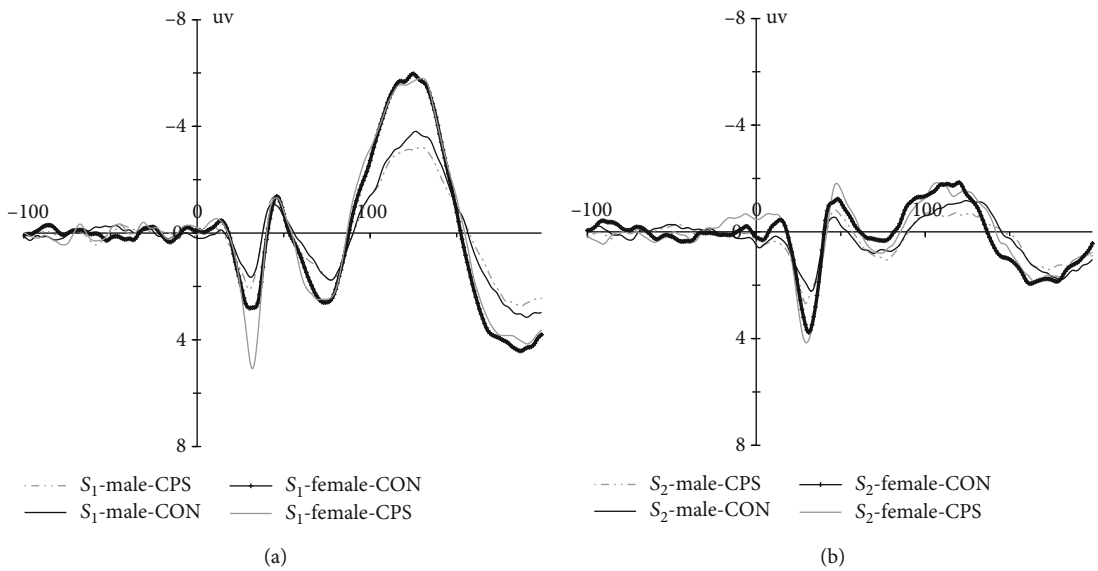

Figure 1: Grand averaged auditory evoked potential waves (C_z) elicited by paired clicks ((a) S_1, (b) S_2) for both genders during two experimental sessions (CON: control condition; CPS: cold pressor stress treatment) (bandpass filter = 10 – 50 Hz).

Table 3: Amplitudes, latencies, gating ratios, and differences for P_{50}, N_{100}, and P_{200}, M (SD).

		Treatment	S_1 Latency	S_1 Amplitude	S_2 Latency	S_2 Amplitude	Gating ratio ($S_2/S_1 \times 100$)	Gating difference
P_{50}	Male	CON	76 (9)	4.1 (2.6)	74 (10)	2.0 (2.0)	52 (40)	2.1 (2.4)
		CPS	75 (8)	3.6 (3.3)	74 (9)	3.1 (4.0)	94 (85)	0.5 (1.4)
	Female	CON	73 (7)	5.5 (4.0)	71 (11)	3.2 (3.1)	59 (28)	2.3 (2.6)
		CPS	72 (7)	4.9 (3.9)	72 (10)	4.2 (3.6)	95 (62)	0.6 (1.9)
N_{100}	Male	CON	122 (12)	−7.7 (4.8)	117 (16)	−1.9 (2.6)	39 (26)	5.8 (3.6)
		CPS	121 (14)	−7.7 (4.7)	118 (18)	−1.9 (2.5)	43 (37)	5.8 (3.6)
	Female	CON	118 (11)	−12.7 (11.6)	111 (14)	−3.8 (4.4)	37 (32)	8.9 (8.8)
		CPS	116 (12)	−12.9 (9.7)	110 (13)	−3.5 (4.1)	34 (20)	9.4 (7.3)
P_{200}	Male	CON	196 (17)	8.8 (7.6)	188 (19)	5.1 (2.9)	67 (49)	3.7 (6.5)
		CPS	198 (18)	7.0 (4.4)	191 (21)	4.5 (2.3)	70 (54)	2.5 (4.3)
	Female	CON	193 (20)	12.9 (7.0)	191 (26)	6.6 (3.0)	54 (24)	6.3 (5.3)
		CPS	198 (15)	11.7 (5.7)	189 (18)	5.2 (2.0)	56 (37)	6.4 (6.1)

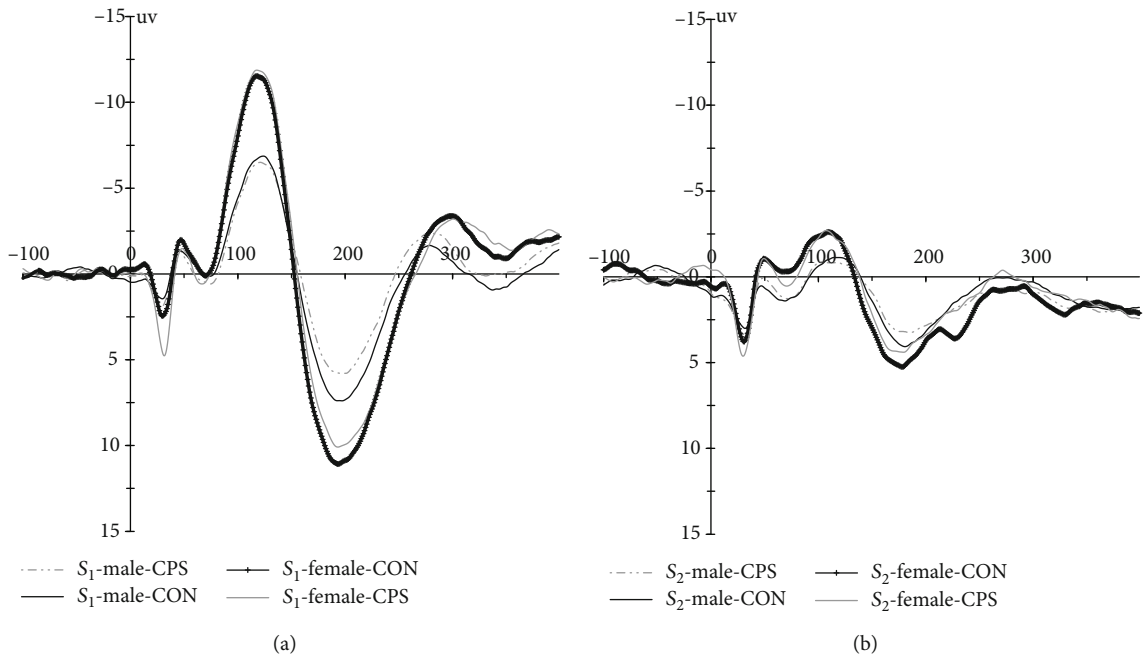

Figure 2: Grand averaged auditory evoked potential waveforms (C_z) elicited by paired clicks ((a) S_1, (b) S_2) for both genders during two experimental sessions (bandpass filter = 1 – 30 Hz).

descriptive results on N_{100} are shown in Table 3. N_{100} amplitudes and latencies were evaluated by performing separate 2 (gender) × 2 (stimuli: S_1 vs. S_2) × 2 (treatment: CPS vs. control) mixed measure ANOVAs.

According to the ANOVA, there was a significant main effect of stimuli with longer latencies for S_1 than S_2 [$F(1, 39) = 6.63$, $p = 0.014$, $\eta 2\,\mathrm{p} = 0.15$] and a borderline main effect of gender [$F(1, 39) = 3.39$, $p = 0.073$, $\eta 2\,\mathrm{p} = 0.08$], with slightly longer latencies for males than females, but there was no main effect of treatment and no interactions on latency (all $p > 0.67$). The results also showed a significant main effect of stimuli [$F(1, 39) = 80.92$, $p < 0.001$, $\eta 2\,\mathrm{p} = 0.68$, $S_1 > S_2$] and of gender [$F(1, 39) = 5.14$, $p = 0.029$, $\eta 2\,\mathrm{p} = 0.12$, larger for females than males] for the mean N_{100} amplitudes and a borderline significant interaction of stimuli × gender [$F(1, 39) = 4.04$, $p = 0.05$, $\eta 2\,\mathrm{p} = 0.09$] without treatment effect. Further analysis showed relatively larger N_{100} amplitudes in women than men for S_1 ($p = 0.028$) and S_2 ($p = 0.077$).

N_{100} gating ratios and gating difference were evaluated by performing 2 (gender) × 2 (treatment) mixed measure ANOVAs. The results showed no main effects of gender ($p = 0.50$) and treatment ($p = 0.99$) and no interaction ($p = 0.51$) for gating ratios. The data showed similar results for gating difference, but a borderline main effect of gender [$F(1, 39) = 4.04$, $p = 0.05$, $\eta 2\,\mathrm{p} = 0.09$], with slightly better N_{100} gating function for females.

3.4. P_{200} Latencies, Amplitudes, and Sensory Gating. The grand averaged potentials are presented in Figure 2, and descriptive results of P_{200} can be found in Table 3. P_{200} amplitudes and latencies were evaluated by performing 2 (gender) × 2 (stimuli) × 2 (treatment) mixed measure ANOVAs. As for latencies, there was only a significant main effect of stimuli [$F(1, 39) = 9.31$, $p = 0.004$, $\eta 2\,\mathrm{p} = 0.19$], with longer P_{200} latencies for S_1 than S_2. As for P_{200} amplitudes, the results showed there were significant main effects of treatment [$F(1, 39) = 4.43$, $p = 0.042$, $\eta 2\,\mathrm{p} = 0.10$], stimuli [$F(1, 39) = 37.89$, $p < 0.001$, $\eta 2\,\mathrm{p} = 0.49$], and gender [$F(1, 39) = 6.34$, $p = 0.016$, $\eta 2\,\mathrm{p} = 0.14$] and a significant interaction of stimuli × gender [$F(1, 39) = 4.47$, $p = 0.041$, $\eta 2\,\mathrm{p} = 0.10$]. Further analysis showed P_{200} responses were attenuated under CPS than control condition ($p = 0.042$), and females had significantly larger S_1 P_{200} amplitude than males ($p = 0.018$), but there was no notable difference in S_2 response amplitude between genders ($p = 0.10$).

P_{200} gating ratios and gating difference were evaluated by performing 2 (gender) × 2 (treatment) mixed measure ANOVAs. The results showed no main effects of gender ($p = 0.26$) and treatment ($p = 0.77$) and no interaction ($p = 0.90$) for gating ratios. The data showed similar results for gating differences, but a significant gender effect [$F(1, 39) = 4.47$, $p = 0.041$, $\eta 2\,\mathrm{p} = 0.10$], with better P_{200} gating function for females.

4. Discussion

To characterize the response to the CPS, salivary cortisol and cardiovascular response were assessed. The results revealed significantly higher blood pressures, as well as an increased activity of the hypothalamus-pituitary-adrenal axis (reflected by higher cortisol concentrations) after CPS treatment, compared to the control procedure session. The findings are well in line with the previous studies (e.g., [4, 51]) and indicate the successful induction of a neuroendocrine stress response [1]. Moreover, a comparable basis was demonstrated by the baseline psychological measures across all conditions.

In the paired-click paradigm, sensory gating is operationally defined as the ratio of the amplitude of the response to S_2 divided by that of S_1 or the amplitude difference between the two clicks (e.g., [9–11]). Higher ratios and smaller absolute difference values mean worse sensory gating, which could be a result of lower amplitudes in response to S_1, thus weaker registration functions, or higher amplitudes in response to S_2, thus weaker inhibition with repetition, according to some authors (e.g., [41–43]). In this view, this study showed diminished P_{50} gating due to enhanced amplitudes to S_2 significantly under CPS relative to control condition, while P_{50} amplitudes to S_1 remaining unaffected, which indicated that CPS disrupted subjects' capacity of inhibition with repetition, but not sensory registration. These results were in right accordance with Johnson and Adler [26] and Atchley [30]. In addition, Ermutlu et al. [29] used an oddball paradigm and also found CPS impaired P_{50} sensory gating. As for Woods et al. [11] reporting no evidence on impairment in P_{50} gating, the most likely explanation is that the CPS procedure used in that study was so weak as only 50 seconds of immersing in cold water that the stress stimuli may not be strong enough to trigger the abundant releasing of norepinephrine (NE) and cortisol to disrupt the sensory gating. A much stronger CPS procedure was used in the current study, and both data of blood pressures and saliva samples proved successful induction of a neuroendocrine stress response. As was known, acute stress can lead to the release of NE from widely distributed synapses, including abundant projections to the PFC, and the rapid activation of the prefrontal dopamine system, and on a slightly longer time scale, the release of cortisol, whose receptors are also abundant in the PFC [3, 39, 40, 52]. However, it was proposed that PFC should be the major neural source of P_{50} suppression by many documents (e.g., [9, 38, 53–56]). Thus, it is reasonable that acute stress disrupts P_{50} sensory gating via the adverse effects of stress hormones and neuromodulators on PFC which might result in impairments of the inhibition of redundant information.

However, White and Yee [27] reported a reduction of S_1 P_{50} amplitude during mental arithmetic stressor, which are different from the results of Johnson and Adler [26], Atchley [30] and the current study that acute stress resulted in an increase of S_2 P_{50} amplitude with unchanged S_1 P_{50} amplitude. Given that consciously directing attention toward the clicks enhanced P_{50} amplitude in healthy subjects (e.g., [16, 31]), oral mental arithmetic stressor task during passively listening task makes less attention resources switched to the clicks and might then a reduction of S_1 P_{50} amplitude, while in the cases of Johnson and Adler [26], Atchley [30] and the current study, CPS was used to induce stress state and there was no specific cognitive processes involved.

No gender difference in P_{50} amplitudes and sensory gating was reported in the current study, which was in accordance with previous studies [6, 22 21, 24, 25]. Freedman, Adler, and Waldo [20] also reported no gender difference in P_{50} sensory gating, but they found women had higher P_{50} amplitude to S_1 than men. However, Franks et al. [19] and Hetrick et al. [10] reported women had significantly larger P_{50} responses to S_2, but Fuerst et al. [23] reported men scored higher than women in P_{50} amplitude to S_1. It is not likely to interpret the discrepancy properly by gender difference in the neuroanatomical origins of the auditory P_{50} response and inhibition, because it was documented that there was no known gender difference in brain structures or neuronal systems relevant to P_{50}, such as auditory cortex, thalamus, and PFC ([57]; e.g., [9, 10]), and the discrepancy is mostly state dependent. As mentioned earlier, menstrual cycles could affect several cognitive processing. In particular, Goldstein et al. [35, 58] found menstrual cycle modulated women's arousal state with less cortical control over the amygdala during early follicular due to low level of estrogen, but an attenuation of brain activity during midcycle in the presence of higher levels of estrogen. Therefore, given different arousals leading to different baseline P_{50} responses [11, 59] and the interplay between acute stress and sex steroid hormone (for a review, see [60]), the mechanisms under the discrepancy is more likely estrogen level dependent.

The results of the current study showed no gender difference in the CPS effects on P_{50} amplitudes and sensory gating. However, White et al. [12] reported a significant gender difference with a significantly reduced P_{50} to S_1 but not S_2 during mental arithmetic stressor for women, not for men, but they did not report any information about menstrual cycles. Therefore, in addition to the defects in design mentioned earlier, the most likely explanation would be that more early follicular phase women participated in that study, while female subjects used in the current study were all in their midluteal phase (days 16 to 24) during which there was a steady rise in estrogen levels forming a second estrogen peak in menstrual cycles [61] and then women might be more comparable to men in arousal and sensory gating because of more cortical control over the amygdala due to high level of estrogen. Future studies should select healthy female subjects during their different menstrual cycles based on direct measurements of gonadal hormone levels instead of self-reported data to precisely determine menstrual phases to further confirm and extend the present findings.

As reviewed earlier, relatively fewer studies using paired-click procedure focused on N_{100} and P_{200} sensory gating. And the relevant findings were also inconsistent. According to Hetrick et al. [10], women had significantly higher N_{100} amplitudes to S_2 and worse N_{100} sensory gating compared to men, but no significant differences were found at P_{200}, and Fuerst et al. [23] found that men had larger N_{100} and P_{200} amplitude to S_1 and better N_{100} and P_{200} sensory gating relative to women. However, other studies reported no gender difference [22, 24]. Data of the current study showed women had larger S_1 N_{100} and P_{200} amplitudes to S_1 and better N_{100} and P_{200} gating function. In addition to the possible effects of arousal due to fluctuations of gonadal hormones mentioned earlier, potential manipulation of attention because of nonstandardized instructions across studies might be an alternative interpretation. Gjini et al. [31] reported attention status had a significant effect on N_{100} and P_{200} amplitudes and gating. However, there is no specific control for attention factors, according to typical instructions in paired-click paradigms. For example, subjects are usually requested to remain awake and try to decrease their eye

movements, close (e.g., [10] and the current study) or open eyes, fixate on an object (e.g., [22]) or not, listen passively or intently to clicks (e.g., [22, 24]), keep relaxed or not, and so on. Thus, different baseline attention status due to different emphases in instructions, combined and interacted with fluctuations of gonadal hormones, leads to complex results.

Some studies suggested that in paired-click paradigm N_{100} could reflect initial direction of attention, and P_{200} reflects early allocation of attention, initial conscious experience, and entrance into working memory of the stimulus [31, 62, 63]. Therefore, women in the current study might be more alert, reflected by larger N_{100} amplitudes than men both to S_1 and S_2. And in the end, women allocated more attention resources to relevant information than men, reflected by significantly larger S_1 P_{200} amplitude for females than males. Additionally, the current study also indicated that CPS disrupted allocation of attention resources, reflected by attenuated activation during P_{200} time window for both clicks after CPS than control procedures, which was in accordance with the majority of the findings in attention studies, and should involve the mechanism that acute stress impairs normal selective attention via disruptions of higher PFC functions (as a review, see [64]).

As for the effects of acute stress on sensory gating of N_{100} and P_{200}, the current study found no stress effect, which was in accordance with Ermutlu et al. [29]. However, White et al. [12] using mental arithmetic stressor reported disrupted N_{100} gating ratios. In typical paired-click paradigm, only pairs of identical clicks are presented and cognitive processing resources are always sufficient. This might be a possible explanation for no effect of CPS on N_{100} amplitude and gating indices in Ermutlu et al. [29] and this current study, but significant stress effects on N_{100} response and gating ratio in White et al. [12] because of the potential inadequate process resources allocated in paired-click listening task due to concurrent mental arithmetic processing and the impairment of inhibition function due to stressful situation.

At last, the data showed significantly longer latencies to S_1 than S_2 both for N_{100} and P_{200} and a similar trend for P_{50} although not statistically significant in this current study, which were in accordance with former studies [10, 23, 24, 65]. We cannot interpret the results properly due to scarcity of relevant documents. Probably, peak latencies reflect the depth of information processing and cognitive process to S_2 is incomplete because of sensory gating, and as a result, the latency to S_1 is longer than S_2. The data of this study also showed a trend of longer N_{100} latencies for men than women, and it might be the fact that the depth of cognitive process during N_{100} time window was less for women than men, although as mentioned earlier, women might be more alert and allocate more attention resources to relevant information than men, according to larger N_{100} and P_{200} amplitudes than men both to S_1 and S_2. In a word, peak latencies in the paired-click paradigm need more concerns and relevant data need to be better understood in the future, but at least the current latency data are in accordance with former studies, which assures in some extent that the components of P_{50}, N_{100}, and P_{200} are extracted precisely.

As for the application of paired-click paradigm in neural pathological studies, based on this study, more emphasis should be paid on the control of all kinds of factors that might induce subjects a stressful state, and we suggest the importance of monitoring stress and anxiety levels of subjects, and furthermore, N_{100} and P_{200} gating indices should be cautiously used because of their strong correlations with high-order cognitive process. But no matter how does one think of the applications of the P_{50}, N_{100}, and P_{200} sensory gating in pathological fields, the primary focus of the work is to standardize the recording of gating data and the extracting procedure of the components.

Data Availability

All data included in this study are available upon request by contact with the corresponding author.

Conflicts of Interest

The authors declare that there are no competing financial interests.

Authors' Contributions

ZX, HL, and YL designed the study; ZX, SG, and WW did the experiments and analyzed the data. ZX, YL, and SG wrote the paper. Zengyou Xin and Simeng Gu contributed equally to this paper.

Acknowledgments

This study is supported by the following: Shenzhen-Hong Kong Institute of Brain Science-Shenzhen Fundamental Research Institutions (2019SHIBS0003); National Natural Science Foundation of China (31871130 and 31671150); Guangdong Key Project (2018B030335001); Guangdong Major Program (2016KZDXM009); Innovative Team Program in Higher Education of Guangdong (2015KCXTD009); Fujian Provincial Department of Education Projects (JA15320); Shenzhen Basic Research Scheme (JCYJ20150729104249783); and Shenzhen Peacock Plan (KQTD2015033016104926).

References

[1] L. Elling, C. Steinberg, A.-K. Bröckelmann, C. Dobel, J. Bölte, and M. Junghofer, "Acute stress alters auditory selective attention in humans independent of HPA: a study of evoked potentials," *PLoS One*, vol. 6, no. 4, article e18009, 2011.

[2] S. Gu, W. Wang, F. Wang, and J. H. Huang, "Neuromodulator and emotion biomarker for stress induced mental disorders," *Neural Plasticity*, vol. 2016, Article ID 2609128, 6 pages, 2016.

[3] E. J. Hermans, H. J. F. van Marle, L. Ossewaarde et al., "Stress-related noradrenergic activity prompts large-scale neural network reconfiguration," *Science*, vol. 334, no. 6059, pp. 1151–1153, 2011.

[4] V. Lai, C. Theppitak, T. Makizuka et al., "A normal intensity level of psycho-physiological stress can benefit working memory performance at high load," *International Journal of Industrial Ergonomics*, vol. 44, no. 3, pp. 362–367, 2014.

[5] C. Kirschbaum, K. M. Pirke, and D. H. Hellhammer, "The 'Trier Social Stress Test'–a tool for investigating

psychobiological stress responses in a laboratory setting," *Neuropsychobiology*, vol. 28, no. 1-2, pp. 76–81, 1993.

[6] M. J. Brinkman and J. E. Stauder, "Development and gender in the P50 paradigm," *Clinical Neurophysiology*, vol. 118, no. 7, pp. 1517–1524, 2007.

[7] G. Zouridakis and N. N. Boutros, "Stimulus parameter effects on the P50 evoked response," *Biological Psychiatry*, vol. 32, no. 9, pp. 839–841, 1992.

[8] R. Freedman, L. E. Adler, G. A. Gerhardt et al., "Neurobiological studies of sensory gating in schizophrenia," *Schizophrenia Bulletin*, vol. 13, no. 4, pp. 669–678, 1987.

[9] L. Jones, P. Hills, K. Dick, S. Jones, and P. Bright, "Cognitive mechanisms associated with auditory sensory gating," *Brain and Cognition*, vol. 102, pp. 33–45, 2016.

[10] W. P. Hetrick, C. A. Sandman, W. E. Bunney, Y. Jin, S. G. Potkin, and M. H. White, "Gender differences in gating of the auditory evoked potential in normal subjects," *Biological Psychiatry*, vol. 39, no. 1, pp. 51–58, 1996.

[11] A. J. Woods, J. W. Philbeck, K. Chelette, R. D. Skinner, E. Garcia-Rill, and M. Mennemeier, "f," *Acta Neurobiologiae Experimentalis*, vol. 71, no. 3, pp. 348–358, 2011.

[12] P. M. White, A. Kanazawa, and C. M. Yee, "Gender and suppression of mid-latency ERP components during stress," *Psychophysiology*, vol. 42, no. 6, pp. 720–725, 2005.

[13] A. Brockhaus-Dumke, R. Mueller, U. Faigle, and J. Klosterkoetter, "Sensory gating revisited: relation between brain oscillations and auditory evoked potentials in schizophrenia," *Schizophrenia Research*, vol. 99, no. 1-3, pp. 238–249, 2008.

[14] J. V. Patterson, W. P. Hetrick, N. N. Boutros et al., "P50 sensory gating ratios in schizophrenics and controls: a review and data analysis," *Psychiatry Research*, vol. 158, no. 2, pp. 226–247, 2008.

[15] T. Popov, T. Jordanov, N. Weisz, T. Elbert, B. Rockstroh, and G. A. Miller, "Evoked and induced oscillatory activity contributes to abnormal auditory sensory gating in schizophrenia," *NeuroImage*, vol. 56, no. 1, pp. 307–314, 2011.

[16] C. M. Yee, T. J. Williams, P. M. White, K. H. Nuechterlein, D. Ames, and K. L. Subotnik, "Attentional modulation of the P50 suppression deficit in recent-onset and chronic schizophrenia," *Journal of Abnormal Psychology*, vol. 119, no. 1, pp. 31–39, 2010.

[17] B. A. Clementz, M. A. Geyer, and D. L. Braff, "Poor P50 suppression among schizophrenia patients and their first-degree biological relatives," *American Journal of Psychiatry*, vol. 155, no. 12, pp. 1691–1694, 1998.

[18] R. Karkal, N. Goyal, S. K. Tikka, R. V. Khanande, A. Kakunje, and C. R. J. Khess, "Sensory gating deficits and their clinical correlates in drug-free/drug-naive patients with schizophrenia," *Indian Journal of Psychological Medicine*, vol. 40, no. 3, pp. 247–256, 2018.

[19] R. D. Franks, L. Adler, M. Waldo, J. Alpert, and R. Freedman, "Neurophysiological studies of sensory gating in mania: comparison with schizophrenia," *Biological Psychiatry*, vol. 18, no. 9, pp. 989–1005, 1983.

[20] R. Freedman, L. E. Adler, and M. Waldo, "Gating of the auditory evoked potential in children and adults," *Psychophysiology*, vol. 24, no. 2, pp. 223–227, 1987.

[21] L. Rasco, R. D. Skinner, and E. Garcia-Rill, "Effect of age on sensory gating of the sleep state-dependent P1/P50 midlatency auditory evoked potential," *Sleep Research Online*, vol. 3, no. 3, pp. 97–105, 2000.

[22] B. A. Clementz and L. D. Blumenfeld, "Multichannel electroencephalographic assessment of auditory evoked response suppression in schizophrenia," *Experimental Brain Research*, vol. 139, no. 4, pp. 377–390, 2001.

[23] D. R. Fuerst, J. Gallinat, and N. N. Boutros, "Range of sensory gating values and test–retest reliability in normal subjects," *Psychophysiology*, vol. 44, no. 4, pp. 620–626, 2007.

[24] M. Lijffijt, F. G. Moeller, N. N. Boutros et al., "The role of age, gender, education, and intelligence in P50, N100, and P200 auditory sensory gating," *Journal of Psychophysiology*, vol. 23, no. 2, pp. 52–62, 2009.

[25] C. Thomas, I. vom Berg, A. Rupp et al., "P50 gating deficit in Alzheimer dementia correlates to frontal neuropsychological function," *Neurobiology of Aging*, vol. 31, no. 3, pp. 416–424, 2010.

[26] M. R. Johnson and L. E. Adler, "Transient impairment in P50 auditory sensory gating induced by a cold-pressor test," *Biological Psychiatry*, vol. 33, no. 5, pp. 380–387, 1993.

[27] P. M. White and C. M. Yee, "Effects of attentional and stressor manipulations on the P50 gating response," *Psychophysiology*, vol. 34, no. 6, pp. 703–711, 1997.

[28] C. M. Yee and P. M. White, "Experimental modification of P50 suppression," *Psychophysiology*, vol. 38, no. 3, pp. 531–539, 2001.

[29] M. N. Ermutlu, S. Karamürsel, E. H. Ugur, L. Senturk, and N. Gokhan, "Effects of cold stress on early and late stimulus gating," *Psychiatry Research*, vol. 136, no. 2-3, pp. 201–209, 2005.

[30] R. M. Atchley, *Mindfulness Meditation Reduces Stress-Related Inhibitory Gating Impairment*, Bowling Green State University, 2014.

[31] K. Gjini, S. Burroughs, and N. N. Boutros, "Relevance of attention in auditory sensory gating paradigms in schizophrenia," *Journal of Psychophysiology*, vol. 25, no. 2, pp. 60–66, 2011.

[32] M. Kurthen, P. Trautner, T. Rosburg et al., "Towards a functional topography of sensory gating areas: invasive P50 recording and electrical stimulation mapping in epilepsy surgery candidates," *Psychiatry Research: Neuroimaging*, vol. 155, no. 2, pp. 121–133, 2007.

[33] A. Gasbarri, A. Pompili, A. d'Onofrio, A. Cifariello, M. C. Tavares, and C. Tomaz, "Working memory for emotional facial expressions: role of the estrogen in young women," *Psychoneuroendocrinology*, vol. 33, no. 7, pp. 964–972, 2008.

[34] V. Kumari, J. Konstantinou, A. Papadopoulos et al., "Evidence for a role of progesterone in menstrual cycle-related variability in prepulse inhibition in healthy young women," *Neuropsychopharmacology*, vol. 35, no. 4, pp. 929–937, 2010.

[35] J. M. Goldstein, M. Jerram, B. Abbs, S. Whitfield-Gabrieli, and N. Makris, "Sex differences in stress response circuitry activation dependent on female hormonal cycle," *Journal of Neuroscience*, vol. 30, no. 2, pp. 431–438, 2010.

[36] M. R. Milad, M. A. Zeidan, A. Contero et al., "The influence of gonadal hormones on conditioned fear extinction in healthy humans," *Neuroscience*, vol. 168, no. 3, pp. 652–658, 2010.

[37] X. Du and B. Jansen, "A neural network model of normal and abnormal auditory information processing," *Neural Networks*, vol. 24, no. 6, pp. 568–574, 2011.

[38] H. Terada, T. Kurayama, K. Nakazawa, D. Matsuzawa, and E. Shimizu, "Transcranial direct current stimulation (tDCS) on the dorsolateral prefrontal cortex alters P50 gating," *Neuroscience Letters*, vol. 602, pp. 139–144, 2015.

[39] E. J. Hermans, M. J. Henckens, M. Joëls, and G. Fernández, "Dynamic adaptation of large-scale brain networks in response to acute stressors," *Trends in Neurosciences*, vol. 37, no. 6, pp. 304–314, 2014.

[40] B. S. McEwen and J. H. Morrison, "The brain on stress: vulnerability and plasticity of the prefrontal cortex over the life course," *Neuron*, vol. 79, no. 1, pp. 16–29, 2013.

[41] N. N. Boutros, K. Gjini, S. B. Eickhoff, H. Urbach, and M. E. Pflieger, "Mapping repetition suppression of the P50 evoked response to the human cerebral cortex," *Clinical Neurophysiology*, vol. 124, no. 4, pp. 675–685, 2013.

[42] A. Brockhaus-Dumke, F. Schultze-Lutter, R. Mueller et al., "Sensory gating in schizophrenia: P50 and N100 gating in antipsychotic-free subjects at risk, first-episode, and chronic patients," *Biological Psychiatry*, vol. 64, no. 5, pp. 376–384, 2008.

[43] J.-C. Shan, M. H. Hsieh, C.-M. Liu, M.-J. Chiu, F.-S. Jaw, and H.-G. Hwu, "More evidence to support the role of S2 in P50 studies," *Schizophrenia Research*, vol. 122, no. 1-3, pp. 270–272, 2010.

[44] C. Kirschbaum, B. M. Kudielka, J. Gaab, N. C. Schommer, and D. H. Hellhammer, "Impact of gender, menstrual cycle phase, and oral contraceptives on the activity of the hypothalamus-pituitary-adrenal axis," *Psychosomatic Medicine*, vol. 61, no. 2, pp. 154–162, 1999.

[45] B. M. Kudielka and C. Kirschbaum, "Sex differences in HPA axis responses to stress: a review," *Biological Psychology*, vol. 69, no. 1, pp. 113–132, 2005.

[46] D. Watson, L. A. Clark, and A. Tellegen, "Development and validation of brief measures of positive and negative affect: the PANAS scales," *Journal of Personality and Social Psychology*, vol. 54, no. 6, pp. 1063–1070, 1988.

[47] A. Beck, R. Steer, and G. Brown, *Beck Depression Inventory-II*, 1996.

[48] D. T. L. Shek, "The Chinese version of the State-Trait Anxiety Inventory: its relationship to different measures of psychological well-being," *Journal of Clinical Psychology*, vol. 49, no. 3, pp. 349–358, 1993.

[49] Y. Yang, D. Koh, V. Ng et al., "Self perceived work related stress and the relation with salivary IgA and lysozyme among emergency department nurses," *Occupational and Environmental Medicine*, vol. 59, no. 12, pp. 836–841, 2002.

[50] J. Rentzsch, M. C. Jockersscherübl, N. N. Boutros, and J. Gallinat, "Test-retest reliability of P50, N100 and P200 auditory sensory gating in healthy subjects," *International Journal of Psychophysiology*, vol. 67, no. 2, pp. 81–90, 2008.

[51] P. R. Zoladz, D. M. Peters, C. E. Cadle et al., "Post-learning stress enhances long-term memory and differentially influences memory in females depending on menstrual stage," *Acta Psychologica*, vol. 160, pp. 127–133, 2015.

[52] E. R. De Kloet, M. Joëls, and F. Holsboer, "Stress and the brain: from adaptation to disease," *Nature Reviews Neuroscience*, vol. 6, no. 6, pp. 463–475, 2005.

[53] R. T. Knight, W. R. Staines, D. Swick, and L. L. Chao, "Prefrontal cortex regulates inhibition and excitation in distributed neural networks," *Acta Psychologica*, vol. 101, no. 2-3, pp. 159–178, 1999.

[54] O. Korzyukov, M. E. Pflieger, M. Wagner et al., "Generators of the intracranial P50 response in auditory sensory gating," *NeuroImage*, vol. 35, no. 2, pp. 814–826, 2007.

[55] J. R. Tregellas, D. B. Davalos, D. C. Rojas et al., "Increased hemodynamic response in the hippocampus, thalamus and prefrontal cortex during abnormal sensory gating in schizophrenia," *Schizophrenia Research*, vol. 92, no. 1-3, pp. 262–272, 2007.

[56] T. J. Williams, K. H. Nuechterlein, K. L. Subotnik, and C. M. Yee, "Distinct neural generators of sensory gating in schizophrenia," *Psychophysiology*, vol. 48, no. 4, pp. 470–478, 2011.

[57] R. C. Gur, F. Gunning-Dixon, W. B. Bilker, and R. E. Gur, "Sex differences in temporo-limbic and frontal brain volumes of healthy adults," *Cerebral Cortex*, vol. 12, no. 9, pp. 998–1003, 2002.

[58] J. M. Goldstein, M. Jerram, R. Poldrack et al., "Hormonal cycle modulates arousal circuitry in women using functional magnetic resonance imaging," *Journal of Neuroscience*, vol. 25, no. 40, pp. 9309–9316, 2005.

[59] I. Griskova-Bulanova, J. Paskevic, K. Dapsys, V. Maciulis, O. Ruksenas, and S. M. Arnfred, "The level of arousal modulates P50 peak amplitude," *Neuroscience Letters*, vol. 499, no. 3, pp. 204–207, 2011.

[60] E. Kajantie and D. I. Phillips, "The effects of sex and hormonal status on the physiological response to acute psychosocial stress," *Psychoneuroendocrinology*, vol. 31, no. 2, pp. 151–178, 2006.

[61] M. A. Farage, T. W. Osborn, and A. B. Maclean, "Cognitive, sensory, and emotional changes associated with the menstrual cycle: a review," *Archives of Gynecology and Obstetrics*, vol. 278, no. 4, pp. 299–307, 2008.

[62] M. Lijffijt, S. D. Lane, S. L. Meier et al., "P50, N100, and P200 sensory gating: relationships with behavioral inhibition, attention, and working memory," *Psychophysiology*, vol. 46, no. 5, pp. 1059–1068, 2009.

[63] A. C. Swann, M. Lijffijt, S. D. Lane et al., "Pre-attentive information processing and impulsivity in bipolar disorder," *Journal of Psychiatric Research*, vol. 47, no. 12, pp. 1917–1924, 2013.

[64] Z. Jafari, B. E. Kolb, and M. H. Mohajerani, "Effect of acute stress on auditory processing: a systematic review of human studies," *Reviews in the Neurosciences*, vol. 28, no. 1, pp. 1–13, 2017.

[65] G. S. Moura, Y. Trinanes-Pego, and M. T. Carrillo-de-la-Pena, "Effects of stimuli intensity and frequency on auditory p50 and n100 sensory gating," in *Brain Inspired Cognitive Systems 2008*, Advances in Experimental Medicine and Biology, vol 657, A. Hussain, I. Aleksander, L. Smith, A. Barros, R. Chrisley, and V. Cutsuridis, Eds., Springer, New York, NY, 2010.

Hindawi
Neural Plasticity
Volume 2020, Article ID 8866386, 8 pages
https://doi.org/10.1155/2020/8866386

Review Article

From Uncertainty to Anxiety: How Uncertainty Fuels Anxiety in a Process Mediated by Intolerance of Uncertainty

Yuanyuan Gu, Simeng Gu, Yi Lei, and Hong Li

Institute for Brain and Psychological Sciences, Sichuan Normal University, Chengdu 610066, China

Correspondence should be addressed to Yi Lei; leiyi821@vip.sina.com

Received 29 April 2020; Revised 16 September 2020; Accepted 10 November 2020; Published 23 November 2020

Academic Editor: Fang Pan

Uncertainty about future events may lead to worry, anxiety, even inability to function. The highly related concept—intolerance of uncertainty (IU)—emerged in the early 1990s, which is further developed into a transdiagnostic risk factor in multiple forms of anxiety disorders. Interests in uncertainty and intolerance of uncertainty have rapidly increased in recent years; little is known about the construct and phenomenology of uncertainty and IU and the association between them. In an attempt to reveal the nature of two concepts, we reviewed broad literature surrounding uncertainty and intolerance of uncertainty (IU). We followed the process in which the whole IU theory developed and extended, including two aspects: (1) from uncertainty to intolerance of uncertainty and (2) definition of uncertainty and intolerance of uncertainty, and further concluded uncertainty fuels to negative emotions, biased expectancy, and inflexible response. Secondly, this paper summarized the experimental research concerning uncertainty and IU, consisted of three parts: (1) uncertainty-based research, (2) measurements of IU, and (3) domain-specific IU. Lastly, we pointed out what remains unknown and needed to be investigated in future research. This result provides a comprehensive overview in this domain, enhancing our understanding of uncertainty and IU and contributing to further theoretical and empirical explorations.

1. Introduction

We live in a world filled with uncertainty. Weather forecast often reports that there is an 80% chance of rain; the possibility never reaches 100%. We cannot be sure about what is going to happen next. What important is how it affects us and how we live and cope with it. Numerous researches have investigated the power of uncertainty, although some of them implicitly include it but did not claim for it. The dictionary definition of uncertainty is "experiencing an unknown" and closely related to unpredictability, ambiguity, unfamiliarity, etc. It is a tremendously hard work to review all the research concerning uncertainty and come to a common conclusion due to the broad definition and confusion between similar concepts. Additionally, some of them are often used interchangeably under certain circumstances ([1]). Here, we narrow down the field by arbitrarily defining the concept of uncertainty which only refers to different contingencies between environmental events in this review [2]. This leads to a clear cut between uncertainty and other similar concepts, such as ambiguity which results from features perceived as equivocal or perceived with insufficient knowledge for a singular definitive interpretation (e.g., figure/ground images like the Rubin vase; apophenia) [3]. Many research use unpredictability to describe stimulus contingencies, whose connotation is consistent with uncertainty according to our definition, allowing us to be as inclusive as possible and regard those two concepts as the same in terms of uncertainty studies. Consequently, studies that are regarding the specific aspect of uncertainty will be subjected to review no matter what particular word they use.

There is an increasing research interest in intolerance of uncertainty and its role in emotional disorders, which broadly refers to response to uncertainty in cognitive, emotional, and behavioral levels [4]. Existing literatures surrounding IU confirm that IU is a key construct in anxiety and worry, but little is known about its exact nature [5]. This paper traces IU definition back to the fundamental

component which is uncertainty, attempting to clarify our understanding of both uncertainty and IU. In line with this thought, there are multiple dimensions of uncertainty, for example, (1) whether an environmental event will occur at all, (2) what kind of environmental event will occur, negative, neutral, or positive, and (3) when will an environmental event occur. So this paper mainly focuses on future-orientated uncertainty and IU construct, hoping to bring insight into uncertainty-related domain.

2. Theoretical Foundation of IU

2.1. From Uncertainty to IU. Many studies have historically demonstrated that uncertainty as a common feature in threat context may elicit fear and anxiety. The idea of "intolerance of uncertainty" emerges from anxiety-related studies; the key component of which was originally identified as fear of the unknown. Psychologists defined fear of the unknown as "an individual's propensity to experience fear caused by the perceived absence of information at any level of consciousness or point of processing" [6]. This fundamental fear is the basic cognitive process underlying all anxiety disorders [7], but different from emotional experience caused by anxiety. Fear is present-oriented and relatively certain while anxiety is future-oriented and relatively uncertain. Uncertainty is a central feature in the conceptual model of fear, which leads to anxiety and worry.

Decades of studies concerning uncertainty lay the foundation of intolerance of uncertainty construct. Unlike unpredictability and uncontrollability, uncertainty is a more diverse and inclusive concept which refers to any forms of unknown and can be specified in different research domains. Prior to the publication of IU construct, responses to uncertainty have been observed in fear, anxiety, and worry. Researchers observed that different emotional responses are affected by the degree of perceived uncertainty: fear is associated with less uncertain future threat while anxiety is related to more uncertain future threat [8]. Also affected by uncertainty are behaviors under environment with no explicit instructions. Intolerant response is a general description and identical feature of these phenomenological experiences in uncertainty-based studies which further conceptualized as IU construct.

2.2. Definition of Intolerance of Uncertainty. In 1994, Freeston et al. defined IU as "cognitive, emotional, and behavioral reactions to uncertainty in everyday life situations." Based on this, researchers revised the definition of IU to clarify its nature, such as adding perception process, and features of uncertain situations [9]. These early definitions sought to include the overall influence of uncertainty, but recent trends are more focused on the cognitive level. Carleton et al. [10] emphasized that individuals high in IU would find possible future negative events unacceptable and threatening regardless of the probability of its occurrence. There is a very similar concept existing prior to IU referred to as "intolerance of ambiguity" [11]. It is necessary to differentiate those two construct, but the distinction between them was very obscure until Krohne [12] proposed that ambiguity of a situation is determined by its unpredictability, complexity, and insolubility. And he further suggested that ambiguity leads to uncertainty, which implies the consistency between them. The definition of intolerance of ambiguity also semantic overlaps with IU which refers to the tendency to perceive ambiguous situations as sources of threat [13].

It is premature to conclude that intolerance of uncertainty is an independent factor underlying high order construct due to the broad and inconsistent definition. The definition, at its core, is about the negative influence brought by uncertainty, such as fear, anxiety, and behavioral inhibition. Previous research shows that intolerance of uncertainty is highly associated with worry in clinical and nonclinical populations. According to the comprehensive definition of worry, it is rooted in thoughts that uncertain future events are negative accompanied by the feeling of anxiety [14]. Definitions of IU and worry demonstrate the fact that worry and IU share many common features regarding future uncertainty and uncertainty-induced maladaptive responses. Noticing that pathological worry is the hallmark of generalized anxiety disorder, it is not surprising that IU can distinguish participants with generalized anxiety disorder (GAD) from healthy controls. Researchers investigated the specificity of the relationship between IU and worry and found that IU was highly related to worry than to obsessions/compulsion and panic sensations ([15]). Does this close association reflect the nature of IU or just confusion in definitions? The definition of IU, at its core, is about the negative influence brought by uncertainty, such as fear, anxiety, and behavioral inhibition. To clear this confusion, researchers in this domain need to extend the conceptual construct from the originator of IU rather than empirical observations.

3. Experimental Research

3.1. Uncertainty-Based Research. Uncertainty regarding future events is inherently implicated in anxiety and worry due to its impact on our emotional state. It has been proposed that anxiety originates from excessive fear overgeneralization which "is quite likely that the summed frequency and intensity of the fear responses of any given individual to clear and imminent physical or psychological threat … would lag far behind the summed amount of fear in response to the anticipation of such events and the myriad anxious "what if …" mental representations of possible future events that are common in daily life" [8]. As pointed out, possible future events may induce the abuse of the associate learning. There is uncertainty in the fear learning and generalizing process all the way through, but the role uncertainty plays in this process is complicated. Reinforcement rate, which has been thoroughly investigated in reinforcement learning studies, can be identified as one of the uncertainty characteristics that we discussed here: whether reinforcement will occur at all. Uncertain condition in which reinforcement rate is between 100% and 0 has different reaction patterns [16].

Uncertainty about a future event may disrupt the anticipatory process which is the key component of adaptive cognitive responses, leading to overestimation of the threat possibility and severity. Former research used fear

conditioning paradigm to investigate expectancy for unconditioned stimulus in an unpredictable context and found that unpredictability induced contextual fear and chronic expectation of potential threats. Participants showed elevated US expectancy in unpredictable context compared to predictable context and sustained expectancy when unpredictable shock is over [17]. Grupe and Nitschke [18] also found evidence to further support this conclusion by using NPU test paradigm which consisted of certain aversive picture, certain neutral picture, and uncertain picture. Self-report data revealed biased expectancies of aversion following uncertain cues, suggesting that participants tend to expect negative events while tolerating uncertain cues. These findings can be interpreted into uncertainty-induced expectancy bias and disrupted anticipatory process. But this association is only observed between threat-related cues and aversive outcomes, neither between threat-irrelevant cues and aversive outcomes nor threat-related cues and neutral outcomes [19–21]. Anticipation or expectation of future events is a very important notion in the domain development and sustenance of anxiety. From an evolutionary and adaptive perspective, it is beneficial for individuals to show hypervigilance to uncertainty and always prepare for the negative outcome.

In addition, expectancy bias as a cognitive factor is also influenced by other coexisting cognitive factors, such as increased selective attention, disrupted sensory processing, and inadequate emotion regulation. The idea that unpredictable future events need more selective attention to make accurate predictions and search for strategies seems to make intuitive sense. A recent study confirmed that uncertainty appeared to enhance the attention allocation in both early and late cognitive processes. Specifically, defensive response concerning uncertainty and prediction errors elicited different attentional dynamics in which participants received unexpected stimulus [22]. In line with this notion, there are other covariation biases regarding uncertainty; that is, uncertainty-related anxiety disrupts sensory processing and impairs the ability to assess stimulus contingencies. For instance, the so-called "illusory correlation" is describing that individual subjectively associate cues indicating potential threat with subsequent outcomes under unrelated circumstances ([18, 23]). It should be pointed out that these factors mentioned above are highly associated and effect cognitive process in different processing stages. Future studies need to clarify the cognitive mechanism of uncertainty processing and disentangle these factors.

Previous researches have showed that uncertainty may affect the acquisition and evaluation process of the predictive properties of uncertain environmental event. Lin et al. [24] conducted a ERP study using classic experimental paradigm called S1-S2 paradigm in which S1 (e.g., a question mark "?" stands for uncertain valence) are cues about certain or uncertain emotional valence of an upcoming event (S2) (e.g., a positive picture) ([25–27]). Results implicated that uncertain cues elicited larger N2 than the certain cues did about both future positive and negative pictures and produced smaller early contingent negative variation (CNV) than did the certain cues about future negative pictures. The results suggest that different attention and anticipation process occurs at the early cognitive processing stages of uncertainty ([24, 28]). What is more, Dieterich et al. [22] used similar paradigm and found that uncertain cues elicited increased P2 and LPP compared to certain cues. It is conceivable that predictable and unpredictable cues have different brain response pattern and uncertainty appears to increase the engagement of early phasic and sustained attention for uncertain events. Taken together, this finding was consistent with previous studies proving uncertainty is associated with biased expectancies and heightened response to aversive stimulus [18, 29, 30]; it also successfully detected uncertainty's modulation on response to positive events. Former studies using similar paradigm failed to find or have sufficient statistical power to detect the analogous effect of uncertainty on response to neutral and positive events ([18]).

Meanwhile, there is also evidence from NPU-threat test which is a developed form of S1-S2 paradigm and consists of three conditions: (1) N condition: no threat; (2) P condition: predictable threat; (3) U condition: unpredictable threat, demonstrating that the modulation effect of uncertainty may be specific to negative events [21]. The most studied predictability in NPU-threat test is temporal and valence predictability which is making the future event onset time and valence predictable. Parisi et al., [31] found that the impact of temporal uncertainty on startle magnitude is not evident for positive or neutral pictures and did not vary as a function of the emotional valence. One plausible explanation for the divergence is that temporary uncertainty and valence uncertainty may be inherently different and have different modulation patterns. Moreover, an individual may have different psychological magnitudes of impending positive and negative events. Notably, the effect of valence uncertainty appears to be consistent giving thought that participants' response to negative stimulus is generally more evident than to neutral and positive stimulus in experiments using NPU paradigm. That leads to one assumption which is uncertainty is specific to aversive events, even uncertainty itself is considered aversive or negative. Further explanation is that negative events might be more arousing and capture more attention relative to positive events such as scary pictures. In addition, an individual is more sensitive to negative events after controlling the effect of arousal level.

Another perspective is that uncertainty impairs our ability to prepare for and response to future events, thus contributing to anxiety, worry, and even fear ([1]). Regardless what kind of external event will occur, the uncertain waiting process before it finally onset contributes to the feeling of distress and worry. Uncertainty is threatening and dangerous, so we have to avoid them and be sure about something likely to happen. Even though we do not know what will happen or whether the worst results that we assume may or may not happen, we just find it hard to tolerate uncertainty and those negative feelings brought by it ([18]). Existing literatures already confirm that faster response can be achieved in a less uncertain condition. Take timing tasks as an example which includes temporal uncertainty; behavioral results showed that reaction time was significantly shorter in cued condition in which a cue signaled the exact onset time of stimulus and allowed participant to make temporal orientation than in an

uncued condition where no cue was provided even though the accuracy was controlled. In addition, accuracy in both conditions was very high; both cued and uncued conditions were very high and showed no difference; one possible explanation was the ceiling effect [32]. At the same time evaluating the elapsed time to anticipate the onset time of forthcoming event, researchers use different approaches to decrease uncertainty during this period, such as providing certain cues to inform participants the exact onset time of stimulus. Certain cues can be divided into implicit (e.g., temporal template) and explicit cues (sensory cues which signal the onset time of stimulus) [33]; both implicit and explicit cues help participants to decrease the perceived uncertainty. Results indicate that decreasing uncertainty can speed up reaction; in another word, increasing uncertainty leads to behavioral inhibition demonstrated by disrupting and slowing down the planned action.

3.2. Measurements of IU. The 27-item Intolerance of Uncertainty Scale is the very first scale to measure IU which is developed on the basis of clinical observations [4]. It is empirical and largely based on descriptive statements which are extending the understanding of the broad definition by using a 5-point Likert scale ranging from 1 to 5. Despite this, IUS showed a highly consisted validity in psychometric testing. It has excellent internal consistency (0.91) and good discriminant and convergent validity and shows good performance as a criterion to distinguish participants with nonclinical GAD from healthy controls [4]. Although the theoretical foundation of IUS is not very solid and we do not know what it exactly measures, it has a face valid construct and has been replicated by latter researchers. Studies use IUS as a standard measurement to obtain the score of IU and distinguish high and low IU groups in their experiments [34, 35] or to investigate the association between IU and multiple emotion disorders and many other factors [36–39].

A large body of research conducts factor analysis of IUS in order to clarify the nature of this construct due to the confounding statement terms which seem similar to terms in trait and state anxiety scale. Birrell et al. [5] carried out an inclusive review regarding factor analyses of IUS and found that there may be two factors that are consistent throughout exploratory factor analyses. These two factors were consistently found to group together across different studies and samples. Therefore, it is necessary to test this two-factor structure of IU using different forms of scale and establish a clear and stable construct for future research. In addition, Carleton et al., [10] tested the fit of unitary-, four-, and five-factor model for 27-item IUS, and results showed that none of these models demonstrated adequate fit. The researchers also found a high-level redundancy within the scale due to the semantic overlap between items. Although the number of factors remains inconsistent in confirmatory factor analyses, a two-factor structure is preferred and supported by many studies which can be described as "unacceptability and avoidance of uncertainty" and "uncertainty leading to the inability to act" [4, 40]. Recent evidence suggests 2 factors can be interpreted into prospective factor (P-IU) and inhibitory factor (I-IU), and P-IU and I-IU are found to be associated with excessive and inflexible avoidance behavior [41] and processing uncertain errors [42]. While P-IU is identical to anxiety disorders characterized by expectancy bias [43] and increased emotional response, I-IU is specifically related to panic disorder and social anxiety [36].

Great efforts have been made to propose different versions of the original 27-item IUS to promote the understanding and application of IU construct. The short form of IUS has 12 items and identically high internal consistencies with two-factor model with less redundancy. It also has excellent convergent validity with the original and been tested repeatedly in clinical and nonclinical samples [44]. The modified version for children gains increased research interest which is adapted from the adult version. Different from adult IU, child IU may be related to more internalizing problems ([45]). Cornacchio et al. [46] performed a study on IUS for children to date its factor construct and found that IUSC shared 2-factor model with IUS-12. But it is too soon to conclude that the prospective/inhibitory model is the general construct underlying all items due to the inconsistent findings in factor analysis studies, and there may be a more ideal construct to conceptualize IU definition.

3.3. Domain-Specific IU. Considerable amount of research have provided evidence that IU is a transdiagnostic dispositional risk factor for the development and maintenance of clinically significant anxiety [3]. Increasing findings demonstrate that IU is associated with a broad range of emotional disorders and other cognitive vulnerability factors, highlighting the theoretical and therapeutic importance of IU [47–49]. Recent researchers argue that disorder-specific IU is more strongly related to disorder symptoms than general IU trait [50]. Dugas et al. investigated the relationship between IU and worry in a nonclinical sample and found that IU was highly related to worry, moderately related to obsessions/compulsions, and weakly related to panic sensations. This pattern revealed that IU is specific to worry since IU was more highly correlated with worry relative to obsessions/compulsions and panic sensation ([15]). Several studies adopted different questionnaires and analytical method to examine the specificity of IU to particular psychological disorders in clinical and nonclinical samples. Evidence was found for the strong association between IU and GAD or OCD symptoms. However, researchers argued that IU got specific association with OCD demonstrated by the strongest association between IU and OCD than that between worry and GAD. Further, individuals with analogue GAD or OCD reported more intolerance of uncertainty than controls, but they did not differ significantly from each other ([47, 51]). To enhance the knowledge on the generality and specificity of IU, Paul et al. also conducted regression analyses among IU and symptom levels of GAD, social anxiety, OCD, and depression. They found that IU explained a significant amount of variance in social anxiety severity when controlling for established cognitive correlates of social anxiety (e.g., fear of negative evaluation) and for neuroticism. In addition, IU appeared to be associated with symptom levels of GAD, OCD, and social anxiety, but not depression, when

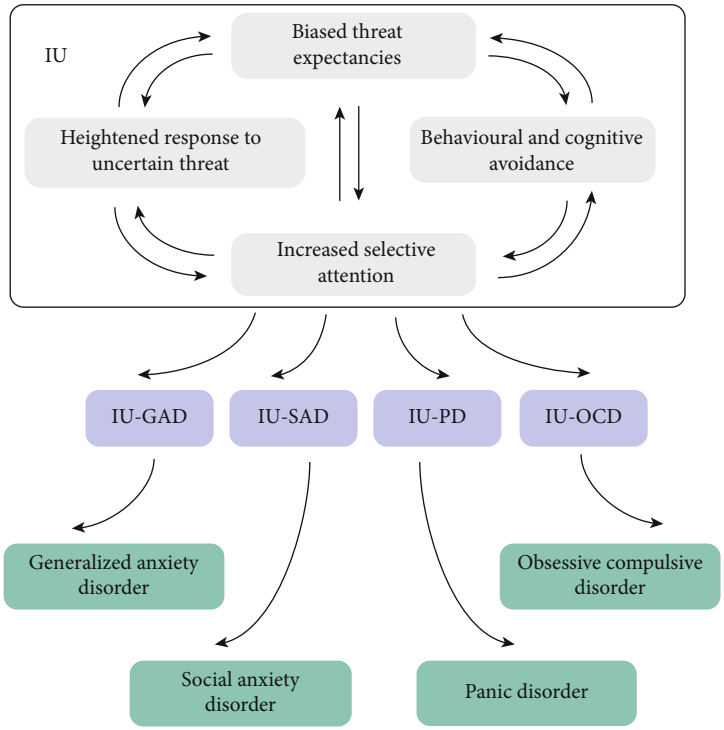

Figure 1: This figure demonstrates the cognitive model of IU across anxiety disorders raised by us. The IU construct consists of multiple factors and the interaction between them. In a process shown in the figure, different combinations.

controlling the share variance among these symptoms [52]. Taken together, we illustrated the complex association of IU and the process from IU to anxiety disorders (shown in Figure 1).

Dugas et al.'s model of GAD illustrates that IU features in the cognitive process where GAD patients receive the mood state and life event inputs and reaction to uncertainty under everyday life situation. There are other cognitive factors in this model coexisting and associated with IU, such as "poor problem orientation" and "cognitive avoidance." The question of how exactly are individuals with GAD influenced by these factors needs more clarification due to complicated mechanism. Recent studies use a hierarchical model to evaluate the unique contribution of IU in anxiety-related pathology. Direct and indirect effects between IU and symptoms are observed through disorder-specific and multiple cognitive vulnerabilities. This model suggests that IU may be a more primary predictor of multiple disorder symptoms than the next-level cognitive factors [53, 54]. In clinical perspective and for potential treatment purpose, IU can be divided into different disorder-specific ingredients which account for most of the difference between relative emotional disorders. Consist of results of factor analysis, it also can be represented as having two dimensions since it mainly causes two kinds of response—prospective response and inhibitory response known as prospective IU (i.e., the cognitively focused dimension of IU; e.g., unforeseen events upset me greatly) and inhibitory IU (i.e., the behaviorally focused dimension of IU; e.g., the smallest doubt can stop me from acting). Likewise, IU is an underlying feature of several emotional disorders, and different dimensions comprise the respective factors which account for different anxiety disorder symptoms [43].

4. Directions for Future Research

Many years of studies yield substantial evidence for the effects of uncertainty and IU construct. The current paper was set up to review the rich body of research concerning this special issue and inspire future researchers. We have to point out that there is relative paucity and unsolved questions in some research domain. Firstly, according to current theories on emotion and motivation, anticipation of emotionally salient stimuli impacts motivational states regardless of valence. It can be proposed that uncertainty during anticipation of upcoming positive events also affects motivation states and response. Uncertainty's duration is rather short which is between cue onset time and the outcome onset time. Once outcome occurs, the mystery is resolved and uncertainty no longer exists. Uncertainty may directly or indirectly mediate the relationship between anticipation and motivation states, and future experimental researches are needed to clarify uncertainty's multiple effects. It remains controversial whether uncertainty serves a role as "fire alarm" which biased the emotional experience towards negative regardless of the actual valence of future events [55]. Or on the contrary, uncertainty could heighten response to negative events while dampening response to positive events.

Secondly, increasing laboratorial studies shed light on temporal uncertainty-related design which generally used cues to provide temporal information for participants. There are mainly two different task types: exogenous-based and

endogenous-based tasks. The former relies on the external cues which have temporal predictive properties to inform the occurrence of stimulus, whereas the latter relies on participants' temporal conception to estimate the stimulus onset time due to the lack of explicit signal. Furthermore, there seems to be a paradox in experiments which manipulate uncertainty by providing an extra signal since signal itself is the opposite of uncertainty. For comparison, signal in control condition does not provide predictive information or does not occur while it does in experimental condition. In fact, invalid signal still alerts participants to uncertainty.

Thirdly, none of the theoretical models of IU construct shows good fit factor analysis research. There are complex associations between cognitive vulnerabilities and overlapping transdiagnostic factors. But the specific process and underlying mechanism are still in a black box. Does IU construct interact with and predict other constructs? More models should be tested by future researchers to explore the determinate factors in IU construct. Last but not least, it is still unclear what role IU plays in the treatment of anxiety disorder, whether trait IU changes or disorder-specific IU changes after the therapy. Researchers need to investigate the mechanisms of such changes across different treatment interventions [56]. Due to the fact that IU is a cognitive bias, exposure treatment may not be sufficient to reduce trait IU. Removing an individual's quest for certainty and safety is not realistic. Changing the negative beliefs about uncertainty and improving coping strategies seem more practical. Generally speaking, clinical applications need to be continuously explored based on cognitive vulnerabilities in the anxiety disorder region.

Data Availability

The original data are available upon request.

Conflicts of Interest

All authors declared that the research was conducted in the absence of any commercial or financial relationships that could be construed as a potential conflict of interest.

Authors' Contributions

Yuanyuan Gu and Simeng Gu are the co-first authors.

Acknowledgments

This work was supported by the National Natural Science Foundation of China (NSFC31571153, 31871130, and 31671150), Guangdong Key Project in "Development of New Tools for Diagnosis and Treatment of Autism" (2018B030335001), Innovative Team Program in Higher Education of Guangdong, China (2015KCXTD009), Major Program of Guangdong, China (2016KZDXM009), Shenzhen Basic Research Scheme (JCYJ20150729104249783), and Shenzhen Peacock Plan (KQTD2015033016104926).

References

[1] D. W. Grupe and J. B. Nitschke, "Uncertainty and anticipation in anxiety: an integrated neurobiological and psychological perspective," *Nature Reviews Neuroscience*, vol. 14, no. 7, pp. 488–501, 2013.

[2] M. E. P. Seligman, S. F. Maier, and R. L. Solomon, "Unpredictable and uncontrollable aversive events," *Aversive Conditioning and Learning*, pp. 347–400, 1971.

[3] R. N. Carleton, M. K. Mulvogue, M. A. Thibodeau, R. E. Mccabe, M. M. Antony, and G. J. Asmundson, "Increasingly certain about uncertainty: intolerance of uncertainty across anxiety and depression," *Journal of Anxiety Disorders*, vol. 26, no. 3, pp. 468–479, 2012.

[4] M. H. Freeston, J. Rhéaume, H. Letarte, M. J. Dugas, and R. Ladouceur, "Why do people worry?," *Personality & Individual Differences*, vol. 17, no. 6, pp. 791–802, 1994.

[5] J. Birrell, K. Meares, A. Wilkinson, and M. Freeston, "Toward a definition of intolerance of uncertainty: a review of factor analytical studies of the Intolerance of Uncertainty Scale," *Clinical Psychology Review*, vol. 31, no. 7, pp. 1198–1208, 2011.

[6] R. N. Carleton, "Into the unknown: a review and synthesis of contemporary models involving uncertainty," *Journal of Anxiety Disorders*, vol. 39, pp. 30–43, 2016.

[7] D. H. Barlow, "Unraveling the mysteries of anxiety and its disorders from the perspective of emotion theory," *American Psychologist*, vol. 55, no. 11, pp. 1247–1263, 2000.

[8] J. B. Rosen and J. Schulkin, "From normal fear to pathological anxiety," *Psychological Review*, vol. 105, no. 2, pp. 325–350, 1998.

[9] R. Ladouceur, P. Gosselin, and M. J. Dugas, "Experimental manipulation of intolerance of uncertainty: a study of a theoretical model of worry," *Behaviour Research and Therapy*, vol. 38, no. 9, pp. 933–941, 2000.

[10] R. N. Carleton, D. Sharpe, and G. J. G. Asmundson, "Anxiety sensitivity and intolerance of uncertainty: requisites of the fundamental fears?," *Behaviour Research and Therapy*, vol. 45, no. 10, pp. 2307–2316, 2007.

[11] S. Budner, "Intolerance of ambiguity as a personality variable," *Journal of Personality*, vol. 30, no. 1, pp. 29–50, 1962.

[12] H. W. Krohne, "Vigilance and cognitive avoidance as concepts in coping research," in *Attention and Avoidance*, H. W. Krohne, Ed., Hogrefe & Huber, Toronto, 1993.

[13] S. Grenier, A. M. Barrette, and R. Ladouceur, "Intolerance of uncertainty and intolerance of ambiguity: similarities and differences," *Personality & Individual Differences*, vol. 39, no. 3, pp. 593–600, 2005.

[14] A. K. Macleod, "Worry is reasonable: the role of explanations in pessimism about future personal events," *Journal of Abnormal Psychology*, vol. 100, no. 4, pp. 478–486, 1991.

[15] M. J. Dugas, P. Gosselin, and R. Ladouceur, "Intolerance of uncertainty and worry: investigating specificity in a nonclinical sample," *Cognitive Therapy & Research*, vol. 25, no. 5, pp. 551–558, 2001.

[16] J. A. Harris and J. S. Carpenter, "Response rate and reinforcement rate in Pavlovian conditioning," *Journal of Experimental Psychology: Animal Behavior Processes*, vol. 37, no. 4, pp. 375–384, 2011.

[17] D. Vansteenwegen, C. Iberico, B. Vervliet, V. Marescau, and D. Hermans, "Contextual fear induced by unpredictability in a human fear conditioning preparation is related to the

chronic expectation of a threatening US," *Biological Psychology*, vol. 77, no. 1, pp. 39–46, 2008.

[18] D. W. Grupe and J. B. Nitschke, "Uncertainty is associated with biased expectancies and heightened responses to aversion," *Emotion*, vol. 11, no. 2, pp. 413–424, 2011.

[19] C. Grillon, S. Lissek, S. Rabin, D. Mcdowell, S. Dvir, and D. S. Pine, "Increased anxiety during anticipation of unpredictable but not predictable aversive stimuli as a psychophysiologic marker of panic disorder," *American Journal of Psychiatry*, vol. 165, no. 7, pp. 898–904, 2008.

[20] C. Grillon, K. O'Connell, L. Lieberman et al., "Distinct responses to predictable and unpredictable threat in anxiety pathologies: effect of panic attack," *Biological Psychiatry Cognitive Neuroscience & Neuroimaging*, vol. 2, no. 7, pp. 575–581, 2017.

[21] A. Schmitz and C. Grillon, "Assessing fear and anxiety in humans using the threat of predictable and unpredictable aversive events (the NPU-threat test)," *Nature Protocols*, vol. 7, no. 3, pp. 527–532, 2012.

[22] R. Dieterich, T. Endrass, and N. Kathmann, "Uncertainty is associated with increased selective attention and sustained stimulus processing," *Cognitive, Affective, & Behavioral Neuroscience*, vol. 16, no. 3, pp. 447–456, 2016.

[23] J. Wiemer, A. Mühlberger, and P. Pauli, "Illusory correlations between neutral and aversive stimuli can be induced by outcome aversiveness," *Cognition & Emotion*, vol. 28, no. 2, pp. 193–207, 2014.

[24] H. Lin, H. Gao, J. You et al., "Larger N2 and smaller early contingent negative variation during the processing of uncertainty about future emotional events," *International Journal of Psychophysiology*, vol. 94, no. 3, pp. 292–297, 2014.

[25] K. Onoda, Y. Okamoto, K. Shishida et al., "Anticipation of affective image modulates visual evoked magnetic fields (VEF)," *Experimental Brain Research*, vol. 175, no. 3, pp. 536–543, 2006.

[26] K. Onoda, Y. Okamoto, K. Shishida et al., "Anticipation of affective images and event-related desynchronization (ERD) of alpha activity: an MEG study," *Brain Research*, vol. 1151, no. 3, pp. 134–141, 2007.

[27] K. Onoda, Y. Okamoto, S. Toki et al., "Anterior cingulate cortex modulates preparatory activation during certain anticipation of negative picture," *Neuropsychologia*, vol. 46, no. 1, pp. 102–110, 2008.

[28] H. Lin, J. Xiang, S. Li et al., "Cued uncertainty modulates later recognition of emotional pictures: an ERP study," *International Journal of Psychophysiology*, vol. 116, pp. 68–76, 2017.

[29] S. M. Gorka, L. Lieberman, K. L. Phan, and S. A. Shankman, "Association between problematic alcohol use and reactivity to uncertain threat in two independent samples," *Drug & Alcohol Dependence*, vol. 164, pp. 89–96, 2016.

[30] B. D. Nelson, G. Hajcak, and S. A. Shankman, "Event-related potentials to acoustic startle probes during the anticipation of predictable and unpredictable threat," *Psychophysiology*, vol. 52, no. 7, pp. 887–894, 2015.

[31] E. A. Parisi, G. Hajcak, E. Aneziris, and B. D. Nelson, "Effects of anticipated emotional category and temporal predictability on the startle reflex," *International Journal of Psychophysiology*, vol. 119, pp. 67–72, 2017.

[32] M. Berchicci, G. Lucci, D. Spinelli, and F. D. Russo, "Stimulus onset predictability modulates proactive action control in a go/no-go task," *Frontiers in Behavioral Neuroscience*, vol. 9, p. 101, 2015.

[33] J. Coull and A. Nobre, "Dissociating explicit timing from temporal expectation with fMRI," *Current Opinion in Neurobiology*, vol. 18, no. 2, pp. 137–144, 2008.

[34] M. Jayne, M. Birthe, and C. M. van Reekum, "What is going on around here? Intolerance of uncertainty predicts threat generalization," *PLoS One*, vol. 11, no. 5, article e0154494, 2016.

[35] J. Morriss, A. Christakou, and C. M. van Reekum, "Intolerance of uncertainty predicts fear extinction in amygdala-ventromedial prefrontal cortical circuitry," *Biology of Mood & Anxiety Disorders*, vol. 5, no. 1, p. 4, 2015.

[36] R. N. Carleton, S. Duranceau, M. H. Freeston, P. A. Boelen, R. E. Mccabe, and M. M. Antony, ""But it might be a heart attack": intolerance of uncertainty and panic disorder symptoms," *Journal of Anxiety Disorders*, vol. 28, no. 5, pp. 463–470, 2014.

[37] T. A. Fergus and W. C. Rowatt, "Intolerance of uncertainty and personality: experiential permeability is associated with difficulties tolerating uncertainty," *Personality & Individual Differences*, vol. 58, no. 2, pp. 128–131, 2014.

[38] S. E. Whiting, W. S. Jenkins, A. C. May, B. M. Rudy, T. E. Davis III, and E. T. Reuther, "The role of intolerance of uncertainty in social anxiety subtypes," *Journal of Clinical Psychology*, vol. 70, no. 3, pp. 260–272, 2014.

[39] C. J. Wright, G. I. Clark, A. J. Rock, and W. L. Coventry, "Intolerance of uncertainty mediates the relationship between adult attachment and worry," *Personality & Individual Differences*, vol. 112, pp. 97–102, 2017.

[40] K. Buhr and M. J. Dugas, "The intolerance of uncertainty scale: psychometric properties of the English version," *Behaviour Research and Therapy*, vol. 40, no. 8, pp. 931–945, 2002.

[41] A. Flores, F. J. López, B. Vervliet, and P. L. Cobos, "Intolerance of uncertainty as a vulnerability factor for excessive and inflexible avoidance behavior," *Behaviour Research and Therapy*, vol. 104, pp. 34–43, 2018.

[42] F. Jackson, B. D. Nelson, and G. Hajcak, "The uncertainty of errors: intolerance of uncertainty is associated with error-related brain activity," *Biological Psychology*, vol. 113, pp. 52–58, 2016.

[43] P. M. McEvoy and A. E. J. Mahoney, "Achieving certainty about the structure of intolerance of uncertainty in a treatment-seeking sample with anxiety and depression," *Journal of Anxiety Disorders*, vol. 25, no. 1, pp. 112–122, 2011.

[44] N. G. Khawaja and L. N. H. Yu, "A comparison of the 27-item and 12-item intolerance of uncertainty scales," *Clinical Psychologist*, vol. 14, no. 3, pp. 97–106, 2010.

[45] M. J. Dugas, N. Laugesen, and W. M. Bukowski, "Intolerance of uncertainty, fear of anxiety, and adolescent worry," *Journal of Abnormal Child Psychology*, vol. 40, no. 6, pp. 863–870, 2012.

[46] D. Cornacchio, A. L. Sanchez, S. Coxe et al., "Factor structure of the intolerance of uncertainty scale for children," *Journal of Anxiety Disorders*, vol. 53, pp. 100–107, 2018.

[47] R. M. Holaway, R. G. Heimberg, and M. E. Coles, "A comparison of intolerance of uncertainty in analogue obsessive-compulsive disorder and generalized anxiety disorder," *Journal of Anxiety Disorders*, vol. 20, no. 2, pp. 158–174, 2006.

[48] M. E. Oglesby and N. B. Schmidt, "The role of threat level and intolerance of uncertainty (IU) in anxiety: an experimental test

of IU theory," *Behavior Therapy*, vol. 48, no. 4, pp. 427–434, 2017.

[49] E. S. Stevens, A. Weinberg, B. D. Nelson, E. E. E. Meissel, and S. A. Shankman, "The effect of panic disorder versus anxiety sensitivity on event-related potentials during anticipation of threat," *Journal of Anxiety Disorders*, vol. 54, pp. 1–10, 2018.

[50] A. E. Mahoney and P. M. Mcevoy, "Trait versus situation-specific intolerance of uncertainty in a clinical sample with anxiety and depressive disorders," *Cognitive Behaviour Therapy*, vol. 41, no. 1, pp. 26–39, 2012.

[51] M. J. Dugas, A. Marchand, and R. Ladouceur, "Further validation of a cognitive-behavioral model of generalized anxiety disorder: diagnostic and symptom specificity," *Journal of Anxiety Disorders*, vol. 19, no. 3, pp. 329–343, 2005.

[52] P. A. Boelen and A. Reijntjes, "Intolerance of uncertainty and social anxiety," *Journal of Anxiety Disorders*, vol. 23, no. 1, pp. 130–135, 2009.

[53] N. P. Allan, D. Cooper, M. E. Oglesby, N. A. Short, K. G. Saulnier, and N. B. Schmidt, "Lower-order anxiety sensitivity and intolerance of uncertainty dimensions operate as specific vulnerabilities for social anxiety and depression within a hierarchical model," *Journal of Anxiety Disorders*, vol. 53, pp. 91–99, 2018.

[54] S. Shihata, P. M. Mcevoy, and B. A. Mullan, "Pathways from uncertainty to anxiety: an evaluation of a hierarchical model of trait and disorder-specific intolerance of uncertainty on anxiety disorder symptoms," *Journal of Anxiety Disorders*, vol. 45, pp. 72–79, 2017.

[55] I. Sarinopoulos, D. W. Grupe, K. L. Mackiewicz et al., "Uncertainty during anticipation modulates neural responses to aversion in human insula and amygdala," *Cerebral Cortex*, vol. 20, no. 4, pp. 929–940, 2010.

[56] S. Shihata, P. M. Mcevoy, B. A. Mullan, and R. N. Carleton, "Intolerance of uncertainty in emotional disorders: what uncertainties remain?," *Journal of Anxiety Disorders*, vol. 41, pp. 115–124, 2016.

Hindawi
Neural Plasticity
Volume 2020, Article ID 8886715, 13 pages
https://doi.org/10.1155/2020/8886715

Research Article

Radix Scutellariae Ameliorates Stress-Induced Depressive-Like Behaviors via Protecting Neurons through the TGFβ3-Smad2/3-Nedd9 Signaling Pathway

Fan Zhao,[1] **Chenyiyu Zhang**,[1] **Dong Xiao**,[2] **Weihua Zhang**,[1] **Liping Zhou**,[1] **Simeng Gu**,[3] **and Rong Qu**[1]

[1]*College of Chinese Medicine, College of Integrated Chinese and Western Medicine, Nanjing University of Chinese Medicine, Nanjing 210046, China*
[2]*Jiangsu Collaborative Innovation Center of Chinese Medicinal Resources Industrialization, National and Local Collaborative Engineering Center of Chinese Medicinal Resources Industrialization and Formulae Innovative Medicine, Nanjing University of Chinese Medicine, Nanjing 210046, China*
[3]*Department of Psychology, Jiangsu University Medical School, Zhenjiang 210023, China*

Correspondence should be addressed to Simeng Gu; gsm_2007@126.com and Rong Qu; qurong@163.com

Received 3 May 2020; Revised 29 June 2020; Accepted 31 October 2020; Published 16 November 2020

Academic Editor: Fang Pan

Chronic stress can impair hippocampal neurogenesis, increase neuronal apoptosis, and cause depressive-like behaviors. Our previous studies found that Radix Scutellariae (RS) can rescue the stress-induced neuronal injury, but the mechanism is not clear. Here, we continued to investigate the underlying antidepressant mechanisms of the RS extract. A 7-week chronic unpredictable mild stress (CUMS) procedure was used to establish a murine depression model. 0.75 g/kg or 1.5 g/kg RS was administered daily to the mice during the last 4 weeks. Depressive-like behaviors were evaluated by the sucrose preference test (SPT), forced swimming test (FST), open field test (OFT), and tail suspension test (TST). The neuroprotective effect of RS was evaluated with the expression of hippocampal neuron-related markers and apoptosis-associated proteins by Nissl staining, immunohistochemistry, and western blot. Transforming growth factor-β3 (TGFβ3) pathway-related proteins were detected by western blot. Results showed that RS could ameliorate depressive-like behaviors, increase the expression of the antiapoptotic protein B-cell lymphoma 2 (BCL-2), reduce the expression of the proapoptotic protein BCL-2-associated X (BAX), and increase the number of doublecortin- (DCX-), microtubule-associated protein 2- (MAP2-), and neuronal nucleus- (NeuN-) positive cells in the hippocampus. Moreover, RS could reverse the CUMS-induced decrease of TGFβ3 protein, promote the phosphorylation of SMAD2/3, and increase the expression of downstream NEDD9 protein. These results suggest that RS could exert antidepressant effects via protecting neurons. And the molecular mechanism might be related to the regulation of the TGFβ3-SMAD2/3-NEDD9 pathway.

1. Introduction

Major depressive disorder (MDD) is an affective disorder with a high risk of morbidity and mortality. Depression produces the greatest decrement in health compared with the chronic diseases angina, arthritis, asthma, and diabetes [1], making it one of the most prevalent health-related causes of human suffering [2]. However, the mechanism of depression are far from clear, the most widely accepted theory about the mechanism of depression points to the monoamine neurotransmitters, and the first line of treatment of depression is the monoamine reuptake inhibitors [3]. However, even though there are many achievements in pharmacological and psychological therapies, an estimated 44% of patients do not respond to two consecutive antidepressant therapies and an estimated 33% do not respond to four consecutive antidepressant therapies [4]. Therefore, it is necessary to look for safe and effective drugs to treat MDD.

Radix Scutellariae (RS), one of the components of Xiao-chai-hu-tang (XCHT), is a dry root of the Lamiaceae plants, *Scutellaria baicalensis* Georgi. XCHT is a famous Chinese herbal formula that has been widely used clinically in depressive disorders in China. In addition, XCHT has been shown to significantly ameliorate depressive-like behavior in several animal models of depression by altering the serotoninergic system and neurotrophic factors in the hippocampus [5, 6]. Zhang and collaborators used an orthogonal array design experiment to show that RS, ginseng, and Radix Glycyrrhizae are supposed to be the core in compatibility of XCHT in antidepressant therapy [7]. Furthermore, baicalin (Figure 1), the major polyphenol component of RS, has potent antidepressant effects by upregulating the expression of α-amino-3-hydroxy-5-methyl-4-isoxazolepropionic acid (AMPA) receptors and the suppression of neuronal apoptosis in CUMS-treated rats [8]. Moreover, baicalin can facilitate the differentiation of neural stem/progenitor cells to neurons and stimulate hippocampal neurogenesis in adult rats [9]. These studies suggest that RS has a well-founded antidepressant effect and the therapeutic effect of RS on depression is associated with the regulation of neurogenesis and apoptosis. However, the details underlying the molecular mechanisms are still elusive.

Recent studies have shown that neurogenesis theory is suggested to compensate for the limitations of the monoamine theory in depression [10]. In the adult hippocampus, neurogenesis is functionally related to regulation of the hypothalamic-pituitary-adrenal (HPA) axis, inflammatory processes, cognitive functions, and other aspects that contribute to etiological factors that lead to MDD and promote recovery from MDD [11]. The human transforming growth factor-β (TGFβ) signaling pathway might regulate the proliferation of neuroepithelial stem cells, which leads to enhanced neurogenesis [12]. Using biotin label-based antibody protein chips to detect the expression levels of TGFβ3 in hippocampal tissues, it has been shown that the expression levels of TGFβ3 were decreased in the CUMS model; however, electroacupuncture therapy can improve the depressive-like state via promoting neurogenesis which might be associated with its effect on upregulating TGFβ3 protein level [13]. In addition, TGFβs were shown to inhibit apoptosis, which contribute to their neuroprotective effects [14]. Importantly, it has been reported that RS can regulate the TGFβ signaling pathway [15]. However, the relationship between the regulation of RS on the TGFβ signaling pathway and the antidepressant effect of RS associated with neuroprotection on neurons has not been reported in the literature.

So we assessed the antidepressant effects of the RS extract on behaviors in a CUMS mouse model and explored the underlying mechanism associated with the TGFβ signaling pathway. Furthermore, we used the HPLC fingerprint to detect the main components of RS.

2. Materials and Methods

2.1. Radix Scutellariae Extract and Chemicals. RS was supplied by Nanjing University of Chinese Medicine and prepared as previously described [16]. Extracts of RS were prepared by macerating the dried herb in distilled water for 2 h and then boiling two times (100 g/800 ml for 2 h; 100 g/800 ml for 1 h). The two decoctions were mixed and filtered, then concentrated to water extracts (0.15 g/ml), and stored in a refrigerator. Baicalin, wogonoside, baicalein, and wogonin were purchased from Liangwei Biological Technology Co., Ltd. (Nanjing, China). The purity of each compound was >98%, determined by HPLC analysis. The chemical structures of these reference compounds are shown in Figure 1.

2.2. Animals. Fifty adult male ICR mice, aged 6-7 weeks and weighing 18-22 g, were purchased from the Jiangsu Provincial Experimental Animal Center (Nanjing, China). They were adapted to animal facilities for 1 week before the experiment. The animals were placed under a 12/12 h light/dark cycle (7 am/7 pm) and the prescribed temperature conditions (22 ± 2°C). Food and water were provided free of charge. All animal experiments are conducted in accordance with the National Institutes of Health guidelines (NIH publication no. 80-23, 1996 revision) and in accordance with the PRC laboratory animal care and use regulations.

2.3. Chronic Unpredictable Mild Stress Procedure. The CUMS program is a slight improvement over the published program described by Willner and our previous research [17, 18]. This paradigm is designed to maximize unpredictability, as the application of stressors seems to be random and at different times. The CUMS mice were exposed to stress twice a day, and the CUMS program was applied for seven weeks (Figure 2). All procedures are conducted in isolated rooms adjacent to the house, with minimal animal handling or transportation requirements.

2.4. Drug Administration and Treatment. After the depressive-like behavior was observed in the third week of the CUMS paradigm, therapeutic administration was given daily for 4 weeks. Fluoxetine hydrochloride (Flu) (positive control drug) is produced by Changzhou Siyao Pharmaceutical Co., Ltd. (Changzhou, P.R. China). Flu is dissolved in normal saline. All drugs and the vehicle (0.9% normal saline) were administered in a volume of 10 ml/kg of body mass via intragastric administration between 8:00 am and 10:00 am. The control group ($n = 10$/group) and CUMS group mice received only normal saline, and the CUMS+Flu group (20 mg/kg) and CUMS+RS group (0.75 g/kg and 1.5 g/kg) mice received the related drugs. Behavioral tests were performed 1 hour after the last administration of d49.

2.5. Behavioral Tests. Behavioral tests mainly include the sucrose preference test (SPT), OPT, FST, and TST. The details of the test methods were performed as in the previously published articles [18, 19, 20]. Briefly, the mice were trained to adapt to the sucrose solution for 24 h; then, the SPT lasts for another 24 h. The OPT was carried out in a 40 × 60 × 50 cm black metal shell. The mice were free to explore for 6 minutes, and the number of crossings was recorded for the last 4 minutes. The FST was carried out in a transparent plexiglass container (20 cm high × 14 cm diameter). Each mouse was individually subjected to swimming freely for 6 minutes, and the immobility time was recorded for the last

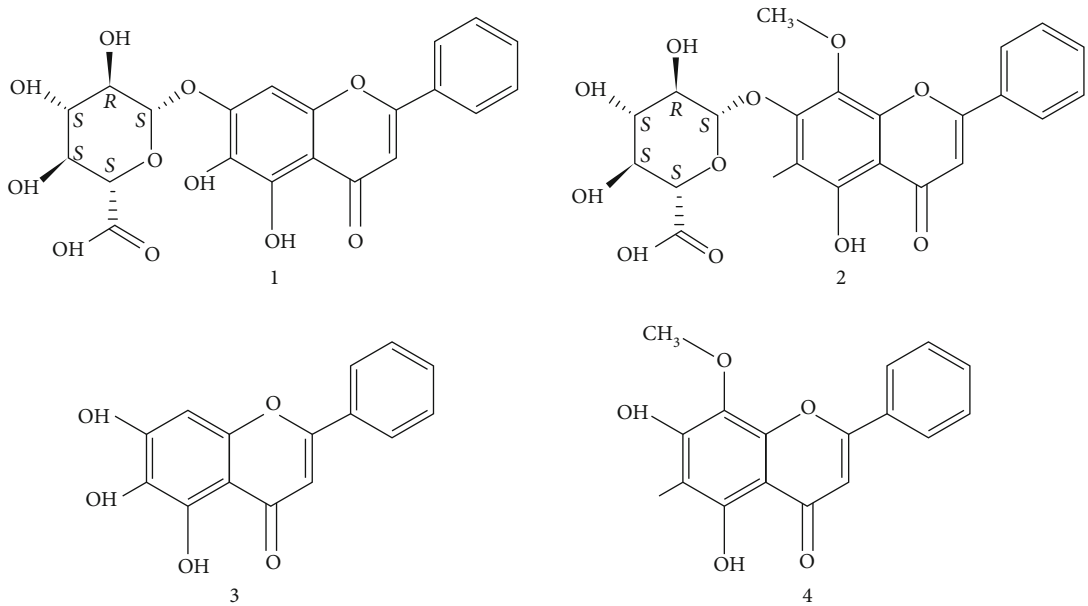

Figure 1: Chemical structures of the 4 identified compounds in RS: baicalin (1), wogonoside (2), baicalein (3), and wogonin (4).

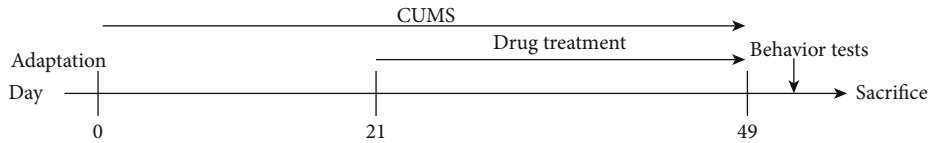

Figure 2: The schematic representation of the experimental procedure.

4 minutes. In the TST, the tail of the mice was fixed 15 cm away from the table for 6 minutes, and the immobility time of the last 4 minutes was recorded.

2.6. Western Blotting. The western blotting method was the same as in our previous publications [18]. On day 50, mice were sacrificed after being deeply anesthetized with sodium pentobarbital (50 mg/kg, i.p.). Brain tissue and hippocampal tissue were rapidly dissected on ice and homogenized. Western blot analysis was performed on three hippocampal tissues from each group. The hippocampal tissue was homogenized with calving tissue buffer ($w : v$ 1 : 5), and the protein concentration was determined according to the manufacturer's instructions using the BCA protein detection kit (Beyotime, Haimen, China). The proteins were run on the SDS-PAGE gel and transferred to a balanced polyvinylidene fluoride (PVDF) membrane (Millipore, Billerica, MA, USA). The main antibodies were anti-HEF1 (ab18056), anti-TGFβ3 (ab15537), anti-Smad2/3 (ab202445), anti-p-Smad2/3 (ab63399), anti-BCL-2 (ab196495), and anti-BAX (sc-20067). After washing, the membrane was incubated with an HRP-conjugated secondary antibody at room temperature for 2 h and developed with an enhanced chemiluminescence (ECL) kit (Millipore, Billerica, MA, USA). ImageJ software was used to analyze the intensity of the blots.

2.7. Immunohistochemistry. Immunohistochemistry was performed as previously reported [21]. The brain was fixed with 10% formalin for 24 hours and embedded in paraffin. Then, the tissue sections were placed in a rotary slicer for immunohistochemical procedures. The brain tissue was cut into 4.5 μm, and the sections containing the hippocampus were incubated with primary antibodies: anti-DCX (ab18723), anti-MAP2 (ab32454), and anti-NeuN (ab177487). After washing with PBS, the sections were incubated with the appropriate secondary antibody. Finally, sections were displayed using 3,3′-diaminobenzidine solution (DAB). The positive expression of target proteins in the dentate gyrus (DG) and cornu ammonis (CA) 1 in the hippocampus was observed under a 10x light microscope. Brown DAB staining was considered positive staining. Then, ImageJ software was used to automatically quantify NeuN-, DCX-, and MAP2-positive cells, and the density of these three positive cells in DG was calculated in three brain sections of each group.

2.8. Nissl Staining. Brain tissues were cut into 4.5 μm in the coronal plane for Nissl staining [22]. The morphological changes in the CA1 region and CA3 region of the hippocampus were observed with a light microscope. The number of positive cells was calculated in three brain sections of each group.

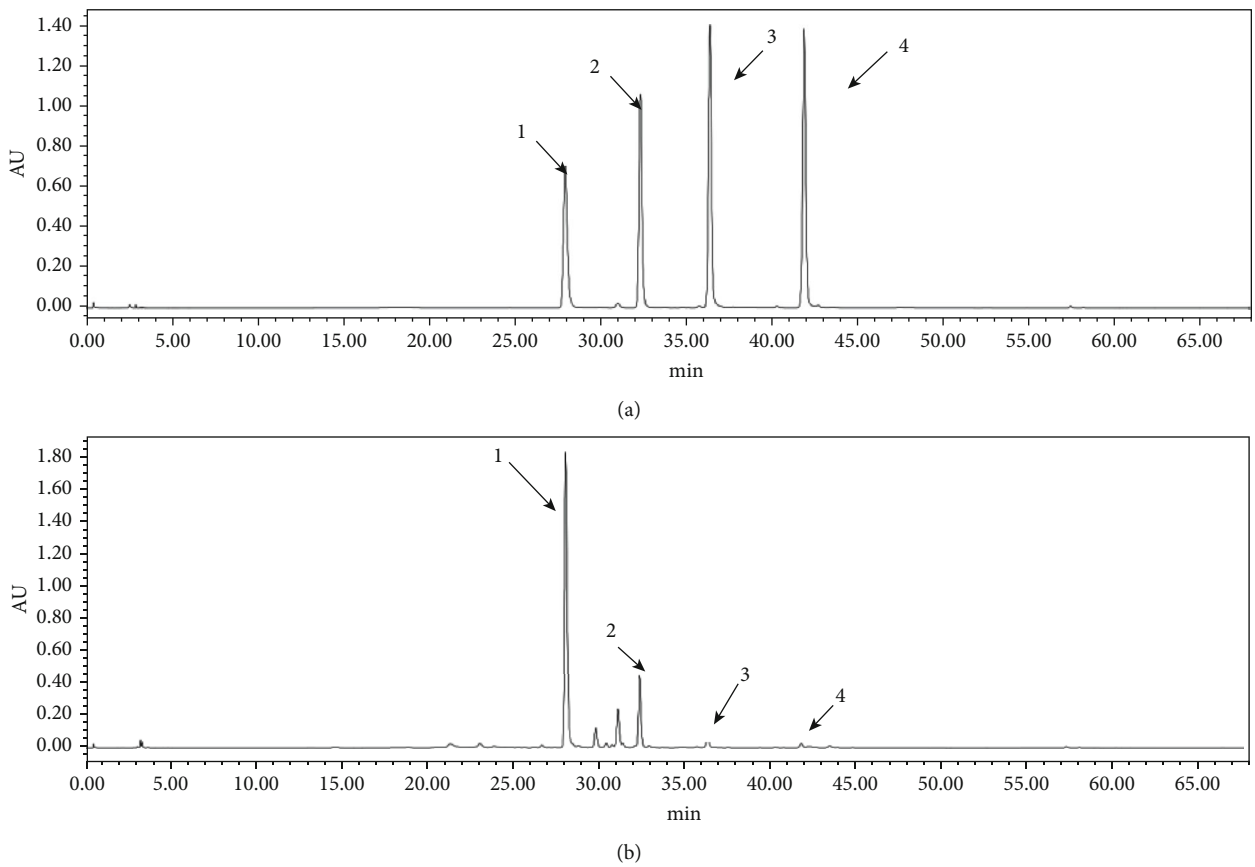

Figure 3: HPLC chromatograms of solution of (a) standards and (b) samples at 274 nm. Peaks: baicalin (1), wogonoside (2), baicalein (3), and wogonin (4).

Table 1: Contents of four compounds in RS.

Analytes*	Contents* of four compounds ($n = 3$) 1	2	3	4
Mean (mg/g)	217.77	42.77	7.14	2.08
SD	1.96	0.38	0.10	0.02

*1: baicalin, 2: wogonoside, 3: baicalein, and 4: wogonin.

2.9. HPLC Analysis and Method Validation. Chromatographic analysis was performed on a Waters 2695 Alliance HPLC system (Waters Corp., Milford, MA, USA) equipped with an Apollo C18 column (250 mm × 4.6 mm, 5 μm). The mobile phase consisted of acetonitrile (A) and 0.1% aqueous formic acid (B). The gradient elution program was as follows: 0-5 min (95% B), 5-50 min (95-50% B), and 50-60 min (50–0% B). The column temperature, flow rate, injection volume, and detection wavelength were set at 30°C, 1.0 ml/min, 10 μl, and 274 nm, respectively. Validation was performed to verify the HPLC methods with pretreatment methods by evaluating the linearity, LOD, LOQ, accuracy, precision, stability, and recovery. Linear calibration curves were established by plotting the peak area (Y) versus the corresponding concentration (X, μg/ml) of baicalin, wogonoside, baicalein, and wogonin, respectively. The correlation coefficients in calibration curves were estimated to examine the linearity. LOD and LOQ at the lowest concentration of calibration standards were calculated with the slope and standard deviation of the analytical response (LOD = 3 σ/S, LOQ = 10 σ/S) [23]. Precision was estimated from the data of intraday and interday tests once a day for three days. After the addition of samples, the stability was observed at 0, 2, 4, 8, 12, 24, and 48 h. Repeatability was confirmed by analyzing six independently prepared solutions of sample RS. The relative standard deviation (RSD%) of the peak area for each marker compound was taken as a measure.

2.10. Statistical Analysis. GraphPad Prism 6.0 software was used for the analysis. Statistical analyses were performed via one-way ANOVA followed by Tukey's test. The significance threshold used was $p < 0.05$. All data were reported as mean ± SEM.

3. Results

3.1. HPLC Analysis of RS and Method Validation. A representative chromatogram of the RS extract along with the chromatogram for the standard compounds is presented in Figure 3. The average proportions of the flavonoids in the extracts of baicalin, wogonoside, baicalein, and wogonin were 217.77 ± 1.96%, 42.77 ± 0.38%, 7.14 ± 0.10%, and 2.08 ± 0.02% (w/w), respectively (Table 1), which is consistent with the results of previous studies [24, 25]. The HPLC method was validated by evaluating the linearity, limit of detection

Table 2: Calibration curve data for four reference compounds ($n = 3$).

Analytes*	Regression equation	R^2	Linear range (μg/ml)	LOD (μg/ml)	LOQ (μg/ml)
1	$Y = 32527X - 17514$	$R^2 = 0.9993$	0.84-84	0.02	0.07
2	$Y = 37321X - 3879.4$	$R^2 = 0.9990$	0.88-88	0.01	0.05
3	$Y = 48267X - 137446$	$R^2 = 0.9991$	1.81-90	0.04	0.14
4	$Y = 56440X - 1223.9$	$R^2 = 0.9992$	0.77-77	0.01	0.04

*1: baicalin, 2: wogonoside, 3: baicalein, and 4: wogonin.

Table 3: Precision, repeatability, stability, and recovery of the analytes.

Analytes*	Precision ($n = 5$)		Repeatability ($n = 6$)	Stability ($n = 6$)	Recovery ($n = 3$)	
	Intraday RSD (%)	Interday RSD (%)	RSD (%)	RSD (%)	Mean (%)	RSD (%)
1	2.91	1.12	2.64	2.13	102.8	3.70
2	1.06	1.69	3.22	1.45	95.6	3.94
3	0.90	1.57	1.73	2.50	95.7	3.72
4	0.65	1.49	2.03	1.81	95.6	2.56

*1: baicalin, 2: wogonoside, 3: baicalein, and 4: wogonin.

(LOD), limit of quantitation (LOQ), precision (interday and intraday), repeatability, stability, and accuracy. All calibration curves exhibited good linearity with a correlation coefficient (R^2) of greater than 0.999 (Table 2). The relative standard deviation (RSD) of the peak area for each marker compound was taken as a measure (Table 3). In intraday and interday tests, the RSD values of standards were in ranges of 0.65%-2.91% and 1.12%-1.69%, respectively. The stability was between 1.45% and 2.50%. In addition, the range of repeatability was 1.73%–3.22%.

3.2. Effects of RS on Body Weight. The results of body weight are illustrated in Figure 4(a). Weight loss is a core feature of depression in the CUMS animal model [17]. There was no significant difference in the initial body weight of each group ($p > 0.05$). After three weeks of CUMS, the mice in the CUMS group gained less weight than the control group ($F(4, 45) = 60.34$, $p < 0.01$), and this condition continued for the following weeks. Four-week treatment of RS (0.75 and 1.5 g/kg) significantly attenuated the body weight reduction induced by CUMS ($F(4, 45) = 73.00$, $p < 0.01$).

3.3. Effects of RS on Depressive-Like Behaviors. As illustrated in Figures 4(b)–4(e), RS significantly ameliorated depressive-like behaviors induced by CUMS. Anhedonia, a prominent feature of depression in humans and rodents, manifested in rodents as a reduced preference for sucrose solutions over water [26]. After the 7-week CUMS program, the sucrose preference ratio (SPR) of CUMS-induced mice was lower (Figure 4(b)) ($F(4, 45) = 21.29$, $p < 0.01$) in comparison with that of the control group. However, in the administration of either 0.75 g/kg or 1.5 g/kg RS for 4 weeks, the SPR was higher than that of the CUMS group ($p < 0.01$).

We next used the FST and the TST, which are widely used for evaluating antidepressant activity, to test the effect of RS treatment on depressive-like behaviors in the CUMS model. Compared with the control group, immobility time in CUMS-induced mice was significantly increased (Figure 4(c)) ($F(4, 45) = 573.0$, $p < 0.01$) in the FST, which is consistent with the depressive phenotype. Compared with the CUMS-induced group, the 0.75 g/kg and 1.5 g/kg RS-treated groups had significantly reduced total immobility times ($p < 0.01$). As shown in Figure 4(d), the results of the TST were similar to the results of the FST. The CUMS-induced mice displayed a depressive-like phenotype as demonstrated by long immobility times in comparison with the control group ($F(4, 45) = 408.7$, $p < 0.01$). This depressive-like phenotype and long immobility times during the TST were significantly improved by the treatment with 0.75 g/kg or 1.5 g/kg RS ($p < 0.01$).

Depression is often accompanied by a decrease in spontaneous activity. As shown in Figure 4(e), the CUMS group showed a significant decrease ($F(4, 45) = 232.6$, $p < 0.01$) in spontaneous locomotor activity in the OFT when compared with the control group. Compared with the untreated and CUMS-induced group, both of the RS-treated (0.75 g/kg and 1.5 g/kg) groups had significantly increased spontaneous locomotor activity ($p < 0.01$). In summary, RS treatment can significantly improve the depressive-like behavior induced by CUMS in mice.

3.4. RS Rescued Neurons from CUMS-Induced Neuronal Injury and Apoptosis. Nissl staining was used to evaluate the effect of RS treatment on CUMS-induced hippocampal neuronal injury. Nissl staining indicated that the CA3 (Figures 5(a) and 5(c)) and CA1 (Figures 5(b) and 5(d)) hippocampal areas of CUMS-induced mice had Nissl body loss, neuronal atrophy, and nuclear atrophy (CA3 region, $F(4, 10) = 432.3$, $p < 0.01$; CA1 region, $F(4, 10) = 70.96$, $p < 0.01$). Compared with the CUMS-induced group, both of the RS-treated (0.75 g/kg and 1.5 g/kg) groups had increased numbers of normal Nissl bodies ($p < 0.01$).

To investigate the potential mechanism of RS treatment in alleviating CUMS-induced neuronal injury, western blot

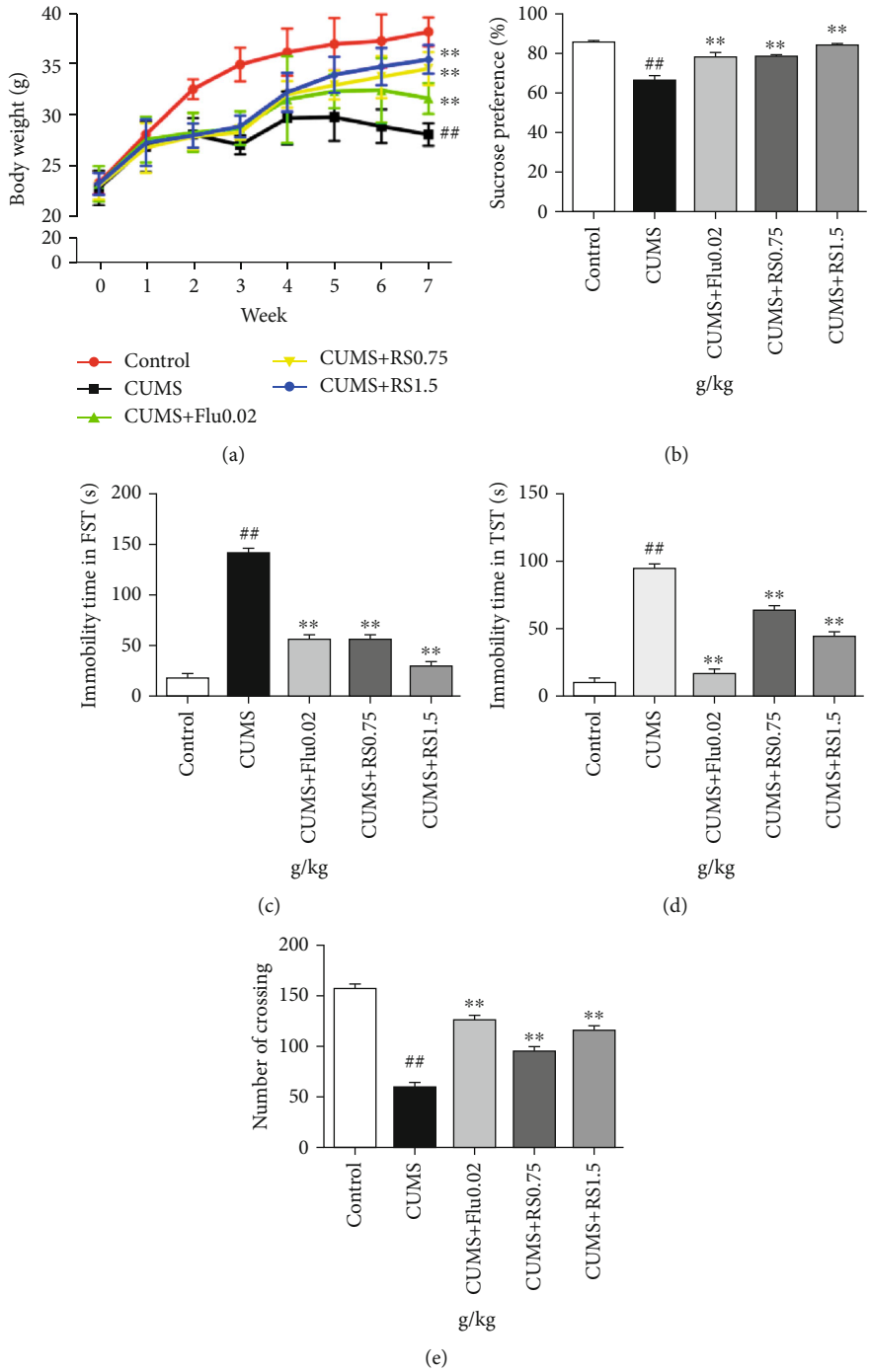

Figure 4: Effects of RS on body weight and behavioral studies: (a) effect of RS on body weight; (b) effect of RS on SPT; (c) effect of RS on immobility time in FST; (d) effect of RS on immobility time in TST; (e) effect of RS on the number of crossing in OFT. Results were reported as means ± SEM ($n = 10$). $^{\#\#}p < 0.01$ versus the control group; $^{**}p < 0.01$ versus the CUMS group.

was used to detect the expression of BCL-2 and BAX in hippocampal tissue. BAX and BCL-2 are two opposite factors that affect whether cells enter the apoptotic process [27]. As shown in Figures 5(e) and 5(f), the BCL-2 levels of CUMS-induced mice decreased ($F(4, 10) = 116.7$, $p < 0.01$) and the BAX levels increased ($F(4, 10) = 46.88$, $p < 0.01$) compared with those of the control group. However, BCL-2 levels increased and BAX levels decreased ($p < 0.01$) in both of the RS-treated (0.75 g/kg and 1.5 g/kg) groups.

3.5. RS Protected Neurons via Promoting the Migration, Differentiation, and Maturation of Neural Stem Cells (NSCs) into Neurons. Neurons are produced by proliferation, migration, and differentiation of NSCs, which occur in the subgranular zone (SGZ) of the DG in the hippocampus. To evaluate the effect of RS treatment on migration, differentiation, and maturation of NSCs to neurons, we detected the levels of DCX-, MAP2-, and NeuN-positive cells in the hippocampus, which are neuronal markers. Immunohistochemical analysis

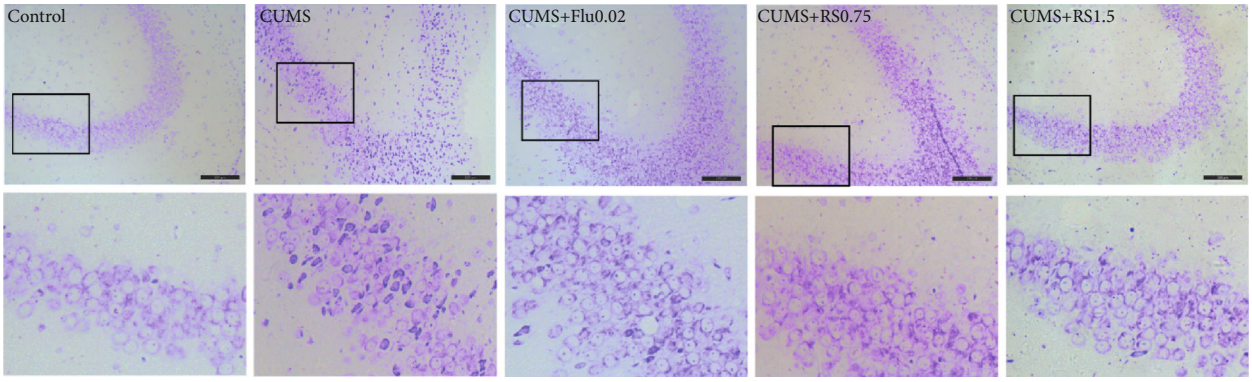

(a)

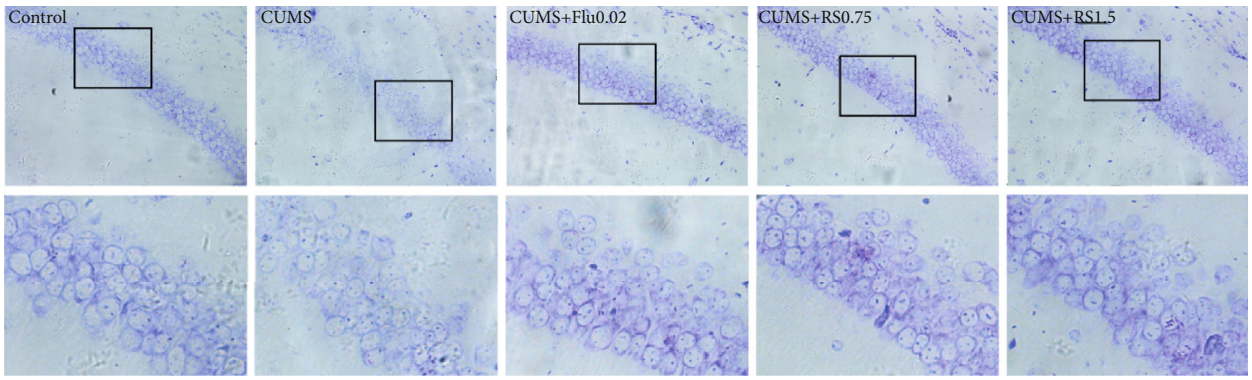

(b)

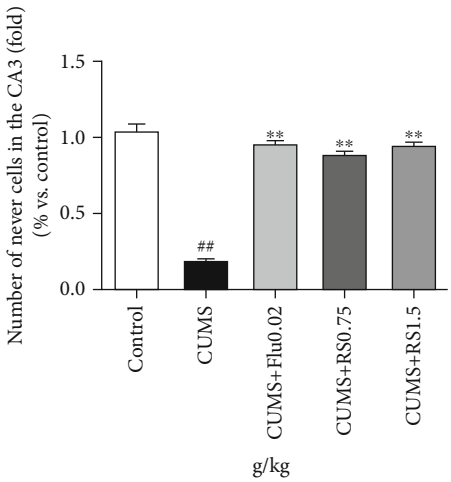

(c)

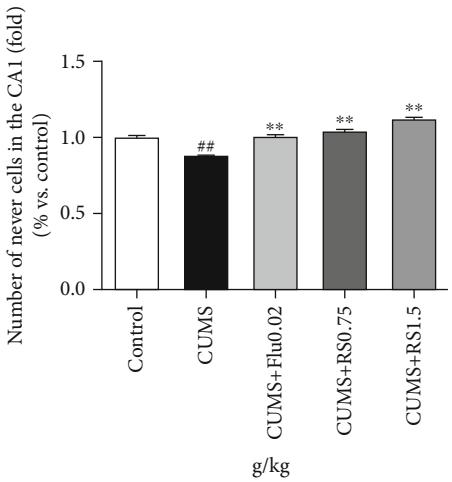

(d)

Figure 5: Continued.

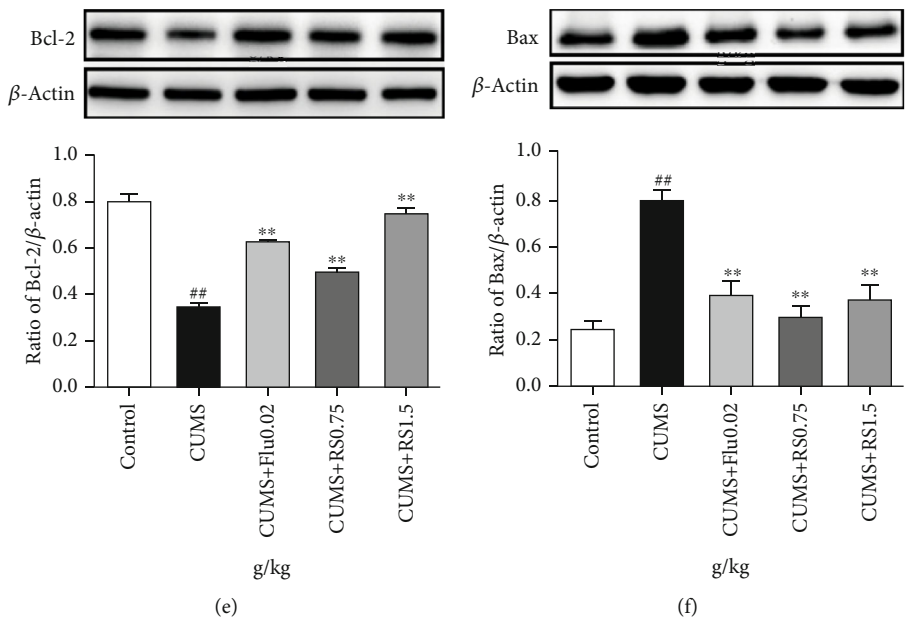

Figure 5: Nissl staining and effects of RS on apoptosis in the hippocampus. (a) Nissl staining in the CA3 area. (b) Nissl staining in the CA1 area. (c) Number of positive cells in the CA3 area. (d) Number of positive cells in the CA1 area. (e) Effect of RS on the Bcl-2 protein. (f) Effect of RS on the BAX protein. Results are reported as means ± SEM ($n = 3$). $^{\#\#}p < 0.01$ versus the control group; $^{**}p < 0.01$ versus the CUMS group. Scale bar, 100 μm.

demonstrated a decreased number of DCX-positive cells (Figures 6(a) and 6(d)) ($F(4, 10) = 39.54$, $p < 0.01$) and NeuN-positive cells (Figures 6(c) and 6(f)) ($F(4, 10) = 29.10$, $p < 0.01$) in the DG region as well as a decreased number of MAP2-positive cells (Figures 6(b) and 6(e)) ($F(4, 10) = 194.5$, $p < 0.01$) in the CA1 region of CUMS-induced mice. With RS treatment for 4 weeks, the number of DCX-positive cells (0.75 g/kg RS, $p < 0.05$; 1.5 g/kg RS, $p < 0.01$), MAP2-positive cells ($p < 0.01$), and NeuN-positive cells ($p < 0.01$) significantly increased. These results suggest that CUMS reduces the number of hippocampal neurons by inhibiting the development and maturation of neurons and that the chronic treatment of RS promotes the migration, differentiation, and maturation of NSCs to neurons in CUMS-induced mice.

3.6. RS Exerted Neuroprotective Effect via Mediating the TGFβ3-Smad2/3-Nedd9 Signal Pathway. The results of western blot showed that the CUMS procedure decreased the expression of TGFβ3 (Figure 7(b)) ($F(4, 10) = 15.04$, $p < 0.01$), repressed the phosphorylation of SMAD2/3 (Figure 7(c)) ($F(4, 10) = 27.38$, $p < 0.01$), and reduced the levels of NEDD9 (Figure 7(d)) ($F(4, 10) = 105.2$, $p < 0.01$) compared with the control group. However, these changes in expression of proteins of the TGFβ3-SMAD2/3-NEDD9 signaling pathway were restored in the RS groups. The expression of TGFβ3 (0.75 g/kg RS, $p < 0.05$; 1.5 g/kg RS, $p < 0.01$), SMAD2/3 ($p < 0.01$), and NEDD9 ($p < 0.01$) increased. These results suggest that the neuroprotective effect of RS may be associated with the modulation of the TGFβ3-SMAD2/3-NEDD9 signaling pathway.

4. Discussion

In this study, we provided evidence that RS treatment modulates neuroprotection in the hippocampus of mice that had undergone the CUMS procedure and we identified the TGFβ3-SMAD2/3-NEDD9 signaling pathway as a potential molecular mechanism. As RS is a water extract of the dry root of the Lamiaceae plants, *Scutellaria baicalensis* Georgi, we also detected the major components including baicalin, wogonoside, baicalein, and wogonin in the RS extract and found that the average proportions of baicalin are the highest. A large number of evidences have indicated that baicalin can protect neurons [28–31], so it is speculated that baicalin may be the main material basis, which requires further study.

So far, no animal model has been able to perfectly replicate the depressive-like phenotype currently observed in humans. It is believed that CUMS is the most commonly used, reliable, and effective rodent model of depression [32, 33]. Consistent with previous study [18], our results suggest that mice exposed to CUMS can display depressive-like behavioral deficits, including anhedonia and desperate behaviors. There is a decrease in the sucrose consumption ratio, an increase in the immobility time of FST and TST, and a decrease in spontaneous activity in CUMS-induced mice. When the treatment with RS was given for 4 weeks, the anhedonia and desperate behaviors caused by CUMS were reduced. In our previous study [34], we have shown that there was no significant alteration in locomotor activity between the control group and control treated with RS group, which revealed that RS did not cause central nervous system excitability. So we think the effect of RS in alleviating the

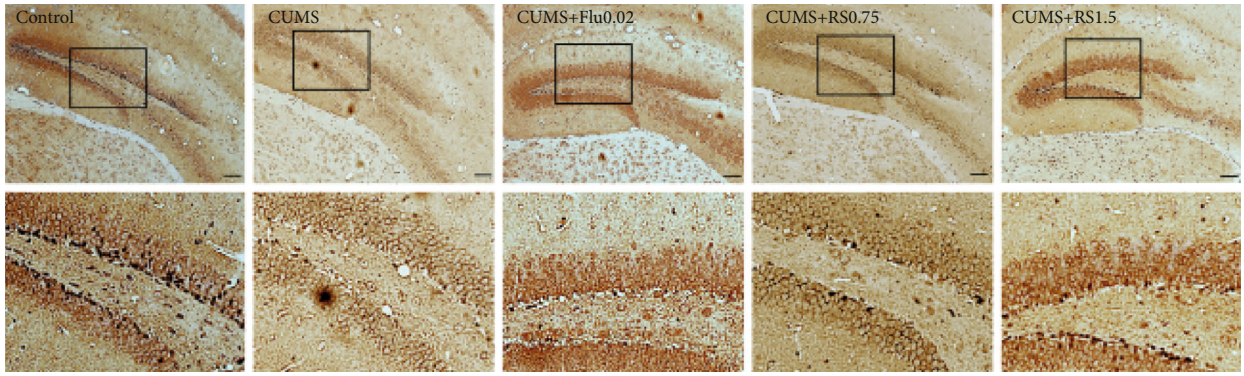

(a)

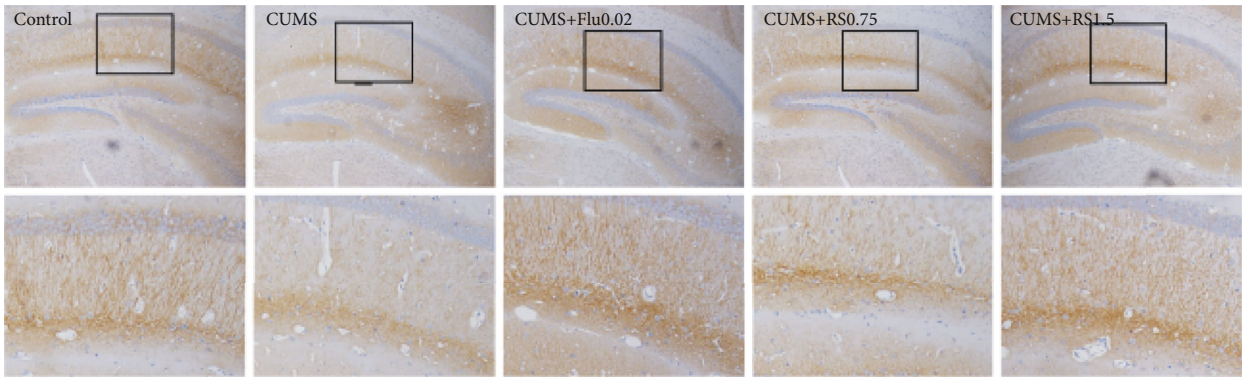

(b)

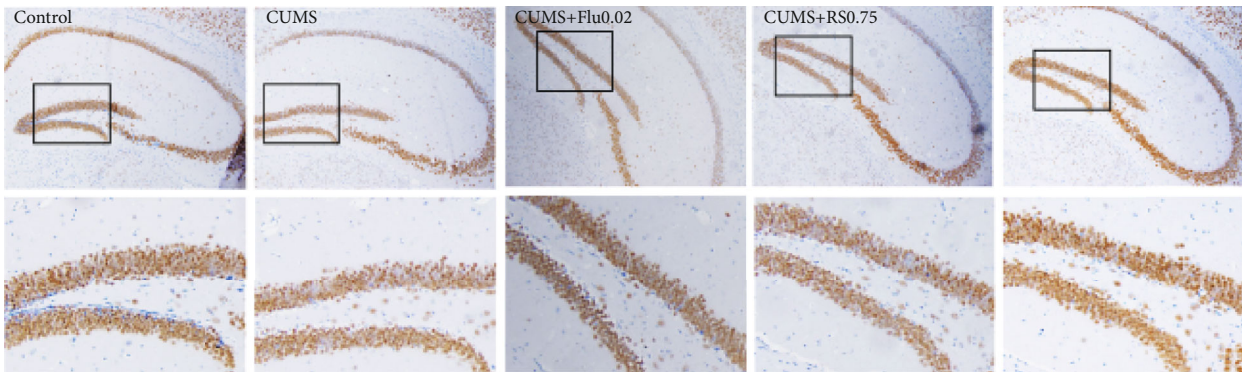

(c)

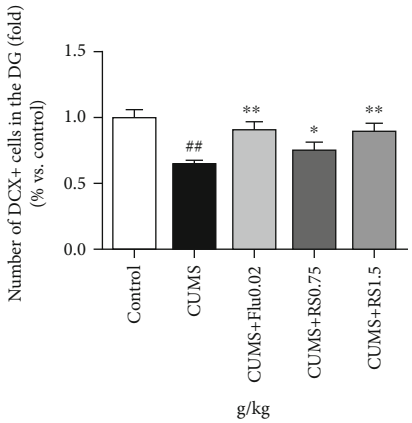

(d)

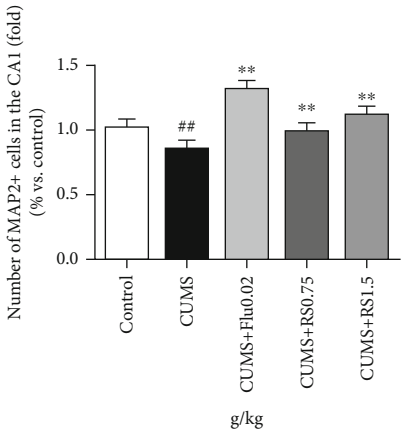

(e)

Figure 6: Continued.

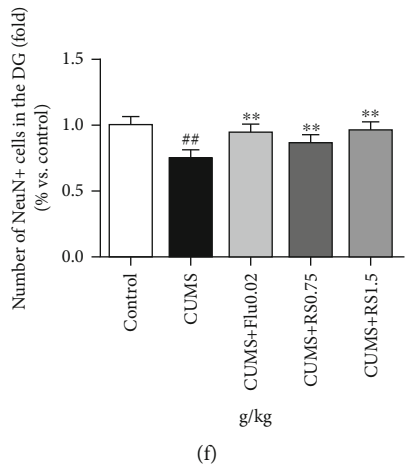

Figure 6: Effects of RS on DCX-, MAP2-, and NeuN-positive neuron numbers in the hippocampus. (a) Immunohistochemistry images of DCX-positive neurons in DG. (b) Immunohistochemistry images of MAP2-positive neurons in CA1. (c) Immunohistochemistry images of NeuN-positive neurons in DG. (d) Effects of RS on DCX-positive neuron numbers. (e) Effects of RS on MAP2-positive neuron numbers. (f) Effects of RS on NeuN-positive neuron numbers. Results are reported as means ± SEM ($n = 3$). $^{\#\#}p < 0.01$ versus the control group, $^{**}p < 0.01$ versus the CUMS group, and $^{*}p < 0.05$ versus the CUMS group. Scale bar, 100 μm.

depressive-like behaviors through its potential antidepressant-like effects.

Clinical studies have shown that patients with chronic depression have smaller hippocampal volume [35] and lower levels of cell proliferation than healthy controls [30]. The neurogenesis hypothesis explains how the hippocampal volume is decreased by the decrease in neurogenesis in the hippocampus [10]. Apoptosis is one of the prominent processes for regulating neurogenesis, including that in adult NSCs, migration neuroblasts, immature neurons, and mature neurons [36]. The decrease in the formation of new neurons in the hippocampus leads to the onset of depression, and enhanced adult hippocampal neuron formation is necessary for successful antidepressant treatment [37]. DCX has been widely used as an immature neuronal marker, and MAP2 and NeuN are the markers of neuronal maturation [38]. Previous studies have shown that CUMS could reduce DCX- and NeuN-positive cells [34, 39]. Therefore, we hypothesized that maintaining a normal hippocampal and neuronal population is critical in chronic depression therapy. In our study, CUMS resulted in decreased Nissl bodies, decreased expression of BCL-2, and increased expression of BAX. After RS treatment, the increase in neuronal apoptosis caused by CUMS was reduced. Meanwhile, the number of DCX-positive cells, NeuN-positive cells, and MAP2-positive cells in the hippocampus was decreased after CUMS, while RS administration could increase the number of positive neurons. These results indicated that RS can protect neurons by inhibiting neuronal apoptosis and increasing neuronal survival and maturation.

TGFβs are well known for their ability to enhance neurogenetic and neuroprotective functions [12, 14]. In the nervous system, TGFβ3, one of the isoforms of TGFβs, is found in neural progenitor cells, differentiating neurons and radial glial cells, and later in mature astrocytes and numerous neuron populations [12]. The SMAD2/3 protein is a direct substrate of TGFβ3 and can be activated to phosphorylated SMAD2/3 (p-SMAD2/3). TGFβ3 can antagonize apoptosis after ischemia by repairing DNA damage [40], and TGFβ3 can play a neuroprotective role through the Smad3 signaling system [41]. In the CUMS model, the expression levels of TGFβ3 protein of the hippocampal tissues were downregulated, but electroacupuncture therapy could upregulate the TGFβ3 protein level [13]. Neural precursor cell expressed, developmentally downregulated 9 (NEDD9) is initially found in the embryonic brain and then downregulated during development, but it remains enriched in neural precursor cells [42, 43]. NEDD9 is induced by TGFβ and directly interacts with SMADs in various types of cells [44, 45]. Like TGFβ, it is implicated in diverse biological processes including cell attachment, migration, and invasion as well as apoptosis and cell cycle regulation [46]. TGFβ2/3 double-knockout mice have fewer neurons in the developing cerebral cortex and hippocampus, which is dependent on the activation of SMAD signaling and the induction of the focal adhesion protein NEDD9 [47]. The study of *Nedd9* expression and function in the nervous system found that NEDD9 is required for the maintenance of dendritic spines in the hippocampus, and NEDD9-knockout mice showed deficits both in the ability to learn the task and in their ability to recall the platform location [48]. Therefore, TGFβ3-SMAD2/3 and NEDD9 play an important role in neuronal survival, maturation, and apoptosis.

RS is commonly used in many antidepressant Chinese medicine prescriptions [49–51]. Baicalein, a flavone derived from RS, has been reported to inhibit cancer cell metastasis via inactivation of the TGFβ-SMAD pathway [15] and inhibit cancer cell proliferation via suppression of NEDD9 expression in cells [52]. However, the role of TGFβ3-SMAD2/3-NEDD9 in depression and the association of RS and TGFβ3-SMAD2/3-NEDD9 are not clear. In our study, the CUMS procedure reduced the expression of TGFβ3, decreased the phosphorylation of SMAD2/3, and led to a decrease in NEDD9 levels. RS could reverse the CUMS-induced decrease in TGFβ3 protein, promote the

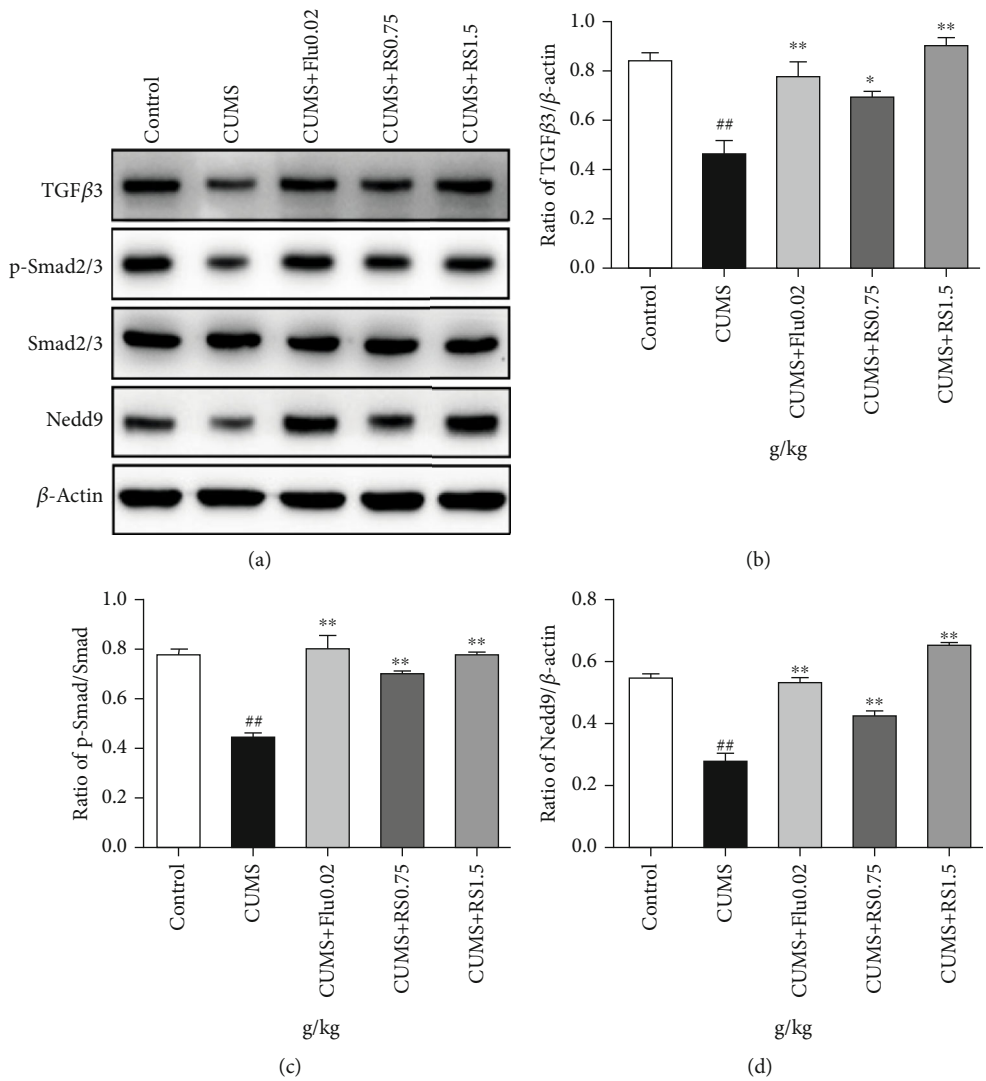

Figure 7: Effects of RS on the TGFβ3-Smad2/3-Nedd9 signal pathway. (a) Effects of RS on the TGFβ3-Smad2/3-Nedd9 signal pathway. (b) Effects of RS on the TGFβ3 protein. (c) Effects of RS on the p-Smad2/3 protein. (d) Effects of RS on the Nedd9 protein. Results are reported as means ± SEM ($n = 3$). $^{\#\#}p < 0.01$ versus the control group, $^{**}p < 0.01$ versus the CUMS group, and $^{*}p < 0.05$ versus the CUMS group.

phosphorylation of SMAD2/3, and increase the expression of downstream NEDD9 protein. These results showed that RS could mediate the TGFβ3-Smad2/3-Nedd9 signaling pathway, which might be the potential mechanism of the neuroprotective effect of RS. Importantly, it is the first time to show that the TGFβ3-SMAD2/3-NEDD9 signaling pathway took part in the process of CUMS-induced depressive-like behaviors and the antidepressant effects of RS.

In summary, RS can improve the depressive-like behaviors through upregulating the levels of TGFβ, p-SMAD2/3, and NEDD9 protein as well as increasing the number of DCX-, MAP2-, and NeuN-positive cells in the hippocampus. These results provide an alluring prospect that RS is used to treat depression in clinic.

Data Availability

The data generated and analyzed during this study are available on request from the corresponding author.

Conflicts of Interest

There is no conflict of interest among the authors.

Authors' Contributions

FZ, SG, and RQ designed the study, FZ, CZ, and DX did the experiments, WZ and LZ analyzed the data, and FZ, CZ, SG, and RQ wrote the paper. Fan Zhao and Chenyiyu Zhang contributed equally to this work.

Acknowledgments

This research was supported by the National Natural Science Foundation of China (No. 81573701), the Postgraduate Research & Practice Innovation Program of Jiangsu Province (KYCX19_1282), and the Priority Academic Program Development of Jiangsu Higher Education Institutions (Integration of Chinese and Western Medicine).

References

[1] S. Moussavi, S. Chatterji, E. Verdes, A. Tandon, V. Patel, and B. Ustun, "Depression, chronic diseases, and decrements in health: results from the world health surveys," *The Lancet*, vol. 370, no. 9590, pp. 851–858, 2007.

[2] S. Gu, L. Jing, Y. Li, J. H. Huang, and F. Wang, "Stress induced hormone and neuromodulator changes in menopausal depressive rats," *Frontiers in Psychiatry*, vol. 9, p. 253, 2018.

[3] Y. Liu, H. Li, X. Xu et al., "The relationship between insecure attachment to depression: mediating role of sleep and cognitive reappraisal," *Neural Plasticity*, vol. 2020, Article ID 1931737, 8 pages, 2020.

[4] A. J. Rush, M. H. Trivedi, S. R. Wisniewski et al., "Acute and longer-term outcomes in depressed outpatients requiring one or several treatment steps: a STAR∗D report," *The American Journal of Psychiatry*, vol. 163, no. 11, pp. 1905–1917, 2006.

[5] G. Y. Su, J. Y. Yang, F. Wang et al., "Antidepressant-like effects of Xiaochaihutang in a rat model of chronic unpredictable mild stress," *Journal of Ethnopharmacology*, vol. 152, no. 1, pp. 217–226, 2014.

[6] G. Y. Su, J. Y. Yang, F. Wang et al., "Xiaochaihutang prevents depressive-like behaviour in rodents by enhancing the serotonergic system," *The Journal of Pharmacy and Pharmacology*, vol. 66, no. 6, pp. 823–834, 2014.

[7] K. Zhang, F. Wang, J. Y. Yang et al., "Analysis of main constituents and mechanisms underlying antidepressant-like effects of Xiaochaihutang in mice," *Journal of Ethnopharmacology*, vol. 175, pp. 48–57, 2015.

[8] H. Y. Yu, Z. J. Yin, S. J. Yang, and S. P. Ma, "Baicalin reverse AMPA receptor expression and neuron apoptosis in chronic unpredictable mild stress rats," *Biochemical and Biophysical Research Communications*, vol. 451, no. 4, pp. 467–472, 2014.

[9] P. W. Zhuang, G. Z. Cui, Y. J. Zhang et al., "Baicalin regulates neuronal fate decision in neural stem/progenitor cells and stimulates hippocampal neurogenesis in adult rats," *CNS Neuroscience & Therapeutics*, vol. 19, no. 3, pp. 154–162, 2013.

[10] B. Shuken, N. Shin, T. Hiroyuki, and H. Akitoyo, "Neural basis of major depressive disorder: beyond monoamine hypothesis," *Psychiatry and Clinical Neurosciences*, vol. 72, pp. 3–12, 2018.

[11] S. C. Park, "Neurogenesis and antidepressant action," *Cell and Tissue Research*, vol. 377, no. 1, pp. 95–106, 2019.

[12] K. Krieglstein, F. Zheng, K. Unsicker, and C. Alzheimer, "More than being protective: functional roles for TGF-β/activin signaling pathways at central synapses," *Trends in Neurosciences*, vol. 34, no. 8, pp. 421–429, 2011.

[13] M. M. Xu, D. M. Zhang, R. X. Shi et al., "Effect of electroacupuncture intervention on behavior changes and levels of hippocampal transforming growth factor beta 3 and basic fibroblast growth factor proteins in depression rats," *Zhen Ci Yan Jiu*, vol. 41, no. 2, pp. 138–143, 2016.

[14] A. Dobolyi, C. Vincze, G. Pál, and G. Lovas, "The neuroprotective functions of transforming growth factor beta proteins," *International Journal of Molecular Sciences*, vol. 13, no. 7, pp. 8219–8258, 2012.

[15] F. Chen, M. Zhuang, J. Peng et al., "Baicalein inhibits migration and invasion of gastric cancer cells through suppression of the TGF-β signaling pathway," *Molecular Medicine Reports*, vol. 10, no. 4, pp. 1999–2003, 2014.

[16] N. Ito, E. Hirose, T. Ishida et al., "Kososan, a Kampo medicine, prevents a social avoidance behavior and attenuates neuroinflammation in socially defeated mice," *Journal of Neuroinflammation*, vol. 14, no. 1, pp. 98–113, 2017.

[17] P. Willner, "Validity, reliability and utility of the chronic mild stress model of depression: a 10-year review and evaluation," *Psychopharmacology*, vol. 134, no. 4, pp. 319–329, 1997.

[18] C. Y. Zhang, M. J. Zeng, L. P. Zhou et al., "Baicalin exerts neuroprotective effects via inhibiting activation of GSK3β/NF-κB/NLRP3 signal pathway in a rat model of depression," *International Immunopharmacology*, vol. 64, pp. 175–182, 2018.

[19] R. D. Porsolt, A. Bertin, and M. Jalfre, "Behavioral despair in mice: a primary screening test for antidepressants," *Archives Internationales de Pharmacodynamie et de Thérapie*, vol. 229, pp. 327–336, 1977.

[20] L. Steru, R. Chermat, B. Thierry, and P. Simon, "The tail suspension test: a new method for screening antidepressants in mice," *Psychopharmacology*, vol. 85, no. 3, pp. 367–370, 1985.

[21] J. S. Purba, W. J. Hoogendijk, M. A. Hofman, and D. F. Swaab, "Increased number of vasopressin- and oxytocin-expressing neurons in the paraventricular nucleus of the hypothalamus in depression," *Archives of General Psychiatry*, vol. 53, no. 2, pp. 137–143, 1996.

[22] R. W. Mays, C. V. Borlongan, T. Yasuhara et al., "Development of an allogeneic adherent stem cell therapy for treatment of ischemic stroke," *Journal of Experimental Stroke and Translational Medicine*, vol. 3, no. 1, pp. 34–46, 2010.

[23] X. Tian, M. Q. Yang, S. Guo et al., "Quantitative analysis and chemical fingerprint similarity for quality control of the seeds of *Paeonia suffruticosa* Andr. by HPLC," *Chemical Research in Chinese Universities*, vol. 33, no. 4, pp. 546–551, 2017.

[24] C. R. Li, L. M. Zhou, G. Lin, and Z. Zuo, "Contents of major bioactive flavones in proprietary traditional Chinese medicine products and reference herb of Radix Scutellariae," *Journal of Pharmaceutical and Biomedical Analysis*, vol. 50, no. 3, pp. 298–306, 2009.

[25] S. J. Wu, A. L. Sun, and R. M. Liu, "Separation and purification of baicalin and wogonoside from the Chinese medicinal plant Scutellaria baicalensis Georgi by high-speed counter-current chromatography," *Journal of Chromatography. A*, vol. 1066, no. 1-2, pp. 243–247, 2005.

[26] H. Anisman and K. Matheson, "Stress, depression, and anhedonia: caveats concerning animal models," *Neuroscience and Biobehavioral Reviews*, vol. 29, no. 4-5, pp. 525–546, 2005.

[27] J. Yang, X. Liu, K. Bhalla et al., "Prevention of apoptosis by bcl-2: release of cytochrome c from mitochondria blocked," *Science*, vol. 275, no. 5303, pp. 1129–1132, 1997.

[28] K. Zhang, X. Pan, F. Wang et al., "Baicalin promotes hippocampal neurogenesis via SGK1- and FKBP5-mediated glucocorticoid receptor phosphorylation in a neuroendocrine mouse model of anxiety/depression," *Scientific Reports*, vol. 6, no. 1, article 30951, 2016.

[29] X. Jin, M.-Y. Liu, D.-F. Zhang et al., "Baicalin mitigates cognitive impairment and protects neurons from microglia-mediated neuroinflammation via suppressing NLRP3 inflammasomes and TLR4/NF-κB signaling pathway," *CNS Neuroscience & Therapeutics*, vol. 25, no. 5, pp. 575–590, 2019.

[30] L. Gao, C. Li, R. Y. Yang et al., "Ameliorative effects of baicalein in MPTP-induced mouse model of Parkinson's disease: a microarray study," *Pharmacology, Biochemistry, and Behavior*, vol. 133, pp. 155–163, 2015.

[31] Y. Li, J. Zhao, and C. Holscher, "Therapeutic potential of baicalein in Alzheimer's disease and Parkinson's disease," *CNS Drugs*, vol. 31, no. 8, pp. 639–652, 2017.

[32] M. Nollet, A. M. Le Guisquet, and C. Belzung, "Models of depression: unpredictable chronic mild stress in mice," *Current Protocols in Pharmacology*, vol. 61, pp. 5–65, 2013.

[33] S. Antoniuk, M. Bijata, E. Ponimaskin, and J. Wlodarczyk, "Chronic unpredictable mild stress for modeling depression in rodents: meta-analysis of model reliability," *Neuroscience and Biobehavioral Reviews*, vol. 99, pp. 101–116, 2019.

[34] R. Y. Zhang, L. T. Guo, Z. Y. Ji et al., "Radix Scutellariae attenuates CUMS-induced depressive-like behavior by promoting neurogenesis via cAMP/PKA pathway," *Neurochemical Research*, vol. 43, no. 11, pp. 2111–2120, 2018.

[35] P. Videbech and B. Ravnkilde, "Hippocampal volume and depression: a meta-analysis of MRI studies," *The American Journal of Psychiatry*, vol. 161, no. 11, pp. 1957–1966, 2004.

[36] J. R. Ryu, C. J. Hong, J. Y. Kim, E. K. Kim, W. Sun, and S. W. Yu, "Control of adult neurogenesis by programmed cell death in the mammalian brain," *Molecular Brain*, vol. 9, no. 1, article 43, 2016.

[37] M. Boldrini, M. D. Underwood, R. Hen et al., "Antidepressants increase neural progenitor cells in the human hippocampus," *Neuropsychopharmacology*, vol. 34, no. 11, pp. 2376–2389, 2009.

[38] H. B. Sarnat, "Clinical neuropathology practice guide 5-2013: markers of neuronal maturation," *Clinical Neuropathology*, vol. 32, no. 9, pp. 340–369, 2013.

[39] J. W. Wang, D. J. David, J. E. Monckton, F. Battaglia, and R. Hen, "Chronic fluoxetine stimulates maturation and synaptic plasticity of adult-born hippocampal granule cells," *The Journal of Neuroscience*, vol. 28, no. 6, pp. 1374–1384, 2008.

[40] F. Wu, H. W. Ye, J. F. Lin et al., "TGF-β3 reduces apoptosis in ischemia-induced adipose-derived stem cells by enhancing DNA repair," *Experimental and Therapeutic Medicine*, vol. 15, no. 5, pp. 4400–4408, 2018.

[41] X. Zhang and W. Y. Lui, "Transforming growth factor-β3 regulates cell junction restructuring via MAPK-mediated mRNA destabilization and Smad-dependent protein degradation of junctional adhesion molecule B (JAM-B)," *Biochimica et Biophysica Acta (BBA) - Gene Regulatory Mechanisms*, vol. 1849, no. 6, pp. 601–611, 2015.

[42] S. Kumar, Y. Tomooka, and M. Noda, "Identification of a set of genes with developmentally down-regulated expression in the mouse brain," *Biochemical and Biophysical Research Communications*, vol. 185, no. 3, pp. 1155–1161, 1992.

[43] N. Abramova, C. Charniga, S. K. Goderie, and S. Temple, "Stage-specific changes in gene expression in acutely isolated mouse CNS progenitor cells," *Developmental Biology*, vol. 283, no. 2, pp. 269–281, 2005.

[44] X. Liu, A. E. Elia, S. F. Law, E. A. Golemis, J. Farley, and T. Wang, "A novel ability of Smad3 to regulate proteasomal degradation of a Cas family member HEF1," *The EMBO Journal*, vol. 19, no. 24, pp. 6759–6769, 2000.

[45] M. Zheng and P. J. McKeown-Longo, "Regulation of HEF1 expression and phosphorylation by TGF-β1 and cell adhesion," *The Journal of Biological Chemistry*, vol. 277, no. 42, pp. 39599–39608, 2002.

[46] M. Singh, L. Cowell, S. Seo, G. M. O'Neill, and E. Golemis, "Molecular basis for HEF1/NEDD9/Cas-L action as a multifunctional co-ordinator of invasion, apoptosis and cell cycle," *Cell Biochemistry and Biophysics*, vol. 48, no. 1, pp. 54–72, 2007.

[47] T. Vogel, S. Ahrens, N. Büttner, and K. Krieglstein, "Transforming growth factor beta promotes neuronal cell fate of mouse cortical and hippocampal progenitors in vitro and in vivo: identification of Nedd9 as an essential signaling component," *Cerebral Cortex*, vol. 20, no. 3, pp. 661–671, 2010.

[48] D. C. Knutson, A. M. Mitzey, L. E. Talton, and M. Clagett-Dame, "Mice null for NEDD9 (HEF1α) display extensive hippocampal dendritic spine loss and cognitive impairment," *Brain Research*, vol. 1632, pp. 141–155, 2016.

[49] Z. Xiong, J. Yang, Y. Huang et al., "Serum metabonomics study of anti-depressive effect of Xiao-chai-Hu-tang on rat model of chronic unpredictable mild stress," *Journal of Chromatography B, Analytical Technologies in the Biomedical and Life Sciences*, vol. 1029-1030, pp. 28–35, 2016.

[50] J. Ma, F. Wang, J. Yang et al., "Xiaochaihutang attenuates depressive/anxiety-like behaviors of social isolation-reared mice by regulating monoaminergic system, neurogenesis and BDNF expression," *Journal of Ethnopharmacology*, vol. 208, pp. 94–104, 2017.

[51] C. Y. Kwon, B. Lee, S. Y. Chung et al., "Herbal medicine Sihogayonggolmoryeo-tang or chai-Hu-Jia-long-Gu-mu-Li-tang for the treatment of post-stroke depression: a protocol for a systematic review and meta-analysis," *Medicine*, vol. 97, no. 38, article e12384, 2018.

[52] R. T. Zhou, M. He, Z. Yu et al., "Baicalein inhibits pancreatic cancer cell proliferation and invasion via suppression of NEDD9 expression and its downstream Akt and ERK signaling pathways," *Oncotarget*, vol. 8, no. 34, pp. 56351–56363, 2017.

Hindawi
Neural Plasticity
Volume 2020, Article ID 8837615, 13 pages
https://doi.org/10.1155/2020/8837615

Research Article

Dynamic Reconfiguration of Functional Topology in Human Brain Networks: From Resting to Task States

Wenhai Zhang,[1,2] **Fanggui Tang**,[1] **Xiaolin Zhou**,[3] **and Hong Li**[4]

[1]*College of Education Science, Hengyang Normal University, Hengyang 421002, China*
[2]*Mental Health Center, Yancheng Institute of Technology, Yancheng 224051, China*
[3]*School of Psychology and Cognition, Peking University, Beijing 100871, China*
[4]*Institute for Brain and Psychological Sciences, Sichuan Normal University, Chengdu 610066, China*

Correspondence should be addressed to Wenhai Zhang; zwh2007106@126.com

Received 4 May 2020; Revised 23 July 2020; Accepted 26 August 2020; Published 8 September 2020

Academic Editor: Fushun Wang

Task demands evoke an intrinsic functional network and flexibly engage multiple distributed networks. However, it is unclear how functional topologies dynamically reconfigure during task performance. Here, we selected the resting- and task-state (emotion and working-memory) functional connectivity data of 81 health subjects from the high-quality HCP data. We used the network-based statistic (NBS) toolbox and the Brain Connectivity Toolbox (BCT) to compute the topological features of functional networks for the resting and task states. Graph-theoretic analysis indicated that under high threshold, a small number of long-distance connections dominated functional networks of emotion and working memory that exhibit distinct long connectivity patterns. Correspondently, task-relevant functional nodes shifted their roles from within-module to between-module: the number of connector hubs (mainly in emotional networks) and kinless hubs (mainly in working-memory networks) increased while provincial hubs disappeared. Moreover, the global properties of assortativity, global efficiency, and transitivity decreased, suggesting that task demands break the intrinsic balance between local and global couplings among brain regions and cause functional networks which tend to be more separated than the resting state. These results characterize dynamic reconfiguration of large-scale distributed networks from resting state to task state and provide evidence for the understanding of the organization principle behind the functional architecture of task-state networks.

1. Introduction

Understanding how the brain shapes mind, such as cognition and emotion, ultimately relies on the knowledge of large-scale brain networks [1]. The Human Connectome Project (HCP) used high-quality neuroimaging to map the structural and functional connectivity of the normal human brain [2], which provides new opportunity to understand general topological principles of brain network organization. Graph theory-based connectivity research has shown that a brain network is composed of functionally separate subnetworks or modules [3]. As a complex system, the brain flexibly processes multiple incoming information through interplaying between distributed subsystems [4, 5]. Moreover, the intrinsic functional network during resting state primarily shapes a standard architecture of task-based functional brain organization and is secondarily evoked by task-relevant networks [6]. However, little is known about how the functional topology dynamically reconfigures for task performance.

In graph-theoretic research, a function network is described as a graph with a collection of nodes representing brain regions and edges representing functional interactions in the brain [7, 8]. Nodes are further grouped into module or community with highly connected within-group links and a minimally possible number of between-group links [9]. Human brain networks have complex local and global topological properties (e.g., hub nodes, modules, transitivity measuring functional separation, and global efficiency measuring functional integration) [8]. When task demands change from resting state to task state, metabolic energy is necessarily redistributed to support the reorganized functional architecture [10] and the functional network is

dynamically reorganized according to the specific cognitive demands of the task [11]. Correspondently, functional topologies such as connections between/within modules, nodal features, and global features (e.g., transitivity and global efficiency) are reconfigured [12–14]. However, there are still the following three unsolved questions.

First, there is lack of enough evidences to determine how long connections switch from resting state to task states, e.g., emotion and working memory (WM). The functional connectivity refers to some forms of statistical dependency between nodes, and short-distance links are distributed mainly within communities while long-distance links are distributed between communities [15, 16]. During tasks, short connections within communities decrease while long connections between communities increase [6, 17]. A recent meta-analysis indicated that the coactivation networks elicited by a wide range of tasks have more long-range connections [18]. Particularly, the default mode network (DMN) actively contributes to function integration [19]: intra-DMN connectivity decreased while inter-DMN connectivity increased during a 2-back versus a 1-back working memory (WM) task [13]. Moreover, emotion processing (e.g., reappraisal) produces distributed alterations in functional connections involving visual, dorsal attention, frontoparietal, and DMN modules [20]. Long connections between communities are particularly important for brain function because they are responsible for intermodular communication [12, 21]. However, performing statistical testing on connectivity values for large networks suffers from multiple comparison problem so that long-links are easily ignored because of their weak connectivity values [7, 22]. The network-based statistic (NBS) has greater power to detect a whole cluster of regions spanning multiple connections and makes it possible to find a set of connections forming a subnetwork associated with an experimental effect [23]. Here, we used the NBS to further clarify how long connections change during the WM and emotional task versus the resting state.

Second, it is unclear how functional hubs dynamically change their nodal roles during the WM and emotional tasks. Resting-state fMRI research has demonstrated functional hubs distributing in the heteromodal association cortex (e.g., the precuneus, posterior and anterior cingulate gyrus, ventromedial frontal cortex, and inferior parietal regions) [3, 24]. Hubs flexibly process multiple information and rapidly update their connectivity pattern according to task demands [25, 26]. Hub nodes are generally divided into three different roles: provincial hubs with the vast majority of links within their module, connector hubs with many links to most of the other modules, and kinless hubs with links homogeneously distributed among all modules [27]. Finc et al. [13] found that the number of connector hubs increased whereas the number of provincial hubs decreased when the WM task became more demanding. Moreover, task-relevant nodes within auditory, visual, salience, and context community become activated in the WM task while subcortical regions (e.g., amygdala and putamen) take an important role in emotional tasks [20, 26, 28–30]. However, the previous studies ignored the shifting of nonhubs to hubs and rarely mentioned kinless hubs.

Third, it is unclear whether intrinsic functional networks become more integrated or separated during the shift from resting state to task state. A number of structural and resting-state fMRI studies have indicated that brain networks exhibit economical small-world topology [31–33], balancing integration and segregation between brain regions [34, 35]. To satisfy ever changing task demands, the global properties (e.g., clustering and modularity) of brain network organization are responsive to the changing task contexts [12]. Some studies have found that functional networks tend to be of higher global network integration at task state: for example, the performance of cognitive tasks (including WM) is associated with increased global efficiency and less segregation of processing relative to resting state [36, 37]. Other studies have proposed that the global topological properties are largely invariant in order to continually maintaining the balance of efficient local and global processing [38, 39]. Another studies demonstrated that functional networks tend to be highly separated (e.g., negative assortativity coefficients) and exhibit a more random configuration at higher levels of task difficulty (e.g., emotional task) [8, 30, 40]. This inconsistency might be because of multiple factors such as different tasks, different signal natures of fMRI and EEG, or different ways to constructing function networks. More high-quality researches are pressed to clarify the consistency.

To address the three questions, we selected the resting-state denoised by FIX (FMRIB's ICA-based X-noiseifier) and task-state (EMOTION and WM) fMRI data from the HCP data with 500 subjects (see Methods for details). Then, we used Pearson's correlation to separately construct three functional networks (FIX, EMOTION, and WM) for each subject. Next, we performed connectivity analysis for EMOTION and WM versus FIX using the NBS toolbox [23] to determine how long connections change during task states versus resting state. We also used the Brain Connectivity Toolbox (BCT) to compute nodal features of participant index (PI) and within-module Z-score and global properties (assortativity, global efficiency, and transitivity) and then performed one-way ANOVA with 3 conditions (FIX, EMOTION, and WM) for global and nodal properties at each threshold of 5-15%. Considering that functional networks at task state need to exchange multiple information between different communities, we firstly predicted that although long connections are of a small proportion, they would become more significant relative to resting state because they are responsible for intermodular communication [12, 21]. We also predicted that with the increase of task demands, the number of task-relevant connector and kinless hubs would increase while the number of provincial hubs would decrease [13]. Finally, we predicted that under the disturbance of active tasks, the balance between integration and segregation at resting state would be disrupted and functional networks would tend to be more separated and randomized [8, 30, 40].

2. Methods

2.1. Participants. After registering an account at ConnectomeDB and agreeing to the Open and Restricted Access Data

Use Terms (http://www.humanconnectome.org/), we were approved to download the HCP data with 500 subjects. After matching age with gender and excluding twins, we selected 81 right-handed healthy adults (age 22-30 years old; 40 males and 41 females). These participants had no prior history of neurological or psychiatric disorders.

2.2. fMRI Data Selection and Processing. The detailed data acquisition and experimental procedure were described at the HCP website [2]. For structural imaging, T1w was acquired using a 32-channel head coil and 3T Siemens product (MPRAGE and SPACE) sequences (TR = 2400 ms, TE = 2.14 ms, flip angle = 8 degrees, FOV = 224 × 224 mm, voxel size = 0.7 mm isotropic). The selected HCP data included the resting-state and task-state fMRI image datasets. The resting-state fMRI data were acquired in four runs of approximately 15 minutes each, two runs in one session and two in another session, with eyes open with relaxed fixation on a projected bright cross hair on a dark background (and presented in a darkened room) (TR = 720 ms, TE = 33.1 ms, flip angle = 52 degrees, FOV = 208 × 108, matrix = 104 × 90, slice thickness = 2 mm isotropic). Following completion of resting-state fMRI in each of the two fMRI scanning sessions, the task-state data were acquired with the same EPI pulse sequence parameters as the resting-state fMRI. These subject-specific images had been preprocessed through the HCP Minimal Processing Pipelines (MPP): (1) to remove spatial artifacts and distortions; (2) to generate cortical surfaces, segmentations, and myelin maps; (3) to make the data easily viewable in the Connectome Workbench visualization software; (4) to generate precise within-subject cross-modal registrations; (5) to handle surface and volume cross-subject registrations to standard volume and surface spaces; and (6) to make the data available in the CIFTI format in a standard grayordinate space (see [41] for details).

The task-state fMRI data included an emotion processing task and a WM task. The emotion processing task is a Hariri matching task [42], in which the participants were asked to decide which of the two faces presented at the bottom of the screen matched the face at the top of the screen or which of two shapes presented at the bottom of the screen matched the shape at the top of the screen [43]. The faces have either angry or fearful expressions and simple geometric shapes (circles, vertical, and horizontal ellipses) were used as control stimuli. The WM task is an n-back task in which 4 different stimulus types (face, places, tools, and body parts) are presented in separate blocks within each run. Within each run, 1/2 of the blocks use a 2-back WM task and 1/2 of the blocks use a 0-back WM task. Each of the two runs contains 8 task blocks (10 trials of 2.5 s each, for 25 s) and 4 fixation blocks (15 s each).

Following Cao et al. [44], the mean average of all task-related signal fluctuations was removed by regression with separate regressors for each experimental condition in order to only account for condition-specific effects, prior to graph construction. The parcellation with 333 parcels developed by Gordon et al. [45] was combined with subcortical areas (bilateral amygdala, hippocampus, accumbens, caudate, pallidum, putamen, thalamus, ventral diencephalon, cerebellum, and the whole brain stem) into a new parcellation with the 352 functional parcels (downloading from https://sites.wustl.edu/petersenschlaggarlab/resources/). Then, we used Connectome Workbench developed by the HCP (http://www.humanconnectome.org/software/connectome-workbench.html) to extract the 352 parcels' time series from the residual task-fMRI data and merged the time series of two scanning orders. Next, we computed the pairwise Pearson's correlation matrices of all these parcel time series for each task. Finally, we removed the rows and columns corresponding to 47 parcels with no original labels in the parcellation developed by Gordon et al. [45] and thus obtained the functional networks with the size 305 × 305.

The resting-state fMRI data contained the FIX data. During the preprocessing, the FIX data had been cleaned of structured noise by a new approach that combines ICA with a more complex automated component classifier referred to as FIX [41]. Similar to the task state, we obtained Pearson's correlation matrices with 305 functional nodes for the FIX data.

2.3. Network Connection Analysis. To identify network connections that varied with the task demand, we used the NBS approach [23]. Full-linking connectivity matrices were entered as repeated measure-dependent variables into the NBS toolbox (freely downloaded from http://www.nitrc.org/projects/nbs/), with the contrast of EMOTION or WM versus FIX. According to Figure 1, the inflection points separately occur at the threshold of $t = 4.6$ for EMOTION versus FIX (i.e., the number of connected edges decreases more sharply when $t < 4.6$; the curve nearly parallels with t-axis when $t > 4.6$) and at the threshold of $t = 6.4$ for WM versus FIX (i.e., the curve nearly parallels with t-axis when $t > 6.4$). Moreover, the networks for EMOTION and WM versus FIX hold comparable edges at these inflection points. Therefore, an individual-connection-level threshold of $t = 4.6$ and 6.4, respectively, for EMOTION versus FIX and WM versus FIX was used with extent-based correction for multiple comparisons, 5000 permutations, and an overall corrected $p < 0.0001$.

2.4. Graph-Theoretic Processing. After these correlation networks were Fisher-Z transformed, their diagonal elements and negative connections were set to zero. We used the BCT (http://www.brain-connectivity-toolbox.net) to sparse functional networks in 1% interval from the threshold 5% to 15%. For each threshold, we constructed weighted networks for the FIX, EMOTION, and WM condition. In these weighted networks, inter/intramodal connections below the threshold were assigned to 0 while the connections above the threshold remained unchanged because weak and non-significant links may represent spurious connections that tend to obscure the topology of strong and significant connections and as a result are often discarded [8].

The graph analyses included nodal and global topological features for each threshold. First, to explore how the hubs change in the different task conditions, we computed the nodal PI (or participation coefficients) and within-module

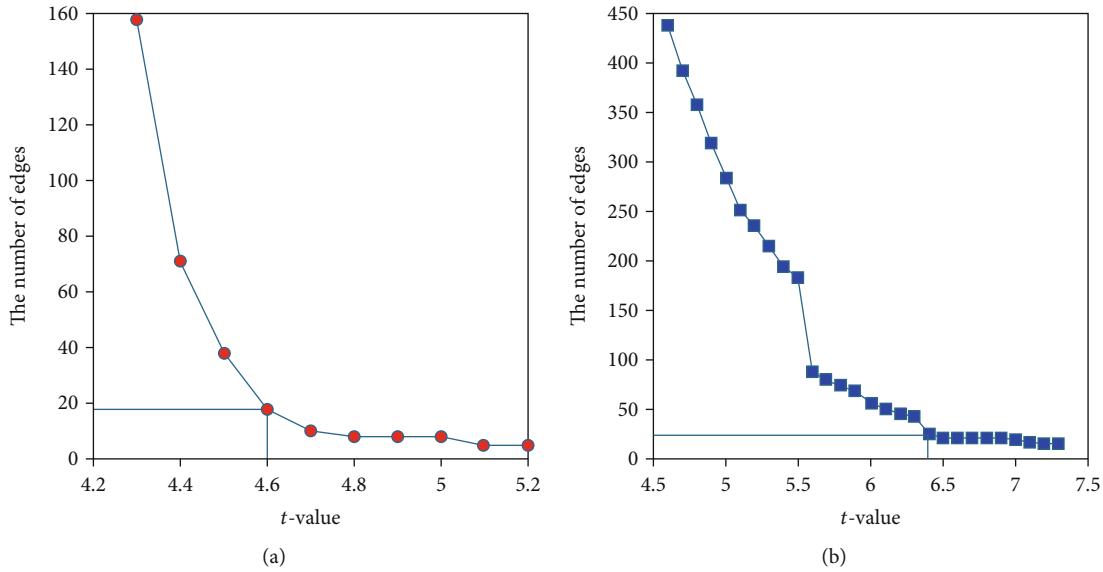

Figure 1: The number of connected edges varies with the threshold of the t-value from the network-based statistic method. (a) The inflection point occurs at the threshold of $t = 4.6$ for EMOTION versus resting state. (b) The inflection point occurs at the threshold of $t = 6.4$ for working memory versus resting state.

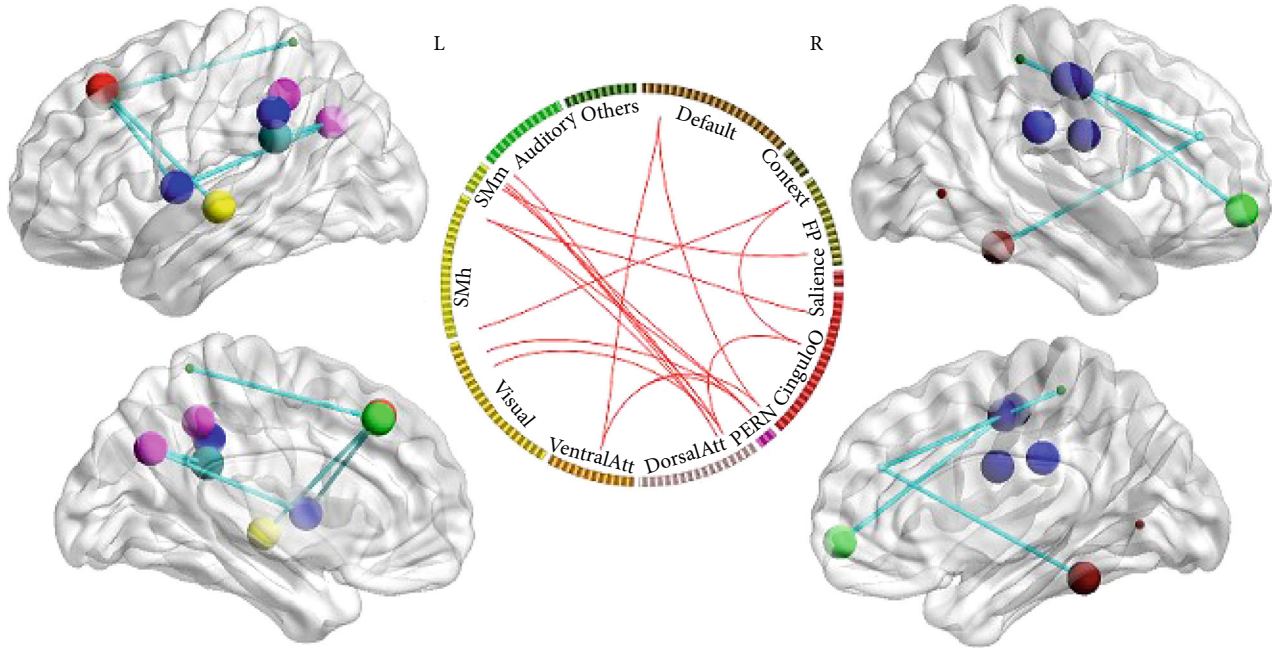

Figure 2: Two-dimension and three-dimension depictions of connectivity analysis result in the EMOTION versus FIX condition. The nodal color denotes affiliative community; the nodal size represents the magnitude of nodal betweenness centrality; the edge depicts binarized edge.

degree Z-score for each threshold. PI measures the diversity of intermodular connections of individual nodes while within-module degree Z-score measures the extent to which a node is connected to other nodes within its module [46]. Following Guimera et al. [27] and Finc et al. [13], we first classified nodes as hubs ($Z_i > 1$) and nonhubs ($Z_i < 1$). Then, the hubs were further divided into three classes: (1) provincial hubs with $Z_i > 1$ and $\mathrm{PI}_i < 0.3$; (2) connector hubs with $Z_i > 1$ and $0.3 < \mathrm{PI}_i < 0.75$; and (3) kinless hubs with $Z_i > 1$ and $\mathrm{PI}_i > 0.75$.

Second, we analyzed the following global network properties to determine functional networks that become integrated or separated from resting to task states. (1) Assortativity is a correlation coefficient between the degrees of all nodes on two opposite ends of a link. A positive assortativity coefficient indicates that nodes tend to link to other nodes with the same or similar degrees. (2) Global efficiency is the inverse of the average shortest path length. (3) Transitivity is the ratio of triangles to triplets in the network and is an alternative to the clustering coefficient.

Table 1: The nodes of connected network in the emotion and working-memory versus the resting-state condition during the network-based statistical analysis.

ID	Parcel label	AAL	Centroid MNI			Role*
			x	y	z	
6	Default_6	Frontal_Sup_L	-19.5	30.1	45.5	P
40	Default_40	Frontal_Mid_R	30.6	18.9	48.7	P
41	Default_41	Temporal_Sup_R	54.4	1.1	-12.9	Nonhub
43	Context_2	Calcarine_L	-8.8	-49.8	4.2	Nonhub
48	Context_7	Fusiform_R	34.6	-23.9	-20.4	Nonhub
52	FrontoParietal_3	Frontal_Sup_Media	-5.5	29.3	44	Nonhub
69	FrontoParietal_20	Frontal_Mid_Orb_R	28.4	57	-5.1	Nonhub
84	CinguloOperc_7	SupraMarginal_L	-57.7	-40.6	35.8	P/C
90	CinguloOperc_13	Insula_L	-28.8	23.7	8.4	P/C
91	CinguloOperc_14	Rolandic_Oper_L	-59.8	-4.1	8.8	P/C
94	CinguloOperc_17	Rolandic_Oper_L	-51.8	-0.6	5	P/C
117	CinguloOperc_40	SupraMarginal_R	54.9	-27	29.6	P/C
119	PERN_2	Precuneus_L	-12.7	-64.9	31.8	C
128	DorsalAttn_6	Parietal_Inf_L	-42.9	-45	43	P/C
130	DorsalAttn_8	Frontal_Inf_Tri_L	-43.6	36.3	8.5	P
165	VentralAttn_11	Temporal_Mid_L	-59	-18	-3	P
205	Visual_28	Occipital_Mid_R	31.7	-85.7	2.4	Nonhub
206	Visual_29	Lingual_R	43.8	-67.2	2	C
208	Visual_31	Temporal_Mid_R	49	-54.5	8.8	Nonhub
209	Visual_32	Lingual_R	31.2	-45.6	-5.8	Nonhub
211	Visual_34	Fusiform_R	34.9	-44	-20	Nonhub
217	SMhand_1	Cuneus_R	-18.8	-48.7	65	P/C
251	SMhand_35	Postcentral_R	39.2	-34.6	57.5	P
260	SMmouth_6	Precentral_R	42.3	-11	47.3	Nonhub
261	SMmouth_7	Postcentral_R	53.9	-8.3	26.1	P/C
262	SMmouth_8	Precentral_R	47.8	-15.1	49.3	P/C
263	Auditory_1	Heschl_L	-32	-29.3	15.6	Nonhub
264	Auditory_2	SupraMarginal_L	-46.3	-41.4	25.9	Nonhub

Note. P: provincial hub; C: connector hub. *Nodal role at the resting state.

We wrote the custom Matlab scripts to perform one-way ANOVA with 3 conditions (FIX, EMOTION, and WM) for global and nodal properties separately in weighted networks at each threshold. The Bonferroni method was used for all post hoc analyses. Significant effects of $p < 0.001$ were reported.

3. Results

3.1. Connectivity-Based Analysis

3.1.1. EMOTION versus FIX Contrast. The NBS analysis revealed that a single connected network with 18 nodes and 18 edges was altered ($t = 4.60$, $p < 0.0001$, corrected) (Figure 2). Table 1 shows the nodes of the connected network. The involved nodal regions included Default_6, two FrontoParietal nodes (3 and 20), three CinguloOperc nodes (7, 17, and 40), PERN_2, two DorsalAttn nodes (6 and 8), one VentralAttn node (11), two Visual nodes (11, 29, and 34), two SMHand nodes (1 and 35), three SMmouth nodes (6, 7, and 8), and one Auditory node (2). All of the connections exhibited increased values in the EMOTION condition compared with the FIX condition. However, there were no significant connections between Context/Salience/Subcortical nodes and other nodes.

3.1.2. WM versus FIX Contrast. The NBS analysis showed a significant increase of connectivity in the WM condition compared with the FIX condition in a single brain network formed by 20 nodes and 23 edges ($t = 6.40$, $p < 0.0001$, corrected) (Figure 3). The involved nodal regions included two Default nodes (40 and 41), two Context nodes (2 and 7), three CinguloOperc nodes (7, 13, and 14), PERN_2, two DorsalAttn nodes (6 and 8), four Visual nodes (28, 31, 32, and 34), SMHand_35, three SMMouth nodes (6, 7, and 8), and two Auditory nodes (1 and 2). There were no significant connections between FrontoParietal/Salience/VentralAttn/Subcortical nodes and other nodes.

3.2. Nodal Feature Analysis. Figures 4(a)–4(f) show the distribution of the hubs within 305 nodes for 81 subjects at the

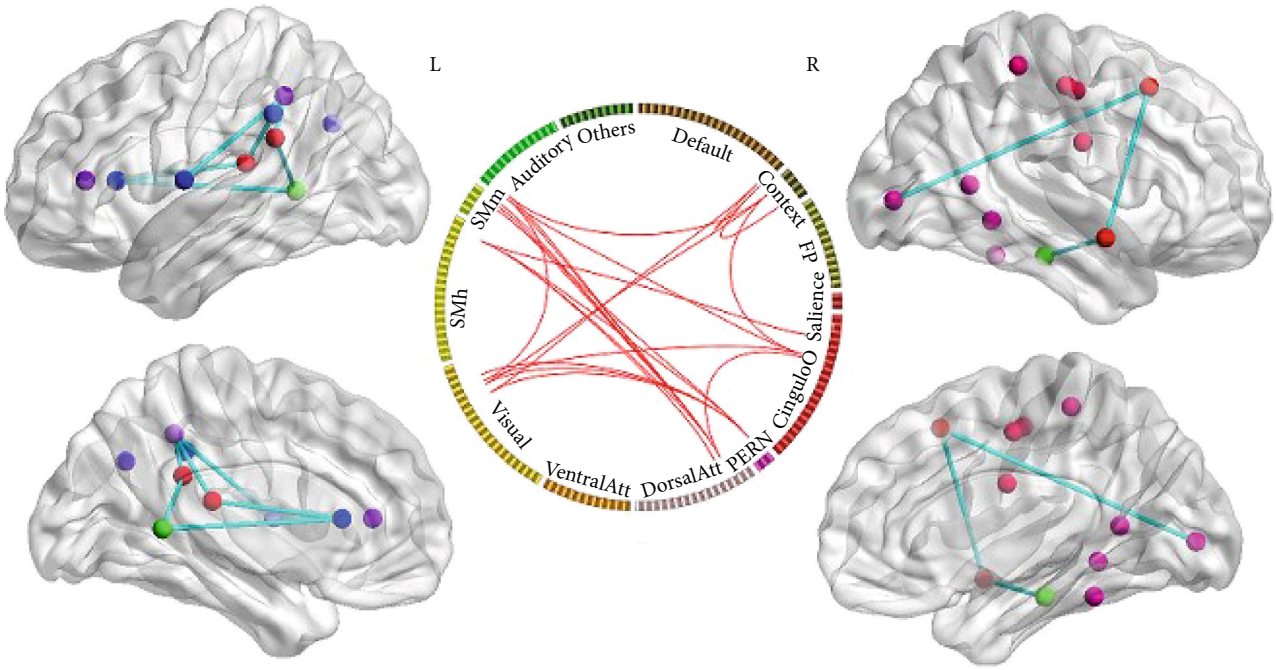

Figure 3: Two-dimension and three-dimension depictions of connectivity analysis result in the WM versus FIX condition. WM: working memory.

threshold of 10%, and Figure 4(g) shows the mean ratio of the hubs across all 305 nodes at the 5-10% threshold. Across each threshold, the number of the nonhubs was approximately 83% while the number of the hubs was approximately 17% in the FIX, EMOTION, and WM networks (Figure 4(g)). On the one hand, FIX networks only included provincial (12.42% ± 0.76%) and connector (4.63% ± 1.08%) hubs (Figures 4(a) and 4(b)) but no kinless hubs; EMOTION networks mainly included connector (12.59% ± 1.08%) and kinless hubs (4.11% ± 1.19%) (Figures 4(c) and 4(d)) but no provincial hubs; WM networks mainly covered kinless (13.72% ± 2.15%) and connector (1.90% ± 2.17%) hubs but no provincial hubs (Figures 4(e) and 4(f)). On the other hand, the ratio of the connector hubs increased with thresholds in FIX networks while the ratio of the kinless hubs increased with thresholds in EMOTION and WM networks. Moreover, ANOVA analyses indicated that the ratio of the connector hubs significantly increased in EMOTION networks relative to FIX and WM networks ($p < 0.001$) while the ratio of the kinless hubs significantly increased in WM networks compared to FIX and EMOTION networks ($p < 0.001$).

When we ignored the hubs whose subject ratio was less than 5%, we found that the Context, Salience, and Subcortical communities did not include any hubs in the FIX condition. The most nodes of these communities shifted from nonhubs in the FIX condition to connector hubs in the EMOTION condition or to kinless hubs in the WM condition. However, Amygdala_1/2, Putamen_1, and Brain Stem became connector hubs only in the EMOTION condition. Additionally, when we considered the nodes as ROIs in Table 1, we found that Default_41, Context_2/7, FrontoParietal_3/20, Visual_28/31/32/34, SMmouth_6, and Auditory_1/2 in the FIX condition shifted from nonhubs of a single role to connector hubs in the EMOTION condition or to kinless hubs in the WM condition (Figure 5). Similarly, Default_6/40, VentralAttn_11, DorsalAttn_8, and SMhand_35 in the FIX condition switched from provincial hubs of a single role to connector hubs in the EMOTION condition or to kinless hubs in the WM condition. PERN_2 and Visual_29 in the FIX and EMOTION condition changed their single role of connector hubs into kinless hubs in the WM condition. However, CinguloOperc_7/13/14/17/40, DorsalAttn_6, SMhand_1, and SMmouth_7/8 in the FIX condition turned their dual roles of provincial/connector hubs into connector hubs in the EMOTION condition or into kinless hubs in the WM condition.

3.3. Global Property Analysis. For FIX, EMOTION, and WM, ANOVA analyses on the global network properties showed significant task effects in global efficiency, transitivity, and assortativity ($p < 0.0001$) (Figure 6). Post hoc comparisons indicated that under the threshold of 5-15%, FIX networks contained greater assortativity values than EMOTION networks while EMOTION networks showed greater assortativity values than WM networks ($p < 0.001$) (Figure 6(a)). Moreover, FIX networks exhibited greater global efficiency than EMOTION networks ($p < 0.001$) while EMOTION networks exhibited greater global efficiency than WM networks ($p < 0.0001$) (Figures 6(b) and 6(d)). Finally, FIX networks had greater transitivity values than EMOTION and WM networks ($p < 0.0001$) while WM networks included greater transitivity values than EMOTION networks ($p < 0.001$) (Figures 6(c) and 6(e)).

4. Discussion

In the present study, we used graph-theoretic approach to analyze the resting-state and task-state (WM and

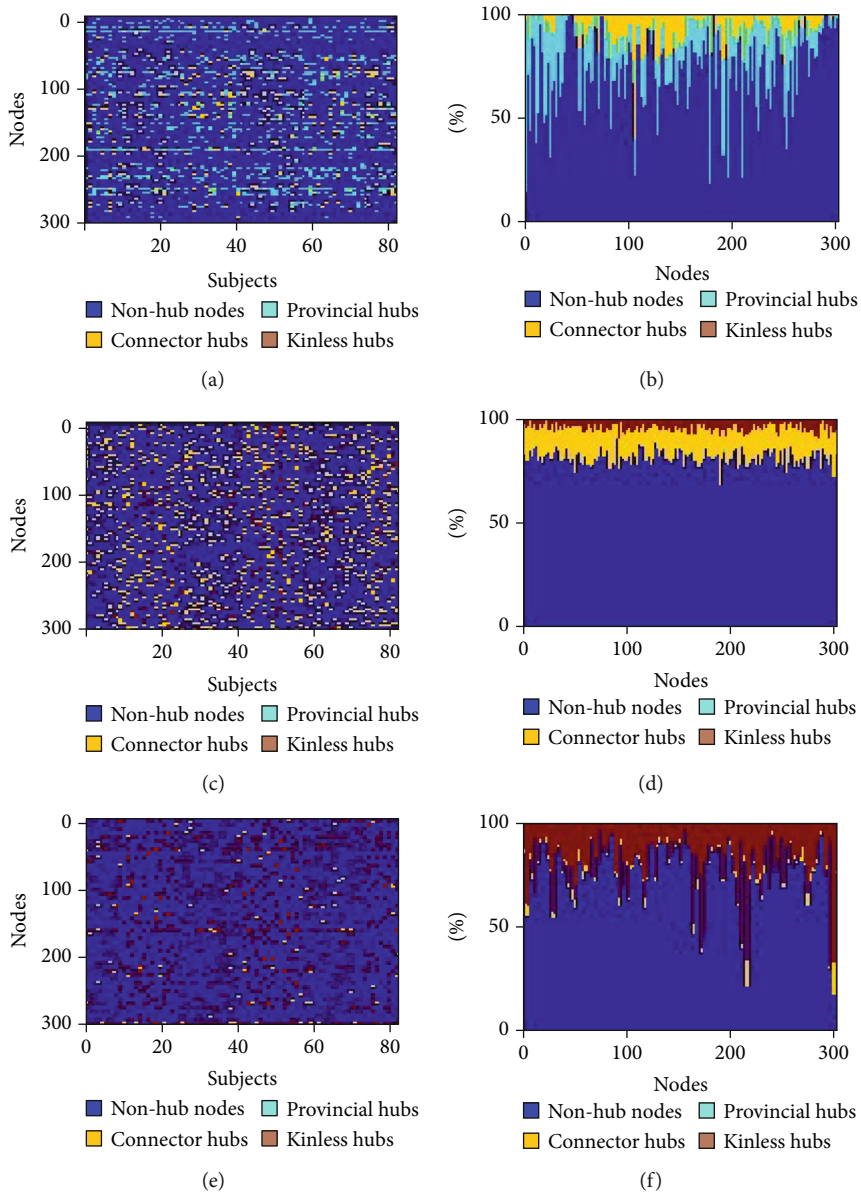

Figure 4: Continued.

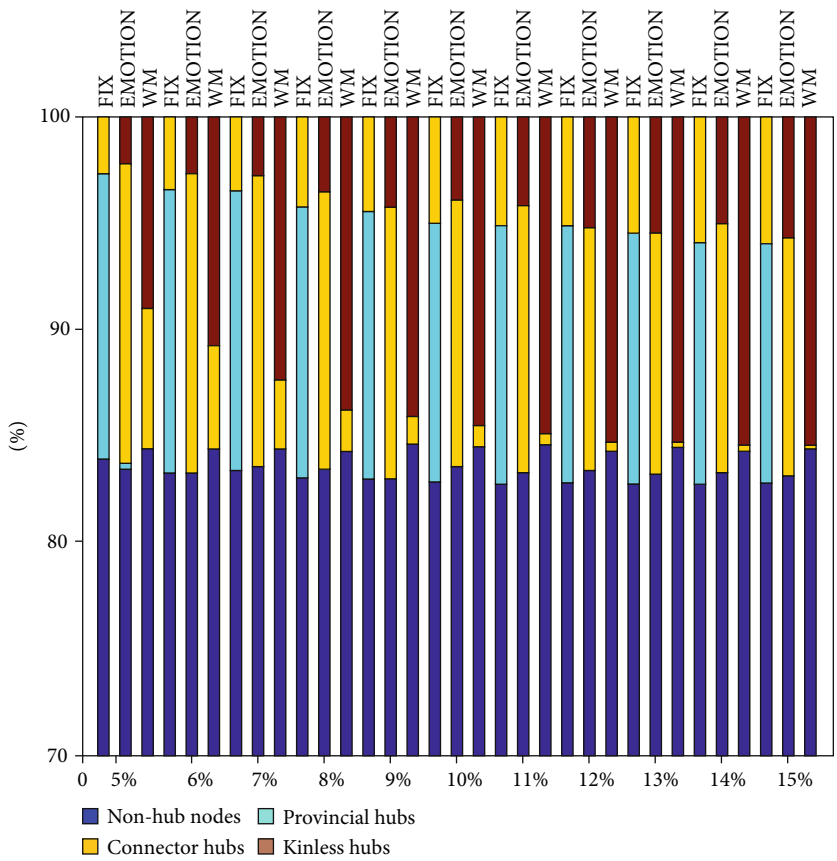

(g)

Figure 4: The hub distribution within 305 nodes for 81 subjects. (a, c, and e) Separately describe the hub distribution of FIX, EMOTION, and WM networks at the threshold of 10%. (b, d, and f) Separately describe the subject ratio of each hub in FIX, EMOTION, and WM networks at the threshold of 10%. (g) Describes the mean ratio of the hubs across all 305 nodes and all subjects at the 5-10% threshold.

EMOTION) fMRI scans of 81 subjects from the HCP to determine how the topological properties of functional networks dynamically change according to task demands. Results indicated that relative to resting state, task demands significantly increase the strength of long-distance connections between modules but not within modules; the number of connector and kinless hubs significantly increases in EMOTION and WM networks while provincial hubs disappeared. Moreover, EMOTION and WM networks seem to become separated: their assortativity is close to zero and both the global efficiency and transitivity decreased. These results suggest that task demands change the architecture of intrinsic functional networks and cause local and global topological properties of functional networks at resting state to redistribute.

4.1. Long-Distance Connections Dominate Intermodular Communication at Task States. The NBS results indicated that the significant increase in connectivity strength occurred between different communities but not within modules at task state versus resting state. Long-distance connections occupy a relatively small ratio in functional networks [18]. However, a small quantity of long-distance connections is necessary to maintain intermodular information communication because long-distance connection shorten the pathway of information transfer but does not significantly increase the wiring cost [3, 20, 47]. Consist with our results, previous MEEG studies also found that task demands (WM and motor performance) promote synchronization between brain networks through long-distance links [34, 40].

Moreover, WM and EMOTION networks show different connectivity patterns. Particularly, the long connection between Defualt_6 (Frontal_Sup_L) and VentralAttn_11 (Temporal_Mid_L) in EMOTION networks significantly increased while the long connections between Default_40/41 (Frontal_Mid_R and Temporal_Sup_R) and Visual_32/34 (Lingual_R and Fusiform_R) significantly increased in WM networks, which is consistent with the flexible reconfiguration in the interactions of DMN with other subnetworks [19]. However, there were no long connections between Subcortical nodes and other modular nodes. This may be partly attributed to very high threshold during the NBS analysis of fully linking networks. Taken together, long-distance connectivity patterns between modules have decisive significance for decoding multiple task-relevant information.

4.2. Connector and Kinless Hubs Dominate Task-State Functional Networks. Consistent with Finc et al. [13], we

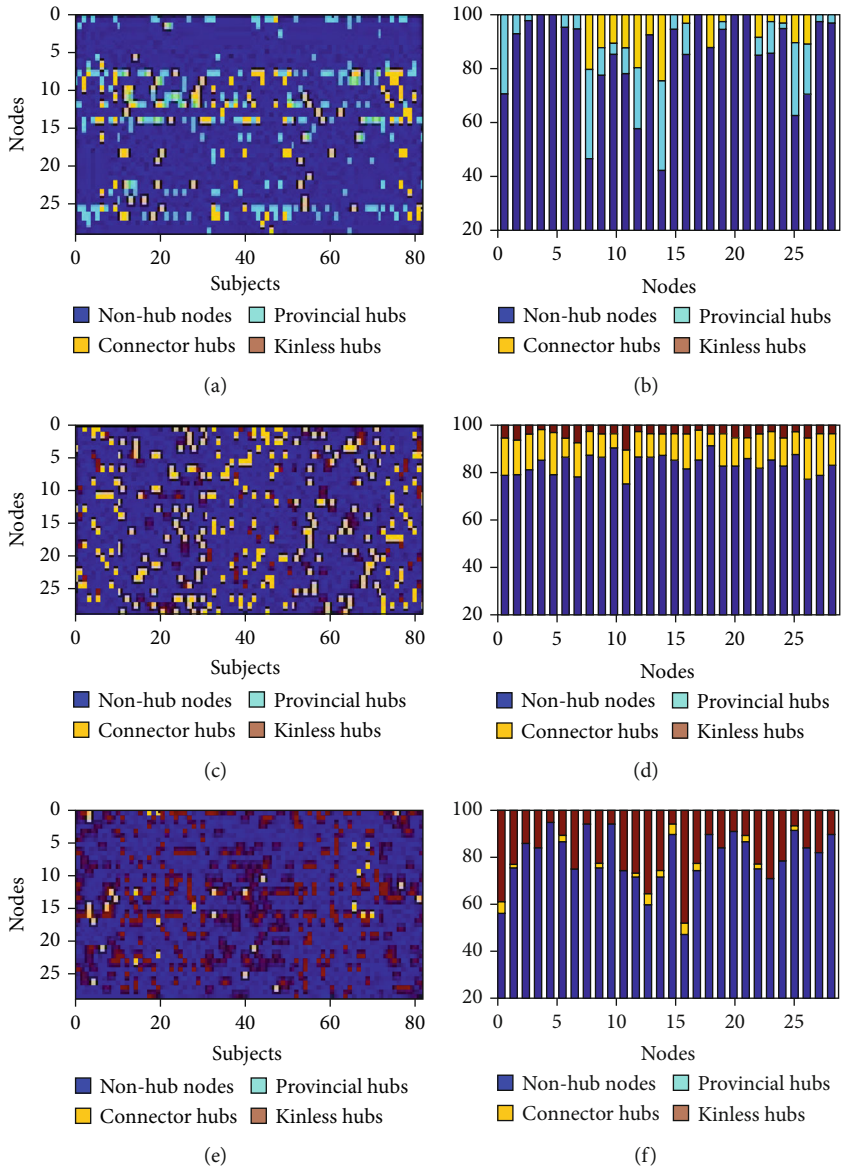

Figure 5: The hub distribution within 28 nodes of FIX (a), EMOTION (c), and WM (e) networks for 81 subjects and the subject ratio of each hub in FIX (b), EMOTION (d), and WM (f) at the threshold of 10%. The nodal order is consistent with Table 1. WM: working memory.

found that the number of connector hubs that have many links to most of the other modules increased in the EMOTION and WM networks relative to the FIX network. To be noted, kinless hubs that have links homogeneously distributing among all modules also increased, particularly in WM networks. However, kinless hubs did not appear in FIX networks, which might explain why kinless hubs were almost ignored in the literature related to functional networks. In addition, provincial hubs that have the vast majority of links within their own module mainly appeared in FIX networks but disappeared in EMOTION and WM networks. The previous MEG research also found that the motor tapping task causes the shift from resting-state networks dominated by provincial hubs to motor networks with a larger number of connector hubs [38]. Thus, consistent with the flexible hub theory [25], task demands need more between-module information communication so that connector and kinless hubs dominate task-state functional networks.

When we neglected the hubs whose subject ratios were less than 5%, the hubs in EMOTION networks mainly consisted of connector hubs while the hubs in WM networks mainly belonged to kinless hubs. This might be attributed to the fact that PI values in WM networks were higher than those in EMOTION networks. This is also consistent with previous results indicating that more task demands need a more globally synchronized system to involve in [40]. Moreover, bilateral Amygdala, the left Putamen, and Brain Stem became connector hubs only in EMOTION networks, consistent with previous results [20, 26, 28–30], which implies that these hubs take a critical role in decoding emotional information. To be noted, in FIX networks, nonhubs (e.g., Defualt_41, Context_2/7, FrontoParietal_3/20, Visual_

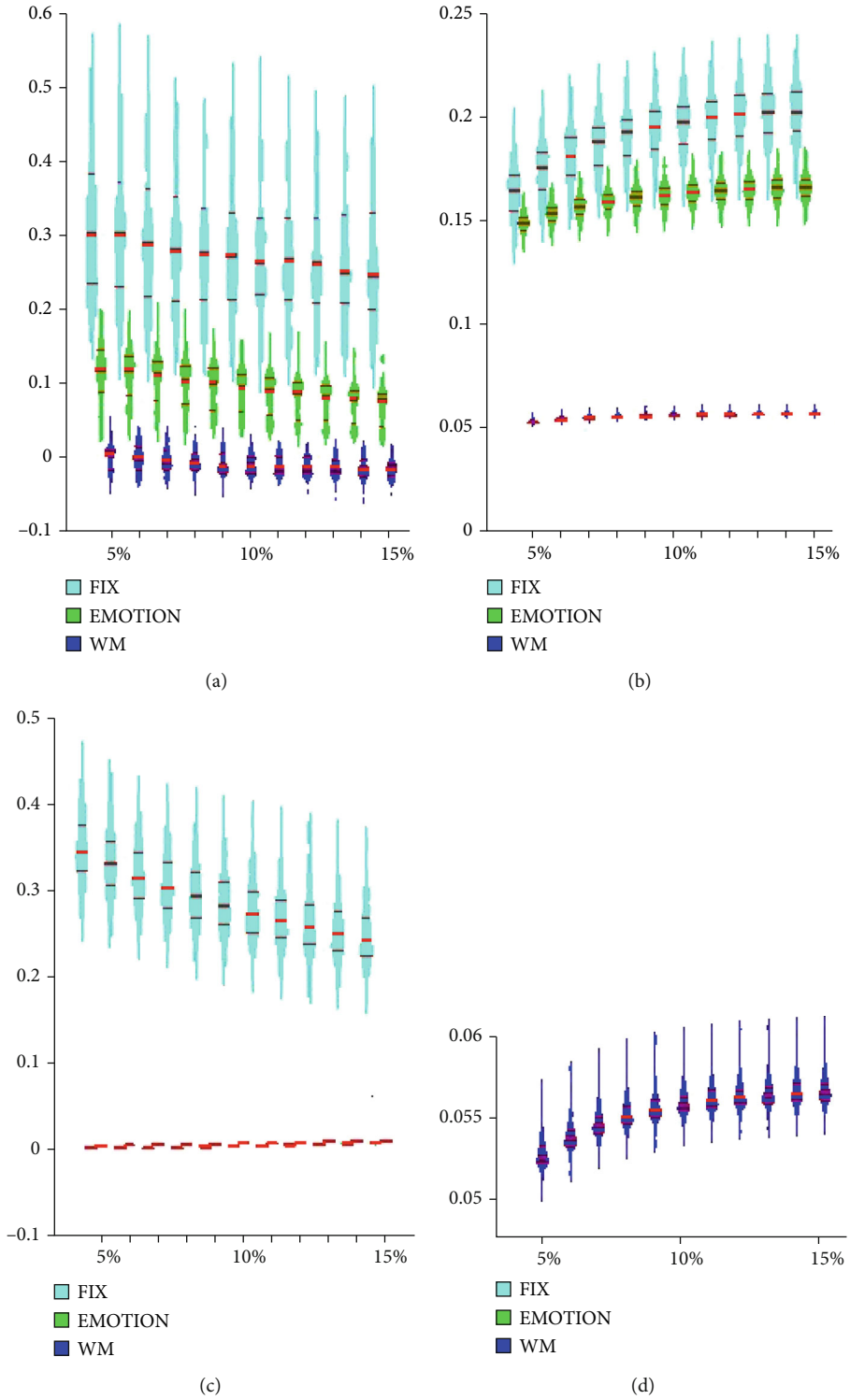

Figure 6: Continued.

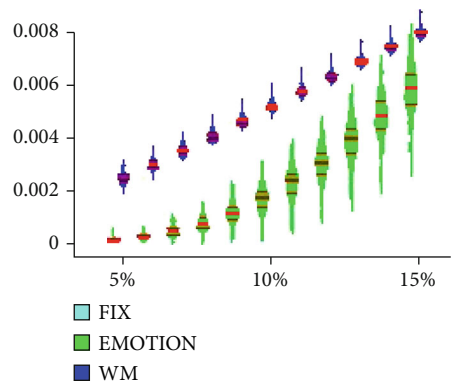

(e)

Figure 6: The ANOVA results of global property analysis for FIX, EMOTION, and WM: (a) assortativity; (b) global efficiency; (c) transitivity; (d) global efficiency graph enlarged for WM; (e) transitivity graph enlarged for EMOTION and WM at the threshold of 10%. WM: working memory.

28/31/32/34, SMmouth_6, and Auditory_1/2) switch to connector hubs in EMOTION networks or kinless hubs in WM networks. These results suggest that task-relevant functional nodes dynamically reconfigure and shift their network roles from within-module to between-module.

4.3. Functional Networks at Task State Tend to Be More Separated Than Those at Resting State. Intrinsic functional networks at resting state represent a standard architecture and maintain the balance between integration and separation, which is evoked by task-relevant network changes [6, 14]. Although less than 24 long-distance connections appeared and less than 17% functional nodes switched their roles in EMOTION and WM as discussed above, the global properties changed significantly. The global efficiency and transitivity significantly decreased in EMOTION and WM versus FIX, which means that task demands cause increase in pathway lengths (e.g., long connections appear) and decrease in clustering coefficients. This is inconsistent with increases in task demands leading to more integrated brain networks [36, 37]. The previous study used a binary network to compute global properties [36] while our study used weighted networks. Undoubtedly, weighted correlation networks occupied more accurate representation than the binary networks.

What is more, the assortativity values reflecting a correlation coefficient between the degrees of all nodes significantly decreased and were close to zero at task state. Similarly, previous results also found that affective networks have negative assortativity and lower global efficiency and exhibit weaker small-worldness [30]. These results suggest that task demands break the balance between local and distant functional couplings at resting state [16] and cause functional networks to reconfigure their topologies. As a result, functional networks at task state tend to become more separated or random, a shift of network architecture to a more random configuration at higher levels of task difficulty [8, 30, 40]. Our result showing that more kinless hubs appeared in WM than in EMOTION networks to some degree provide direct evidence for this opinion. However, functional brain network topology was never completely randomized because of the constraint of structural network [8]. These explanations are not in agreement with previous MEG/EEG results that the clustering coefficient was conserved over a wide range of frequencies and increasing memory load increased clustering coefficient [38, 39]. One possibility is because of the difference in signal measurement nature between fMRI and MEEG. Another possible interpretation is because the previous research absolutized the correlation between wavelet coefficients for each pair of sensors [38] or used EEG phase synchronization (positive and negative value) as a functional connectivity index [39], while the present study only contained positive connections. To clarify these inconsistencies, future studies necessarily combine fMRI with MEEG and select hard- and soft-thresholding approach of functional networks [48].

In summary, task demands break the balance between local and global coupling among brain regions in intrinsic functional networks. Long-distance functional connections dominated intermodular communication of functional networks at task states under high threshold. Correspondently, task-relevant connector or kinless hubs between modules were flexibly redistributed to promote task performance while provincial hubs within modules disappeared. Moreover, task-state networks significantly change their global topologies and tend to become more random. These observations provide important and direct evidences for the understanding of the organization principle behind the functional architecture of task-state networks. To be cautious, it is unclear whether our results can be generalized to other task-state network. Future studies should use more other tasks with other network properties to further confirm our observations.

Data Availability

The data that support the findings of this study are available from the corresponding author upon reasonable request.

Ethical Approval

All procedures performed in the study were in accordance with the ethical standards of both the HCP and the research

committee of Hengyang Normal University and with the 1964 Helsinki declaration and its later amendments or comparable ethical standards.

Consent

Informed consent was obtained from all individual participants included in the study.

Conflicts of Interest

All the authors declared no conflict of interest.

Authors' Contributions

All authors contributed to the study conception and design and performed the material preparation, data collection, and analysis. The first draft of the manuscript was written by Wenhai Zhang, and all authors commented on previous versions of the manuscript. All authors read and approved the final manuscript.

Acknowledgments

This study was funded by the National Natural Scientific Foundation of China (31470997 and 81171289), Jiangsu Provincial Social Science Foundation of China (19JYD009), and Hunan Provincial Natural Science Foundation of China (2018JJ2008).

References

[1] V. Menon, "Large-scale brain networks and psychopathology: a unifying triple network model," *Trends in Cognitive Sciences*, vol. 15, no. 10, pp. 483–506, 2011.

[2] D. van Essen, K. Ugurbil, E. Auerbach et al., "The human connectome project: a data acquisition perspective," *NeuroImage*, vol. 62, no. 4, pp. 2222–2231, 2012.

[3] R. L. Buckner, J. Sepulcre, T. Talukdar et al., "Cortical hubs revealed by intrinsic functional connectivity: mapping, assessment of stability, and relation to alzheimer's disease," *Journal of Neuroscience*, vol. 29, no. 6, pp. 1860–1873, 2009.

[4] D. S. Bassett and O. Sporns, "Network neuroscience," *Nature Neuroscience*, vol. 20, no. 3, pp. 353–364, 2017.

[5] C. Gratton, E. M. Nomura, F. Pérez, and M. D'Esposito, "Focal brain lesions to critical locations cause widespread disruption of the modular organization of the brain," *Journal of Cognitive Neuroscience*, vol. 24, no. 6, pp. 1275–1285, 2012.

[6] M. W. Cole, D. S. Bassett, J. D. Power, T. S. Braver, and S. E. Petersen, "Intrinsic and task-evoked network architectures of the human brain," *Neuron*, vol. 83, no. 1, pp. 238–251, 2014.

[7] A. Fornito, A. Zalesky, and M. Breakspear, "Graph analysis of the human connectome: promise, progress, and pitfalls," *NeuroImage*, vol. 80, pp. 426–444, 2013.

[8] M. Rubinov and O. Sporns, "Complex network measures of brain connectivity: uses and interpretations," *NeuroImage*, vol. 52, no. 3, pp. 1059–1069, 2010.

[9] M. Girvan and M. E. J. Newman, "Community structure in social and biological networks," *Proceedings of the National Academy of Sciences*, vol. 99, no. 12, pp. 7821–7826, 2002.

[10] X. Liang, Q. Zou, Y. He, and Y. Yang, "Coupling of functional connectivity and regional cerebral blood flow reveals a physiological basis for network hubs of the human brain," *PNAS*, vol. 110, no. 5, pp. 1929–1934, 2013.

[11] X. N. Zuo, R. Ehmke, M. Mennes et al., "Network centrality in the human functional connectome," *Cerebral Cortex*, vol. 22, no. 8, pp. 1862–1875, 2012.

[12] R. F. Betzel, J. D. Medaglia, L. Papadopoulos et al., "The modular organization of human anatomical brain networks: accounting for the cost of wiring," *Network Neuroscience*, vol. 1, no. 1, pp. 42–68, 2017.

[13] K. Finc, K. Bonna, M. Lewandowska et al., "Transition of the functional brain network related to increasing cognitive demands," *Human Brain Mapping*, vol. 38, no. 7, pp. 3659–3674, 2017.

[14] C. Gratton, T. O. Laumann, E. M. Gordon, B. Adeyemo, and S. E. Petersen, "Evidence for two independent factors that modify brain networks to meet task goals," *Cell Reports*, vol. 17, no. 5, pp. 1276–1288, 2016.

[15] A. M. Hermundstad, D. S. Bassett, K. S. Brown et al., "Structural foundations of resting-state and task-based functional connectivity in the human brain," *Proceedings of the National Academy of Sciences*, vol. 110, no. 15, pp. 6169–6174, 2013.

[16] J. Sepulcre, H. Liu, T. Talukdar, I. Martincorena, B. T. T. Yeo, and R. L. Buckner, "The organization of local and distant functional connectivity in the human brain," *PLoS Computational Biology*, vol. 6, no. 6, article e1000808, 2010.

[17] X. di, S. Gohel, E. H. Kim, and B. B. Biswal, "Task vs. rest—different network configurations between the coactivation and the resting-state brain networks," *Frontiers in Human Neuroscience*, vol. 7, no. 2, 2013.

[18] N. A. Crossley, A. Mechelli, P. E. Vertes et al., "Cognitive relevance of the community structure of the human brain functional coactivation network," *Proceedings of the National Academy of Sciences*, vol. 110, no. 28, pp. 11583–11588, 2013.

[19] D. Vatansever, D. K. Menon, A. E. Manktelow, B. J. Sahakian, and E. A. Stamatakis, "Default mode dynamics for global functional integration," *Journal of Neuroscience*, vol. 35, no. 46, pp. 15254–15262, 2015.

[20] C. Sripada, M. Angstadt, D. Kessler et al., "Volitional regulation of emotions produces distributed alterations in connectivity between visual, attention control, and default networks," *NeuroImage*, vol. 89, no. 5, pp. 110–121, 2014.

[21] N. T. Markov, M. Ercsey-Ravasz, C. Lamy et al., "The role of long-range connections on the specificity of the macaque interareal cortical network," *Proceedings of the National Academy of Sciences*, vol. 110, no. 13, pp. 5187–5192, 2013.

[22] M. Kaiser and C. C. Hilgetag, "Nonoptimal component placement, but short processing paths, due to long-distance projections in neural systems," *PLoS Computional Biology*, vol. 2, no. 7, article e95, 2006.

[23] A. Zalesky, L. Cocchi, A. Fornito, M. M. Murray, and E. Bullmore, "Connectivity differences in brain networks," *NeuroImage*, vol. 60, no. 2, pp. 1055–1062, 2012.

[24] M. P. V. D. van den Heuvel and A. O. Sporns, "Network hubs in the human brain," *Trends in Cognitive Sciences*, vol. 17, no. 12, pp. 683–696, 2013.

[25] M. W. Cole, J. R. Reynolds, J. D. Power, G. Repovs, A. Anticevic, and T. S. Braver, "Multi-task connectivity reveals

flexible hubs for adaptive task control," *Nature Neuroscience*, vol. 16, no. 9, pp. 1348–1355, 2013.

[26] T. Osada, Y. Adachi, K. Miyamoto, K. Jimura, R. Setsuie, and Y. Miyashita, "Dynamically allocated hub in task-evoked network predicts the vulnerable prefrontal locus for contextual memory retrieval in macaques," *PLoS Biology*, vol. 13, no. 6, article e1002177, 2015.

[27] R. Guimerà and L. A. Nunes Amaral, "Functional cartography of complex metabolic networks," *Nature*, vol. 433, no. 7028, pp. 895–900, 2005.

[28] U. Braun, A. Schäfer, H. Walter et al., "Dynamic reconfiguration of frontal brain networks during executive cognition in humans," *Proceedings of the National Academy of Sciences*, vol. 112, no. 37, pp. 11678–11683, 2015.

[29] K. A. Lindquist and L. F. Barrett, "A functional architecture of the human brain: emerging insights from the science of emotion," *Trends in Cognitive Sciences*, vol. 16, no. 11, pp. 533–540, 2012.

[30] W. Zhang, H. Li, and X. Pan, "Positive and negative affective processing exhibit dissociable functional hubs during the viewing of affective pictures," *Human Brain Mapping*, vol. 36, no. 2, pp. 415–426, 2015.

[31] O. Sporns, "The human connectome: a complex network," *Annals of the New York Academy of Sciences*, vol. 1224, no. 1, pp. 109–125, 2011.

[32] B. M. Tijms, P. Seriès, D. J. Willshaw, and S. M. Lawrie, "Similarity-based extraction of individual networks from gray matter mri scans," *Cerebral Cortex*, vol. 22, no. 7, pp. 1530–1541, 2012.

[33] C. Yan, G. Gong, J. Wang et al., "Sex- and brain size-related small-world structural cortical networks in young adults: a DTI tractography study," *Cerebral Cortex*, vol. 21, no. 2, pp. 449–458, 2011.

[34] D. S. Bassett, E. T. Bullmore, A. Meyer-Lindenberg, J. A. Apud, D. R. Weinberger, and R. Coppola, "Cognitive fitness of cost-efficient brain functional networks," *Proceedings of the National Academy of Sciences*, vol. 106, no. 28, pp. 11747–11752, 2009.

[35] O. Sporns and C. J. Honey, "Small worlds inside big brains," *Proceedings of the National Academy of Sciences*, vol. 103, no. 51, pp. 19219-19220, 2006.

[36] M. Alavash, P. Doebler, H. Holling, C. M. Thiel, and C. Gießing, "Is functional integration of resting state brain networks an unspecific biomarker for working memory performance?," *NeuroImage*, vol. 108, pp. 182–193, 2015.

[37] A. Fornito, J. Yoon, A. Zalesky, E. T. Bullmore, and C. S. Carter, "General and specific functional connectivity disturbances in first-episode schizophrenia during cognitive control performance," *Biological Psychiatry*, vol. 70, no. 1, pp. 64–72, 2011.

[38] D. S. Bassett, A. Meyer-Lindenberg, S. Achard, T. Duke, and E. Bullmore, "Adaptive reconfiguration of fractal small-world human brain functional networks," *Proceedings of the National Academy of Sciences*, vol. 103, no. 51, pp. 19518–19523, 2006.

[39] L. Li, J. X. Zhang, and T. Jiang, "Visual working memory load-related changes in neural activity and functional connectivity," *PLoS One*, vol. 6, no. 7, article e22357, 2011.

[40] M. G. Kitzbichler, R. N. A. Henson, M. L. Smith, P. J. Nathan, and E. T. Bullmore, "Cognitive effort drives workspace configuration of human brain functional networks," *Journal of Neuroscience*, vol. 31, no. 22, pp. 8259–8270, 2011.

[41] M. F. Glasser, S. N. Sotiropoulos, J. A. Wilson et al., "The minimal preprocessing pipelines for the Human Connectome Project," *NeuroImage*, vol. 80, pp. 105–124, 2013.

[42] A. R. Hariri, A. Tessitore, V. S. Mattay, F. Fera, and D. R. Weinberger, "The amygdala response to emotional stimuli: a comparison of faces and scenes," *NeuroImage*, vol. 17, no. 1, pp. 317–323, 2002.

[43] D. M. Barch, G. C. Burgess, M. P. Harms et al., "Function in the human connectome: task-fMRI and individual differences in behavior," *NeuroImage*, vol. 80, pp. 169–189, 2013.

[44] H. Cao, M. M. Plichta, A. Schäfer et al., "Test-retest reliability of fMRI-based graph theoretical properties during working memory, emotion processing, and resting state," *NeuroImage*, vol. 84, pp. 888–900, 2014.

[45] E. M. Gordon, T. O. Laumann, B. Adeyemo, J. F. Huckins, W. M. Kelley, and S. E. Petersen, "Generation and evaluation of a cortical area parcellation from resting-state correlations," *Cerebral Cortex*, vol. 26, no. 1, pp. 288–303, 2015.

[46] M. Rubinov and O. Sporns, "Weight-conserving characterization of complex functional brain networks," *NeuroImage*, vol. 56, no. 4, pp. 2068–2079, 2011.

[47] L. F. Barrett and A. B. Satpute, "Large-scale brain networks in affective and social neuroscience: towards an integrative functional architecture of the brain," *Current Opinion in Neurobiology*, vol. 23, no. 3, pp. 361–372, 2013.

[48] A. J. Schwarz and J. Mcgonigle, "Negative edges and soft thresholding in complex network analysis of resting state functional connectivity data," *NeuroImage*, vol. 55, no. 3, pp. 1132–1146, 2011.

Hindawi
Neural Plasticity
Volume 2020, Article ID 8866187, 22 pages
https://doi.org/10.1155/2020/8866187

Research Article

GPER-Deficient Rats Exhibit Lower Serum Corticosterone Level and Increased Anxiety-Like Behavior

Yi Zheng,[1,2] Meimei Wu,[2] Ting Gao,[2] Li Meng,[2] Xiaowei Ding,[2] Youqiang Meng,[1] Yingfu Jiao,[3] Ping Luo,[2] Zhenquan He,[4] Tao Sun,[4] Guohua Zhang,[2] Xueyin Shi,[1] and Weifang Rong[1,2,4]

[1]*Department of Anesthesiology, Xinhua Hospital, Shanghai Jiaotong University School of Medicine, Shanghai, China*
[2]*Department of Anatomy and Physiology, Shanghai Jiaotong University School of Medicine, Shanghai, China*
[3]*Department of Anesthesiology, Renji Hospital, Shanghai Jiaotong University School of Medicine, Shanghai, China*
[4]*Key Laboratory of Cerebrocranial Diseases, Ningxia Medical University, Yinchuan 750004, China*

Correspondence should be addressed to Xueyin Shi; shixueyin1128@163.com and Weifang Rong; weifangrong@shsmu.edu.cn

Received 7 May 2020; Revised 3 June 2020; Accepted 11 June 2020; Published 28 August 2020

Academic Editor: Fushun Wang

Ample evidence suggests that estrogens have strong influences on the occurrence of stress-related mood disorders, but the underlying mechanisms remain poorly understood. Through multiple approaches, we demonstrate that the G protein-coupled estrogen receptor (GPER) is widely distributed along the HPA axis and in brain structures critically involved in mood control. Genetic ablation of GPER in the rat resulted in significantly lower basal serum corticosterone level but enhanced ACTH release in response to acute restraint stress, especially in the female. GPER$^{-/-}$ rats of either sex displayed increased anxiety-like behaviors and deficits in learning and memory. Additionally, GPER deficiency led to aggravation of anxiety-like behaviors following single-prolonged stress (SPS). SPS caused significant decreases in serum corticosterone in WT but not in GPER-deficient rats. The results highlight an important role of GPER at multiple sites in regulation of the HPA axis and mood.

1. Introduction

Women are at least twice as likely to develop mood disorders such as anxiety, depression, and posttraumatic stress syndromes [1–3]. Such gender-related differences in the occurrence of mood disorders manifest after puberty, implicating an important role of the female hormone estrogens in modulation of anxiety [4, 5]. Indeed, numerous clinical and preclinical observations have indicated a strong interaction between mood and estrogen levels in females. Paradoxically, however, in most human studies, high and constant estrogen levels have been described as anxiolytic and "emotionally positive," whereas low or fluctuating estrogen levels have been shown to correlate with increased anxiety [6–8]. Similarly, in rodents, low estrogen levels have been associated with increased anxiety and exogenous estrogen administration has been shown to alleviate anxiety [9–13]. These findings suggest that estrogens may play important but complicated roles in the regulation of mood. Understanding the mechanisms of estrogenic actions in mood regulation may be important for the prevention and effective management of mood disorders, particularly in the female population.

Mood disorders are closely related to abnormalities in the stress responses, which are also sex-biased and are modulated by estrogens [14, 15]. It has been well documented that stressful events trigger negative emotions with greater intensity in women than in men [16, 17], which may be attributable to differences in the corticolimbic circuitry comprising the amygdala, prefrontal cortex and the hippocampal formation [18, 19]. The autonomic and neuroendocrine responses to stress are also sex-biased, such that females generally have

higher basal glucocorticoid levels and greater increases in glucocorticoid release in response to stress than males, whereas basal and stress-induced adrenaline release is lower in females than in males [2, 20].

Until now, at least three types of estrogen receptors have been identified: the nuclear receptors ERα and ERβ, which mediate slow genomic effects, and the G protein-coupled estrogen receptor (GPER or GPER-1, formerly known as GPER30), which mediates rapid nongenomic effects [21]. The distribution of ERα and ERβ within the CNS and their roles in sex-biased stress responses or mood disorders have been studied extensively, with recent evidence suggesting sex-specific involvement of ERα and ERβ in behavioral responses to stress [22]. ERβ likely plays an anxiolytic role since E2 had an antianxiety effect in wild-type but not in ERβ knockout mice [23]. It has also been reported that serum concentration of corticosterone was increased in ERβ knockout mice [24], whilst ERα knockout mice had similar serum corticosterone level as WT mice at least in the male [25].

On the other hand, the involvement of GPER in sex-biased stress responses has not been as vigorously investigated, although immunohistochemical mapping indicated widespread distribution of GPER in the CNS. High-level expression of GPER or GPER mRNA has been reported in the cortical, the hippocampus, the amygdala, and the hypothalamus, but the results were not always consistent [26–28]. Moreover, although several studies have implicated GPER in the modulation of anxiety, there have been conflicting reports as to whether this receptor is anxiogenic or anxiolytic. For example, Hart et al. reported that systematic application of the GPER agonist G-1 led to a decrease in anxiety-like behavior in gonadectomized male mice without significant effect in ovariectomized female mice [29]. In contrast, Kastenberger et al. reported an increase in anxiety-like behavior following systematic G-1 treatment in ovariectomized mice and intact male mice in the elevated plus maze and open field test [30]. A subsequent follow-up study by the same group revealed a phenotype of reduced anxiety-like behavior in male but not female GPER knockout mice [31]. Therefore, further studies are needed in order to determine the distribution of GPER in the CNS and its role in the regulation of stress response and anxiety.

In the current investigation, complementary measures were taken to systematically analyze the distribution of GPER in the corticolimbic circuit and the HPA axis. The possible role of GPER in the regulation of anxiety-like behaviors and the HPA axis was explored using GPER-deficient (GPER$^{-/-}$) rats. Our results indicate that GPER is anatomically positioned to influence the cognitive, autonomic, and neuroendocrine responses to stress and plays prominent roles in the regulation of anxiety.

2. Material and Methods

2.1. Animals. Gper-Cre transgenic mice were generated in Shanghai Model Organisms Inc. (Shanghai) with a knock-in of the 2A-Cre gene fragment into the GPER gene stop codon based on CRISPR/Cas9 system. GPER reporter (GPER Cre/tdTomato) mice were obtained by crossing the Gper-Cre mice with Ai14(RCL-tdT)-D mice. GPER-deficient Sprague Dawley (SD) rats (GPER$^{-/-}$ rats, with a 139 bp deletion of GPER gene, Gene ID 171104) were generated through the CRISPR/Cas9 gene-editing approach in BIORAY BIOTECHNOLOGY (Shanghai, China), which has been described previously [32]. Age-matched WT SD rats were provided by Shanghai Jiaotong University School of Medicine. The animals were housed (5 per cage) in an air-conditioned room (23°C with 60% humidity) with a 12 h light-dark cycle (lights on 7 a.m. to 7 p.m.) and free access to food and water. Cages were changed weekly and no more than 48 h before any behavioral test. All the experimental procedures were in compliance with the Guiding Principles in the Care and Use of Animals and the Animal Management Rule of the Ministry of Public Health, People's Republic of China (documentation 545, 2001), and had been approved by the Institutional Ethic Committee for Experimental Use of Animals of Shanghai Jiaotong University School of Medicine (document #SYXK-2013-0050). Every effort was taken to minimize the number of animals used.

2.2. Ovariectomy. Bilateral ovariectomy (OVX) was performed on a group of female rats at the age of 8 weeks under anesthesia (ketamine 25 mg/kg, ip for induction, and 2% sevoflurane for maintenance of anesthesia) and aseptic condition. Their back was cleaned and shaved, and a 1 cm incision was made in the skin. Incisions were made bilaterally in the muscle above the ovaries, the ovaries were drawn out and clamped at the uterus, and the ovary was incised above the clamp. The uterus was then put back into the abdominal cavity, and the incision in the skin was closed with 1 or 2 MikRon wound clips (MikRon Precision Inc., Gardena, CA). A single dose of 2 mg/kg meloxicam was administered for postsurgical analgesia. Rats were single housed following surgery and were allowed 2 weeks of recovery before behavior tests.

2.3. Single-Prolonged Stress (SPS) Model. Eight-week-old GPER$^{-/-}$ and WT rats of either sex were randomly assigned to the SPS or control groups. SPS rats were exposed to three consecutive stressors: two hours of restraint, followed by 20 min of forced swimming and 5 min of general anesthesia with sevoflurane. Rats were then returned to their home cages for a 14-day quiescent period. The control groups were left undisturbed in their home cages for the duration of the experiment.

2.4. Immunofluorescence and Nissl Staining. Adult (16 weeks of age) WT or GPER$^{-/-}$ rats or mice were euthanized by an overdose of sodium pentobarbital and were immediately perfused with phosphate-buffered saline (PBS) followed by 4% paraformaldehyde (PFA). The brain was dissected out and postfixed in 4% PFA. After fixation, the tissue was dehydrated in 30% sucrose solution for 24 h and embedded in OCT on the dry ice. For immunofluorescence, the brain was cut into 15 μm thick coronal sections. Sections were blocked with 5% normal donkey serum (NDS, Interchim) in PBS for 1 h and were then incubated with the primary antibodies (anti-GPER, 1 : 300, #A4272, Lifespan, Seattle, WA;

anti-S100β, 1 : 300, #ab52642, Abcam, Cambridge, MA) diluted in PBS containing 1% NDS. Sections were washed 4 times with PBS, then incubated with the secondary antibodies (Alexa Fluor-conjugated goat anti-rabbit IgG, 1 : 1000, #A11304, Invitrogen, Carlsbad, CA) for 2 h at room temperature. Sections were examined with a LEICA DM 2500 microscope equipped for epifluorescence. Nissl staining was conducted on 30 μm brain slices following the protocol described by Mantamadiotis et al. [33].

2.5. GPER RNAscope In Situ Hybridization

2.5.1. Tissue Preparation. WT or GPER Cre/tdTomato mice were euthanized by an overdose of sodium pentobarbital and were perfused transcardially with normal saline and 4% PFA (freshly prepared with PBS). Tissues (brain, pituitary, adrenal gland, or sympathetic ganglia) were collected and postfixed in 4% PFA at 4°C for 24 h, thereafter transferred to 30% sucrose solution until the tissues sank to the bottom of the container. The tissues were embedded with OCT and stored at -80°C. For GPER RNAscope in situ hybridization, the tissue mass was equilibrated at -20°C for at least 1 h and was subsequently cut into 15 μm thick sections using a cryostat. Tissue sections were mounted onto slides, equilibrated at -20°C for 20 min, and then dried at 60°C for 30 min. The sections were then fixed in freshly prepared 4% PFA for 15 min, washed in PBS for 5 min to remove OCT, treated with hydrogen peroxide for 10 min, and subsequently washed with distilled water. The slides were submerged into the target repair reagent (preheated to 98-102°C) for 5 min, washed with distilled water 3 times, treated with 100% ethanol for 3 min, and then dried at room temperature. The tissue sections were covered with Drop protease III reagent, and the slides were left in HybEZ™ hybrid oven (40°C, preheated for 30 min) for 20 min. The slides were washed with distilled water 3 times.

2.5.2. RNAscope® In Situ Hybridization. RNAscope® multichannel fluorescent second generation kit (cat. 323100), customized double Z oligonucleotide probes including Probe-Mm_gpr30 (cat.318191), Duplex Positive Control Probe (cat. 321651), and 2-plex Negative Control Probe (cat. 320751) were all purchased from Advanced Cell Diagnostics (ACD, USA). Opal fluorescent dye (Opal520) was from PerkinElmer. We followed the instructions accompanying the kit to carry out target probe hybridization (only one probe is used for each tissue section), hybridization signal amplification, and probe signal marking using Opal520. Sections were examined under a LEICA DM 2500 microscope.

2.6. Determination of Serum Levels of Stress Hormones. Rats were killed by decapitation. Blood samples were collected in blank EP tubes (for serum separation) or in EP tubes containing aprotinin 0.6 TIU/ml and saturated EDTA-Na2 (for plasma separation). For serum separation, the blood samples were kept at 4°C overnight and then centrifuged (1500 rpm) at 4°C for 20 min. For plasma separation, the blood samples were immediately centrifuged (1500 rpm) at 4°C for 20 min. Serum and plasma were collected into new EP tubes and stored at -80°C until assay.

Serum levels of endogenous corticosterone, 17β-estradiol, and adrenaline were determined by liquid chromatography-mass spectrometry (LC-MS). Briefly, 100 μl serum was added to 400 μl precooled acetonitrile and vortexed for 30 s. The mixture was centrifuged for 10 min at 4°C, 150000 g, and the supernatant was vacuum dried and redissolved in 150 μl of 50% acetonitrile solution. After being vortexed for 60 s, the sample was centrifuged for 10 min (150000 g, 4°C). 100 μl of the supernatant was collected, filtered through a 0.22 μm filter, and then entered into liquid chromatography tandem mass spectrometry for quantitative analysis. Concentration of corticosterone, estradiol, and adrenaline in each sample was extrapolated from their respective standard curves (10, 20, 50, 100, 200, 500, and 1000 ng/ml for corticosterone and adrenaline; 0.2, 1, 2, 5, 10, 20, 50, and 100 ng/ml for estradiol).

Plasma levels of peptide hormones were determined by ELISA. The detection sensitivity of the ELISA kits (all from Phoenix Pharmaceuticals, Inc., Burlingame, CA, USA) was 0.33 ng/ml for CRH (cat. EK-022-33), 0.08 ng/ml for ACTH (cat. EK-001-21), 0.04 ng/ml for AVP (cat. EK-065-07), and 0.17 ng/ml for β-endorphin (cat. EK-022-33).

2.7. Elevated Plus Maze (EPM) Test. The EPM consisted of 4 arms, forming the shape of a plus, elevated 70 cm above the floor. Two opposing arms were closed by black walls; the other two arms were open. All four arms were connected by a neutral field. The dimensions were 30 × 5 cm for the arms and 5 × 5 cm for the neutral field, and the framing of the closed arm had a height of 15 cm. Illumination in the neutral field was set to 180 lx. Each rat was placed gently on the neutral field facing an open arm and allowed to explore the maze for 5 min. The time spent and the number of entries into the open arm were taken as measures of trait anxiety levels.

2.8. Open Field Test. The test apparatus was a 70 × 70 cm synthetic box. The arena was divided into 3 areas. The border area was 15 cm from the wall, the center (25 × 25 cm) covered 13% of the total area, and the area in-between was the intermediate zone. Illumination was set to 150 lx in the center of the open field. When tested, each rat was placed in the middle of the open field and recorded for 5 min. The time the rat spent, the distance traveled, and the number of visits to the center of the open field were taken as measures of anxiety levels.

2.9. Morris Water Maze. A white circular tank (150 cm in diameter, 80 cm in height) was filled with water (24°C, 60 cm in height) and was surrounded by a variety of extra maze cues. The tank was divided into four quadrants, and four start positions were located at the intersections of the quadrants. A platform (10 cm in diameter, 2 cm beneath the water) was placed singly in the center of the quadrants. Data were recorded using an automated tracking system. The protocols include the following. (1) Adaptive training: one day before the experiment, animals were forced to swim in the water without platform twice (90 s each time). (2) Positioning navigation: the experiment lasted five days. On each testing

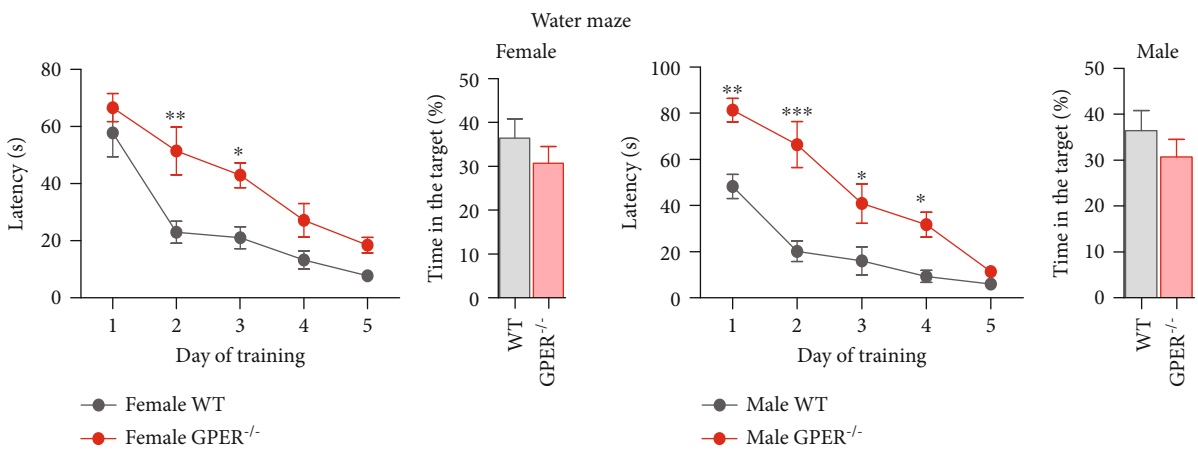

(a)

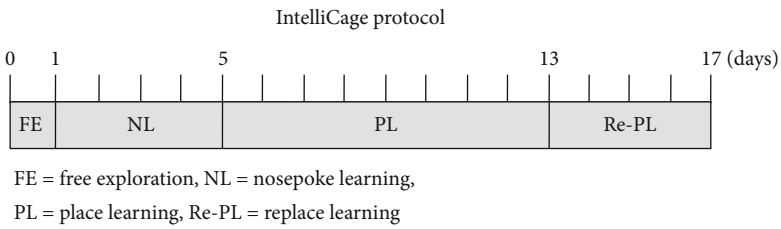

(b)

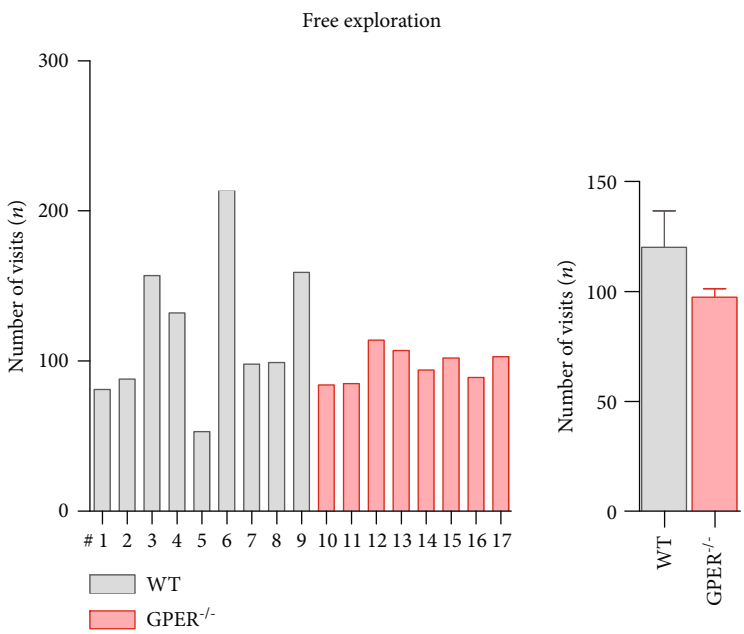

(c)

Figure 1: Continued.

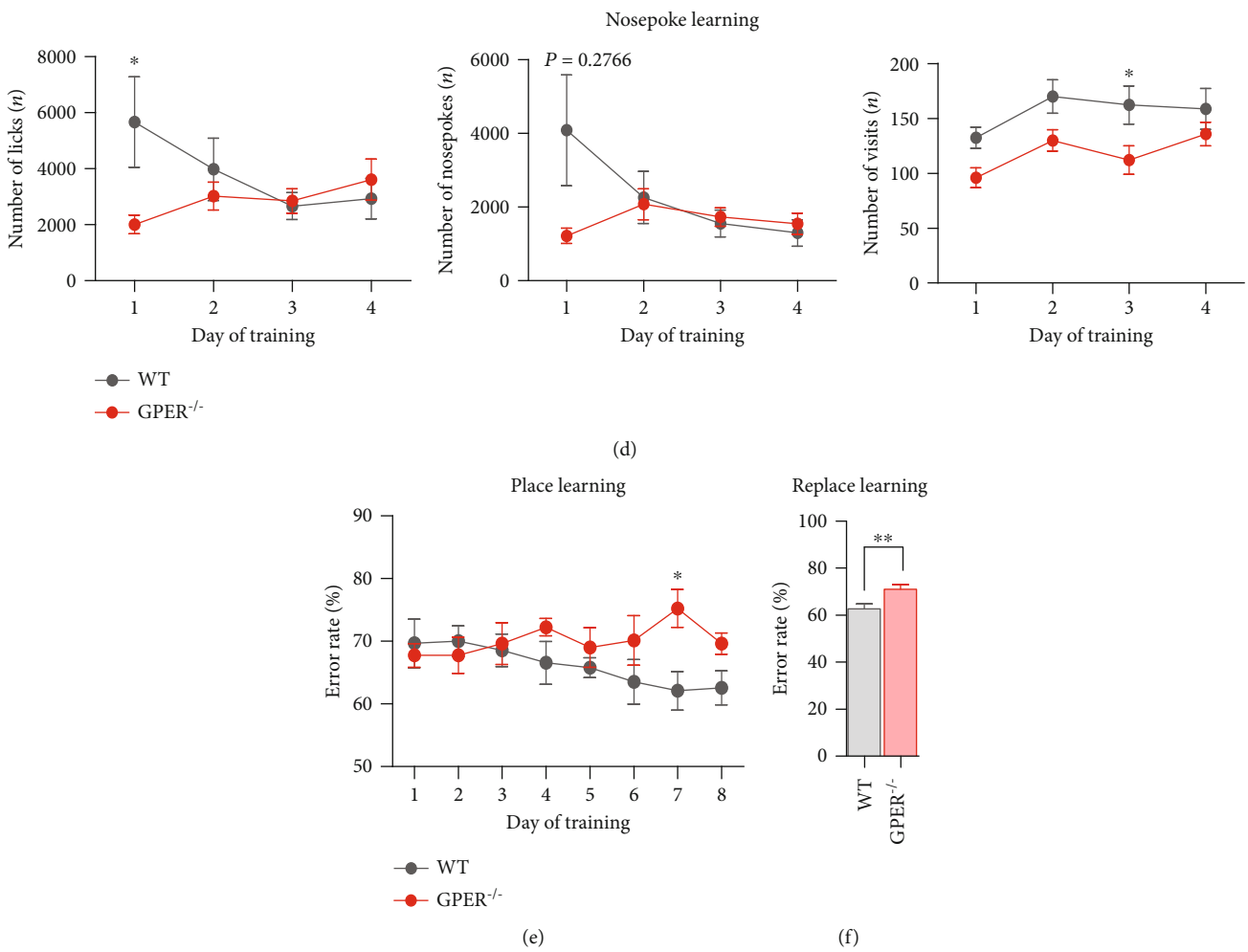

Figure 1: GPER-deficient rats exhibit deficits in learning and memory. (a) Comparison of the latency to find the platform and the percentage of time in the target quarter in Morris water maze test between WT and GPER$^{-/-}$ rats ($n = 7$ for each group). Note that in the positioning navigation period, GPER$^{-/-}$ rats spent more time to find the platform than WT rats. (b) Protocol of the IntelliCage test to evaluate learning and memory of female WT ($n = 9$) and GPER$^{-/-}$ ($n = 8$) rats. (c) Comparison of the number of corner visits in IntelliCage free exploration (FE) period between female WT and GPER$^{-/-}$ rats. The left panel shows the number of corner visits of individual rats, and the right panel shows the averaged number of corner visits of WT and GPER$^{-/-}$ rats. (d) Comparison of the number of licks, nosepokes, and visits in the nosepoke learning (NL) period between female WT and GPER$^{-/-}$ rats. Note that GPER$^{-/-}$ rats showed fewer number of licks, nosepokes, and visits than WT rats, indicating decreased basic skill learning ability. (e) Comparison of the error rate of corner visits in the place learning (PL) period between WT and GPER$^{-/-}$ rats, with the GPER$^{-/-}$ group showing higher error rate of corner visits. (f) Comparison of the error rate of corner visits in the replace learning (Re-PL) period between WT and GPER$^{-/-}$ rats, with the GPER$^{-/-}$ rats showing higher error rate than WT rats. $*P < 0.05$, $**P < 0.01$, and $***P < 0.001$, unpaired t-test.

day, the rat was put into the water atone quadrant facing the wall of the pool. When the rat found the platform, it was allowed to stand on the platform for 30 s. The rat was then taken off the platform and allowed to rest for 60 s. The experiment was repeated three times by placing the rat into the water at another random quadrant. If the platform could not be found within 90 s, the rat was guided to the platform and rested for 30 s, and the latency was recorded as the highest score of 90 s. The time of rats finding the platform (escape latency) was recorded. (3) Space exploration: on the sixth day, the platform was withdrawn and the rats were placed into the pool at random in a quadrant; the time of rats swimming in the quadrant of the platform within 90 s was recorded.

2.10. IntelliCage. IntelliCage was used to study individual animal's behaviors related to anxiety, learning, and memory in a social environment. Before the test, each rat (WT or GPER$^{-/-}$) was implanted with a unique microchip, allowing individual animal's behavior to be registered. The cage ($140 \times 140 \times 45$ cm) is equipped with four operant conditioning chambers located in each corner. Each conditioning chamber contains two drinking bottles accessible by a small opening containing a transponder reader antenna that registers the microchip of the entering rat. Access to each water bottle is controlled by a nosepoke hole containing infrared beam-break sensors, which can be programmed to open or remain closed upon visit or nosepoke. There is also a high-pressure jet at the opening

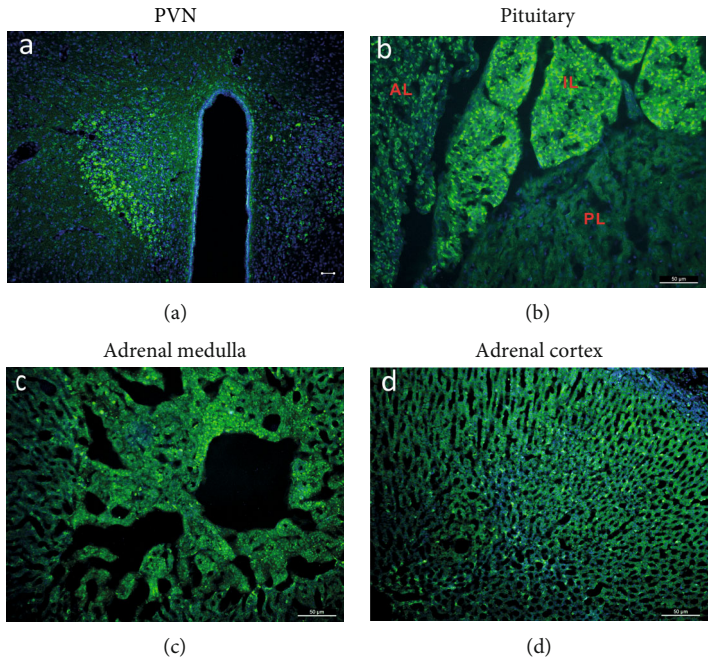

Figure 2: GPER immunoreactivity along the HPA axis in the rat. (a) GPER immunofluorescence (green) in the PVN. (b) GPER immunofluorescence in pituitary (AL = anterior lobe; IL = intermediate lobe; PL = posterior lobe). Note that GPER is enriched in the intermediate lobe (IL) of pituitary. (c) GPER immunofluorescence in the adrenal medulla. (d) GPER immunofluorescence in the adrenal cortex. Horizontal bars = 50 μm.

of each corner, which can punitively spray animals when needed.

2.10.1. Learning and Memory-Related Behavior Test. Ten-week-old female GPER$^{-/-}$ ($n = 8$) and WT ($n = 9$) rats were transferred to the IntelliCage, which was programmed to study learning and memory-related behaviors over a period of 17 days, consisting of the following (Figure 1(b)):

(1) Free exploration, in which animals were allowed to get familiar with the cage environment for 1 day: all doors were opened so animals have free access to the water bottle. The numbers of corner visits were counted to assess the exploratory activity and corner preference

(2) Nosepoke learning, which lasted for 4 days: all doors were closed and rats must complete the nosepoke to open the door to access water. The numbers of corner visits and nosepokes were counted to assess the exploratory activity and corner preferences

(3) Place learning, which lasted for a total of 8 days: the rat's least preferred corner of the nosepoke learning period was designated as "correct," whilst the remaining corners were designated as "error." All rats were able to visit all the corners, but only when the corner was "correct," the door could be opened and drinking allowed. The place learning ability was measured by calculating the number of correct corner visits

(4) Replace learning, which lasted for 4 days: the opposite corner of the "correct" corner in the position learning was designated as the new "correct" corner and the remaining corners were designated as "error." Rats were allowed to visit all corners freely. Replace learning ability was measured by calculating the number of correct corner visits

2.10.2. Anxiety-Related Behavior Test. Another cohort of ten-week-old female GPER$^{-/-}$ ($n = 6$) and WT ($n = 9$) rats were transferred to the IntelliCage, which was programmed for evaluation of anxiety-like behaviors as follows:

(1) Training period: in the first two days, rats were forbidden to drink water for 20 h each day (01:00-21:00) and then allowed to drink water for 4 h (21:00-01:00) but only in a specific corner

(2) Testing period: in this stage, rats were forbidden to drink water for 20 h each day (01:00-21:00) and then allowed to drink for 4 h (21:00-01:00) in a specific corner. Each animal received a punitive air puff the first time it accessed water each day. This was repeated for 3 days. The average drinking latency (latency between the second drink and the first drink) and the average number of corner visits within the 4 h drinking period over the 3 days were calculated to measure the anxiety level of the rats

2.11. Statistics. Statistics analysis was performed using GraphPad PRISM 5. Numerical data are presented as mean ± SEM. Unpaired t-test was used to compare between two genotypes. To compare more than 2 groups, one-way or two-way ANOVA with Bonferroni or Tukey's post hoc test

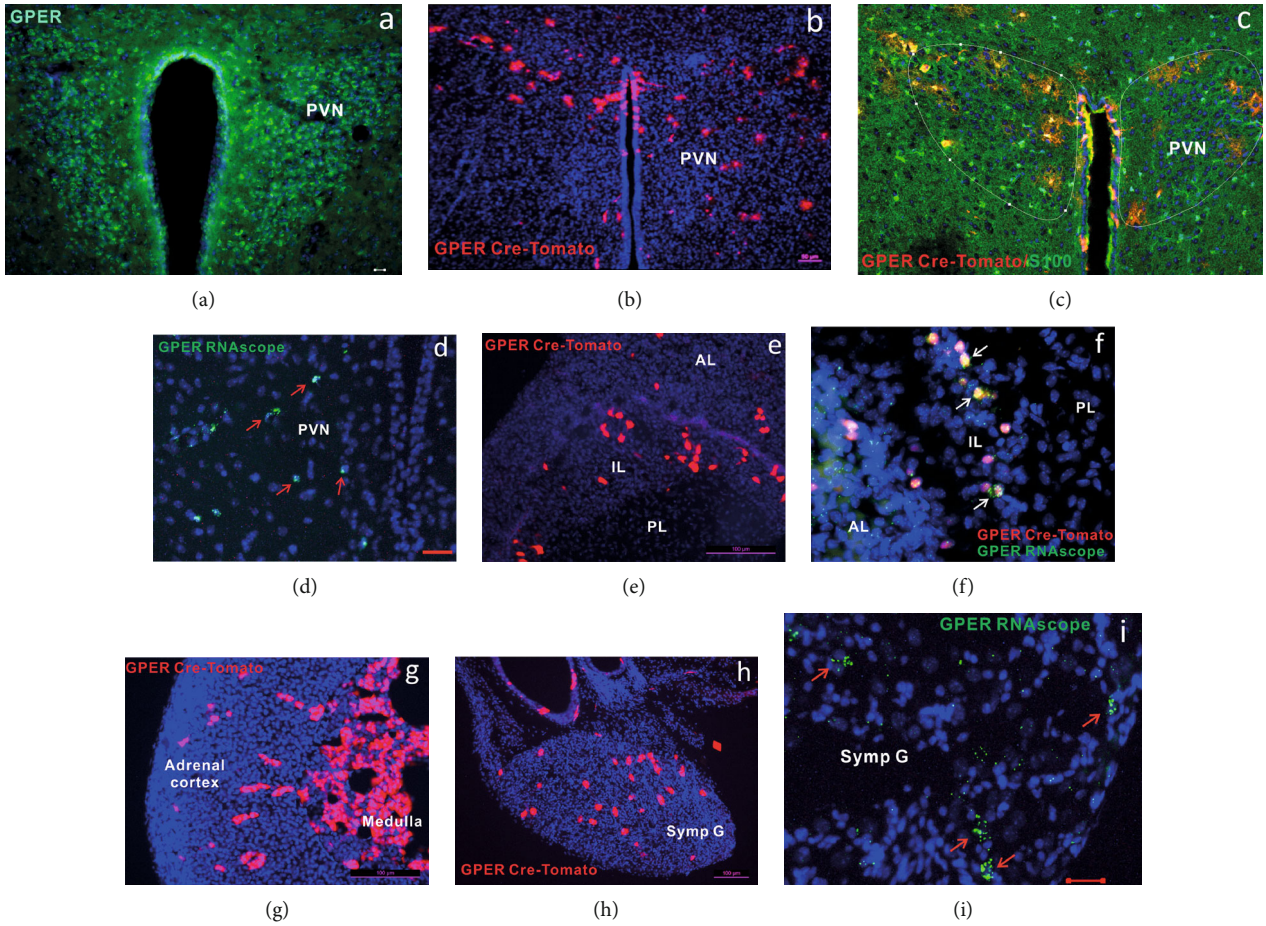

Figure 3: Distribution of GPER along the HPA axis in the mouse. (a) GPER immunofluorescence (green) in the PVN; (b) presence of Tomato$^+$ cells (red) in the PVN of GPER reporter (GPER Cre/tdTomato) mice; (c) immunohistochemistry shows Tomato$^+$ (red) cells express astrocyte marker S100 (green) in the PVN of GPER reporter mice. Note that only a fraction of S100$^+$ cells are Tomato$^+$. (d) GPER RNAscope in situ hybridization signal (green) in mouse PVN. (e) Presence of Tomato$^+$ (red) cells in the intermediate lobe (IL) and anterior lobe (AL) but not in the posterior lobe (PL) of the pituitary. (f) GPER RNAscope signal (green) in the pituitary of GPER reporter mice. Note the presence of clustered RNAscope signal (green) in Tomato$^+$ (red) cells in the intermediate lobe and weak sporadic RNAscope signal in the anterior lobe, but the absence of RNAscope signal in the posterior lobe. (g) Presence of Tomato$^+$ cells in the adrenal gland. Note that most cells in the adrenal medulla are Tomato$^+$ (red). Some cells in the adrenal cortex, particularly in the zona fasciculata, are Tomato$^+$. (h) Presence of Tomato$^+$ cells in the superior cervical sympathetic ganglion of GPER reporter mice. (i) GPER RNAscope signal in the superior cervical sympathetic ganglion of WT mice. Horizontal bars = 100 μm.

was performed. A P value less than 0.05 was considered as statistically significant.

3. Results

3.1. GPER Is Widely Distributed along the HPA Axis and in Brain Structures Involved in the Regulation of Anxiety. The distribution of GPER along the HPA axis and in the prefrontal cortex, the hippocampal formation, and the amygdala was addressed by three complementary approaches: immunohistochemistry, GPER reporter mice, and RNAscope. Immunohistochemistry revealed widespread distribution of GPER immunofluorescence in these areas in rats and mice. Within the rat HPA axis, strong GPER immunofluorescence was detected in the paraventricular nucleus (PVN) of the hypothalamus, the intermediate lobe of the pituitary, and the adrenal medulla, whereas moderate GPER immunofluorescence was seen in the anterior lobe of the pituitary and the adrenal cortex (Figure 2). A similar pattern of GPER immunofluorescence was detected in the PVN (Figure 3(a)), the pituitary, and the adrenal medulla (data not shown) in the mice. The distribution of GPER immunofluorescence was consistent with the distribution of GPER/tdTomato cells in the GPER reporter mice. Thus, Tomato$^+$ cells were clustered within the PVN (Figure 3(b)), the intermediate lobe of the pituitary (Figure 3(e)), and the adrenal medulla (Figure 3(g)), whereas sporadic Tomato$^+$ cells were seen within the anterior lobe of the pituitary (Figure 3(e)) and adrenal cortex, especially in the zona fasciculata (Figure 3(g)). Tomato$^+$ cells within the PVN were immunoreactive to S100 (Figure 3(c)), indicating that they were astrocytes rather than neurons. By RNAscope, GPER transcripts were clearly detected within the PVN (Figure 3(d)). Within the pituitary taken from GPER reporter mice, strong GPER RNAscope signal was detected in Tomato$^+$ cells in the intermediate lobe, with weak GPER

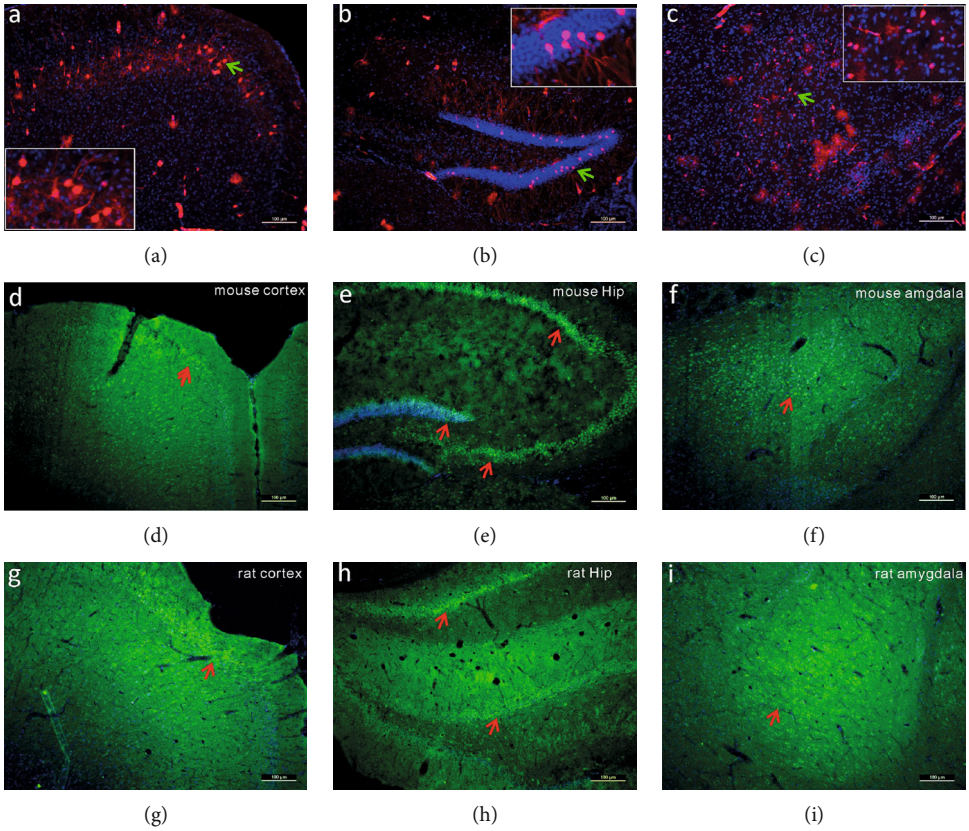

Figure 4: Distribution of GPER in the prefrontal cortex, hippocampus, and basal lateral amygdala. (a–c) Distribution of Tomato fluorescence (red) in the prefrontal cortex (PFC), the hippocampus (Hip), and the basolateral amygdala (BLA) in the GPER reporter (GPER Cre/tdTomato) mice. Green arrows indicate regions shown in higher magnification in the insets. (d–f) Distribution of GPER immunofluorescence (green) in mouse PFC, Hip, and BLA. Arrows point to positive staining. (g–i) Distribution of GPER immunofluorescence (green) in rat PFC, Hip, and BLA. Arrows point to positive staining. Horizontal bars = 100 μm.

RNAscope signal being clearly visible in the anterior but not in the posterior lobe of the pituitary (Figure 3(f)). Additionally, in the GPER reporter mice, Tomato$^+$ neurons were seen in the superior cervical sympathetic ganglion and this is consistent with positive GPER RNAscope signal being present in this ganglion (Figures 3(h) and 3(i)). These results indicate that estrogens may act via GPER at multiple levels to modulate the physiological and neuroendocrine responses to stress.

The prefrontal cortex, the hippocampal formation, and the amygdala are critically involved in the cognitive and behavioral responses to stress. We found that these structures were enriched with GPER immunofluorescence, both in mice and in rats (Figures 4(d)–4(i)). Consistently, Tomato$^+$ cells were present in these structures in the GPER reporter mice (Figures 4(a)–4(c)). Interestingly, within the hippocampal formation, whilst GPER immunofluorescence seemed to be ubiquitous in the dentate gyrus (DG), CA1, CA2, and CA3 regions (Figures 4(e) and 4(h)), Tomato$^+$ neuronal bodies were only seen in DG but not in CA1, CA2, CA3, and the hilum regions, where instead dense Tomato$^+$ terminal fibers and synaptic boutons were clearly visible (Figure 5). GPER RNAscope signal was also detected in the prefrontal cortex (Figure 6(a)), basolateral amygdala (BLA, Figure 6(b)), CA3 (Figure 6(c)), and DG (Figure 6(d)). It was interesting to note

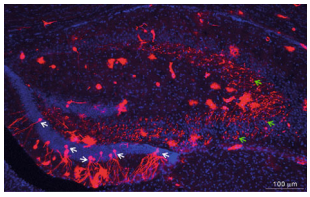

Figure 5: Distribution of the reporter gene (Tomato) in the hippocampal formation of the GPER reporter mice. Tomato$^+$ neuronal cell bodies (white arrows) are localized in the dentate gyrus (DG) but not in the hilum, CA3, CA2, or CA1 regions, where Tomato$^+$ fibers and terminal boutons (green arrows) are numerous.

that clustered RNAscope signal (likely present in neuronal bodies) was seen in the prefrontal cortex, BLA, and DG, whereas sporadic RNAscope signal (presumably present in terminal fibers) was detected in CA3, which was consistent with the distribution of Tomato$^+$ cell bodies and fibers within these regions. These results revealed widespread but unique pattern of distribution of GPER within brain structures implicated in the regulation of anxiety.

3.2. GPER-Deficient Rats Had Lower Basal Serum Corticosterone Levels. Given the widespread distribution of

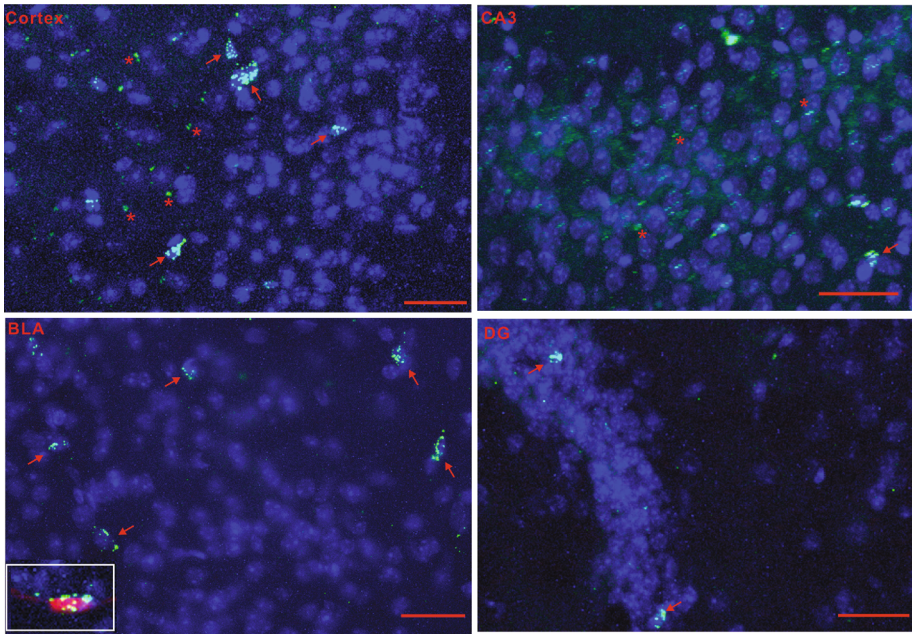

Figure 6: Distribution of GPER RNAscope in situ hybridization signal (green) in the prefrontal cortex, hippocampus (CA3 and DG regions), and basal lateral amygdala (BLA). Red arrows point to clustered signal indicative of expression in cell bodies. Red stars indicate weak sporadic RNAscope signal presumably in fiber terminals. The inset shows a representative Tomato^{+} neuronal body in the BLA of GPER reporter mice with strong clustered RNAscope signal. Horizontal bars = 50 μm.

GPER within the HPA axis and the sympathetic nervous system (adrenal medulla and sympathetic ganglia), we next investigated whether GPER deficiency may impact serum or plasma levels of stress hormones. Consistent with previous reports [34], WT female rats had significantly higher basal serum corticosterone but lower basal adrenaline levels than WT male rats (Figures 7(a) and 7(c)). Strikingly, the basal serum corticosterone level of GPER-deficient (GPER$^{-/-}$) female rats was markedly lower than that of WT female rats (Figure 7(a)), whereas serum adrenaline level was slightly but significantly increased in GPER$^{-/-}$ female rats as compared to the WT female rats (Figure 7(c)). It was interesting to note that GPER$^{-/-}$ male rats also had a lower basal corticosterone level than WT male rats (Figure 7(a)), but serum adrenaline levels were not significantly different between GPER$^{-/-}$ and WT male rats (Figure 7(c)). Plasma level of CRH was slightly increased in GPER$^{-/-}$ female rats as compared with the WT female rats (Figure 7(f)), which was likely explained by decreased negative feedback (i.e., due to lower serum corticosterone level). However, GPER deficiency did not significantly affect plasma ACTH levels either in female or in male rats (Figure 7(g)). These results imply that peripheral GPER (i.e., GPER in the adrenal cortex) might be responsible for the higher basal corticosterone level in female than in male rats.

GPER$^{-/-}$ female rats had significantly lower serum E2 in the proestrus phase than the WT female rats, but no difference in serum E2 level was found between GPER$^{-/-}$ and WT male rats (Figures 7(b) and 7(e)). We also analyzed the impact of GPER deficiency on serum corticosterone levels at different phases of the menstrual cycle, with lower levels found in diestrus, estrous, and metestrus phases but not in proestrus phase in GPER$^{-/-}$ rats compared with the WT rats (Figure 7(d)).

Given the markedly lower basal corticosterone level in GPER$^{-/-}$ than WT rats, we wondered how GPER deficiency would affect HPA axis responses to stress. Therefore, in another cohort of GPER$^{-/-}$ and WT rats, we measured the serum or plasma levels of stress hormones following 30 min of restraint stress. Surprisingly, neither serum corticosterone nor adrenaline levels were significantly different between GPER$^{-/-}$ and WT female or between GPER$^{-/-}$ and WT male rats following acute restraint stress (Figures 8(a) and 8(b)). However, plasma ACTH level was significantly higher in GPER$^{-/-}$ female than in WT female rats following the acute stress, despite no significant difference in plasma CRH levels between these two groups (Figures 8(c) and 8(d)). The results imply that GPER at the level of the pituitary may negatively regulate stress responses of the HPA axis, such that removal of this negative modulation (in GPER$^{-/-}$ rats) may enhance ACTH and corticosterone release during acute stress.

3.3. GPER-Deficient Rats Display Increased Anxiety-Like Behaviors. Seeing that GPER is widely distributed in the corticolimbic circuit comprising the prefrontal cortex, the hippocampal formation, and the amygdala, we next investigated whether GPER deficiency may impact animal behaviors related to mood, learning, and memory. It is worthy of mentioning here that Nissl staining indicated that hippocampal morphology of GPER$^{-/-}$ rats was intact compared with the WT rats (Figure 9).

Anxiety-like behaviors were investigated by elevated plus maze (EPM), open field, and IntelliCage tests. In the EPM test, GPER$^{-/-}$ female rats of three age groups (10, 16, and 22

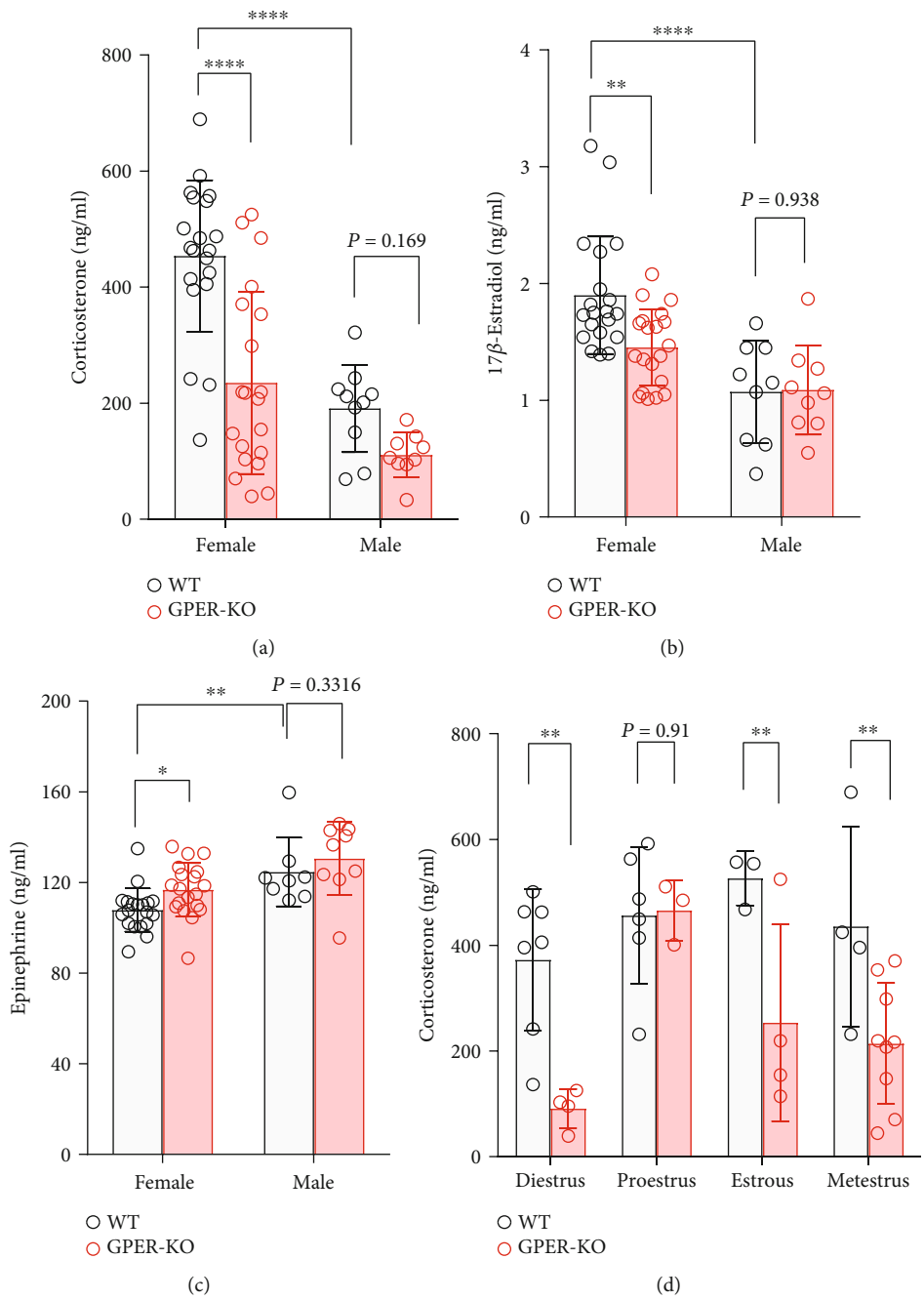

Figure 7: Continued.

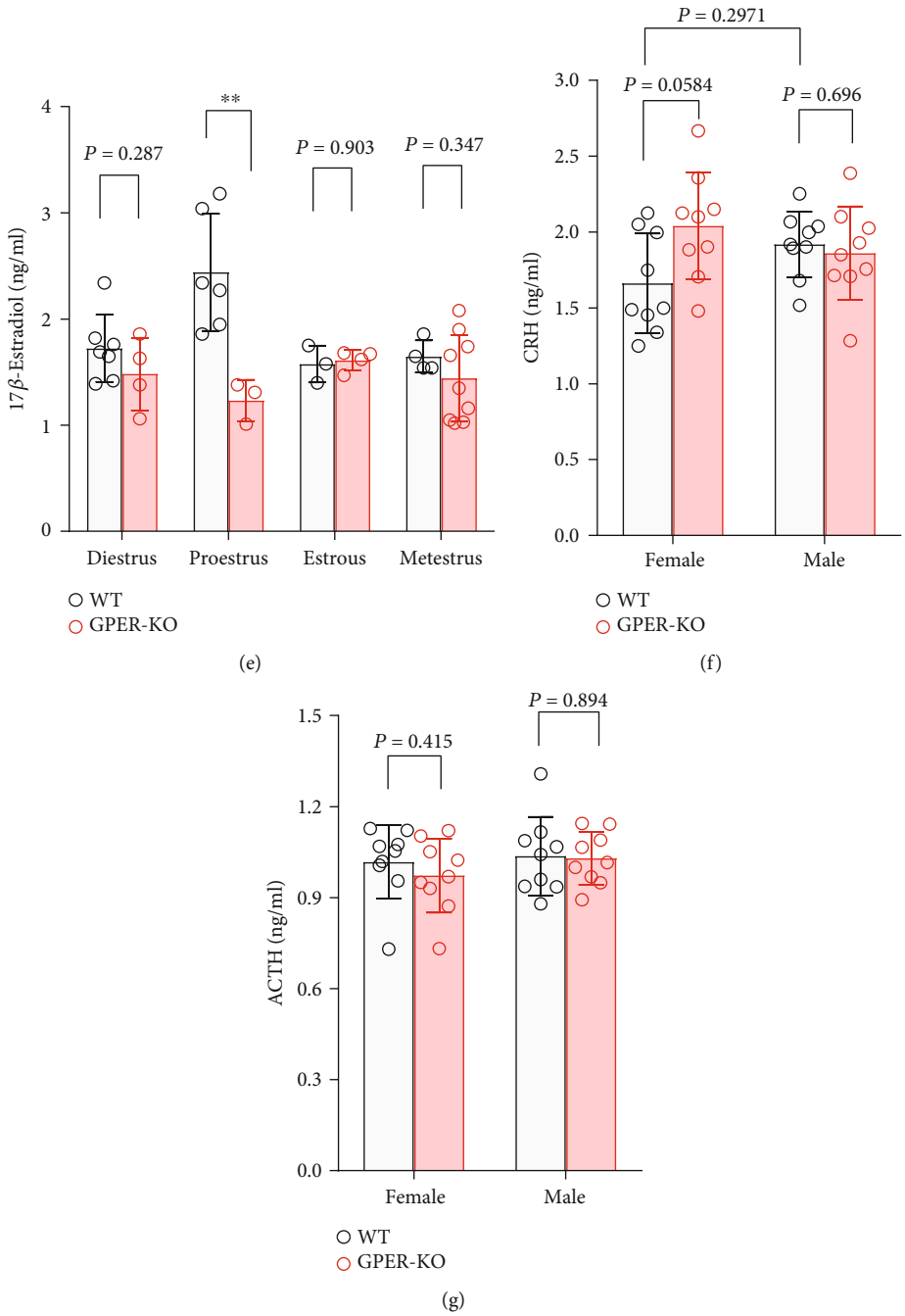

Figure 7: GPER-deficient rats had lower basal serum corticosterone level. (a) Basal serum corticosterone level (detected by HPLC-MS) in WT and GPER$^{-/-}$ rats of either sex. Note that serum corticosterone of GPER$^{-/-}$ female rats ($n = 20$) is significantly lower than that of WT female rats ($n = 20$). GPER$^{-/-}$ male rats ($n = 10$) also seemed to have lower serum corticosterone level than WT males ($n = 10$), but the difference did not reach statistical significance. (b) Basal serum17β-estradiol level (detected by HPLC-MS) in WT and GPER$^{-/-}$ rats of either sex. Note that serum 17β-estradiol of GPER$^{-/-}$ female rats ($n = 20$) is significantly lower than that of WT female rats ($n = 20$). (c) Basal serum adrenaline level (detected by HPLC-MS) in WT and GPER$^{-/-}$ rats of either sex. Note that serum adrenaline of GPER$^{-/-}$ female rats ($n = 20$) is significantly higher than that of WT female rats ($n = 20$). (d) Basal serum corticosterone level in WT and GPER$^{-/-}$ rats of different menstrual cycle. (e) Basal serum 17β-estradiol level in WT and GPER$^{-/-}$ rats of different menstrual cycle. (f) Basal plasma CRH level (detected by ELISA) in WT and GPER$^{-/-}$ rats of either sex. Note that plasma CRH of GPER$^{-/-}$ female rats ($n = 10$) is significantly higher than that of WT female rats ($n = 10$). (g) Basal plasma ACTH level (detected by ELISA) in WT and GPER$^{-/-}$ rats of either sex. $*P < 0.05$, $**P < 0.01$, $***P < 0.001$, and $****P < 0.0001$, two-way ANOVA with Tukey post hoc test.

weeks) all showed remarkable decreases in open-arm time (percentage of time spent in the open arm) and number of open-arm visits compared with their WT counterparts (Figure 10(a)). In the 10- and 16-week-old male rats, open-arm time or number of open-arm visits was not significantly different between GPER$^{-/-}$ and WT groups. However, in the

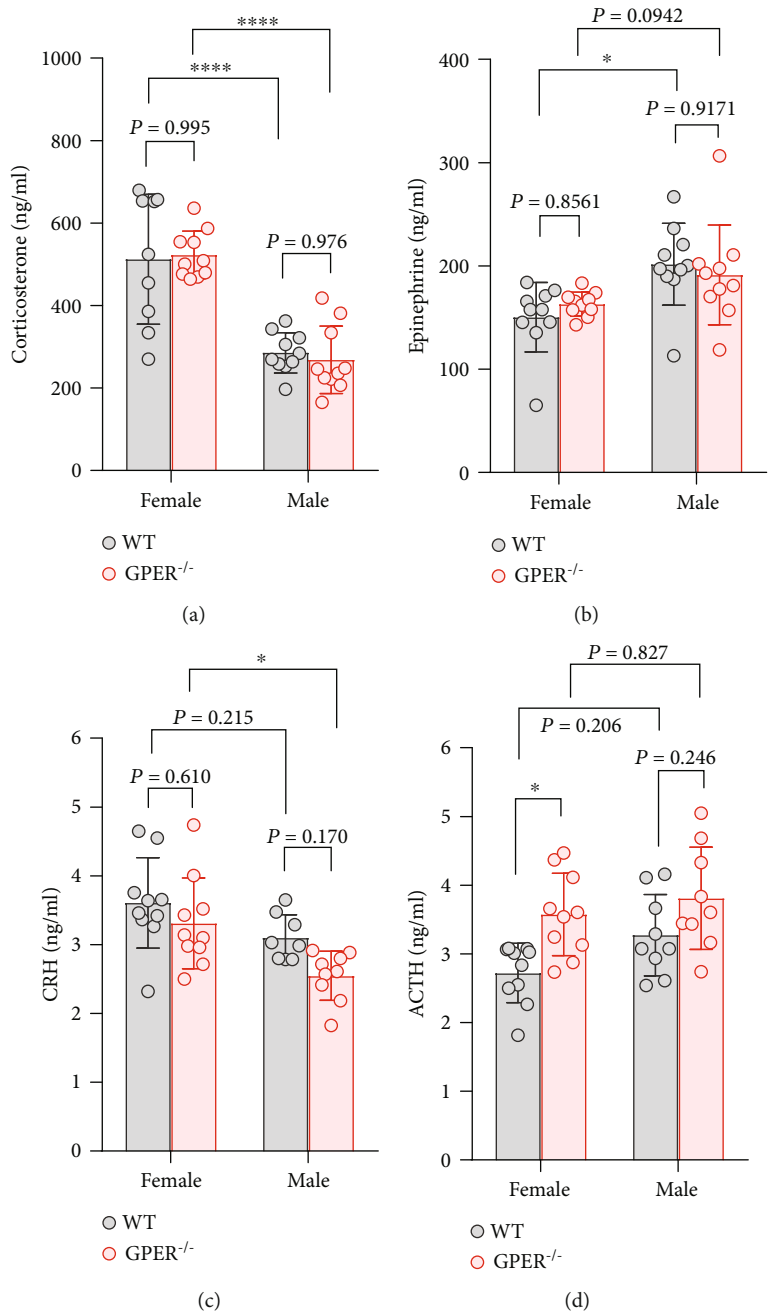

Figure 8: Serum levels of stress hormones following acute restraint stress in wild-type and GPER-deficient rats. (a) Serum corticosterone level following 30 min acute restraint stress in WT and GPER$^{-/-}$ rats of either sex ($n = 10$ for each group). (b) Serum adrenaline level in WT and GPER$^{-/-}$ rats of either sex following acute restraint stress. (c) Plasma CRH level in WT and GPER$^{-/-}$ rats of either sex following acute restraint stress. Note that GPER$^{-/-}$ rats ($n = 10$) of either sex seemed to have lower plasma CRH level than WT ($n = 10$) following acute restraint stress, but the difference did not reach statistical significance. (d) Plasma ACTH level in WT and GPER$^{-/-}$ rats of either sex following acute restraint stress. Note that GPER$^{-/-}$ rats had higher plasma ACTH level than the WT rats, particularly in the female. $*P < 0.05$ and $****P < 0.0001$, two-way ANOVA with Tukey post hoc test.

22-week-old male rats, there were significant decreases in open-arm time and number of open-arm visits in GPER$^{-/-}$ than the WT controls (Figure 10(a)). Similar results were obtained in the open field test. Thus, center time, center distance, and center visits were all decreased in female GPER$^{-/-}$ compared with their WT counterparts in all three age groups (Figure 10(c)). For the male rats, only the 22-week-old GPER$^{-/-}$ group showed significant decreases in center time and center distance compared with the WT control group (Figure 10(c)). The IntelliCage test, with the advantage of enabling evaluation of animal's anxiety level in a social environment, was carried out in 10-week-old female WT and GPER$^{-/-}$ rats. The animals were trained to drink water at a specific corner, and on the testing days, they received a punitive air puff when they first drank water after 20 h of water deprivation. The latency taken for the animals to access water

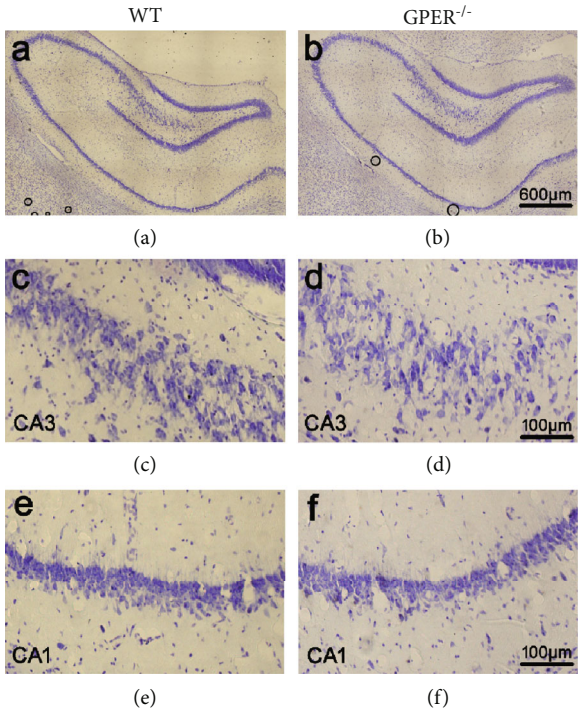

Figure 9: GPER deficiency in the rat did not significantly affect hippocampal morphology. (a, b) Nissl-stained hippocampal formation of WT and GPER$^{-/-}$ rats. (c, d) Nissl-stained CA3 region of WT and GPER$^{-/-}$ rats. (e, f) Nissl-stained CA1 region of WT and GPER$^{-/-}$ rats.

again (drinking latency) and frequency of access (visits) during a 4 h period were registered. GPER$^{-/-}$ rats were found to have significantly longer drinking latency and fewer visits compared with their WT counterparts (Figure 10(b)). These results demonstrated that GPER deficiency, particularly in the females, may lead to behaviors indicative of increased anxiety level in the rats.

To further explore the role of GPER in the modulation of anxiety, we conducted EPM and open field tests to observe the effects of ovariectomy (OVX) and systemically administered E2 (endogenous GPER agonist, 10 μg/kg, s.c.) or G-1 (synthetic GPER agonist, 10 μg/kg, s.c.) on anxiety-like behaviors in 10-week-old female rats. As shown in Figures 10(e) and 10(f), OVX resulted in behaviors indicative of increased anxiety (less open-arm time and fewer open-arm visits in EPM test; less center time and center distance and fewer center visits in open field test), which were reversed by E2 and G-1 (Figures 10(e) and 10(f)).

Imbalanced excitatory and inhibitory neurotransmissions are regarded as an important mechanism underlying anxiety disorders [35, 36], which is the mechanistic basis of mainstream medications such as diazepam ($GABA_A$ agonist) and chlorpromazine (dopamine receptor antagonist). We wondered whether diazepam or chlorpromazine may affect the anxiety-like behavior of GPER$^{-/-}$ rats. To answer such a question, WT and GPER$^{-/-}$ rats of either sex were injected with diazepam (1 mg/kg, ip) or chlorpromazine (1 mg/kg, ip) 1 h before the EPM test. Diazepam did not significantly alter open-arm time or open-arm visits in the WT rats. In the GPER$^{-/-}$ rats, however, diazepam caused significant increases in open-arm time and open-arm visits (Figure 11(b)). In contrast, chlorpromazine had no significant effect on open-arm time or open-arm visits either in WT or GPER$^{-/-}$ rats (Figure 11(c)).

3.4. GPER Deficiency Accentuates Anxiety-Like Behavior and Alters Neuroendocrine Profile following Single-Prolonged Stress. Women are more likely than men to develop posttraumatic stress disorders (PTSD) following life-threatening tragic events [37], and a dysfunctional HPA axis has been implicated in the pathogenesis of PTSD [38, 39]. We wondered whether GPER deficiency in the rat may alter the anxiety-like behavior and the neuroendocrine profile following an episode of intense stress. To answer such a question, 8-week-old GPER$^{-/-}$ and WT rats of either sex were subjected to single-prolonged stress (SPS). Following 2 weeks of quiescence period, they were tested for anxiety-like behaviors on EPM and serum or plasma levels of stress hormones. In female WT rats, the stressed group had significantly less open-arm time (reduced by 73%) and fewer open-arm visits (reduced by 57%) than the unstressed (WT control) group (Figure 12(b)). In female GPER$^{-/-}$ rats, the stressed group barely visited or stayed in the open arm (open-arm time reduced by 94% and open-arm visits reduced by 92%) (Figure 12(b)). Similar results were found in male rats with the stressed GPER$^{-/-}$ group being least likely to visit or stay in the open arm compared with other groups (Figure 12(b)). These results indicate that GPER deficiency may accentuate anxiety-like behaviors following SPS.

Interestingly, we noted that GPER$^{-/-}$ rats of either sex showed significantly less body weight gain than their WT counterparts following SPS and this was primarily evident in the first 3 days after stress, when GPER$^{-/-}$ rats showed zero weight gains (Figure 12(c)).

In line with the literature [40], we found that 2 weeks after SPS, WT rats of either sex had significantly lower serum corticosterone level compared with the unstressed controls (Figure 12(d)). In contrast, the serum corticosterone level of stressed GPER$^{-/-}$ female rats was comparable with that of the unstressed GPER$^{-/-}$ female group (Figure 12(d)). The serum corticosterone level of the stressed GPER$^{-/-}$ male group seemed to be lower than that of the unstressed control group, but the difference did not reach statistical significance (Figure 12(d)). In addition, stressed WT female rats had lower serum 17β-estradiol than unstressed WT females (Figure 12(e)), whilst stressed WT male rats had lower serum adrenaline than unstressed WT males (Figure 12(f)). Such differences were not seen in GPER$^{-/-}$ rats (Figures 12(e) and 12(f)). We did not find significant effects of SPS or GPER deficiency on plasma levels of CRH, ACTH, vasopressin (AVP), or β-endorphin (Figures 12(g)–12(j)). However, it was noted that SPS led to slightly lower plasma CRH, ACTH, and AVP levels in WT but not in GPER$^{-/-}$ rats.

3.5. GPER-Deficient Rats Display Impaired Learning and Memory. Morris water maze (MWM) and IntelliCage tests were conducted to evaluate learning and memory-related behavior. In MWM test, GPER$^{-/-}$ rats, whether female or

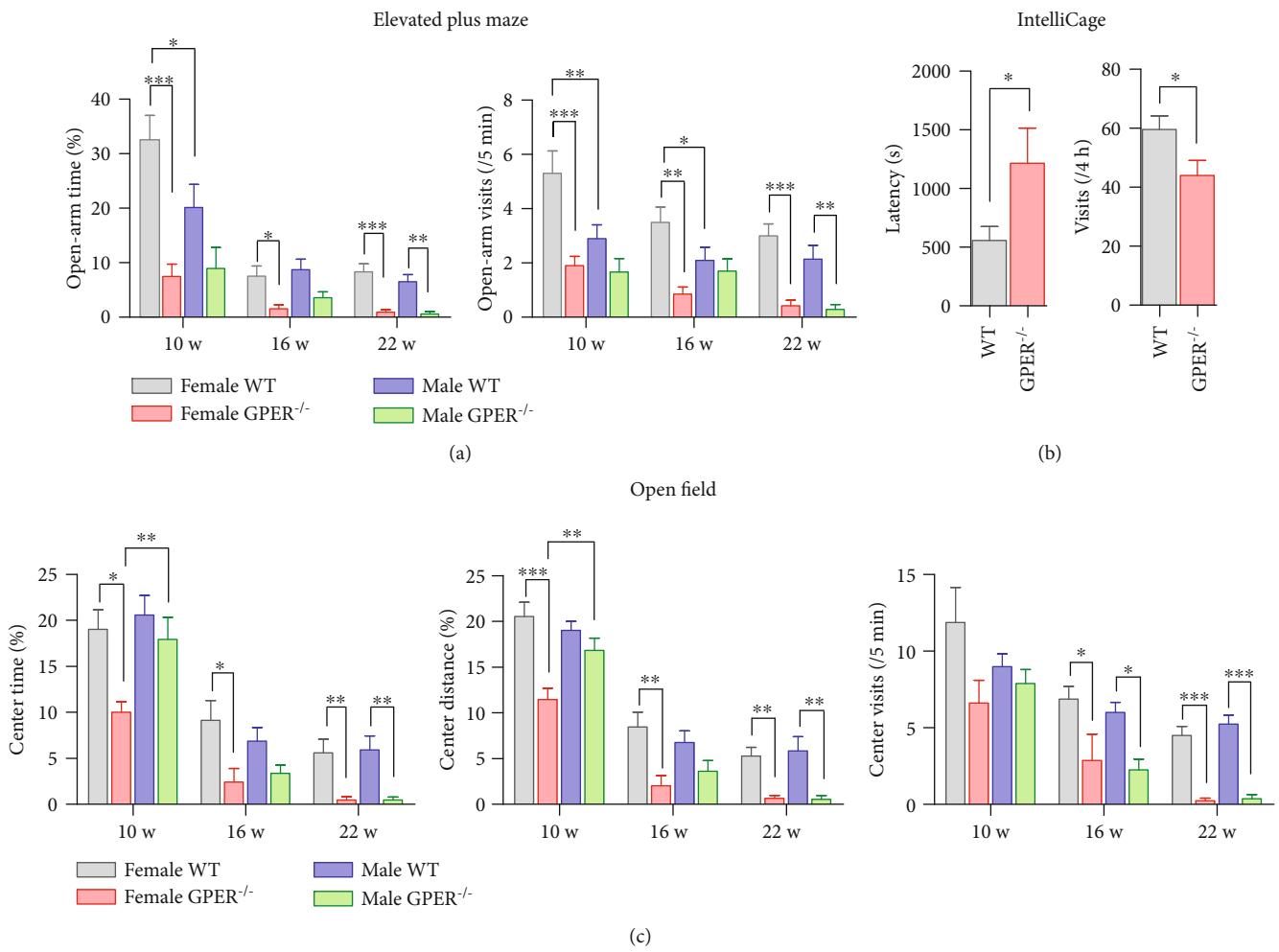

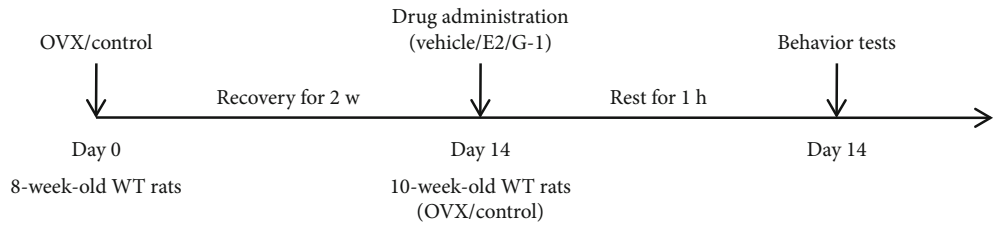

Figure 10: Continued.

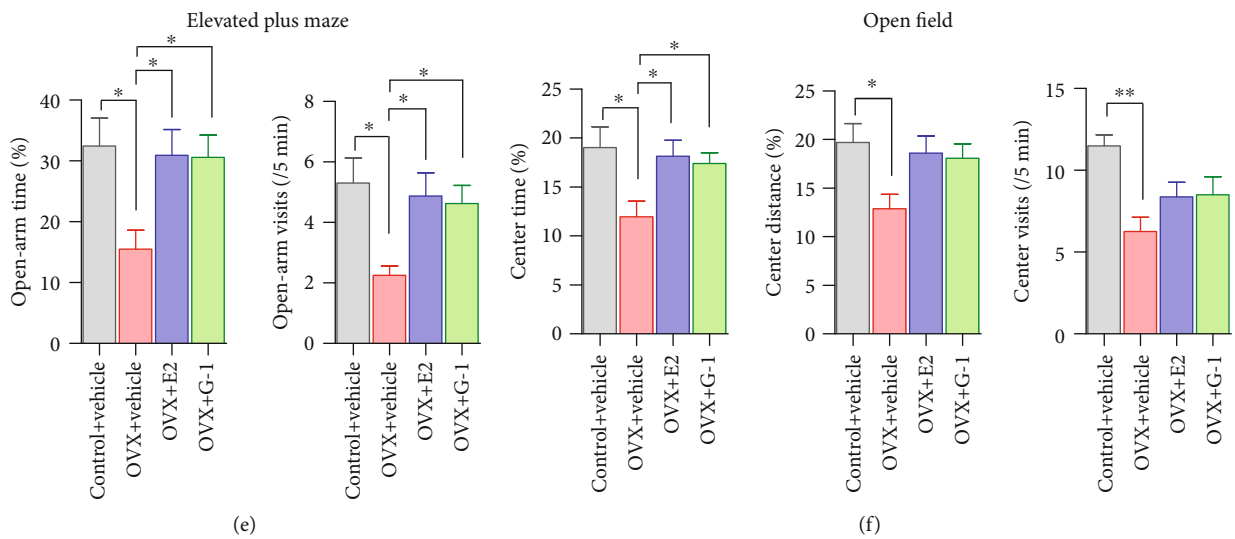

Figure 10: GPER-deficient rats exhibit anxiety-like behavior. (a) Comparison of the open-arm time and open-arm visits in the elevated plus maze (EPM) between WT and GPER$^{-/-}$ rats of three age groups (10 weeks old, $n = 10$; 16 weeks old, $n = 10$; and 22 weeks old, $n = 7$). (b) Comparison of the latency to drink and corner visits after punitive air puff in the IntelliCage between WT ($n = 9$) and GPER$^{-/-}$ ($n = 6$) female rats. (c) Comparison of the center time, center distance, and center visits in the open field test between WT and GPER$^{-/-}$ rats of three age groups (10 w, $n = 8$; 16 w, $n = 8$; and 22 w, $n = 8$). (d) Protocol of the OVX test to further explore the role of GPER in modulation of anxiety. (e) Comparison of the open-arm time and open-arm visits in the EPM test among control ($n = 10$), ovariectomized (OVX, $n = 10$), and OVX rats treated with E2 ($n = 10$) or G-1 ($n = 10$). Note that OVX rats showed anxiety-like behaviors, which were reversed by E2 and G-1. (f) Comparison of the center time, center distance, and center visits in the open field test among control ($n = 8$), OVX ($n = 8$), and OVX rats treated with E2 ($n = 8$) or G-1 ($n = 8$). Note that E2 and G-1 can reverse OVX-induced anxiety-like behaviors. $*P < 0.05$, $**P < 0.01$, and $***P < 0.001$, two-way ANOVA with Bonferroni posttests for elevated plus maze and open field, unpaired t-test for IntelliCage.

male, showed significantly longer latency to find the platform compared with their WT counterparts during the 5-day positioning navigation tests (Figure 1(a)). On the 6th day (spatial exploration test), GPER$^{-/-}$ female and male rats showed slightly lower percentage of time in the target quarter than their WT counterparts, but the differences did not reach statistical significance (Figure 1(a)).

In the IntelliCage test (Figure 1(b)), GPER$^{-/-}$ and WT rats showed similar corner visits during the free exploration period (Figure 1(c)). During the 4-day nosepoke learning period, GPER$^{-/-}$ rats had fewer corner visits than the WT rats (Figure 1(d)), indicative of decreased simple skill learning ability in GPER$^{-/-}$ rats. GPER$^{-/-}$ rats had fewer numbers of licks and nosepokes than the WT rats on the first day of nosepoke learning. Lastly, during the place and replace learning period, GPER$^{-/-}$ rats showed higher error rates than the WT rats, indicative of decreased spatial learning and memory (Figures 1(e) and 1(f)). These results demonstrated that GPER-deficient rats had impaired learning and memory.

4. Discussion

Organizational and activational effects of estrogens are presumably responsible for the gender difference in the stress responses and the higher prevalence of stress-related disorders in females [2, 3, 7]. Estrogens may not only act via the nuclear receptors ERα and ERβ to mediate classical slow genomic effects but also bind to GPER to mediate rapid nongenomic effects. The current investigation has systematically analyzed the distribution and function of GPER in the corticolimbic circuit and the HPA axis. Our findings support GPER as a major player in mediating the estrogenic influences on the HPA axis and anxiety.

We took three complementary approaches to analyze GPER expression in the HPA axis and the corticolimbic circuit at transcription and protein levels. GPER immunofluorescence could be detected at every level of the HPA axis, with high expressions seen in the PVN and the intermediate lobe of pituitary and moderate expressions seen in the anterior pituitary and adrenal cortex in rats and mice, which was consistent with some previous reports [26, 41]. Importantly, GPER reporter (GPER Cre/tdTomato) mice and GPER RNAscope *in situ* hybridization revealed similar pattern of GPER expression at the transcription level. Within the corticolimbic circuit, moderate GPER immunofluorescence was ubiquitously present in the prefrontal cortex, the hippocampal formation, and the basolateral amygdala, which was in agreement with previous findings [26, 41]. GPER reporter mice and GPER RNAscope confirmed GPER transcription in these structures. The distribution pattern of Tomato and RNAscope signal in the hippocampal formation seemed to suggest that GPER-expressing granular neurons in DG may project extensively to CA3, CA2, CA1, and the hilum regions, where GPER may be expressed presynaptically. These results confirm that GPER is well positioned to mediate rapid estrogenic effects on the corticolimbic circuit [28] and the HPA axis.

It is well documented that females generally have higher basal and stress-induced glucocorticoid levels but lower basal and stress-induced adrenaline level than males [2, 20]. We

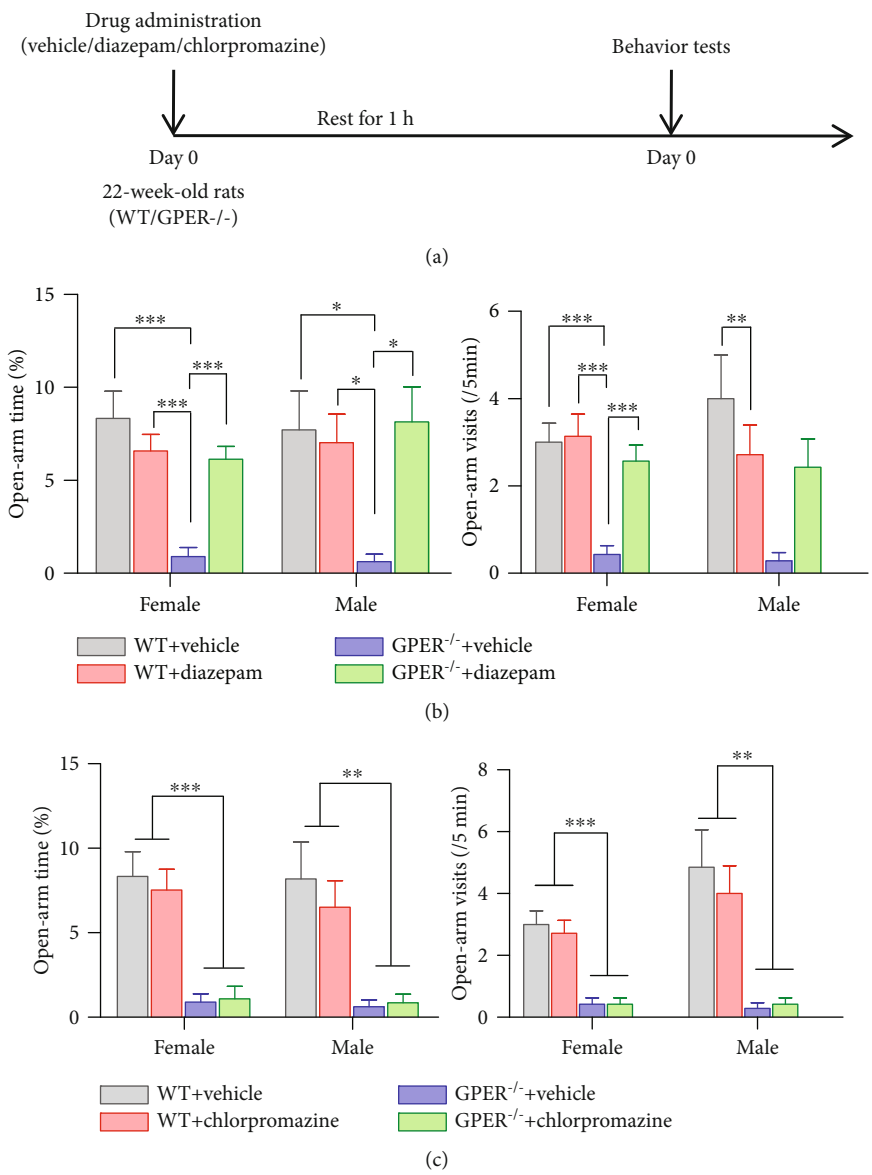

Figure 11: Diazepam reverses anxiety-like behavior in GPER-deficient rats. (a) Protocol of the drug administration test to explore the possible neurotransmitter which can be the mechanistic basis of the anxiety-like behavior of GPER$^{-/-}$ rats. (b) Comparison of the open-arm time and open-arm visits in the elevated plus maze test in WT and GPER$^{-/-}$ rats treated with diazepam or vehicle ($n = 7$ for each group). Note that diazepam can reduce the anxiety-like behavior of GPER$^{-/-}$ rats. (c) Comparison of the open-arm time and open-arm visits in the elevated plus maze test in WT and GPER$^{-/-}$ rats treated with chlorpromazine or vehicle ($n = 7$ for each group). Note that chlorpromazine did not seem to affect the anxiety-like behavior of GPER$^{-/-}$ rats. $*P < 0.05$, $**P < 0.01$, and $***P < 0.001$, two-way ANOVA with Bonferroni post hoc tests.

argue that GPER may be primarily responsible for such gender differences, since the loss of GPER caused a dramatic decrease in basal serum corticosterone and a significant increase of basal serum adrenaline in female rats. We reason that GPER within the adrenal cortex facilitates basal corticosterone secretion since basal plasma concentration of ACTH was not significantly different between GPER$^{-/-}$ and WT female rats. It may also be likely that GPER in the adrenal cortex inhibits adrenaline secretion, thereby contributing to the lower basal serum adrenaline level in females than in males. The profile of stress hormones following acute restraint stress was suggestive of an inhibitory role of GPER at the level of the pituitary on the HPA reactivity to stress. Thus, despite the significantly lower basal corticosterone level, GPER$^{-/-}$ rats had similar serum level of corticosterone and concomitantly greater ACTH (but not CRH) response compared with the WT rats. Interestingly, physiologically relevant doses of E2 reportedly inhibit ACTH release but significantly increase adrenal sensitivity in OVX female rats [42]. It seems possible that those effects may be mediated by GPER.

We conducted the elevated plus maze (EPM), open field, and IntelliCage tests to explore the effects of GPER deficiency on behaviors related to anxiety. Seeing that besides gender,

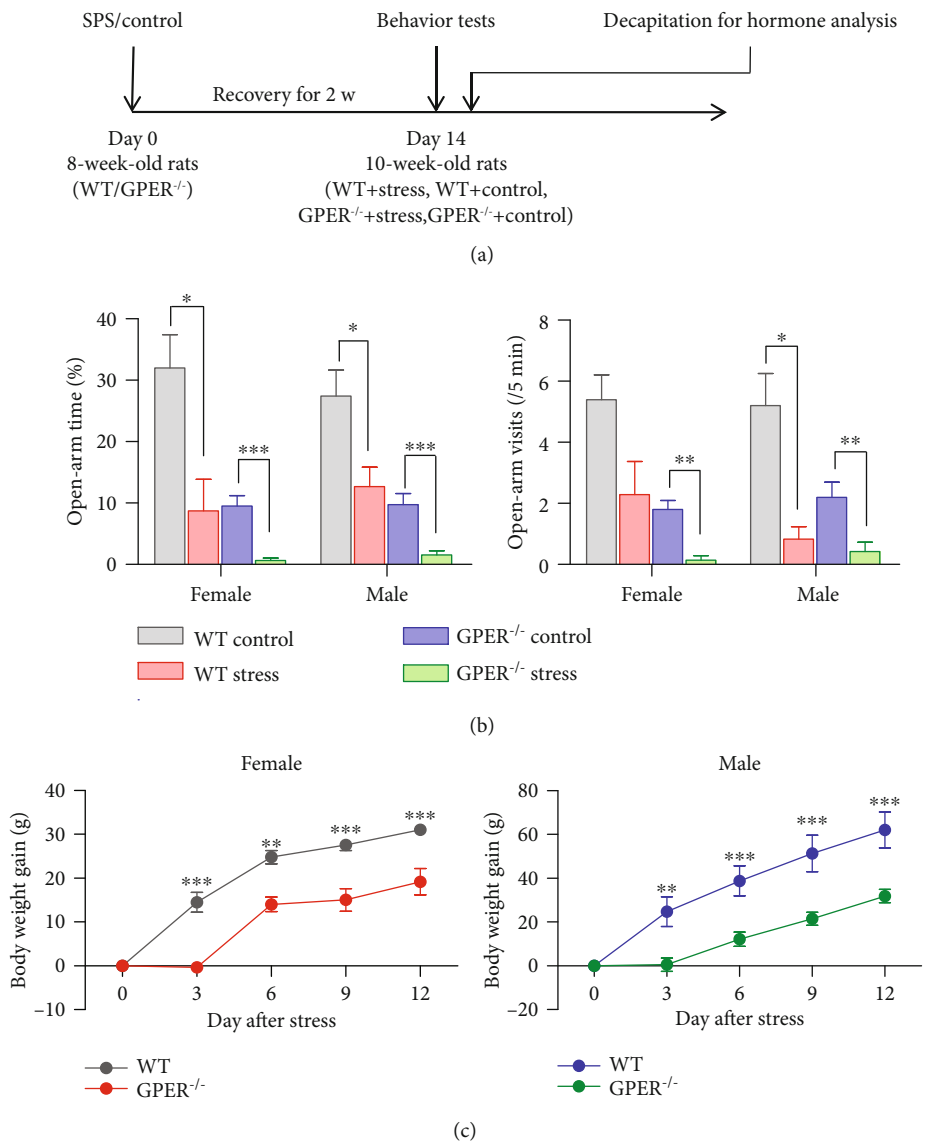

Figure 12: Continued.

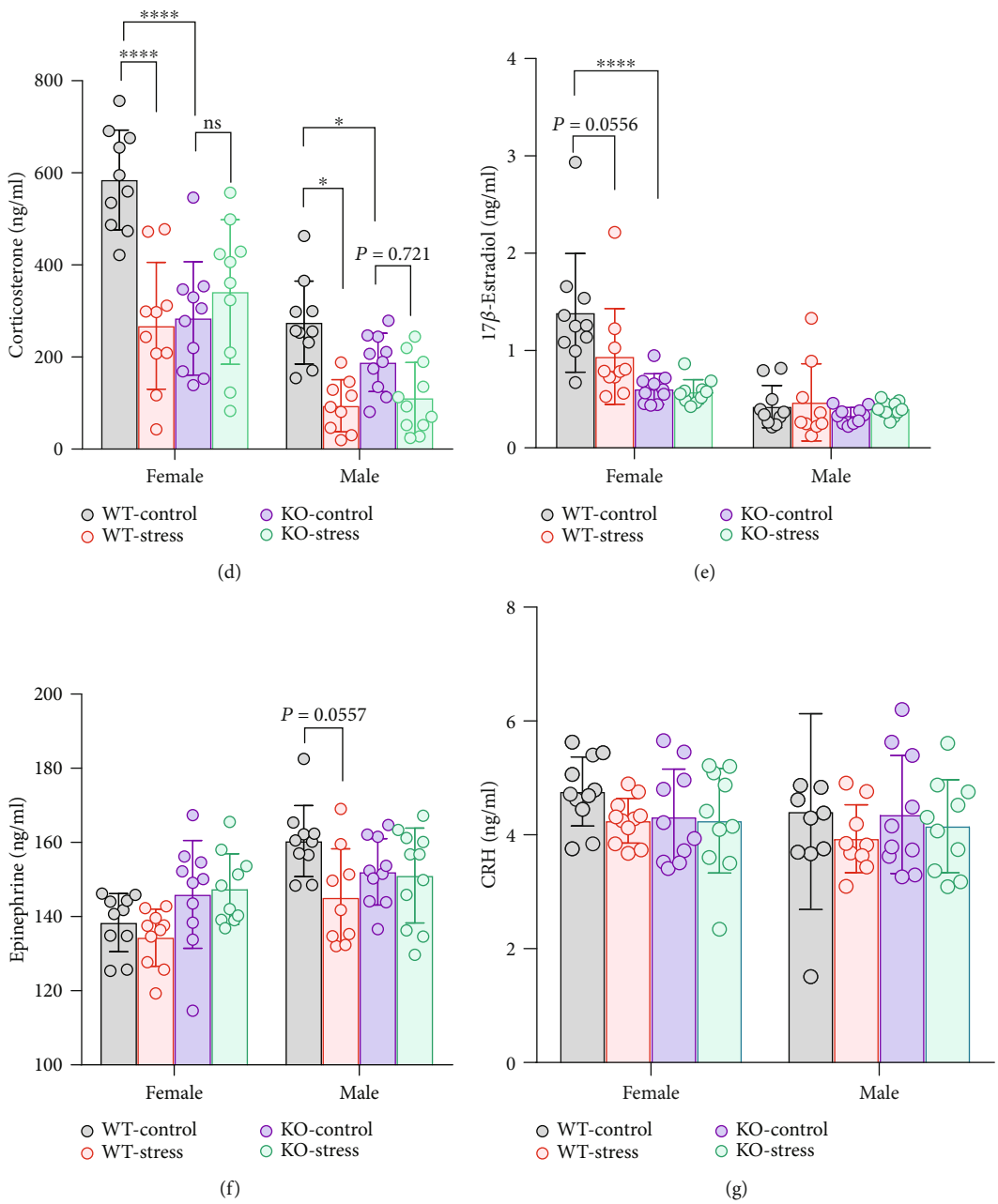

Figure 12: Continued.

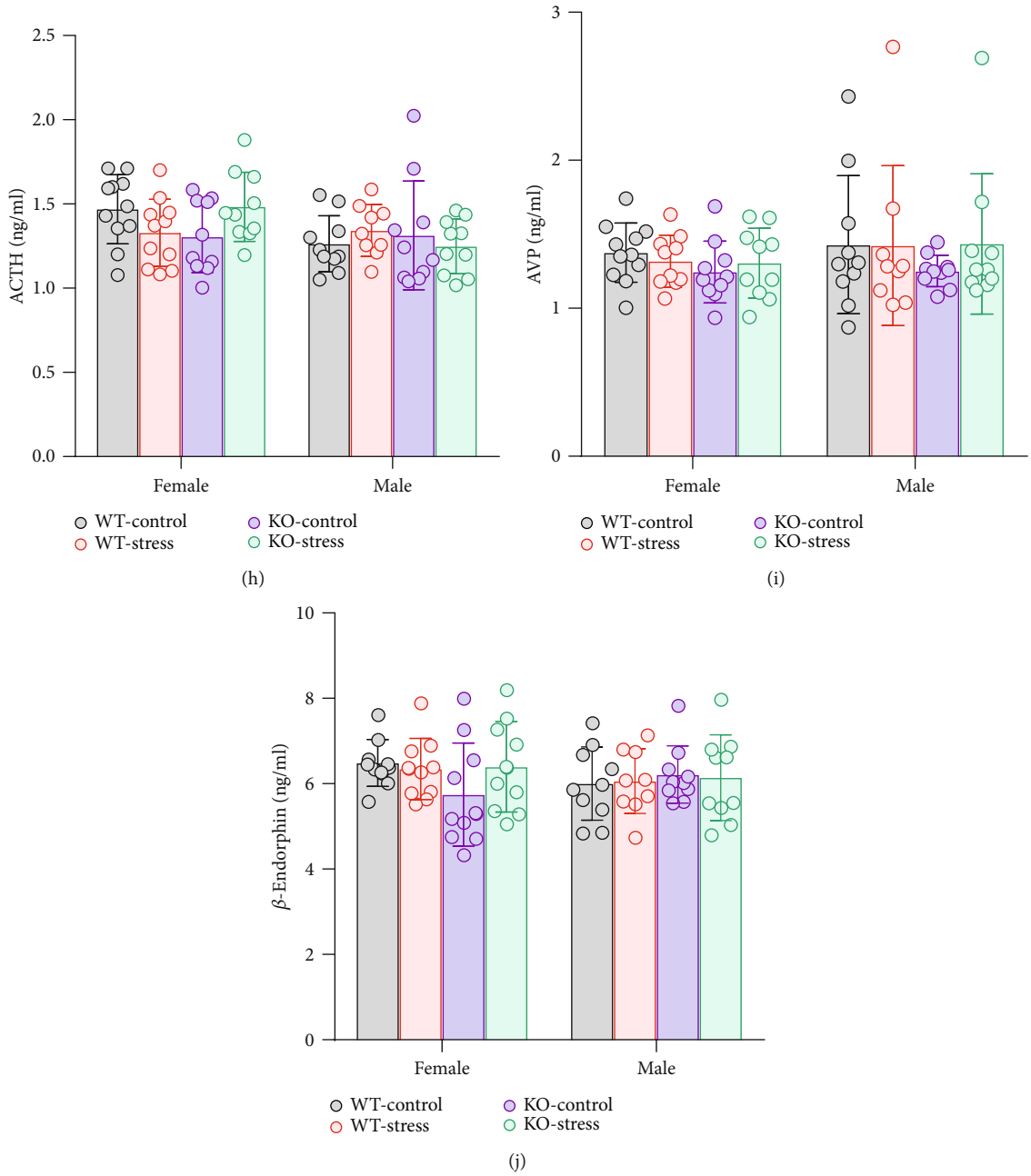

Figure 12: GPER deficiency accentuates anxiety-like behaviors and alters neuroendocrine profile following single-prolonged stress. (a) Timeline of the SPS model and the following tests to explore whether GPER deficiency in the rat may alter the anxiety-like behavior and the neuroendocrine profile following stress. (b) Comparison of open-arm time and open-arm visits in the elevated plus maze (EPM) between unstressed or stressed (with single-prolonged stress (SPS)) WT and GPER$^{-/-}$ rats of either sex. $n = 10$ for each unstressed group, $n = 7$ for each stressed group. Note that stressed GPER$^{-/-}$ rats of either sex were least likely to visit or to stay in the open arm, indicative of higher anxiety levels, compared with other groups. (c) Comparison of the body weight gain between WT ($n = 7$ each gender) and GPER$^{-/-}$ ($n = 7$ each gender) rats following SPS. (d–j) Comparison of serum or plasma levels of corticosterone, 17β-estradiol, adrenaline, CRH, ACTH, vasopressin (AVP), and β-endorphin between unstressed or stressed WT and GPER$^{-/-}$ rats ($n = 10$ for each group). Note that SPS caused a significant decrease in serum corticosterone levels and slightly lower serum adrenaline levels in WT but not GPER$^{-/-}$ rats. $*P < 0.05$, $**P < 0.01$, and $*** P < 0.001$, two-way ANOVA with Bonferroni or Tukey post hoc tests.

age is also an important factor in anxiety [43–45], we studied male and female rats of three age groups (10, 16, and 22 weeks of age, which correspond to adolescent, adult, and middle age of humans). GPER$^{-/-}$ rats of all three age groups displayed behaviors indicative of increased anxiety particularly in the females. The greater effects seen in the female were suggestive of the involvement of circulating estrogens in mood regulation via GPER, which was further supported by the findings that OVX rats showed behaviors indicative of increased anxiety, which could be reversed by

subcutaneous administration of E2 or G-1. An earlier study also showed that GPER agonists ameliorated anxiety-like behaviors in rats [46]. These results indicate that GPER generally mediates a positive anxiolytic effect. However, there have also been reports that systemic G-1 led to decreased anxiety-like behaviors in gonadectomized male but not female mice [29] or led to increased anxiety level in OVX mice [30]. In addition, GPER-deficient male but not female mice reportedly displayed reduced anxiety-like behaviors [31]. The inconsistencies are not surprising, given the widespread distribution of GPER in the corticolimbic regions and the HPA axis. It may well be possible that GPER at different sites may modulate anxiety differently.

Given the distinct distribution of GPER in the hippocampal formation, we also investigated whether GPER deficiency may affect learning and memory. Morris water maze and IntelliCage tests showed impaired learning and spatial memory in the GPER$^{-/-}$ female rats. There have been reports that the activation of GPER may improve the performance of rats in T-maze task and the inhibition of GPER has the opposite effect [47, 48]. Therefore, GPER appears to play a favorable role promoting learning and memory.

In summary, the present study has revealed widespread expression of GPER in the corticolimbic circuit, the HPA axis, and the sympathetic ganglia in rats and mice. GPER appears to play a major role in mediating gender differences in the HPA axis and in regulation of the cognitive, autonomic, and neuroendocrine responses to stress. Since GPER deficiency in the rat resulted in significant phenotypes including altered stress hormone profile in basal and stressed conditions, vulnerability to homeostatic disturbance such as reduced body weight gain and hypertension following stress [33], increased anxiety-like behaviors, and impaired learning and memory, more detailed analysis of GPER at different levels is warranted.

Data Availability

All data supporting the results of this study are included in the article.

Conflicts of Interest

The authors declare that they have no conflicts of interest.

Authors' Contributions

All authors listed have made important contributions to this study. WR, XS, TS, and GZ made substantial contributions to the conception and design of this study, acquired funding, supervised the experiments and data analysis, and critically revised the manuscript. YZ, MW, TG, LM, and XD conducted most of the experiments, analyzed the data, and drafted the manuscript. YM, YJ, PL, ZH, and BH took part in some of the experiments or provided technical support. Yi Zheng and Meimei Wu contributed equally to this work.

Acknowledgments

We thank Dr. Xuefeng Wu for the gift of Ai14(RCL-tdT)-D mice. This study was supported by the National Natural Science Foundation of China (grant #81570493 and 81873728), the Science and Technology Commission of Shanghai Municipality (grant #18JC1420302), and the Xinhua Hospital Affiliated to Shanghai Jiaotong University School of Medicine (grant #JZPI201705).

References

[1] K. Lebron-Milad and M. R. Milad, "Sex differences, gonadal hormones and the fear extinction network: implications for anxiety disorders," *Biology of Mood & Anxiety Disorders*, vol. 2, no. 1, article 3, 2012.

[2] A. L. Heck and R. J. Handa, "Sex differences in the hypothalamic-pituitary-adrenal axis' response to stress: an important role for gonadal hormones," *Neuropsychopharmacology*, vol. 44, no. 1, pp. 45–58, 2019.

[3] L. R. Hammerslag and J. M. Gulley, "Sex differences in behavior and neural development and their role in adolescent vulnerability to substance use," *Behavioural Brain Research*, vol. 298, no. Part A, pp. 15–26, 2016.

[4] C. Hayward and K. Sanborn, "Puberty and the emergence of gender differences in psychopathology," *The Journal of Adolescent Health*, vol. 30, no. 4, pp. 49–58, 2002.

[5] P. Llaneza, M. P. García-Portilla, D. Llaneza-Suárez, B. Armott, and F. R. Pérez-López, "Depressive disorders and the menopause transition," *Maturitas*, vol. 71, no. 2, pp. 120–130, 2012.

[6] W. Wittmann, E. Schunk, I. Rosskothen et al., "Prodynorphin-derived peptides are critical modulators of anxiety and regulate neurochemistry and corticosterone," *Neuropsychopharmacology*, vol. 34, no. 3, pp. 775–785, 2009.

[7] H. Cohen and R. Yehuda, "Gender differences in animal models of posttraumatic stress disorder," *Disease Markers*, vol. 30, no. 2-3, p. 150, 2011.

[8] J. S. Moser, T. P. Moran, C. Kneip, H. S. Schroder, and M. J. Larson, "Sex moderates the association between symptoms of anxiety, but not obsessive compulsive disorder, and error-monitoring brain activity: a meta-analytic review," *Psychophysiology*, vol. 53, no. 1, pp. 21–29, 2016.

[9] C. A. Frye, S. M. Petralia, and M. E. Rhodes, "Estrous cycle and sex differences in performance on anxiety tasks coincide with increases in hippocampal progesterone and 3α,5α-THP," *Pharmacology, Biochemistry, and Behavior*, vol. 67, no. 3, pp. 587–596, 2000.

[10] F. K. Marcondes, K. J. Miguel, L. L. Melo, and R. C. Spadari-Bratfisch, "Estrous cycle influences the response of female rats in the elevated plus-maze test," *Physiology & Behavior*, vol. 74, no. 4-5, pp. 435–440, 2001.

[11] M. A. Morgan and D. W. Pfaff, "Estrogen's effects on activity, anxiety, and fear in two mouse strains," *Behavioural Brain Research*, vol. 132, no. 1, pp. 85–93, 2002.

[12] N. Danilovich, N. Harada, M. R. Sairam, and D. Maysinger, "Age-related neurodegenerative changes in the central nervous system of estrogen-deficient follitropin receptor knockout mice," *Experimental Neurology*, vol. 183, no. 2, pp. 559–572, 2003.

[13] C. A. Frye, M. E. Rhodes, and B. Dudek, "Estradiol to aged female or male mice improves learning in inhibitory avoidance and water maze tasks," *Brain Research*, vol. 1036, no. 1-2, pp. 101–108, 2005.

[14] A. Caspi, K. Sugden, T. E. Moffitt et al., "Influence of life stress on depression: moderation by a polymorphism in the 5-HTT gene," *Science*, vol. 301, no. 5631, pp. 386–389, 2003.

[15] J. S. Snyder, A. Soumier, M. Brewer, J. Pickel, and H. A. Cameron, "Adult hippocampal neurogenesis buffers stress responses and depressive behaviour," *Nature*, vol. 476, no. 7361, pp. 458–461, 2011.

[16] D. A. Bangasser and R. J. Valentino, "Sex differences in stress-related psychiatric disorders: neurobiological perspectives," *Frontiers in Neuroendocrinology*, vol. 35, no. 3, pp. 303–319, 2014.

[17] R. A. Kloner, "Lessons learned about stress and the heart after major earthquakes," *American Heart Journal*, vol. 215, no. 1, pp. 20–26, 2019.

[18] E. V. Goldfarb, D. Seo, and R. Sinha, "Sex differences in neural stress responses and correlation with subjective stress and stress regulation," *Neurobiology of Stress*, vol. 11, no. 1, article 100177, 2019.

[19] D. Seo, A. Ahluwalia, M. N. Potenza, and R. Sinha, "Gender differences in neural correlates of stress-induced anxiety," *Journal of Neuroscience Research*, vol. 95, no. 1-2, pp. 115–125, 2017.

[20] D. Dyball, S. Evans, C. J. Boos, S. A. M. Stevelink, and N. T. Fear, "The association between PTSD and cardiovascular disease and its risk factors in male veterans of the Iraq/Afghanistan conflicts: a systematic review," *International Review of Psychiatry*, vol. 31, no. 1, pp. 34–48, 2019.

[21] B. Olde and L. M. F. Leeb-Lundberg, "GPR30/GPER1: searching for a role in estrogen physiology," *Trends in Endocrinology and Metabolism*, vol. 20, no. 8, pp. 409–416, 2009.

[22] P. Georgiou, P. Zanos, C. E. Jenne, and T. D. Gould, "Sex-specific involvement of estrogen receptors in behavioral responses to stress and psychomotor activation," *Frontiers in Psychiatry*, vol. 10, no. 1, article 81, 2019.

[23] D. B. Imwalle, J. A. Gustafsson, and E. F. Rissman, "Lack of functional estrogen receptor β influences anxiety behavior and serotonin content in female mice," *Physiology & Behavior*, vol. 84, no. 1, pp. 157–163, 2005.

[24] A. A. Walf, C. Koonce, K. Manley, and C. A. Frye, "Proestrous compared to diestrous wildtype, but not estrogen receptor beta knockout, mice have better performance in the spontaneous alternation and object recognition tasks and reduced anxiety-like behavior in the elevated plus and mirror maze," *Behavioural Brain Research*, vol. 196, no. 2, pp. 254–260, 2009.

[25] S. Yellayi, C. Teuscher, J. A. Woods et al., "Normal development of thymus in male and female mice requires estrogen/estrogen receptor-alpha signaling pathway," *Endocrine*, vol. 12, no. 3, pp. 207–213, 2000.

[26] G. G. J. Hazell, S. T. Yao, J. A. Roper, E. R. Prossnitz, A. M. O'Carroll, and S. J. Lolait, "Localisation of GPR30, a novel G protein-coupled oestrogen receptor, suggests multiple functions in rodent brain and peripheral tissues," *The Journal of Endocrinology*, vol. 202, no. 2, pp. 223–236, 2009.

[27] K. Matsuda, H. Sakamoto, H. Mori et al., "Expression and intracellular distribution of the G protein-coupled receptor 30 in rat hippocampal formation," *Neuroscience Letters*, vol. 441, no. 1, pp. 94–99, 2008.

[28] E. M. Waters, L. I. Thompson, P. Patel et al., "G-protein-coupled estrogen receptor 1 is anatomically positioned to modulate synaptic plasticity in the mouse hippocampus," *The Journal of Neuroscience*, vol. 35, no. 6, pp. 2384–2397, 2015.

[29] D. Hart, M. Nilges, K. Pollard et al., "Activation of the G-protein coupled receptor 30 (GPR30) has different effects on anxiety in male and female mice," *Steroids*, vol. 81, no. 1, pp. 49–56, 2014.

[30] I. Kastenberger, C. Lutsch, and C. Schwarzer, "Activation of the G-protein-coupled receptor GPR30 induces anxiogenic effects in mice, similar to oestradiol," *Psychopharmacology*, vol. 221, no. 3, pp. 527–535, 2012.

[31] I. Kastenberger and C. Schwarzer, "GPER1 (GPR30) knockout mice display reduced anxiety and altered stress response in a sex and paradigm dependent manner," *Hormones and Behavior*, vol. 66, no. 4, pp. 628–636, 2014.

[32] P. Luo, M. M. Wu, P. Gao et al., "Stress-related arterial hypertension in Gper-deficient rats," *Sheng Li Xue Bao*, vol. 69, no. 5, pp. 532–540, 2017.

[33] T. Mantamadiotis, T. Lemberger, S. C. Bleckmann et al., "Disruption of CREB function in brain leads to neurodegeneration," *Nature Genetics*, vol. 31, no. 1, pp. 47–54, 2002.

[34] T. J. Shors, C. Chua, and J. Falduto, "Sex differences and opposite effects of stress on dendritic spine density in the male versus female hippocampus," *The Journal of Neuroscience*, vol. 21, no. 16, pp. 6292–6297, 2001.

[35] C. Gross, X. Zhuang, K. Stark et al., "Serotonin$_{1A}$ receptor acts during development to establish normal anxiety-like behaviour in the adult," *Nature*, vol. 416, no. 6879, pp. 396–400, 2002.

[36] N. V. Weisstaub, M. Zhou, A. Lira et al., "Cortical 5-HT2A receptor signaling modulates anxiety-like behaviors in mice," *Science*, vol. 313, no. 5786, pp. 536–540, 2006.

[37] D. F. Tolin and E. B. Foa, "Sex differences in trauma and posttraumatic stress disorder: a quantitative review of 25 years of research," *Psychological Bulletin*, vol. 132, no. 6, pp. 959–992, 2006.

[38] C. S. de Kloet, E. Vermetten, E. Geuze, A. Kavelaars, C. J. Heijnen, and H. G. M. Westenberg, "Assessment of HPA-axis function in posttraumatic stress disorder: pharmacological and non-pharmacological challenge tests, a review," *Journal of Psychiatric Research*, vol. 40, no. 6, pp. 550–567, 2006.

[39] M. C. Morris, B. E. Compas, and J. Garber, "Relations among posttraumatic stress disorder, comorbid major depression, and HPA function: a systematic review and meta-analysis," *Clinical Psychology Review*, vol. 32, no. 4, pp. 301–315, 2012.

[40] P. Pervanidou and G. P. Chrousos, "Chapter 5 - neuroendocrinology of post-traumatic stress disorder," *Progress in Brain Research*, vol. 182, pp. 149–160, 2010.

[41] E. Brailoiu, S. L. Dun, G. C. Brailoiu et al., "Distribution and characterization of estrogen receptor G protein-coupled receptor 30 in the rat central nervous system," *The Journal of Endocrinology*, vol. 193, no. 2, pp. 311–321, 2007.

[42] H. F. Figueiredo, Y. M. Ulrich-Lai, D. C. Choi, and J. P. Herman, "Estrogen potentiates adrenocortical responses to stress in female rats," *American Journal of Physiology. Endocrinology and Metabolism*, vol. 292, no. 4, pp. E1173–E1182, 2007.

[43] R. J. Blanchard, R. Agullana, L. McGee, S. Weiss, and D. C. Blanchard, "Sex differences in the incidence and sonographic characteristics of antipredator ultrasonic cries in the

laboratory rat (Rattus norvegicus)," *Journal of Comparative Psychology*, vol. 106, no. 3, pp. 270–277, 1992.

[44] A. L. Johnston and S. E. File, "Sex differences in animal tests of anxiety," *Physiology & Behavior*, vol. 49, no. 2, pp. 245–250, 1991.

[45] B. Zimmerberg and M. J. Farley, "Sex differences in anxiety behavior in rats: role of gonadal hormones," *Physiology & Behavior*, vol. 54, no. 6, pp. 1119–1124, 1993.

[46] Z. Tian, Y. Wang, N. Zhang et al., "Estrogen receptor GPR30 exerts anxiolytic effects by maintaining the balance between GABAergic and glutamatergic transmission in the basolateral amygdala of ovariectomized mice after stress," *Psychoneuroendocrinology*, vol. 38, no. 10, pp. 2218–2233, 2013.

[47] R. Hammond, R. Mauk, D. Ninaci, D. Nelson, and R. B. Gibbs, "Chronic treatment with estrogen receptor agonists restores acquisition of a spatial learning task in young ovariectomized rats," *Hormones and Behavior*, vol. 56, no. 3, pp. 309–314, 2009.

[48] W. R. Hawley, E. M. Grissom, N. M. Moody, G. P. Dohanich, and N. Vasudevan, "Activation of G-protein-coupled receptor 30 is sufficient to enhance spatial recognition memory in ovariectomized rats," *Behavioural Brain Research*, vol. 262, no. 1, pp. 68–73, 2014.

Hindawi
Neural Plasticity
Volume 2020, Article ID 8814531, 10 pages
https://doi.org/10.1155/2020/8814531

Review Article

Neuropharmacological Effects of Mesaconitine: Evidence from Molecular and Cellular Basis of Neural Circuit

Zhihui Sun,[1] Limin Yang,[1] Lihong Zhao,[2] Ranji Cui,[2] and Wei Yang[2]

[1]*Cultivation Base of State Key Laboratory for Ecological Restoration and Ecosystem Management of Jilin Province and Ministry of Science and Technology, College of Chinese Medicinal Materials, Jilin Agricultural University, 130118, Changchun, Jilin, China*
[2]*Jilin Provincial Key Laboratory on Molecular and Chemical Genetic, The Second Hospital of Jilin University, Changchun, China*

Correspondence should be addressed to Limin Yang; ylmh777@126.com and Wei Yang; wyang2002@jlu.edu.cn

Received 25 May 2020; Revised 27 June 2020; Accepted 16 July 2020; Published 21 August 2020

Academic Editor: Fushun Wang

Mesaconitine (MA), a diester-diterpenoid alkaloid in aconite roots, is considered to be one of the most important bioactive ingredients. In this review, we summarized its neuropharmacological effects, including analgesic effects and antiepileptiform effects. Mesaconitine can act on the central noradrenergic system and the serotonin system; behaving like the norepinephrine reuptake inhibitors and tricyclic antidepressants that increase norepinephrine levels in stress-induced depression. Therefore, the possible perspectives for future studies on the depression of MA were also discussed as well. The pharmacological effect of MA on depression is worthy of further study.

1. Introduction

Many antidepressants have been developed based on the catecholamine deficiency hypothesis, but these drugs cannot meet people's needs. The latency period in antidepressant efficacy is a problem in Major Depressive Disorder (MDD) treatment because the depressive states are often connected with a higher risk of suicide [1, 2]. Representative antidepressants like NA reuptake inhibitors (NRIs) and selective serotonin reuptake inhibitors (SSRIs) require long-term therapy [3, 4]. Besides, only about 50% of MDD patients who received currently available antidepressants (AD) showed complete remission, including several drug trials with or without concurrent psychotherapy, but up to 80% of patients showed partial response [5]. Tricyclic antidepressants may have cardiotoxicity and atropine-like side effects [6]. Many new antidepressants are variants of classic antidepressants and have similar limitations [7, 8]. Therefore, there is a need to develop better antidepressants.

Mesaconitine (MA) is a predominant and representative component of alkaloids contained in the plant of the genera Aconitum [9]. MA possesses multiple pharmacological activities, such as vaso-relaxing effects [10–12], analgesic effects [13], and antiepileptiform effects [14]. Currently, only Nesterova et al. reported that MA possesses antidepressant activity [15]. However, the mechanisms of MA in analgesia and antiepileptiform effects are similar to that of antidepressants. The biological and pharmaceutical properties of MA can be improved by structural modification (Figure 1). So, the pharmacological effect of MA on depression is worthy of further study. In this review, we summarized the analgesic effects and antiepileptic effects. Besides, the possible perspectives for future studies on the depression of MA were also discussed as well.

2. Neuropharmacological Effects of MA

2.1. Analgesic Effects of MA. Mesaconitine (MA) possesses antinociceptive activity in nociceptive test models, such as writhing and tail immersion test [16–18]. Also, several components of Fuzi (genera Aconitum) possess analgesic effects, such as hypaconitine, fuziline, neoline, aconitine, songorine, and mesaconitine [18–20]. Benzoylmesaconine, hydrolyte of mesaconitine [21], possesses antinociceptive action in hyperalgesic rats as well [22]. Among these alkaloids, mesaconitine exhibited the strongest analgesic effects [23]. Mesaconitine

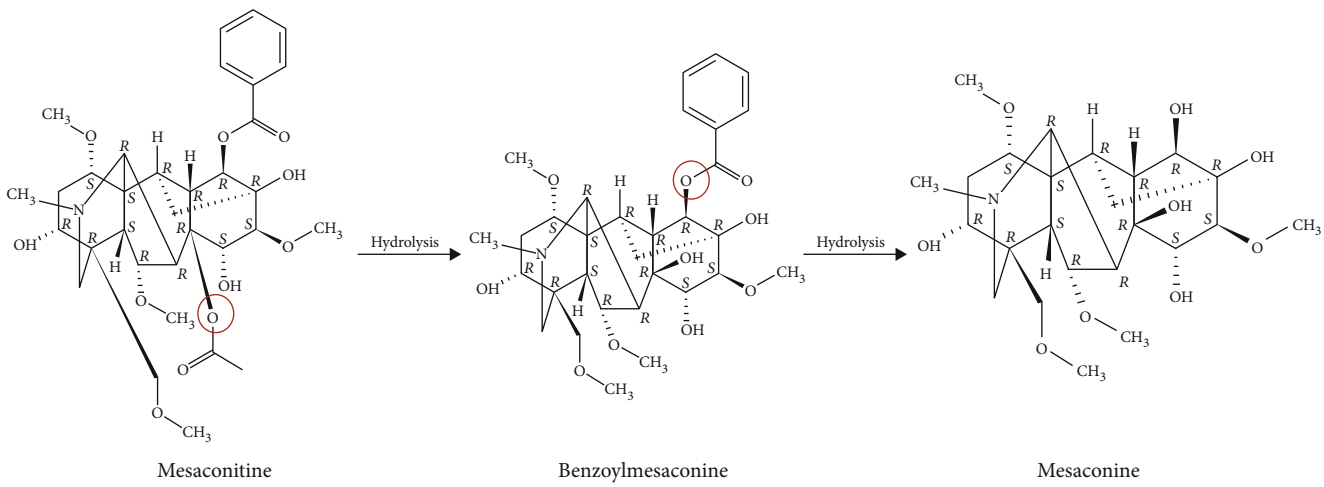

Figure 1: Absolute stereochemistry of mesaconitine and catabolite.

exerted analgesic effects via the periaqueductal gray (PAG), the nucleus reticularis gigantocellularis (NRGC), the lumbar enlargement, the nucleus raphe magnus (NRM), and the nucleus reticularis paragigantocellularis (NRPG) [17, 22, 24]. Microinjection of mesaconitine into the NRPG, NRM, and PAG produced dose-dependent analgesic activity; The analgesic effect of MA in NRM was more potent and sensitive than PAG and NRPG. [22]. Analgesic activity of the benzoylmesaconine (BM) may be through the activation of the NRM [22]. In the medulla oblongata, NRM is involved in the serotonergic descending inhibitory systems and NRPG acts in noradrenergic descending inhibitory systems. In the mesencephalon, PAG is involved in the descending pain inhibitory systems. Analgesic action of MA and BM appears to be through a descending serotonin system. MA promoted the turnover rate of norepinephrine in the brain stem and spinal cord. Norepinephrine activated adenylate cyclase through β-adrenoceptors, thereby significantly increased the level of cyclic adenosine monophosphate (cAMP), which enhanced the analgesic activity of MA [25, 26]. Murayama et al. reported that in isolated guinea-pig vas deferens, MA promoted the release of norepinephrine through excitatory sympathetic nerve fibers. Its analgesic effect may be the result of the release of noradrenaline from nerve endings and increased receptor sensitivity [26]. The analgesic effect of MA was enhanced by the injection of norepinephrine or isoproterenol intracerebroventricularly (i.c.v.) and attenuated by β-adrenoceptors antagonist [17, 26]. Therefore, the analgesic effect of MA seems to be through the activation of the noradrenergic system and serotonergic descending systems. This information is outlined in Table 1 and Figure 2.

Some studies have shown that the aromatic ester group of MA bound to site 2 of Na^+channels, resulting in sodium ion influx, causing neuronal depolarization and ultimately inhibiting the transmission of pain [18]. Besides, MA has the highest concentration in aconitine-type alkaloids of water extract of Radix Aconiti Carmichaeli (Chuan Wu) as quantified by high-performance liquid chromatography; the analgesic and anti-inflammatory activity of aqueous extracts may be due to high concentration of MA [13]. Heishunpian, Baifupian, and Yan-Fuzi are processed products of Fuzi. Interestingly, compared to Heishunpian and Baifupian, Yan-Fuzi possesses less toxic and antinociceptive activity of Yan-Fuzi is similar to crude Fuzi [27], which may be differences in processing methods that resulted in different alkaloid contents [28].

2.2. Antiepileptiform Effects of MA. From the above statements, we already know that mesaconitine exerts analgesic effects by stimulating the noradrenergic system. Mesaconitine also inhibited epileptic field potentials through α-adrenoceptors in a concentration-dependent manner. Important components of epileptiform discharge include presynaptic fiber peaks, the first postsynaptic population spike, and succeeding spikes, which define epileptiform activity. Stimulation-triggered epileptiform activity (a nominal Mg^{2+}-free perfusate) and spontaneous epileptiform activity (a nominal Mg^{2+}-free perfusate with elevated K+ concentration (5 mM)) are inhibited by MA (30 nM), which was antagonized by the α-adrenoceptors antagonist yohimbine (YOH) [14]. However, MA (300 nM and 1 μM) completely inhibited trigger-induced epileptiform activity and yohimbine cannot antagonize the inhibitory effect of MA [14]. These results indicated that MA (30 nM) activated the α-adrenoceptors when it inhibited experimentally induced epilepsy-like activity in the hippocampus.

Norepinephrine is believed to have both a convulsive and anticonvulsant effect depending on the receptors that are activated [29]. The hippocampus receives a diffuse projection of norepinephrine fibers from the locus coeruleus, and the activation of noradrenergic afferents affect hippocampal neuron activity [24]. The activation of alpha-adrenergic receptors reduced epileptiform discharges, whereas activation of beta-adrenergic receptors increased epileptiform discharges in the hippocampus. The rate of discharges induced by either picrotoxin or elevated extracellular potassium ($[K+]_o$) was slowed by NA($\geq$10 μM) [29]. Both α_1-adrenergic receptors agonists (phenylephrine) and α_2-adrenergic receptors antagonists (yohimbine) slowed epileptiform discharge rates [29]. However, some scholars have reported that the anticonvulsant activity of norepinephrine was mediated by α_2-adrenergic receptors and the α_2-selective agonist inhibited epileptiform

Table 1: Experimental information of the analgesic effect of MA.

Animal	Route	Most intense analgesia	ED_{50} values	Mode of action	Medicine	Method	References
Male mice (20-24 g) of the Std:ddY strain Male rats (200-220 g) of the Wistar strain.	s.c. MA (60 μg/kg) s.c. MA (20 μg/kg) i.c.	40 min after s.c	28 μg/kg (95% confidence limit: 11-37) in acetic acid-induced writhing 11 μg/kg (4-28) in tail flick	Dose-dependent and time-dependent	Mesaconitine hydrobromide	Acetic acid-induced writhing tail-flick	[26]....
Male Sprague-Dawley rats (250-350 g)	Intracerebral cannulation 10 ng/rats into NRPG 5 ng/rats into NRM 5 ng/rats into PAG	10 min 5 min 5 min		Dose-dependent and time-dependent	Mesaconitine hydrobromide	Paw pressure test	[22]....
Male rats of the Sprague-Dawley strain (200-250 g)	Intracerebral cannulation 50 and 100 ng/rat into the NRPG 50 ng/rat into the NRGC 50 ng/rat into the PAG 0.5 and 1.0 μg/rat into the lumbar enlargement	20 to 120 min 20 to 120 min 5 to 120 min 10 to 60 min	9.1 μg/kg- (95% confidence limits: 5.1-16.2) intravenously	Dose-dependent and time-dependent	Mesaconitine hydrobromide	Tail immersion test	[17]....
Male NMRI mice (25-30 g)	i.v.		0.025 (0.021-0.034)	Dose-dependent and time-dependent	Mesaconitine	Formalin test	[18]....

Abbreviations: MA: mesaconitine; NRPG: nucleus reticularis paragigantocellularis; NRM: nucleus raphe magnus; NGF: nerve growth factor; PAG: periaqueductal gray.

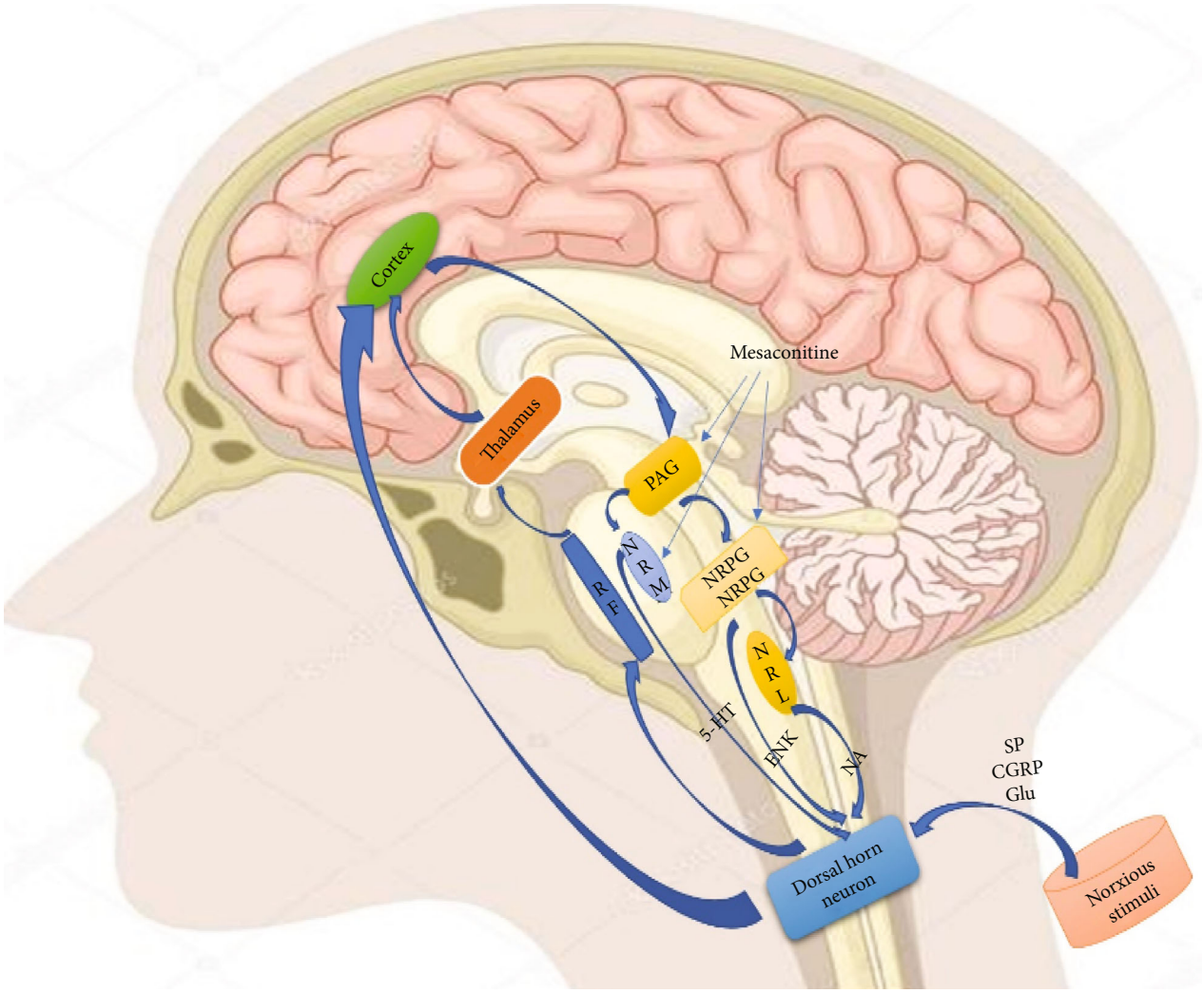

Figure 2: Schematic drawing of the nociceptive system with ascending and descending fibers. RF: reticular formation; PAG: periaqueductal gray; NRM: nucleus raphe magnus; NRGC: nucleus reticularis gigantocellularis; NRPG: nucleus reticularis paragigantocellularis; NRL: nucleus reticularis lateralis; 5-HT: 5-hydroxytryptamine; ENK: enkephalin; NA: noradrenaline.

discharges [30, 31]. The difference in the antiepileptiform mechanism of NA may be due to the different brain parts and concentrations of applied drugs. Consistently, the antiepileptiform effect is exerted by α-adrenergic receptors, and it is yet to be proven which specific α-adrenergic receptors have worked. It has been reported that mesaconitine induced contractions of the guinea-pig vas deferens by an enhanced neuronal release of noradrenaline [32]. So, MA (like the agonist) may act on α-adrenergic receptors to promote the release of norepinephrine and exert antiepileptiform effects (Figure 3). Besides, the specific molecular mechanism of antiepileptiform effects of MA needs further clarification.

2.3. Antidepressant Effects of MA. Our previous studies have demonstrated that Fuzi total alkaloids exerted anticonvulsant and antidepressant effects [33, 34]. Also, the antiepileptiform activity of MA has been reported. Some scholars have demonstrated the antidepressant effect of MA, possibly due to the altering of sensitivity to serotonin [15]. It is similar to the mechanism of the analgesic effects of MA. There are other possible reasons to support further the study of the pharmacological effect of MA on depression.

First, at least half of patients with chronic pain and itching are accompanied by depression and anxiety; chronic pain and itching can be found in as much as 60% of depressed patients. Tricyclic antidepressants have analgesic and antipruritic effects. Drugs treating psychosis can be used for analgesia, and analgesic drugs can also be used for depression [35]. We already knew that MA has an analgesic effect. Second, some scholars have demonstrated that the locus coeruleus noradrenergic neuron α_2-adrenergic receptors are functionally blocked in stress-depressed states. Injecting α_2-adrenergic receptor agonist intra-clonidine reduced the frequency of neuronal firing and reversed the animals' depressed state [36]. The antiepileptiform effect of MA was blocked by the α_2-adrenergic receptor antagonist [14]. So, MA may act on α_2-adrenergic receptors like clonidine. Third, dual-acting antidepressants like serotonin and norepinephrine

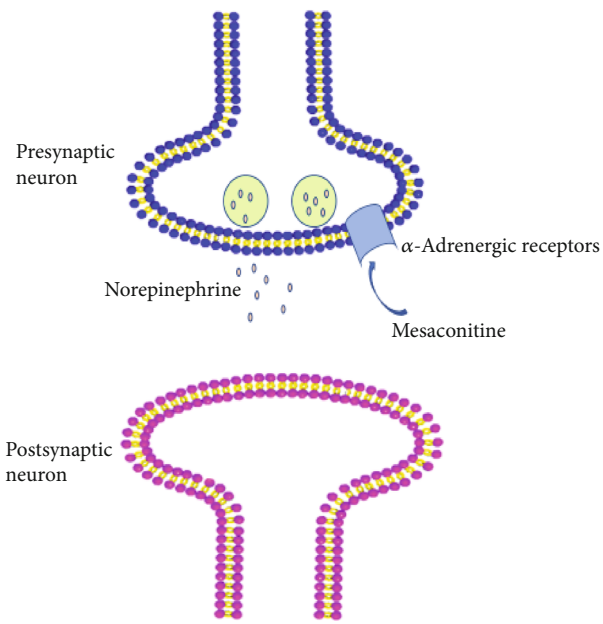

Figure 3: Schematic drawing of the antiepileptiform mechanism of mesaconitine on a noradrenergic neuron in the pyramidal stratum of the hippocampus.

reuptake inhibitors (SNRIs) as well as norepinephrine and dopamine reuptake inhibitors (NDRIs) have better efficacy than one system because of the multisystem monoaminergic pathway. They are the primary choices for clinicians in reducing residual symptoms and remission [37, 38]. MA exerted an analgesic effect through both the adrenergic system and the serotonin system. It is also possible to exert antidepressant effects through these two systems.

Moreover, the lack of monoamines is thought to be the leading cause of major depressive disorder (MDD), and some antidepressants work by increasing monoamine levels in the brain [39]. Representative antidepressants such as reboxetine [40], atomoxetine [41], and nortriptyline [42] inhibit noradrenergic transporters and increase norepinephrine in the brain. It has been reported that MA may promote the release of norepinephrine from neurons [24]. The neurotransmitter norepinephrine plays an important role in cognition, behavior, stress responses, and vigilance [43–45]. When the neurogenesis of the adult animal's hippocampus is destroyed by irradiation, the behavioral effects of antidepressants disappear [46]. Depression leads to atrophy of hippocampal neurons. Antidepressants enhance hippocampal neurogenesis [47–49] and reverse hippocampal volume shrinkage as well as hippocampal neuron loss [39]. NA greatly increased the dentate gyrus-derived neural precursor cells (NPCs) proliferation by activating the β_2-adrenergic receptor [50]. Jhaveri et al. reported that an increased amount of NA activated the neurogenic precursors and stem cells via β_3-adrenergic receptors [51]. Increasing norepinephrine by antidepressant promotes hippocampal neurogenesis through augmenting the survival and differentiation of new granule cells (DG) [52]. MA may increase hippocampal neurogenesis by norepinephrine acting on β-adrenergic receptors.

Finally, injection of norepinephrine or isoproterenol intracerebroventricularly (i.c.v.) enhanced analgesic effects of MA, and this effect was attenuated by β-adrenoceptors antagonist [17, 26]. MA seems to produce an analgesic effect by activating the β-adrenoceptors. The β-adrenoceptors can activate Gs. And then Gs activates adenylate cyclase (AC) to produce cyclic adenosine monophosphate (cAMP). cAMP further promotes phosphorylation of cAMP response element-binding (CREB), which in turn produces brain-derived neurotrophic factor (BDNF) [53] (Figure 4). Norepinephrine activated AC through β-adrenoceptors and increased the level of cAMP [25]. It is consistent with the previous description that MA promoted the release of norepinephrine. Moreover, some antidepressants act on CREB/BDNF pathway [54–57]. Increased expression of BDNF is considered to be an important mechanism of synaptic plasticity [58–60] and neurogenesis [61–63]. CREB plays an important role in neurogenesis and in reducing depressive symptoms in mice [64]. β_3-adrenergic receptor agonists reduced the immobility time of mice in forced swimming tests. The increase of NA by norepinephrine reuptake inhibitor in the synaptic cleft increased BDNF expression in the dentate gyrus (DG) of the hippocampus through β_3-adrenoceptor [39]. It seems that the antidepressant effects require the activation of β_3-adrenergic receptors. MA may activate β_3-adrenoceptor through norepinephrine (Figure 4).

Synaptic plasticity is currently considered to be an important basis for the formation of learning and memory. It is the fastest-growing research field in neuroscience. Synaptic plasticity includes structural plasticity and functional plasticity. The plasticity of the structure refers to the change in synaptic morphology and quantity caused by repeated synaptic activity. Functional plasticity refers to changes in synaptic transmission efficiency, including long-term potentiation (LTP) and long-term depression (LTD) [65]. Various forms of stress impair long-term potentiation and enhance long-term inhibition [66–69]. Tricyclic antidepressants increase synaptic plasticity at different levels [70]. Norepinephrine facilitates or induces LTP of the population spike through the β-adrenergic receptor [53]. Activation of β-adrenergic receptors increases the concentration of the cAMP, followed by activation of protein kinase A(PKA) and mitogen-activated protein kinase (MAPK) [71]. Also, norepinephrine-induced long-term potentiation may require activation of N-methyl-D-aspartic acid receptor (NMDA) receptors [72]. Calcium ions enter the cell through the activated NMDA receptors, then bind to intracellular calmodulin and activate adenylate cyclase to increase cAMP levels [73]. Activation of adenylate cyclase, PKA, and MAPK is involved in long-term potentiation induction [74–77]. Besides, norepinephrine reduces the threshold of LTP through phosphorylation of AMPA receptor subunit GluR1 [78]. Therefore, MA may affect synaptic plasticity through increasing norepinephrine. The possible mechanisms of the antidepressant effects induced by MA are outlined in Figure 4.

3. Side Effects of MA

Mesaconitine, a diester-diterpenoid alkaloid in aconite roots, is considered to be one of the most important bioactive

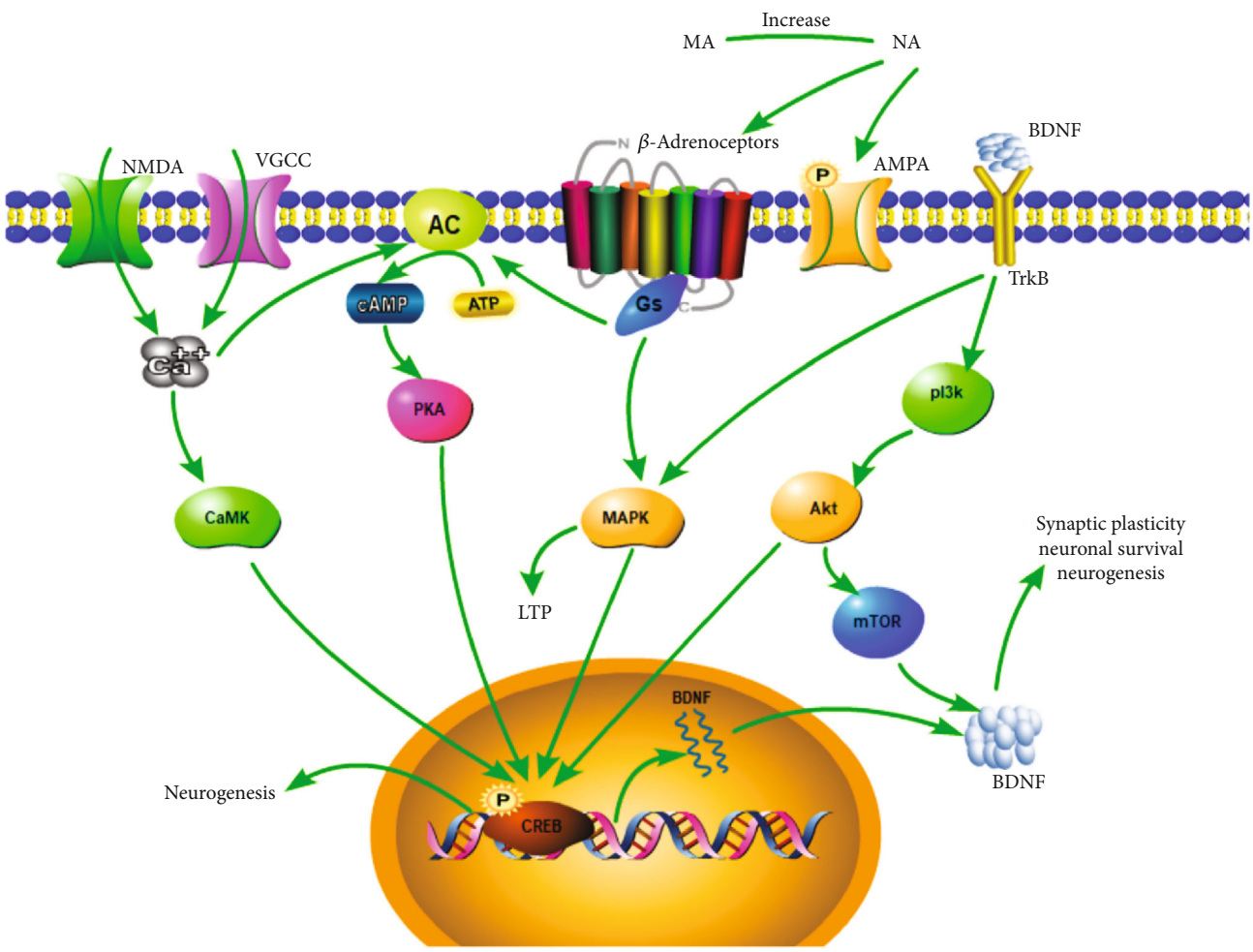

Figure 4: Role of β-adrenoceptors on antidepressant effect. All arrows indicate activation arrows. Gs: stimulating adenylate cyclase g protein; ATP: adenosine triphosphate; AC: adenylate cyclase; cAMP: cyclic adenosine monophosphate; PKA: protein kinase A; CREB: cAMP-response element-binding protein; BDNF: brain-derived neurotrophic factor; LTP: long-term potentiation; AMPA: α-amino-3-hydroxy-5-methyl-4-isoxazole propionate receptor.

Table 2: LD_{50} of mesaconitine.

Alkaloid	LD_{50} (mg/kg)			
	p.o.	s.c.	i.p.	i.v.
Mesaconitine	1.90 (mice)	0.20–0.38 (mice) 0.204 (rat)	0.20–0.30 (mice)	0.068–0.13 (mice)

ingredients and toxic ingredients [79]. Understanding the toxicity and toxicokinetic of MA is important for the application of MA and risk control. The therapeutic window of MA is narrow [80]: studies have shown that the median lethal dose (LD_{50}) of a single oral administration MA was 1.9 mg/kg in animal [81] and the half-life of MA was around 2.8–5.8 h [82]. The intravenous LD_{50} value in mice was 0.068 mg/kg [83]. Data from toxicological tests for MA have been presented by Zhou et al. [84] (Table 2). Although there are few reports on the toxicity of MA, three major diterpenoid alkaloids aconitine (AC), MA, and hypaconitine (HA) may share similar cardiotoxicity and mechanisms because of similar core structures [79]. Aconitine-type alkaloids are unstable and unsafe [28, 84–86]. Studies on the metabolism of MA in organisms have been reported [10, 87]. However, a comprehensive MA metabolism database still needs to be built for future pharmacological studies and clinical use [80]. In order to better understand the toxicity of MA, other advanced methods like an electrocardiogram, histopathology, serum biomarkers, and lipidomic profile changes need to be applied [79].

The diester diterpene alkaloids (DAs) with acetyl group at the C-8 position and ester group the C-14 benzoyl are toxic [84]. As the ester bond is hydrolyzed, the toxicity of MA is reduced [83, 87]. However, its pharmacological activity has not been affected [84]. Therefore, it is possible to improve the biological and pharmaceutical properties of MA through structural modification [19].

4. Conclusion

MA exerted analgesic effects and antidepressant effects through the serotonin system. Besides, MA exerted analgesic and antiepileptiform effects through the noradrenergic system. Like norepinephrine reuptake inhibitors and tricyclic antidepressants, MA can also increase norepinephrine levels, possibly through norepinephrine acting on related targets to produce multiple neuropharmacological effects. Therefore, the pharmacological effect of MA on depression is worthy of further study. Moreover, a thorough understanding of the toxicity and toxicokinetics of MA is required through advanced methods.

Abbreviations

BDNF: Brain-derived neurotrophic factor
CREB: cAMP-response element-binding protein
NRPG: Nucleus reticularis paragigantocellularis
NRM: Nucleus raphe magnus
NGF: Nerve growth factor
PAG: Periaqueductal gray
BM: Benzoylmesaconine
cAMP: Cyclic adenosine monophosphate
LD50: Median lethal dose
NA: Noradrenaline
PKA: Protein kinase A
MAPK: Mitogen-activated protein kinase
LTP: Long-term potentiation
NMDA: N-methyl-D-aspartic acid receptor.

Conflicts of Interest

The authors declare no conflict of interest.

Authors' Contributions

ZHS, LHZ, LMY, and WY contributed to drafting the article. All authors have revised the manuscript critically for important intellectual content and approved the final version to be published.

Acknowledgments

This work was supported by grants from the Natural Science Foundation of China (NSFC) (81971276), the National Key R&D Program of China (Grant #2018YFC1311600), and the Jilin Province Medical and Health Talents (2019SCZT007 and 2019SCZT013).

References

[1] J. Wang, L. Jing, J. C. Toledo-Salas, and L. Xu, "Rapid-onset antidepressant efficacy of glutamatergic system modulators: the neural plasticity hypothesis of depression," *Neuroscience Bulletin*, vol. 31, no. 1, pp. 75–86, 2015.

[2] N. Li, B. Lee, R. J. Liu et al., "mTOR-dependent synapse formation underlies the rapid antidepressant effects of NMDA antagonists," *Science*, vol. 329, no. 5994, pp. 959–964, 2010.

[3] G. A. Farber and J. F. Goldberg, "Regarding "combining norepinephrine and serotonin reuptake inhibition mechanisms for treatment of depression: A double-blind randomized study": Optimizing initial interventions," *Biological Psychiatry*, vol. 56, no. 7, pp. 535–535; author reply 536, 2004.

[4] L. R. Aleksandrova, Y. T. Wang, and A. G. Phillips, "Evaluation of the Wistar-Kyoto rat model of depression and the role of synaptic plasticity in depression and antidepressant response," *Neuroscience and Biobehavioral Reviews*, vol. 105, pp. 1–23, 2019.

[5] B. Haenisch and H. Bonisch, "Depression and antidepressants: insights from knockout of dopamine, serotonin or noradrenaline re-uptake transporters," *Pharmacology & Therapeutics*, vol. 129, no. 3, pp. 352–368, 2011.

[6] P. K. Gillman, "Tricyclic antidepressant pharmacology and therapeutic drug interactions updated," *British Journal of Pharmacology*, vol. 151, no. 6, pp. 737–748, 2007.

[7] G. Sanacora and A. F. Schatzberg, "Ketamine: promising path or false prophecy in the development of novel therapeutics for mood disorders?," *Neuropsychopharmacology*, vol. 40, no. 2, pp. 259–267, 2015.

[8] P. Willner, J. Scheel-Kruger, and C. Belzung, "Resistance to antidepressant drugs," *Behavioural Pharmacology*, vol. 25, no. 5 and 6, pp. 352–371, 2014.

[9] B. Sun, M. Zhang, Q. Zhang et al., "Metabonomics study of the effects of pretreatment with glycyrrhetinic acid on mesaconitine-induced toxicity in rats," *Journal of Ethnopharmacology*, vol. 154, no. 3, pp. 839–846, 2014.

[10] L. Ye, L. Tang, Y. Gong et al., "Characterization of metabolites and human P450 isoforms involved in the microsomal metabolism of mesaconitine," *Xenobiotica*, vol. 41, no. 1, pp. 46–58, 2010.

[11] M. Mitamura, K. Boussery, S. Horie, T. Murayama, and J. Van de Voorde, "Vasorelaxing effect of mesaconitine, an alkaloid from Aconitum japonicum, on rat small gastric artery: possible involvement of endothelium-derived hyperpolarizing factor," *Japanese Journal of Pharmacology.*, vol. 89, no. 4, pp. 380–387, 2002.

[12] M. Mitamura, S. Horie, M. Sakaguchi et al., "Mesaconitine-induced relaxation in rat aorta: involvement of Ca2+ influx and nitric-oxide synthase in the endothelium," *European Journal of Pharmacology*, vol. 436, no. 3, pp. 217–225, 2002.

[13] M. C. Lai, I.-M. Liu, S.-S. Liou, and Y.-S. Chang, "Mesaconitine plays the major role in the antinociceptive and anti-inflammatory activities of Radix Aconiti Carmichaeli (Chuan Wu)," *Journal of Food and Drug Analysis*, vol. 19, no. 3, 2011.

[14] A. Ameri, "Inhibition of stimulus-triggered and spontaneous epileptiform activity in rat hippocampal slices by the Aconitum alkaloid mesaconitine," *European Journal of Pharmacology*, vol. 342, no. 2-3, pp. 183–191, 1998.

[15] Y. V. Nesterova, T. N. Povetieva, N. I. Suslov, A. A. Semenov, and S. V. Pushkarskiy, "Antidepressant activity of diterpene alkaloids of Aconitum baicalense Turcz," *Bulletin of Experimental Biology and Medicine.*, vol. 151, no. 4, pp. 425–428, 2011.

[16] T. Oyama, T. Isono, Y. Suzuki, and Y. Hayakawa, "Anti-nociceptive effects of aconiti tuber and its alkaloids," *The American Journal of Chinese Medicine*, vol. 22, no. 2, pp. 175–182, 2012.

[17] H. Hikino and M. Murayama, "Mechanism of the antinociceptive action of mesaconitine: participation of brain stem and

lumbar enlargement," *British Journal of Pharmacology*, vol. 85, no. 3, pp. 575–580, 1985.

[18] J. Friese, J. Gleitz, U. T. Gutser et al., "Aconitum sp. alkaloids: the modulation of voltage-dependent Na+ channels, toxicity and antinociceptive properties," *European Journal of Pharmacology*, vol. 337, no. 2-3, pp. 165–174, 1997.

[19] Y. V. Nesterova, T. N. Povet'yeva, N. I. Suslov et al., "Analgesic activity of diterpene alkaloids from Aconitum baikalensis," *Bulletin of Experimental Biology and Medicine*, vol. 157, no. 4, pp. 488–491, 2014.

[20] D. Zhao, Y. Shi, X. Zhu et al., "Identification of Potential Biomarkers from Aconitum carmichaelii, a Traditional Chinese Medicine, Using a Metabolomic Approach," *Planta Medica*, vol. 84, no. 6/7, pp. 434–441, 2018.

[21] Y. Liu, X. Chen, R. He, and P. Tan, "Analysis of the metabolites of mesaconitine in rat blood using ultrafast liquid chromatography and electrospray ionization mass spectrometry," *Pharmacognosy magazine*, vol. 10, no. 38, pp. 101–105, 2014.

[22] Y. Suzuki, T. Oyama, A. Ishige et al., "Antinociceptive mechanism of the Actonitine alkaloids mesaconitine and benzoylmesaconine," *Planta Medica*, vol. 60, no. 5, pp. 391–394, 1994.

[23] L. Zhao, Z. Sun, L. Yang, R. Cui, W. Yang, and B. Li, "Neuropharmacological effects of aconiti lateralis radix praeparata," *Clinical and Experimental Pharmacology and Physiology*, vol. 47, no. 4, pp. 531–542, 2020.

[24] A. Ameri, "The effects of Aconitum alkaloids on the central nervous system," *Progress in Neurobiology*, vol. 56, no. 2, pp. 211–235, 1998.

[25] M. Murayama and H. Hikino, "Effect of cyclic AMP on mesaconitine-induced analgesia in mice," *European Journal of Pharmacology*, vol. 108, no. 1, pp. 19–23, 1985.

[26] M. Murayama, T. Ito, C. Konno, and H. Hikino, "Mechanism of analgesic action of mesaconitine. I. Relationship between analgesic effect and central monoamines or opiate receptors," *European Journal of Pharmacology*, vol. 101, no. 1-2, pp. 29–36, 1984.

[27] S. S. Liou, I. M. Liu, M. C. Lai, and J. T. Cheng, "Comparison of the antinociceptive action of crude Fuzei, the root of Aconitum, and its processed products," *Journal of Ethnopharmacology*, vol. 99, no. 3, pp. 379–383, 2005.

[28] S. Liu, F. Li, Y. Li, W. Li, J. Xu, and H. Du, "A review of traditional and current methods used to potentially reduce toxicity of Aconitum roots in traditional Chinese medicine," *Journal of Ethnopharmacology*, vol. 207, pp. 237–250, 2017.

[29] P. A. Rutecki, "Noradrenergic modulation of epileptiform activity in the hippocampus," *Epilepsy Research*, vol. 20, no. 2, pp. 125–136, 1995.

[30] A. L. Mueller and T. V. Dunwiddie, "Anticonvulsant and proconvulsant actions of alpha- and beta-noradrenergic agonists on epileptiform activity in rat hippocampus in vitro," *Epilepsia*, vol. 24, no. 1, pp. 57–64, 1983.

[31] M. N. Shouse, J. Langer, M. Bier et al., "The alpha 2-adrenoreceptor agonist clonidine suppresses seizures, whereas the alpha 2-adrenoreceptor antagonist idazoxan promotes seizures in amygdala-kindled kittens: a comparison of amygdala and pontine microinfusion effects," *Epilepsia*, vol. 37, no. 8, pp. 709–717, 1996.

[32] H. Sato, Y. Ohizumi, and H. Hikino, "Mechanism of mesoconitine-induced contractile response in Guinea pig vas deferens," *European Journal of Pharmacology*, vol. 55, no. 1, pp. 83–92, 1979.

[33] B. Li, F. Tang, L. Wang et al., "Anticonvulsant effects of Fuzi total alkaloid on pentylenetetrazole-induced seizure in mice," *Journal of Pharmacological Sciences*, vol. 123, no. 2, pp. 195–198, 2013.

[34] L. Liu, B. Li, Y. Zhou et al., "Antidepressant-like effect of Fuzi total alkaloid on ovariectomized mice," *Journal of Pharmacological Sciences*, vol. 120, no. 4, pp. 280–287, 2012.

[35] D. A. Belinskaia, M. A. Belinskaia, O. I. Barygin, N. P. Vanchakova, and N. N. Shestakova, "Psychotropic drugs for the management of chronic pain and itch," *Pharmaceuticals*, vol. 12, no. 2, p. 99, 2019.

[36] J. M. Weiss and P. E. Simson, "Neurochemical and electrophysiological events underlying stress-induced depression in an animal model," *Advances in Experimental Medicine and Biology*, vol. 245, pp. 425–440, 1988.

[37] C. B. Nemeroff, A. F. Schatzberg, D. J. Goldstein et al., "Duloxetine for the treatment of major depressive disorder," *Psychopharmacology Bulletin*, vol. 36, no. 4, pp. 106–132, 2002.

[38] D. Smith, C. Dempster, J. Glanville, N. Freemantle, and I. Anderson, "Efficacy and tolerability of venlafaxine compared with selective serotonin reuptake inhibitors and other antidepressants: a meta-analysis," *The British Journal of Psychiatry*, vol. 180, no. 5, pp. 396–404, 2002.

[39] K. Seki, S. Yoshida, and M. K. Jaiswal, "Molecular mechanism of noradrenaline during the stress-induced major depressive disorder," *Neural Regeneration Research*, vol. 13, no. 7, pp. 1159–1169, 2018.

[40] G. Chuluunkhuu, N. Nakahara, S. Yanagisawa, and I. Kamae, "The efficacy of reboxetine as an antidepressant, a meta-analysis of both continuous (mean HAM-D score) and dichotomous (response rate) outcomes," *The Kobe Journal of Medical Sciences*, vol. 54, no. 2, pp. E147–E158, 2008.

[41] C. J. Kratochvil, J. H. Newcorn, L. E. Arnold et al., "Atomoxetine alone or combined with fluoxetine for treating ADHD with comorbid depressive or anxiety symptoms," *Journal of the American Academy of Child and Adolescent Psychiatry*, vol. 44, no. 9, pp. 915–924, 2005.

[42] C. F. Reynolds III, E. Frank, J. M. Perel et al., "Nortriptyline and interpersonal psychotherapy as maintenance therapies for recurrent major depression," *JAMA*, vol. 281, no. 1, p. 39, 1999.

[43] S. Bouret, "Locus Coeruleus, noradrenaline, and behavior: network effect, network effects?," *Neuron*, vol. 103, no. 4, pp. 554–556, 2019.

[44] A. W. Goddard, S. G. Ball, J. Martinez et al., "Current perspectives of the roles of the central norepinephrine system in anxiety and depression," *Depression and Anxiety*, vol. 27, no. 4, pp. 339–350, 2010.

[45] L. K. Kuehl, C. E. Deuter, J. Hellmann-Regen, M. Kaczmarczyk, C. Otte, and K. Wingenfeld, "Enhanced noradrenergic activity by yohimbine and differential fear conditioning in patients with major depression with and without adverse childhood experiences," *Progress in Neuro-Psychopharmacology & Biological Psychiatry*, vol. 96, p. 109751, 2020.

[46] L. Santarelli, M. Saxe, C. Gross et al., "Requirement of hippocampal neurogenesis for the behavioral effects of antidepressants," *Science*, vol. 301, no. 5634, pp. 805–809, 2003.

[47] S. C. Park, "Neurogenesis and antidepressant action," *Cell and Tissue Research*, vol. 377, no. 1, pp. 95–106, 2019.

[48] L. Micheli, M. Ceccarelli, G. D'Andrea, and F. Tirone, "Depression and adult neurogenesis: Positive effects of the antidepressant fluoxetine and of physical exercise," *Brain Research Bulletin*, vol. 143, pp. 181–193, 2018.

[49] E. Tunc-Ozcan, C. Y. Peng, Y. Zhu, S. R. Dunlop, A. Contractor, and J. A. Kessler, "Activating newborn neurons suppresses depression and anxiety-like behaviors," *Nature Communications*, vol. 10, no. 1, p. 3768, 2019.

[50] T. Masuda, S. Nakagawa, S. Boku et al., "Noradrenaline increases neural precursor cells derived from adult rat dentate gyrus through beta2 receptor," *Progress in Neuro-Psychopharmacology & Biological Psychiatry*, vol. 36, no. 1, pp. 44–51, 2012.

[51] D. J. Jhaveri, E. W. Mackay, A. S. Hamlin et al., "Norepinephrine directly activates adult hippocampal precursors via beta3-adrenergic receptors," *The Journal of Neuroscience*, vol. 30, no. 7, pp. 2795–2806, 2010.

[52] P. Rizk, J. Salazar, R. Raisman-Vozari et al., "The alpha2-adrenoceptor antagonist dexefaroxan enhances hippocampal neurogenesis by increasing the survival and differentiation of new granule cells," *Neuropsychopharmacology*, vol. 31, no. 6, pp. 1146–1157, 2006.

[53] A. Marzo, J. Bai, and S. Otani, "Neuroplasticity regulation by noradrenaline in mammalian brain," *Current Neuropharmacology*, vol. 7, no. 4, pp. 286–295, 2009.

[54] P. Wang, B. Li, J. Fan et al., "Additive antidepressant-like effects of fasting with β-estradiol in mice," *Journal of Cellular and Molecular Medicine*, vol. 23, no. 8, pp. 5508–5517, 2019.

[55] S. Keshavarzi, S. Kermanshahi, L. Karami, M. Motaghinejad, M. Motevalian, and S. Sadr, "Protective role of metformin against methamphetamine induced anxiety, depression, cognition impairment and neurodegeneration in rat: the role of CREB/BDNF and Akt/GSK3 signaling pathways," *Neurotoxicology*, vol. 72, pp. 74–84, 2019.

[56] J. Li, Y. Luo, R. Zhang, H. Shi, W. Zhu, and J. Shi, "Neuropeptide trefoil factor 3 reverses depressive-like behaviors by activation of BDNF-ERK-CREB signaling in olfactory Bulbectomized rats," *International Journal of Molecular Sciences*, vol. 16, no. 12, pp. 28386–28400, 2015.

[57] Y. Li, J. Liu, X. Liu et al., "Antidepressant-like action of single facial injection of Botulinum neurotoxin a is associated with augmented 5-HT levels and BDNF/ERK/CREB pathways in mouse brain," *Neuroscience Bulletin*, vol. 35, no. 4, pp. 661–672, 2019.

[58] C. Bjorkholm and L. M. Monteggia, "BDNF - a key transducer of antidepressant effects," *Neuropharmacology*, vol. 102, pp. 72–79, 2016.

[59] D. T. Radecki, L. M. Brown, J. Martinez, and T. J. Teyler, "BDNF protects against stress-induced impairments in spatial learning and memory and LTP," *Hippocampus*, vol. 15, no. 2, pp. 246–253, 2005.

[60] E. T. Kavalali and L. M. Monteggia, "Synaptic mechanisms underlying rapid antidepressant action of ketamine," *The American Journal of Psychiatry*, vol. 169, no. 11, pp. 1150–1156, 2012.

[61] J. E. Malberg, A. J. Eisch, E. J. Nestler, and R. S. Duman, "Chronic antidepressant treatment increases neurogenesis in adult rat hippocampus," *The Journal of Neuroscience*, vol. 20, no. 24, pp. 9104–9110, 2000.

[62] B. Chen, D. Dowlatshahi, G. M. MacQueen, J.-F. Wang, and L. T. Young, "Increased hippocampal BDNF immunoreactivity in subjects treated with antidepressant medication," *Biological Psychiatry*, vol. 50, no. 4, pp. 260–265, 2001.

[63] Y. Jin, R. Cui, L. Zhao, J. Fan, and B. Li, "Mechanisms of Panax ginseng action as an antidepressant," *Cell Proliferation*, vol. 52, no. 6, p. e12696, 2019.

[64] S. Gascon, F. Ortega, and M. Gotz, "Transient CREB-mediated transcription is key in direct neuronal reprogramming," *Neurogenesis*, vol. 4, no. 1, p. e1285383, 2017.

[65] J. Jedrzejewska-Szmek and K. T. Blackwell, "From membrane receptors to protein synthesis and actin cytoskeleton: mechanisms underlying long lasting forms of synaptic plasticity," *Seminars in Cell & Developmental Biology*, vol. 95, pp. 120–129, 2019.

[66] S. Chattarji, A. Tomar, A. Suvrathan, S. Ghosh, and M. M. Rahman, "Neighborhood matters: divergent patterns of stress-induced plasticity across the brain," *Nature Neuroscience*, vol. 18, no. 10, pp. 1364–1375, 2015.

[67] W. N. Marsden, "Synaptic plasticity in depression: molecular, cellular and functional correlates," *Progress in Neuro-Psychopharmacology & Biological Psychiatry*, vol. 43, pp. 168–184, 2013.

[68] N. Maggio and M. Segal, "Persistent changes in ability to express long-term potentiation/depression in the rat hippocampus after juvenile/adult stress," *Biological Psychiatry*, vol. 69, no. 8, pp. 748–753, 2011.

[69] R. Holderbach, K. Clark, J. L. Moreau, J. Bischofberger, and C. Normann, "Enhanced long-term synaptic depression in an animal model of depression," *Biological Psychiatry*, vol. 62, no. 1, pp. 92–100, 2007.

[70] R. S. Duman, G. K. Aghajanian, G. Sanacora, and J. H. Krystal, "Synaptic plasticity and depression: new insights from stress and rapid-acting antidepressants," *Nature Medicine*, vol. 22, no. 3, pp. 238–249, 2016.

[71] Y. W. Lin, M. Y. Min, T. H. Chiu, and H. W. Yang, "Enhancement of associative long-term potentiation by activation of beta-adrenergic receptors at CA1 synapses in rat hippocampal slices," *The Journal of Neuroscience*, vol. 23, no. 10, pp. 4173–4181, 2003.

[72] E. C. Burgard, G. Decker, and J. M. Sarvey, "NMDA receptor antagonists block norepinephrine-induced long-lasting potentiation and long-term potentiation in rat dentate gyrus," *Brain Research*, vol. 482, no. 2, pp. 351–355, 1989.

[73] D. M. Chetkovich and J. D. Sweatt, "nMDA receptor activation increases cyclic AMP in area CA1 of the hippocampus via calcium/calmodulin stimulation of adenylyl cyclase," *Journal of Neurochemistry*, vol. 61, no. 5, pp. 1933–1942, 1993.

[74] N. A. Otmakhova, N. Otmakhov, L. H. Mortenson, and J. E. Lisman, "Inhibition of the cAMP pathway decreases early long-term potentiation at CA1 hippocampal synapses," *The Journal of Neuroscience*, vol. 20, no. 12, pp. 4446–4451, 2000.

[75] M. Makhinson, J. K. Chotiner, J. B. Watson, and T. J. O'Dell, "Adenylyl cyclase activation modulates activity-dependent changes in synaptic strength and Ca2+/calmodulin-dependent kinase II autophosphorylation," *The Journal of Neuroscience*, vol. 19, no. 7, pp. 2500–2510, 1999.

[76] Y. Y. Huang, K. C. Martin, and E. R. Kandel, "Both protein kinase a and mitogen-activated protein kinase are required in the amygdala for the macromolecular synthesis-dependent late phase of long-term potentiation," *The Journal of Neuroscience*, vol. 20, no. 17, pp. 6317–6325, 2000.

[77] M. G. Giovannini, R. D. Blitzer, T. Wong et al., "Mitogen-activated protein kinase regulates early phosphorylation and delayed expression of Ca2+/calmodulin-dependent protein kinase II in long-term potentiation," *The Journal of Neuroscience*, vol. 21, no. 18, pp. 7053–7062, 2001.

[78] H. Hu, E. Real, K. Takamiya et al., "Emotion enhances learning via norepinephrine regulation of AMPA-receptor trafficking," *Cell*, vol. 131, no. 1, pp. 160–173, 2007.

[79] M. Yang, X. Ji, and Z. Zuo, "Relationships between the toxicities of Radix Aconiti Lateralis Preparata (Fuzi) and the toxicokinetics of its main diester-diterpenoid alkaloids," *Toxins.*, vol. 10, no. 10, p. 391, 2018.

[80] L. Liu, C. Liu, Y. Wang, P. Wang, Y. Li, and B. Li, "Herbal medicine for anxiety, depression and insomnia," *Current Neuropharmacology*, vol. 13, no. 4, pp. 481–493, 2015.

[81] J. Singhuber, M. Zhu, S. Prinz, and B. Kopp, "Aconitum in traditional Chinese medicine: a valuable drug or an unpredictable risk?," *Journal of Ethnopharmacology*, vol. 126, no. 1, pp. 18–30, 2009.

[82] Y. Fujita, K. Terui, M. Fujita et al., "Five cases of aconite poisoning: toxicokinetics of aconitines," *Journal of Analytical Toxicology*, vol. 31, no. 3, pp. 132–137, 2007.

[83] L. Ye, S. Gao, Q. Feng et al., "Development and validation of a highly sensitive UPLC-MS/MS method for simultaneous determination of aconitine, mesaconitine, hypaconitine, and five of their metabolites in rat blood and its application to a pharmacokinetics study of aconitine, mesaconitine, and hypaconitine," *Xenobiotica*, vol. 42, no. 6, pp. 518–525, 2011.

[84] G. Zhou, L. Tang, X. Zhou, T. Wang, Z. Kou, and Z. Wang, "A review on phytochemistry and pharmacological activities of the processed lateral root of Aconitum carmichaelii Debeaux," *Journal of Ethnopharmacology*, vol. 160, pp. 173–193, 2015.

[85] T. Y. K. Chan, "Aconite poisoning," *Clinical Toxicology*, vol. 47, no. 4, pp. 279–285, 2009.

[86] J. J. Wu, Z. Z. Guo, Y. F. Zhu et al., "A systematic review of pharmacokinetic studies on herbal drug Fuzi: implications for Fuzi as personalized medicine," *Phytomedicine*, vol. 44, pp. 187–203, 2018.

[87] L. Ye, X. S. Yang, Z. Yang et al., "The role of efflux transporters on the transport of highly toxic aconitine, mesaconitine, hypaconitine, and their hydrolysates, as determined in cultured Caco-2 and transfected MDCKII cells," *Toxicology Letters.*, vol. 216, no. 2-3, pp. 86–99, 2013.

Hindawi
Neural Plasticity
Volume 2020, Article ID 9814978, 10 pages
https://doi.org/10.1155/2020/9814978

Research Article

Toll-Like Receptor 2 Attenuates Traumatic Brain Injury-Induced Neural Stem Cell Proliferation in Dentate Gyrus of Rats

Xin Zhang,[1,2] Yue Hei,[1] Wei Bai,[1] Tao Huang,[3] Enming Kang,[1] Huijun Chen,[1] Chuiguang Kong,[1] Yongxiang Yang,[1] Yuqin Ye,[1] and Xiaosheng He[1]

[1]*Department of Neurosurgery, Xijing Hospital, Air Force Medical University, Xi'an, 710032 Shaanxi, China*
[2]*Health Team of PLA 75768 Troops, Xiangyang, 441500 Hubei, China*
[3]*Department of Neurosurgery, Tangdu Hospital, Air Force Medical University, Xi'an, 710032 Shaanxi, China*

Correspondence should be addressed to Xiaosheng He; hexiaos@fmmu.edu.cn

Received 24 March 2020; Revised 10 July 2020; Accepted 24 July 2020; Published 17 August 2020

Academic Editor: Fushun Wang

It was not clear how and whether neural stem cells (NSCs) responded to toll-like receptor 2 (TLR2) in the inflammatory environment after traumatic brain injury (TBI). The current study investigated the correlation of TLR2 and NSC proliferation in the dentate gyrus (DG) using the TBI model of rats. Immunofluorescence (IF) was used to observe the expression of BrdU, nestin, and TLR2 in the DG in morphology. Proliferating cells in the DG were labelled by thymidine analog 5-bromo-2-deoxyuridine (BrdU). Three-labelled BrdU, nestin, and DAPI was used for the identification of newly generated NSCs. Western blotting and real-time polymerase chain reaction (PCR) were used to observe the expression of TLR2 from the level of protein and mRNA. We observed that $BrdU^+/nestin^+/DAPI^+$ cells accounted for $84.30\% \pm 6.54\%$ among $BrdU^+$ cells; $BrdU^+$ and $nestin^+$ cells in the DG were also $TLR2^+$ cells. $BrdU^+$ cells and the expression of TLR2 (both protein and mRNA levels) both elevated immediately at 6 hours (h), 24 h, 3 days (d), and 7 d posttrauma and peaked in 3 d. Results indicated that TLR2 was expressed on proliferating cells in the DG (NSCs possibly) and there was a potential correlation between increased TLR2 and proliferated NSCs after TBI. Taken together, these findings suggested that TLR2 was involved in endogenous neurogenesis in the DG after TBI.

1. Introduction

Neurogenesis occurs not only in the immature brain but also in the mature brain of mammals. In the adult brain, it is a complicated process including proliferation, differentiation, migration, and integration of neural stem cells (NSCs) into a neural network [1]. It is well known that NSCs exist mainly in two regions of the adult brain—the subgranular zone (SGZ) of the hippocampal dentate gyrus (DG) [2] and the subventricular zone (SVZ) of lateral ventricles [3]. Cells in these regions have potential self-renewal capacity and can turn out to become newborn neurons, microglia, oligodendrocytes, and astrocytes [4]. Such neurogenesis can be activated in some pathological conditions and play a key role in regeneration, repair, and functional recovery of the central nervous system (CNS) [5–8]. Although many studies have demonstrated that endogenous neurogenesis in the adult brain can be regulated by inflammatory reaction after neural trauma [9–11], it is still not clear how the inflammation within the brain influences the process of neurogenesis through NSC proliferation, differentiation, migration, and integration after traumatic brain injury (TBI).

As the essential innate immune receptors and members of the pattern recognition receptor family, TLRs can initiate primary defense mediated by pathogen-associated molecular pattern (PAMP) and endogenous ligand-induced damage-associated molecular pattern (DAMP) in the CNS [12–16]. TLRs can become stimulated by endogenous ligand released through damaged tissue, which comes from TBI, such as heat-shock proteins (HSPs), molecular degradation products, and intracellular components of damaged cells, which are called DAMPs. TLR signaling pathways contain two main parts, which are the MYD88-dependent pathway and the MYD88-independent pathway [17]. The inflammatory

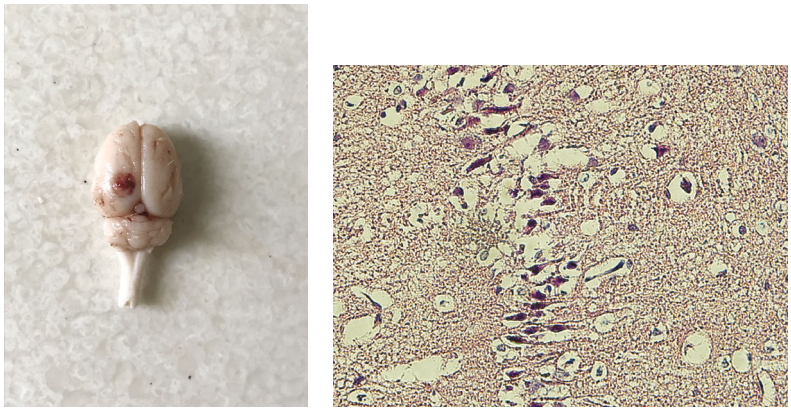

(a) (b)

Figure 1: Whole rat brain and injured cortex image. (a) Contusion and bleeding area on the surface at the parietal and occipital brain; (b) a large number of shrink neurons with pyknosis occurred in the injured cortex. Scale bar: 50 μm.

reaction caused by TBI can initiate activation of NF-κB and inflammatory cytokine genes. TLR2 is an identified TLR analog in mammals, and evidences have shown that TLR2 can be seen on several brain cells including neurons, microglia, oligodendrocytes, and astrocytes [18–20]. As known, it is important in the identification of an inflammatory environment in CNS-associated disorders, such as brain hemorrhage, infarction, and trauma [21–24]. Activation of TLR2 can mediate activation of NF-κB through the MYD88-independent pathway. Some recent investigations exhibit that the TLR2 expressed on the surface of NSCs and participated in the proliferation and differentiation of NSCs [25–27]. Nevertheless, it is not known what a potential role TLR2 plays in neurogenesis and whether and how NSCs respond to TLR2 in the inflammatory environment in the DG after TBI [28]. The current study observed NSC proliferation and TLR2 expression using a rat TBI model with an aim of exploring the potential correlation of TLR2 and endogenous neurogenesis (mainly NSCs involved) in the DG after TBI.

2. Results

2.1. Neurological Function Deficiency and Morphological Abnormality. After being performed by controlled cortical impact (CCI), all injured rats were back-arched, hair-erected, and in a rapid and shallow breath. These above manifestations disappeared in 1-2 hours; meanwhile, the rats were kept on the heating plate. It was observed that their right limbs were paralyzed. Sections of cortex containing injury sites 1 day after trauma were prepared for hematoxylin and eosin staining (H&E). Contusion and bleeding were seen on the surface at the parietal and occipital cortex (Figure 1(a)), and pyknosis among lots of shrink neurons was observed under microscopy (Figure 1(b)).

2.2. NSC Proliferation. Compared with the sham group, BrdU-positive cells in the DG increased markedly in rats after TBI ($p < 0.05$). BrdU$^+$ cells increased right after brain trauma, reached the peak in the 3rd day, and then decreased gradually (Figure 2(b)). BrdU, nestin, and DAPI three-labelled immunofluorescence (IF) images showed NSC proliferation in the DG. The proliferating cells, NSCs, and cell nuclei were indicated as red fluor (BrdU$^+$), green fluor (nestin$^+$), and blue fluor (DAPI$^+$), respectively. BrdU$^+$/-nestin$^+$/DAPI$^+$ cells accounted for 84.30% ± 6.54% among all BrdU$^+$ cells (Figure 3(a)). The percentage was consistent with the increasing of proliferating NSCs in the DG.

2.3. Expression of IF, Morphology, Protein, and mRNA of TLR2 in the Dentate Gyrus. TLR2$^+$ cells could be seen with red fluor on cytomembrane in the DG (Figures 2(a) and 3(b)). TLR2$^+$/nestin$^+$/DAPI$^+$ three-labelled fluor showed TLR2 expression on NSCs (Figure 3(b)). BrdU$^+$/TLR2$^+$/-DAPI$^+$ three-labelled fluor showed TLR2 expression in proliferating cells (mainly NSCs) in the DG (Figure 2(a)). Quantitative analysis indicated that BrdU$^+$/TLR2$^+$/DAPI$^+$ cells increased immediately after trauma and peaked in the 3rd day, then decreased gradually in the 7th day (Figure 2(c)). The TLR2 protein expression in the DG increased immediately after trauma, peaked in the 3rd day, and decreased in the 7th day posttrauma, but significantly higher compared with sham ($p < 0.05$) (Figures 4(a) and 4(b)). The expression of TLR2 mRNA elevated immediately after trauma, peaked in the 3rd day, and then decreased to a level still significantly higher than in sham ($p < 0.05$) (Figure 4(c)).

3. Discussion

Neurogenesis is a continuous process including proliferation, differentiation, and migration of NSCs after TBI [16, 29]. The current study focused on the proliferation process of NSCs. The rats were injected with BrdU intraperitoneally which was used to label newly generated or proliferating cells in the DG [30]. Meanwhile, nestin was expressed on the early stage of NSCs and it was used here to identify the NSCs among all of the proliferating cells in the DG and cortex. The expression of nestin was relatively stable in the proliferation of NSCs; however, it might change in the differentiation

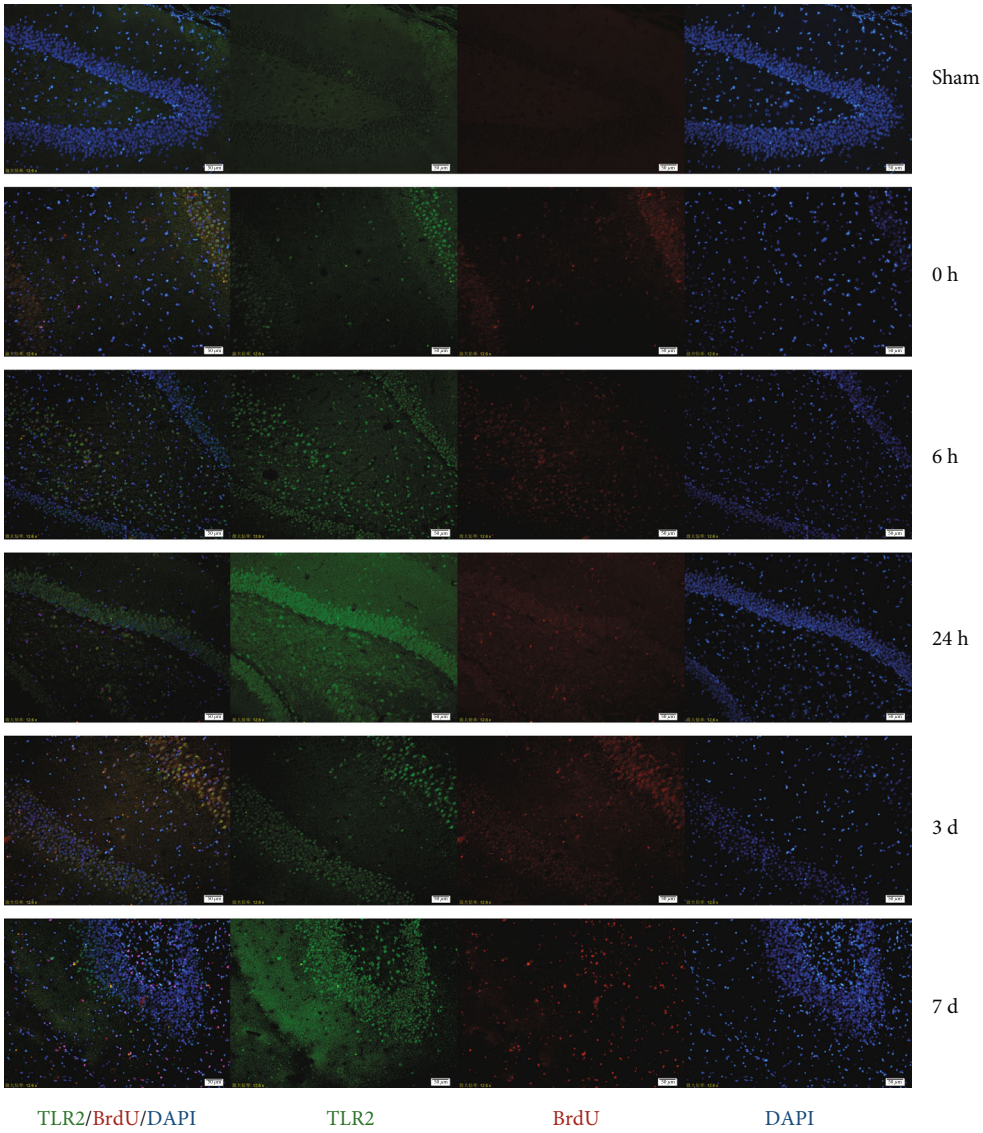

(a)

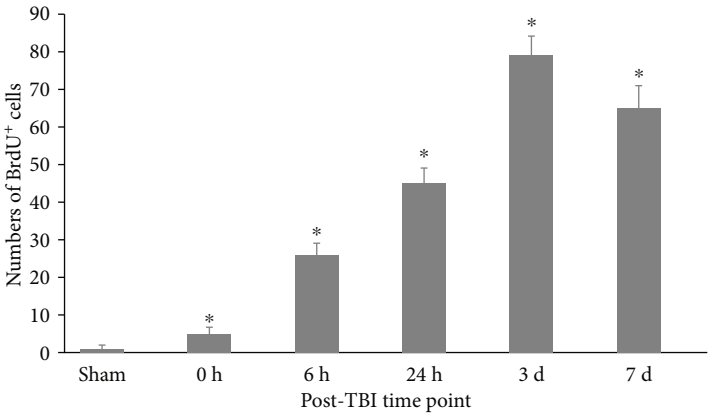

(b)

Figure 2: Continued.

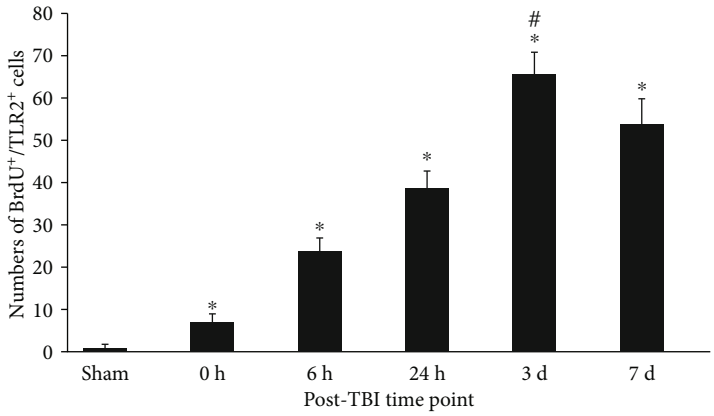

(c)

Figure 2: Immunofluorescence (IF) microphotographs in the dentate gyrus (DG) of the DG in sham and TBI groups at different time points. (a) BrdU-labelled NSCs (red fluor), expression of TLR2 (green fluor), cell nuclei (blue fluor), and $BrdU^+/TLR2^+/DAPI^+$ cells indicated that TLR2 expression in labelled proliferating cells was possible NSCs; (b) $BrdU^+$ cells showed the proliferation of NSCs in the DG during different time points posttrauma. $BrdU^+$ cells were more in the TBI group than that in the sham group ($^*p < 0.05$), and numbers of these cells were significantly different among different time points posttrauma ($^\#p < 0.05$); (c) numbers of $BrdU^+/TLR2^+$ cells indicated that the expression of TLR2 was quite different in proliferating cells of the DG among different time points posttrauma. There were more $BrdU^+$ cells in the TBI group than that in the sham group ($^*p < 0.05$), and the numbers of these cells are obviously different among different time points posttrauma ($^\#p < 0.05$). Scale bar: 50 μm; data is shown as mean ± SEM.

of NSCs into neurons, microglia, oligodendrocytes, and astrocytes. The current results revealed that $BrdU^+/nestin^+/DAPI^+$ cells accounted for 84.30% ± 6.54% among $BrdU^+$ cells, which suggested that the main proliferating cells in the DG were BrdU, nestin, and DAPI three-labelled positive cells. It was to say that these proliferating cells were highly suggested NSCs, although some of these cells could be composed of other cells, such as astrocytes or others.

In the current study, we observed that the protein and mRNA expression of TLR2 in the DG increased immediately after trauma, peaked in the 3rd day, and fell gradually from the 3rd day to the 7th day but still higher than the sham level. Moreover, $BrdU^+$ cells, $BrdU^+/TLR2^+$, and $BrdU^+/TLR2^+/DAPI^+$ cells all increased in a similar way over the various time points posttrauma. More importantly, $TLR2^+/nestin^+/DAPI^+$ three-labelled IF demonstrated that TLR2 was expressed on the NSCs in vivo.

It was accepted that NSC proliferation (often considered as $BrdU^+$ cells increasing) was actually a kind of secondary events after TBI. Our results revealed that NSC proliferation was accompanied by the upregulation of TLR2 in the DG. The synchronous change of the expression of TLR2 and BrdU-positive cells posttrauma revealed that there could be a possible correlation between each other [9, 16, 30], which implied that TLR2 might play a potential role in NSC proliferation after TBI.

Recent studies indicate that endogenous neurogenesis occurs continuously throughout the whole life of all cells [31–33]. Injuries, such as trauma, stroke, inhalation injury, and also oxygen-glucose deprivation (OGD), can easily trigger neurogenesis in the brain [9, 34]. Also, trauma triggers, activates, and enhances the ability of NSCs to regenerate neurons in the DG [35]. These newborn neurons can integrate into the existed neural network and contribute to the repair process in the DG [33]. The current study based on the TBI model of rats demonstrated the pyknosis in lots of shrunken neurons in the area of the injured cortex (H&E stain). The lesions and the possibly enhanced neurogenesis in the DG (BrdU-labelled proliferating cells) coexisted. These proliferating cells maintained a higher level than sham within posttrauma in 7 days with a peak in the 3rd day. Our findings were in accordance with previous studies that reported endogenous neurogenesis in the adult brain after TBI [33].

More and more evidences showed that activated endogenous neurogenesis in the DG is essential not only for learning and memory but also for other detrimental outcomes caused by TBI [11, 36]. Nevertheless, endogenous neurogenesis of NSCs is not sufficient that is used to repair brain injury post-TBI. Therefore, strategies that effectively activate endogenous NSCs to produce more functional neural cells are needed for tissue repair and functional reconstruction posttrauma.

Recent investigations focused on the TLR2 expression on NSCs in vitro and collected the evidences on the effect of TLR2 on NSC proliferation and differentiation. Rolls et al. declared that TLR2 was expressed on NSCs in the hippocampus of the adult brain [25]. In the study of Covacu et al. [27], it was observed that the expression of TLR2 on NSCs and NSC culture, which separated from the DG in the hippocampus of the adult rat brain, was exposed on different inflammatory factors, such as IFN-γ, TNF-α, IL-1β, and IL-6 [37, 38]. At the same time, TLR2 mRNA was also upregulated while IFN-γ was put into NSC culture with supernatants from activated macrophages, but it could not be seen when TNF-α was put into. TLR2 agonist could activate NSCs to produce TNF-α in a medium, but there were no solid evidences whether there was any promotion of TLR2 agonist on the proliferation and differentiation of NSCs in vitro

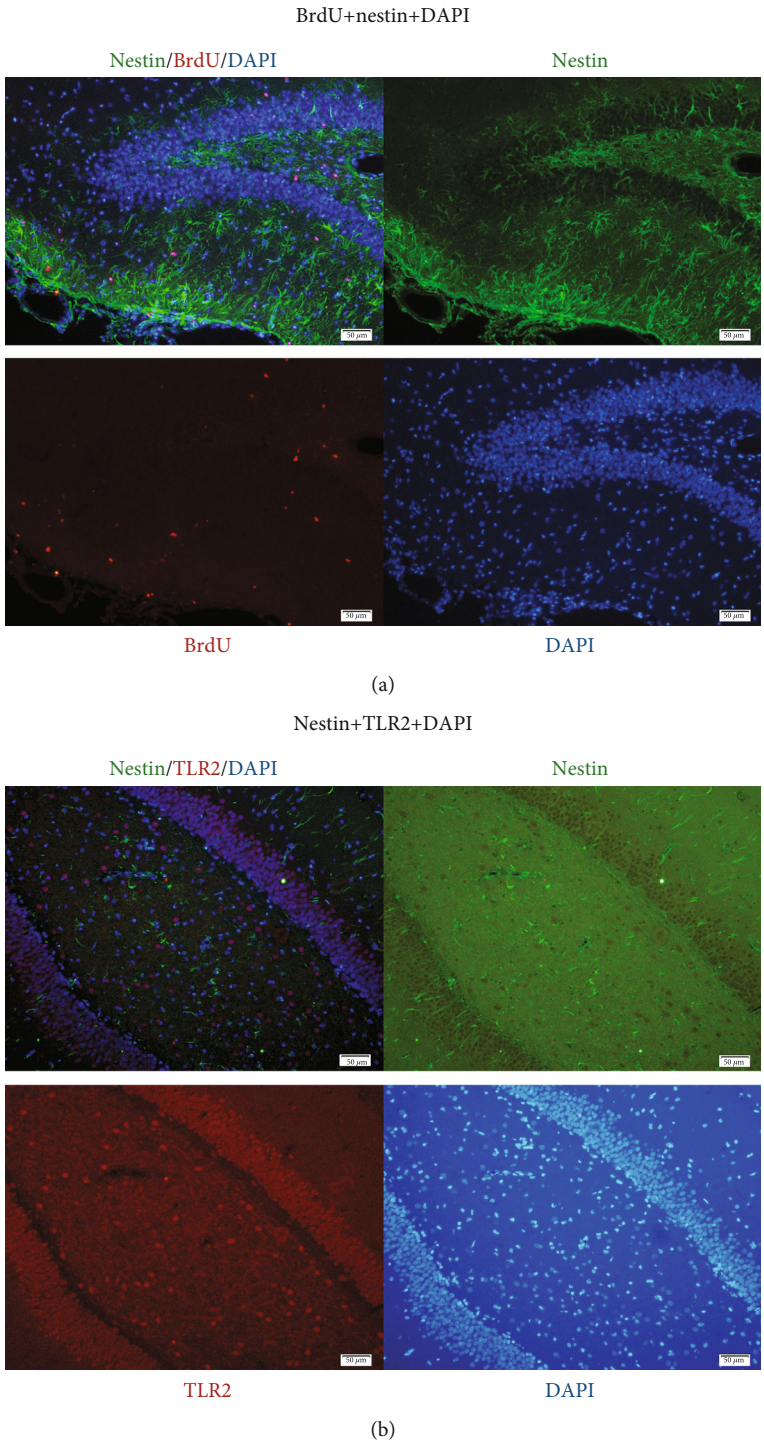

Figure 3: IF in the DG of the TBI group (mouse brain got from 3 days posttrauma). (a) BrdU (red), nestin (green), and DAPI (blue), respectively, exhibited proliferating cells, NSCs, and cell nuclei in the DG. Merged pictures of $BrdU^+/nestin^+/DAPI^+$ showed NSCs (the percentage of NSCs in proliferating cells was 84.30% ± 6.54%); scale bar: 50 μm; data were expressed as mean ± SEM. (b) Nestin (green), TLR2 (red), and DAPI (blue), respectively, exhibited NSCs, TLR2 expression, and cell nuclei in the DG. Merged pictures of $nestin^+/TLR2^+/DAPI^+$ showed the expression of TLR2 on NSCs. Scale bar: 50 μm; data were expressed as mean ± SEM.

[39]. On the contrary, compared with NSCs separated from wild-type rats, neurogenesis around the DG from TLR2-deficiency rats was destroyed, and adult neural cell differentiation could not be seen. It is to say that TLR2 plays an important role in both proliferation and differentiation of NSCs [25, 26]. Based on existed studies, it was inferred that TLR2 activation could lead to neuronal and other neural cells' death [40] but whether the numbers of neural cells decreased needed further exploration. Moreover, because of different species of animals, different trauma models, and different

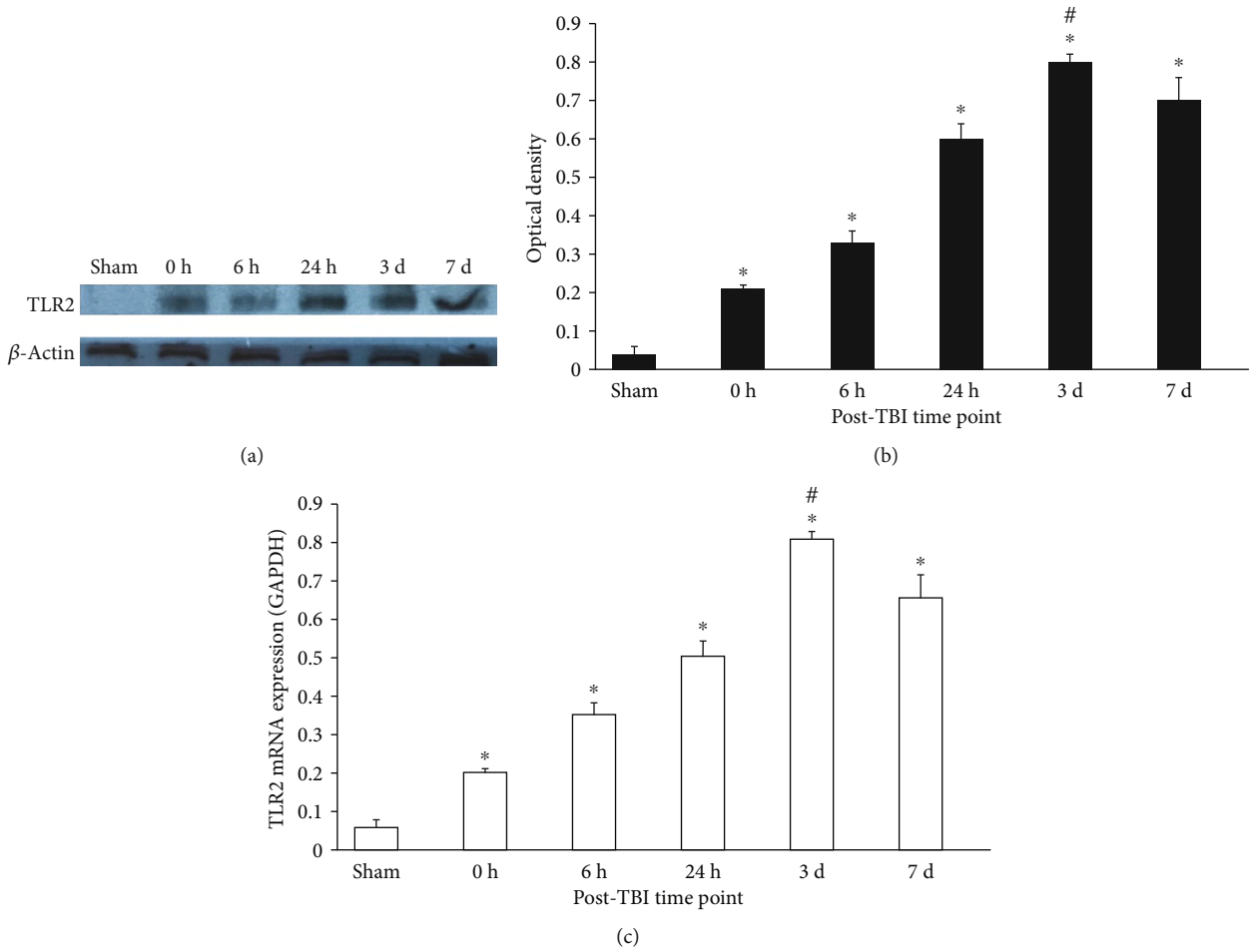

Figure 4: Expression of TLR2 protein and mRNA in the DG (western blotting and PCR). (a) Western blotting: electrophoresis bands of TLR2 protein controlled with β-actin; (b) western blotting: the optical density of TLR2 electrophoresis; (c) real-time PCR: the expression of TLR2 mRNA and GAPDH was used as the endogenous reference gene. The TLR2 expression in the protein and mRNA level was significantly higher in the TBI group than that in the sham group ($^{*}p < 0.05$), and the TLR2 expression was significantly different among various time points ($^{\#}p < 0.05$). Data were expressed as mean ± SEM.

functional stages of NSCs, different results should also need to be investigated.

TLR2 can also express on other cells in the brain besides NSCs, and the cells which can express TLR2 are helpful for the process of neurogenesis and inflammation in the environment of neurogenesis in the brain [11, 26, 41]. However, the growth environment of the NSC medium in vitro is different from that in vivo. Less study focused on the correlation of TLR2 expression in the DG in vivo after TBI and neurogenesis. The current study based on the TBI model helped us to observe that the level of morphology, protein, and mRNA upregulated from immediately after trauma to the 7th day in vivo after TBI [42]. It demonstrated the morphological evidences of TLR2 on NSC expression in the DG and suggested a potential correlation of TLR2 expression and NSC proliferation in the DG.

To sum up, the current experiments investigated the potential correlation between TLR2 expression and NSC proliferation in the DG in vivo. Because there was a limitation in experimental design in vivo, the results were not able to show the expression of TLR2 on the other cells, such as oligodendrocytes and neurons, in the level of protein and mRNA in the DG after trauma. Therefore, more studies are needed to precisely describe the effect of TLR2 in purer NSCs in endogenous neurogenesis in the DG after TBI. Moreover, other explorations are required to investigate the inflorescences of TLR2 to the differentiation of NSCs following the proliferation in the DG post-TBI.

4. Materials and Methods

4.1. Animals and Group. A total of 108 healthy adult male SD rats, weighing 226 ± 25 g, were purchased from the center of experimental animals of the Air Force Military Medical University. They were raised in the environment with stable temperature and humidity, 12-hour day and night cycle, and were allowed to eat and drink freely. Methods were used in order to minimize the pain and uncomfortableness of animals. Experimental procedures were in accordance with the guidelines of the National Experimental Animals, approved by the Ministry of Science and Technology of China (023915137, 09 January 2001).

An independent group design was adopted. Rats were randomly divided into the sham group ($n = 18$) and the TBI group ($n = 90$). TBI rats were divided into 5 subgroups ($n = 18$ each), sacrificed, respectively, in 6 hours postinjury, 1 day, 3 days, 7 days, and 14 days after trauma. The sham group was divided into 3 subgroups ($n = 6$ each) as controls. IF, western blotting, and real-time PCR were performed with each individual brain sample in both the TBI and sham groups.

4.2. TBI Model Establishment. A CCI device (Hatteras Instruments, Cary, NC, USA) was used to establish the TBI model [43]. Rats were anesthetized intraperitoneally with sodium pentobarbital (60 mg/kg) and then placed on a stereotaxic frame (Kopf Instruments, Tujunga, CA, USA). Rats were secured with ear pins and incisor bar on a frame floor. A midline scalp incision was made, and a craniotomy was performed, using a bone harvest drill with a 3.5 mm diameter, at 2 mm left to the sagittal suture and 2 mm in front of the lambdoidal suture. The bone flap was smoothly removed, and the window was in a diameter of 10 cm. A one-time injury was performed with the flat end of a metal stick with a diameter of 3 mm to contact the surface of the exposed dura. The impact parameters were as follows: 1.0 mm dura shift vertically, 100 ms contact time, and 3 m/s velocity. The scalp incision was sewed up after the operation. The above surgical procedures were done in sham rats without any injury. Animals were put on a constant temperature plate to maintain their core temperature at not below 37°C after the operation.

4.3. Administration of 5-Bromo-2-Deoxyuridine (BrdU). BrdU (Sigma-Aldrich, B5002, St. Louis, Missouri, USA) was dissolved in sterile saline to the concentration of 10 mg/ml. The TBI and sham groups were injected intraperitoneally with BrdU (50 mg/kg) once a day to label NSCs in the DG in order to assess proliferation.

4.4. Tissue Preparation. At the established time points, rats in the TBI and sham groups were weighed and anesthetized by intraperitoneal injection of pentobarbital sodium (60 mg/kg) and then treated with heart-perfusion through the left ventricle with 100 ml 10% heparin saline for 3-5 min and 500 ml 10% paraformaldehyde phosphate buffer saline (PBS) for 2-4 h. The whole brain was removed and placed in 10% paraformaldehyde PBS (pH = 7.4) at 4°C overnight, then dehydrated in alcohol gradient and embedded in paraffin. A microtome (Leica, Nussloch, Germany) was used to cut the brain DG area into 3 μm thick coronal sections containing the site of the DG which were dried and maintained at 70°C overnight. Ten coronal sections of each animal were three-labelled with BrdU/TLR2/DAPI. In order to identify NSCs in proliferating cells and verify the expression of TLR2 on NSCs after TBI, half of 10 more sections at the same plane in 6 rats in the 3-day group were prepared for to get BrdU/-nestin/DAPI three-labelled treatment, and another half for nestin/TLR2/DAPI three-labelled treatment.

The TBI severity was assessed by animal behavior, such as its posture and mobility, and gross morphological change of brain tissue.

4.5. IF. Sections were deparaffinized by alcohol and dimethylbenzene and then incubated in citric acid and sodium citrate antigen retrieval solution (pH = 6.0) at 100°C for 100 s. The sections were incubated in hydrogen peroxide for 20 min and donkey serum for 45 min to block nonspecific signals at room temperature. The primary antibodies were used as the following to illustrate, respectively, the expression of BrdU, nestin, and TLR2: sheep anti-BrdU antibody (1 : 160, abcam, ab1893, Cambridge Science Park, Cambridge, UK), mouse anti-rat nestin antibody (1 : 100, Millipore, MAB353, Burlington, Massachusetts, USA), and mouse anti-TLR2 antibody (1 : 100, GeneTex, GTX31279, Alton Pkwy, Irvine, CA, USA). Each body was dissolved in PBS at 4°C overnight. After being washed 5 times by PBS with tween-20 (PBST), the secondary antibodies were used as follows: Alexa Fluor 594 donkey anti-sheep IgG antibody (1 : 2000, ThermoFisher SCIENTIFIC, A11016, Waltham, Massachusetts, USA), Alexa Fluor 594 donkey anti-mouse IgG antibody (1 : 2000, ThermoFisher SCIENTIFIC, A-21203, Waltham, Massachusetts, USA), Alexa Fluor 488 donkey anti-rabbit IgG antibody (1 : 2000, ThermoFisher SCIENTIFIC, A21206, Waltham, Massachusetts, USA), and Alexa Fluor 488 donkey anti-mouse IgG antibody (1 : 2000, ThermoFisher SCIENTIFIC, A21202, Waltham, Massachusetts, USA). Each body was dissolved in PBS for 3 h at room temperature. After being washed 5 times by PBST, sections were mounted with antifade mounting medium (Beyotime, P0131, Songjiang, Shanghai, China) and coverslipped. All experimental procedures are required to minimize light exposure to the tissue.

4.6. Microscopy and Quantification. Sections were observed by an upright fluorescence microscope (OLYMPUS, BX53, Shinjuku, Tokyo, Japan) and a high-power mercury lamp (OLYMPUS, U-RFL-T, Shinjuku, Tokyo, Japan) through the cellSens Standard system (OLYMPUS, Shinjuku, Tokyo, Japan) and photographed by a camera (OLYMPUS, DP72, Shinjuku, Tokyo, Japan).

Proliferating cells in the DG were assessed by $BrdU^+$ cells in the ipsilateral DG of the injured cortex [44]. BrdU/TLR2/-DAPI three-labelled fluor was used to observe $BrdU^+$, $TLR2^+$, and $BrdU^+/TLR2^+$ cells. Positive cells were measured in 5 consecutive fields in sections containing the DG using a fluorescence microscope. The average cell number of all 5 fields was considered as the positive cell number of each section, and the average of the positive cell number of all 5 sections was considered as the positive cell number of each brain sample of rats. Data was expressed as mean ± SEM.

The $BrdU^+/nestin^+/DAPI^+$ three-labelling was used to show proliferating NSCs in the DG after TBI. The percentage of $BrdU^+/nestin^+/DAPI^+$ cells in $BrdU^+$ cells was counted, and $nestin^+/TLR2^+/DAPI^+$ three-labelling were taken to analyze the expression of TLR2 in possible NSCs.

4.7. Western Blotting. At each time point, the rats' brains were removed immediately after the rats were sacrificed by

Table 1: Gene sequences for primer synthesis.

Gene	Primers	Sequence 5′-3′
TLR2	Sense	TGGAAGCAGGTGACAACC
	Antisense	ACCTTCGTCCACTGTTGG
GAPDH	Sense	ACAGCAACAGGGTGGTGGAC
	Antisense	TTTGAGGGTGCAGCGAACTT

excessively intraperitoneal anesthesia. Hippocampal tissues were separated as quickly as possible on ice and then dissolved in a buffer in homogenizers, which contained RIPA lysis buffer (Beyotime, P0013, Songjiang, Shanghai, China) and phenylmethylsulfonyl fluoride (Beyotime, ST506, Songjiang, Shanghai, China). The above solution was put around the ice for 30 min and then centrifuged for 20 min in 15000 rpm at 4°C. Supernate was taken for protein quantification through the Bicinchoninic Acid Protein Assay kit (Beyotime, P0010, Songjiang, Shanghai, China). Protein samples were added with loading buffer and boiled at 100°C for 10 min. Samples containing 40 μg protein were used for gel electrophoresis, and then, the protein on the gel was transferred to nitrocellulose membranes. Primary antibodies were used as follows: mouse anti-TLR2 antibody (1 : 500, Biorbyt, orb191498, San Francisco, CA, USA) and mouse anti-β-actin antibody (1 : 3000, TDY BIOTECH, TDY041, Beijing, China) overnight at 4°C. After washed 4 times by PBST, membranes were incubated with HRP- (horseradish peroxidase-) Conjugated Goat anti-Mouse IgG (H+L) antibody (1 : 40000, TDY BIOTECH, S001, Beijing, China) for 1 h in room temperature. The protein bands were observed through Western LumaxLight Superior (ZETA LIFE, 310208, USA), and the greyscale of TLR2 to β-actin was considered as the expression of TLR2.

4.8. Real-Time PCR. At each time point, rats were sacrificed in the way as used above. The tissue of the DG was removed. Total RNA was extracted by the MiniBEST Universal RNA Extraction Kit (TaKaRa, 9767, Toyko, Japan). Prime Script™ one-step RT-PCR Kit Ver.2 (TaKaRa, RR055, Toyko, Japan) was used to synthesis cDNA. TB Green™ Fast qPCR Mix (TaKaRa, RR430, Toyko, Japan) was used in the CFX96 real-time PCR detection system (Bio-Rad, Hercules, CA, USA). GAPDH was adopted as the endogenous reference gene for the expression of the TLR2 gene.

The sequences of primers were as follows (Table 1): TLR2 forward: 5′-TGGAAGCAGGTGACAACC-3′; TLR2 reserve: 5-ACCTTCGTCCACTGTTGG-3; GAPDH forward: 5-ACAGCAACAGGGTGGTGGAC-5; GAPDH reserve: 5-TTTGAGGGTGCAGCGAACTT.

4.9. Statistical Analysis. All of the data was expressed as mean ± SEM. Multiple comparisons in TLR2 and proliferation-related factors in the DG were analyzed using one-way ANOVA followed by post hoc Bonferroni's test using SPSS 22.0.0 and GraphPad prism (v.7.0.1, GraphPad software, San Diego, CA, USA). The $p < 0.05$ was considered to be statistically significant.

5. Conclusion

The current study illustrated that BrdU$^+$ and nestin$^+$ cells were TLR2$^+$ cells in the DG after trauma through the TBI model of rats, indicating that obvious cell proliferation (considered as newly NSC formation) was followed with an increased expression of TLR2. It suggested that NSC proliferation might be correlated with TLR2 upregulation in the DG and TLR2 might play a potential role in endogenous neurogenesis in the DG after TBI. The results demonstrated that there was evident NSC proliferation in the DG. Because newborn neurons and other cells grew mixed in the process of NSC differentiation, specific markers should be used to identify cell types and their possible origin, which was the goal of future investigations.

Data Availability

All data generated or analyzed during this study are included in this article.

Conflicts of Interest

The authors declare no conflicts of interest.

Authors' Contributions

Xin Zhang performed the experiments, Yue Hei analyzed the results, and Wei Bai made statistical treatments. Tao Huang, Enming Kang, Huijun Chen, Chuiguang Kong, Yongxiang Yang, and Yuqin Ye assisted the first author in performing the immunofluorescence, western blotting, and real-time PCR. Xiaosheng He designed the study, monitored the whole research process, and wrote the article. Xin Zhang, Yue Hei, and Wei Bai contributed equally to this work.

Acknowledgments

The current study was supported by the Natural Science Foundation of China (NSFC) (Nos. 81171155 and 81171246).

References

[1] A. H. Yao, L. Y. Jia, Y. K. Zhang et al., "Early blockade of TLRs MyD88-dependent pathway may reduce secondary spinal cord injury in the rats," *Evidence-Based Complementary and Alternative Medicine*, vol. 2012, Article ID 591298, 13 pages, 2012.

[2] K. Obernier and A. Alvarez-Buylla, "Neural stem cells: origin, heterogeneity and regulation in the adult mammalian brain," *Development*, vol. 146, no. 4, 2019.

[3] S. Biswas, S. H. Chung, P. Jiang, S. Dehghan, and W. Deng, "Development of glial restricted human neural stem cells for oligodendrocyte differentiation in vitro and in vivo," *Scientific Reports*, vol. 9, no. 1, p. 9013, 2019.

[4] C. Grochowski, E. Radzikowska, and R. Maciejewski, "Neural stem cell therapy–brief review," *Clinical Neurology and Neurosurgery*, vol. 173, pp. 8–14, 2018.

[5] R. Pérez-Sen, M. J. Queipo, J. C. Gil-Redondo et al., "Dual-specificity phosphatase regulation in neurons and glial cells,"

International Journal of Molecular Sciences, vol. 20, no. 8, p. 1999, 2019.

[6] M. Kolahdouzan, N. C. Futhey, N. W. Kieran, and L. M. Healy, "Novel molecular leads for the prevention of damage and the promotion of repair in neuroimmunological disease," *Frontiers in Immunology*, vol. 10, p. 1657, 2019.

[7] K. Berry and Q. Richard Lu, "Chromatin modification and epigenetic control in functional nerve regeneration," *Seminars in Cell & Developmental Biology*, vol. 97, pp. 74–83, 2020.

[8] F. Riganello, S. K. Larroque, C. di Perri, V. Prada, W. G. Sannita, and S. Laureys, "Measures of CNS-autonomic interaction and responsiveness in disorder of consciousness," *Frontiers in Neuroscience*, vol. 13, p. 530, 2019.

[9] J. M. Parent, "Injury-induced neurogenesis in the adult mammalian brain," *The Neuroscientist*, vol. 9, no. 4, pp. 261–272, 2016.

[10] N. Stella, "Neuroscience. Inflammation to rebuild a brain," *Science*, vol. 338, no. 6112, pp. 1303-1304, 2012.

[11] R. A. Kohman and J. S. Rhodes, "Neurogenesis, inflammation and behavior," *Brain, Behavior, and Immunity*, vol. 27, no. 1, pp. 22–32, 2013.

[12] S. Akira and K. Takeda, "Toll-like receptor signalling," *Nature Reviews. Immunology*, vol. 4, no. 7, pp. 499–511, 2004.

[13] H. Tada, R. Suzuki, E. Nemoto, H. Shimauchi, K. Matsushita, and H. Takada, "Increases in IL-33 production by fimbriae and lipopeptide from Porphyromonas gingivalis in mouse bone marrow-derived dendritic cells via toll-like receptor 2," *Biomedical Research*, vol. 38, no. 3, pp. 189–195, 2017.

[14] S. Esser, L. Göpfrich, K. Bihler et al., "Toll-like receptor 2-mediated glial cell activation in a mouse model of cuprizone-induced demyelination," *Molecular Neurobiology*, vol. 55, no. 8, pp. 6237–6249, 2018.

[15] V. Kumar, "Toll-like receptors in the pathogenesis of neuroinflammation," *Journal of Neuroimmunology*, vol. 332, pp. 16–30, 2019.

[16] Y. Ye, H. Xu, X. Zhang et al., "Association between toll-like receptor 4 expression and neural stem cell proliferation in the hippocampus following traumatic brain injury in mice," *International Journal of Molecular Sciences*, vol. 15, no. 7, pp. 12651–12664, 2014.

[17] D. S. Weiss, K. Takeda, S. Akira, A. Zychlinsky, and E. Moreno, "MyD88, but not toll-like receptors 4 and 2, is required for efficient clearance of Brucella abortus," *Infection Immunity*, vol. 73, no. 8, pp. 5137–5143, 2005.

[18] M. Carty and A. G. Bowie, "Evaluating the role of toll-like receptors in diseases of the central nervous system," *Biochemical Pharmacology*, vol. 81, no. 7, pp. 825–837, 2011.

[19] M. Sanchez-Ruiz, N. K. Polakos, T. Blau et al., "TLR signals license CD8 T cells to destroy oligodendrocytes expressing an antigen shared with a Listeria pathogen," *European Journal of Immunology*, vol. 49, no. 3, pp. 413–427, 2019.

[20] J. Wang, Z. Chen, J. D. Walston, P. Gao, M. Gao, and S. X. Leng, "Interferon-γ potentiates α-synuclein-induced neurotoxicity linked to toll-like receptors 2 and 3 and tumor necrosis factor-α in murine astrocytes," *Molecular Neurobiology*, vol. 56, no. 11, pp. 7664–7679, 2019.

[21] M. L. Hanke and T. Kielian, "Toll-like receptors in health and disease in the brain: mechanisms and therapeutic potential," *Clinical Science*, vol. 121, no. 9, pp. 367–387, 2011.

[22] L. Zuo, Q. Feng, Y. Han et al., "Therapeutic effect on experimental acute cerebral infarction is enhanced after nanoceria labeling of human umbilical cord mesenchymal stem cells," *Therapeutic Advances in Neurological Disorders*, vol. 12, p. 1756286419859725, 2019.

[23] H. Zhu, Z. Wang, J. Yu et al., "Role and mechanisms of cytokines in the secondary brain injury after intracerebral hemorrhage," *Progress in Neurobiology*, vol. 178, p. 101610, 2019.

[24] T. Otsuka, T. Imura, K. Nakagawa et al., "Simulated microgravity culture enhances the neuroprotective effects of human cranial bone-derived mesenchymal stem cells in traumatic brain injury," *Stem Cells and Development*, vol. 27, no. 18, pp. 1287–1297, 2018.

[25] A. Rolls, R. Shechter, A. London et al., "Toll-like receptors modulate adult hippocampal neurogenesis," *Nature Cell Biology*, vol. 9, no. 9, pp. 1081–1088, 2007.

[26] E. Okun, K. J. Griffioen, and M. P. Mattson, "Toll-like receptor signaling in neural plasticity and disease," *Trends in Neurosciences*, vol. 34, no. 5, pp. 269–281, 2011.

[27] R. Covacu, L. Arvidsson, Å. Andersson et al., "TLR activation induces TNF-alpha production from adult neural stem/progenitor cells," *Journal of Immunology*, vol. 182, no. 11, pp. 6889–6895, 2009.

[28] S. M. Krieg, F. Voigt, P. Knuefermann, C. J. Kirschning, N. Plesnila, and F. Ringel, "Decreased secondary lesion growth and attenuated immune response after traumatic brain injury in Tlr2/4(-/-) mice," *Frontiers in Neurology*, vol. 8, p. 455, 2017.

[29] G. Furlan, V. Cuccioli, N. Vuillemin et al., "Life-long neurogenic activity of individual neural stem cells and continuous growth establish an outside-in architecture in the teleost pallium," *Current Biology*, vol. 27, no. 21, pp. 3288–3301.e3, 2017, e3.

[30] S. Sauerzweig, K. Baldauf, H. Braun, and K. G. Reymann, "Time-dependent segmentation of BrdU-signal leads to late detection problems in studies using BrdU as cell label or proliferation marker," *Journal of Neuroscience Methods*, vol. 177, no. 1, pp. 149–159, 2009.

[31] H. J. Kim and W. Sun, "Adult neurogenesis in the central and peripheral nervous systems," *International Neurourology Journal*, vol. 16, no. 2, pp. 57–61, 2012.

[32] J. G. Emsley, B. D. Mitchell, G. Kempermann, and J. D. Macklis, "Adult neurogenesis and repair of the adult CNS with neural progenitors, precursors, and stem cells," *Progress in Neurobiology*, vol. 75, no. 5, pp. 321–341, 2005.

[33] P. K. Dash, S. A. Mach, and A. N. Moore, "Enhanced neurogenesis in the rodent hippocampus following traumatic brain injury," *Journal of Neuroscience Research*, vol. 63, no. 4, pp. 313–319, 2001.

[34] J. D. Bernstock, L. Peruzzotti-Jametti, T. Leonardi et al., "SUMOylation promotes survival and integration of neural stem cell grafts in ischemic stroke," *eBioMedicine*, vol. 42, pp. 214–224, 2019.

[35] E. M. Millon and T. J. Shors, "Taking neurogenesis out of the lab and into the world with _MAP Train My Brain_ ™," *Behavioural Brain Research*, vol. 376, p. 112154, 2019.

[36] R. M. Richardson, D. Sun, and M. R. Bullock, "Neurogenesis after traumatic brain injury," *Neurosurgery Clinics of North America*, vol. 18, no. 1, pp. 169–181, 2007, xi.

[37] J. Zan, H. Zhang, M. Y. Lu et al., "Isosteviol sodium injection improves outcomes by modulating TLRs/NF-κB-dependent inflammatory responses following experimental traumatic brain injury in rats," *Neuroreport*, vol. 29, no. 10, pp. 794–803, 2018.

[38] G. D. Silveira, M. E. Ishimura, D. Teixeira et al., "Improvement of mesenchymal stem cell immunomodulatory properties by heat-killed Propionibacterium acnes via TLR2," *Frontiers in Molecular Neuroscience*, vol. 11, p. 489, 2018.

[39] T. J. Albin, J. K. Tom, S. Manna et al., "Linked toll-like receptor triagonists stimulate distinct, combination-dependent innate immune responses," *ACS Central Science*, vol. 5, no. 7, pp. 1137–1145, 2019.

[40] D. Trudler, D. Farfara, and D. Frenkel, "Toll-like receptors expression and signaling in glia cells in neuro- amyloidogenic diseases: towards future therapeutic application," *Mediators of Inflammation*, vol. 2010, 12 pages, 2010.

[41] H. Song, C. F. Stevens, and F. H. Gage, "Astroglia induce neurogenesis from adult neural stem cells," *Nature*, vol. 417, no. 6884, pp. 39–44, 2002.

[42] G. Z. Li, Y. Zhang, J. B. Zhao, G. J. Wu, X. F. Su, and C. H. Hang, "Expression of myeloid differentiation primary response protein 88 (Myd88) in the cerebral cortex after experimental traumatic brain injury in rats," *Brain Research*, vol. 1396, pp. 96–104, 2011.

[43] T. T. Logan, S. Villapol, and A. J. Symes, "TGF-β superfamily gene expression and induction of the Runx1 transcription factor in adult neurogenic regions after brain injury," *PLoS One*, vol. 8, no. 3, article e59250, 2013.

[44] D. G. Amaral, H. E. Scharfman, and P. Lavenex, "The dentate gyrus: fundamental neuroanatomical organization (dentate gyrus for dummies)," *Progress in Brain Research*, vol. 163, pp. 3–22, 2007.

Hindawi
Neural Plasticity
Volume 2020, Article ID 7235734, 8 pages
https://doi.org/10.1155/2020/7235734

Research Article

Biases of Happy Faces in Face Classification Processing of Depression in Chinese Patients

Yuying Tong,[1] Gang Zhao,[2] Jinbo Zhao,[1] Nianxiang Xie,[1] Dong Han,[3,4] Bowen Yang,[1] Qi Liu,[1] Hailian Sun,[5] and Yanjie Yang[4]

[1]*Department of Psychology, School of Education, Heilongjiang University, China*
[2]*Department of Child Health Care, Maternity and Child Healthcare, Hospital of Nanshan District, Shenzhen, China*
[3]*Department of Human Movement and Sport Science, Harbin Sport University, China*
[4]*Public Health College of Harbin Medical University, Heilongjiang Province, China*
[5]*The First Affiliated Hospital of Harbin Medical University, China*

Correspondence should be addressed to Yanjie Yang; yanjie1965@163.com

Received 18 March 2020; Revised 25 July 2020; Accepted 31 July 2020; Published 17 August 2020

Academic Editor: Fushun Wang

We explored the face classification processing mechanism in depressed patients, especially the biases of happy faces in face classification processing of depression. Thirty patients with the first episode of depression at the First Affiliated Hospital of Harbin Medical University were selected as the depression group, while healthy people matched for age, gender, and educational level were assigned to the control group. The Hamilton Depression Scale and Hamilton Anxiety Scale were used to select the subjects; then, we used the forced face classification paradigm to collect behavioral (response time and accuracy) and event-related potential (ERP) data of the subjects. The differences between the groups were estimated using a repeated measurement analysis of variance. The total response time of classified faces in the depression group was longer than that in the control group, the correct rate was lower, and the difference was statistically significant ($P < 0.05$). N170 component analysis demonstrated that the latency of the depression group was prolonged, and the difference was statistically significant ($P < 0.05$). When classifying happy faces, the depressed patients demonstrated a decrease in N170 amplitude and a prolongation of latency in some brain regions compared with the healthy individuals. The cognitive bias in depression may be due to prolonged processing of positive facial information and difficulty in producing positive emotional responses.

1. Introduction

Depression is the leading cause of ill health and disability worldwide, and >300 million individuals live with depression [1]. Between 10% and 15% of patients with depression are at risk for suicide [2]. According to a survey, the economic burden in China due to depression exceeds 60 billion yuan [2].

Scholars have explored the etiologic mechanism underlying depression from genetic, biochemical, and psychosocial aspects, but the specific mechanism remains unclear. Cognitive factors, especially cognitive biases (processing biases to negative stimuli), are one of the major reasons for the occurrence, continuation, and development of depressive symptoms [3]. The cognitive model of depression demonstrates that depressed individuals tend to attribute negative meanings to neutral stimuli and enhance the treatment of depressive stimuli. Subsequently, many studies have confirmed that depressive patients tend to choose negative information consistent with their negative schema because of the negative cognitive schema in their brain when processing external information [4]. Studies have demonstrated that depressive patients have significant impairment of facial expression recognition [5]. The literature has also demonstrated that depressed individuals tend to exaggerate negative stimuli [6, 7] and are more excited about sad faces [8]. Depressed patients are more likely to judge happy faces as neutral stimulation, neutral faces as negative stimulation, and indistinguishable blurred faces as negative stimulation. Healthy individuals are more likely to interpret neutral expression as positive expression [6, 7]. Many event-related potential (ERP) studies have demonstrated that depressive patients have a bias

for emotional processing and have a higher score in evaluating the intensity of sad faces [9].

However, the evidence has been inconsistent. Some scholars have not found that patients with depression have a special sense of perception (emotional and facial expression judgment) deficiencies [10]. Several studies have demonstrated no difference in the processing of emotional stimuli in major depressive disorder [6, 9, 11]; others have reported differences in the processing of either sad or happy expressions or both [4, 12]. Scholars have also posited that the impairment of negative information processing in patients with depression is due to the decline in positive expression recognition ability and the enhancement of negative expression stimulus recognition ability, which is closely related to the severity of depressive symptoms. Some scholars believe that the negative preference of depression is due to the decrease in the response to positive stimuli [13, 14].

Notably, in normal subjects, happy facial advantage (HFA) exists in normal face classification processing [10, 15], but in depressed patients, obstacles have been observed in processing happy facial expressions. Depressed patients have difficulty distinguishing positive social stimuli (e.g., happy expressions) [6, 16, 17]. The subtle difference is that patients with depression have a lack of positive emotion recognition, especially happy face recognition disorder, which may lead to the aggravation of a negative state or produce negative social effects. The score of happy face evaluation in patients with depression is significantly decreased and is significantly lower than that in the healthy and depression groups [18]. The study also confirmed that evaluation of positive emotional stimuli is decreased in depressed patients, which made them feel inadequate when processing positive materials. Depressed patients cannot be induced by positive stimuli to emerge from the depressive state, and depressed patients have a negative face attention preference [19]. The "attention avoidance" of positive faces has also been described which aggravates the negative cognitive bias of depressed individuals and makes it difficult for them to get rid of the negative mood and reach the normal state [20].

In summary, the results of the research on face classification and processing of depressed patients are inconsistent because of the differences in research paradigms, research methods, severity, and age of depression. According to other studies on emotional processing of depression, the most often used methods of emotional processing of depression have been the face recognition task [21], point detection task [22], and visual search task [16]. In contrast, the task of face classification based on classification speed has been less involved, and most of those studies have focused on the recognition of sadness and depression in patients with depression. A comparison of the accuracy of happy faces was also conducted [23]. Whether there is an HFA effect in the facial expression classification of depressed patients remains unresolved. Whether the classification pattern of depressed patients is the same as that of healthy individuals has not been reported in the relevant literature.

1.1. Aims of the Study. The aim of the present study was to determine whether the HFA effect exists in first-episode, drug-naïve, depressed patients, especially the biases of happy face in face classification processing of depression. The purpose of this study was to analyze the classification and processing mechanism of depressed patients' faces and to provide a basis for the diagnosis and clinical prediction of depression.

2. Materials and Methods

2.1. Subjects. The subjects for the study included 30 depressed patients and 30 healthy individuals selected from the outpatient department at a hospital in Harbin, China. The subjects in the depression and control groups were matched for gender, age, and educational level; there were no significant differences between the groups ($P > 0.05$). All the subjects were right-handed with normal or corrected vision. The experimental plan complied with the Helsinki Declaration and was approved by the Ethics Committee. After understanding the purpose and content of the study, all subjects signed an informed consent form.

Subjects were diagnosed with a first episode of depression, as described in DSM-IV. The subjects were between 18 and 55 years of age and took no psychiatric drugs, and the familial genetic history was unremarkable. The control and depression groups were matched for age, gender, and education level. The following criteria were also fulfilled: no serious physical diseases, no neuropsychiatric diseases, and no history of taking antianxiety, depression, and psychiatric drugs.

2.2. Methods

2.2.1. Research Tools. The General Situation Questionnaire collected the gender, age, marital status, and educational level of the subjects, as well as whether they had taken psychotropic drugs within 1 month and whether there were depressed patients in the family.

(1) Hamilton Rating Scale for Depression (HRSD). The HRSD was compiled by Hamilton. The evaluation method of the scale is simple, and the standard is clear. Seventeen items were used in this study. The scale was comprised of seven factors: anxiety, somatization, cognitive impairment, weight, day and night change, sleep disorder, retardation, and despair. If the total score of depression was <7, the individual had no symptoms of depression. If the total score of depression was >17, the individual may have mild or moderate depression. If the total score was >24, the individual may have severe depression [24].

(2) Hamilton Anxiety Rating Scale (HAMA). The HAMA is comprised of 14 items divided into two dimensions (physical and mental anxiety). The scale is scored by five grades of 0–4 points (total score > 29 points, possible severe anxiety; total score > 21 points, obvious anxiety; and total score > 14 points, anxiety). The general demarcation value was 14 points.

2.2.2. Stimuli. The stimulus sequence was presented by E-prime software. The stimulus material was extracted from

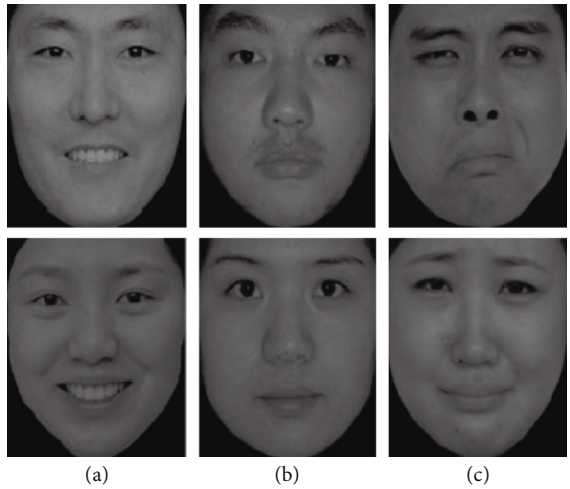

Figure 1: Example of the happy (a), neutral (b), and sad (c) faces used in the experiment.

the facial system of the Chinese Emotional Picture System [25]. Ninety emotional faces, 30 happy faces, 30 neutral faces, and 30 sad faces were selected. The gender ratio of each face was 1 : 1. Examples of the stimuli are shown in Figure 1. The recognition and strong degrees between different facial expressions were obtained. No significant difference was observed in degree, and the size, brightness, contrast, and spatial frequency of all pictures were the same after software processing.

2.2.3. Procedure. The experiment was conducted in a quiet and light-appropriate electrophysiology laboratory. The subjects sat in front of a 17-inch computer screen with a resolution of 1280 × 800 pixels. The refresh rate was 60 Hz. The distance between the eyes and the screen was 80 cm. The background of the experimental screen was light gray. The experiment was divided into two stages (practice and experiment stages). During the exercise, 18 pictures were presented. The subjects judged the facial expression information (happy, neutral, and sad) represented by the face, then responded to the key as soon as possible. The correct rate of practice reached >90%, and only then could the subjects enter the formal experiment.

In the formal experiment, there were four blocks. Each block contained 102 trials. Each face was presented for 300 ms. When the face was presented on the screen, the participants were asked to judge the facial expression information represented by the face (happy, neutral, and sad). Next, they were asked to press the button as soon as possible, to record the response time and correct rate of the participants. Each face was presented immediately and could not be the same. When three or more faces had the same expression, the keyboard adopted the principle of balanced matching. Before the experiment, 18 trials were trained. Between each block, participants could rest for 1–2 min.

2.2.4. Electroencephalogram (EEG) Recording and Analysis. The EEG was recorded by 32 Ag/AgCl electrodes mounted on a custom-made cap (ECI; Eaton, OH, USA). According to the extended 10-20 system, the EEG was sampled with a 0.20–100 Hz band pass. The tip of the nose was used as a reference during recording, and electrode impedances were kept below 5 k Ω.

The EEG was segmented to obtain epochs starting 200 ms prior to and ending 800 ms following picture onset. Artifact correction for conventional artifacts (e.g., eye blinks) was performed by means of the "statistical correction of artifacts in dense array studies." The EEG segments were averaged separately for each participant and for each face stimuli (at least 50 trials for each condition). The averaged waveforms were digital and had a low-pass of 30 Hz (24 dB/octave). Based on the literature [26, 27] and on scrutiny of the present scalp distribution of the N170 amplitudes, the statistical analysis was restricted to posterior lateral regions (T5, T6, A1, and A2) over the right hemisphere and the homolog sites over the left. For each subject, the peak of each ERP component [26, 27] was determined as the most negative peak between 120 and 220 ms (for N170). Subsequent visual scrutiny ensured that the most negative values represented real peaks rather than the endpoints of the epoch.

2.2.5. Data Analysis. The general demographic data and behavioral results, such as age, education level, HRSD score, and HAMA score, were analyzed. The correct rate was calculated, and the wrong data were deleted. Next, the response time was analyzed by repeated measurement analysis of variance, with a $P < 0.05$ as the significant level of statistical difference.

These measurements were submitted to mixed model repeated measures three-way ANOVAs, with face emotion (happy, neutral, and sad), hemisphere (left and right), and site (A1/A2 and T5/T6) as the within-subject factors and group (depression and control) as the between-subject factor. Degrees of freedom were corrected whenever necessary using the Greenhouse–Geisser epsilon correction factor.

3. Results

3.1. Comparison of Demographic Data between the Depression and Control Groups. Table 1 presents the

Table 1: Comparison of demographic data between depression and control groups.

Variables	Depression group, $n = 30$ Mean ± SD	Control group, $n = 30$ Mean ± SD	P value
Age	44.88 ± 13.28	46.60 ± 9.41	0.217
Depression score	22.75 ± 3.10	3.38 ± 1.09	0.000
Anxiety score	4.37 ± 2.44	3.43 ± 1.14	0.063

Table 2: Accuracy (%) of facial expression category in the depression group and control group ($n = 30$).

Variables	Happy Mean ± SD	Neutral Mean ± SD	Sad Mean ± SD
Depression group	87.68 ± 7.50	82.87 ± 10.14	75.06 ± 13.32
Control group	95.97 ± 5.36	95.07 ± 5.48	78.77 ± 16.91

Table 3: Response time of facial expression category between depression and control groups ($n = 30$).

Variables	Happy Mean ± SD	Neutral Mean ± SD	Sad Mean ± SD
Depression group	1106.11 ± 356.10	1210.02 ± 327.03	1293.92 ± 301.74
Control group	857.12 ± 117.66	1115.25 ± 652.12	1138.31 ± 363.12

demographic data of the depression and control groups. There was no significant difference in the age and anxiety scores between the depression and healthy control groups ($P > 0.05$). The depression score of the depression group was higher than that of the obvious control group, and the difference was statistically significant ($P < 0.05$).

3.2. Behavioral Results

3.2.1. Accuracy Comparison between the Depression and Control Groups. Types of facial expressions (happy, neutral, and sad) were used as within-group factors, and groups (depression and control groups) were used as between-group factors for repeated measurement of variance analysis. The results demonstrated that the main effect of the accuracy of the facial expression category was significant ($F_{(2,57)} = 28.81$, $P < 0.05$, $\eta^2_p = 0.391$). A significant difference was observed between the depression and control groups in the accuracy of facial expression classification ($P < 0.05$). The accuracy of classifying facial expressions in the depression group was significantly lower than that in the control group. The interaction between facial expressions and groups was nonsignificant ($F_{(2,57)} = 2.46$, $P > 0.05$, $\eta^2_p = 0.061$). The detailed information is shown in Table 2.

3.2.2. Comparison of Reaction Time between the Depression and Control Groups. Before calculating the response time, the data collected from each participant were pretreated to delete the data beyond the standard deviation (±3). Approximately 7% of the data were deleted, and the classification response time of different facial expressions was deleted. The response time of the facial expression category between the depression and control groups is shown in Table 3. Using facial expression (happy, neutral, and sad) as the within-group factors and groups (depression and control groups) as the between-group factor, repeated measurement variance analysis demonstrated that the main effect of facial expression classification was significant ($F_{(2,57)} = 19.75$, $P < 0.01$, $\eta^2_p = 0.405$) and that the overall response time of the depression group (1203.35 ± 53.98 ms) was significantly longer than that of the control group (1036.89 ± 54.87 ms; Table 3); the difference was statistically significant ($P < 0.05$). No significant interaction was observed between facial expressions and groups ($F_{(2,57)} = 1.03$, $P > 0.05$, $\eta^2_p = 0.034$).

3.2.3. Comparison of N170 Components between the Depression and Control Groups. The results demonstrated that N170 was the most obvious negative component in the posterior temporal and occipital regions between 120 and 220 ms after the stimulus was presented (Figures 2 and 3).

The N170 amplitude of the T5 and T6 electrodes was analyzed. The results demonstrated no significant difference in the amplitude of N170 between the depression and control groups ($P > 0.05$). The results showed a significant difference in the main effect of facial expression ($F_{(2,57)} = 4.30$, $P < 0.05$, $\eta^2_p = 0.137$), the interaction effect of the facial expression × group ($F_{(2,57)} = 4.74$, $P < 0.05$, $\eta^2_p = 0.149$), and the interaction effect of the facial expression × group × hemisphere ($F_{(2,57)} = 3.44$, $P < 0.05$, $\eta^2_p = 0.113$). There was no significant difference in the interaction effects between the hemispheres ($P > 0.05$). Further analysis demonstrated that when classifying happy faces, there was a significant difference in the amplitude of N170 between the two groups ($P < 0.05$), whereas the amplitude of N170 in the depression group decreased (Figure 2). There was no significant difference in the

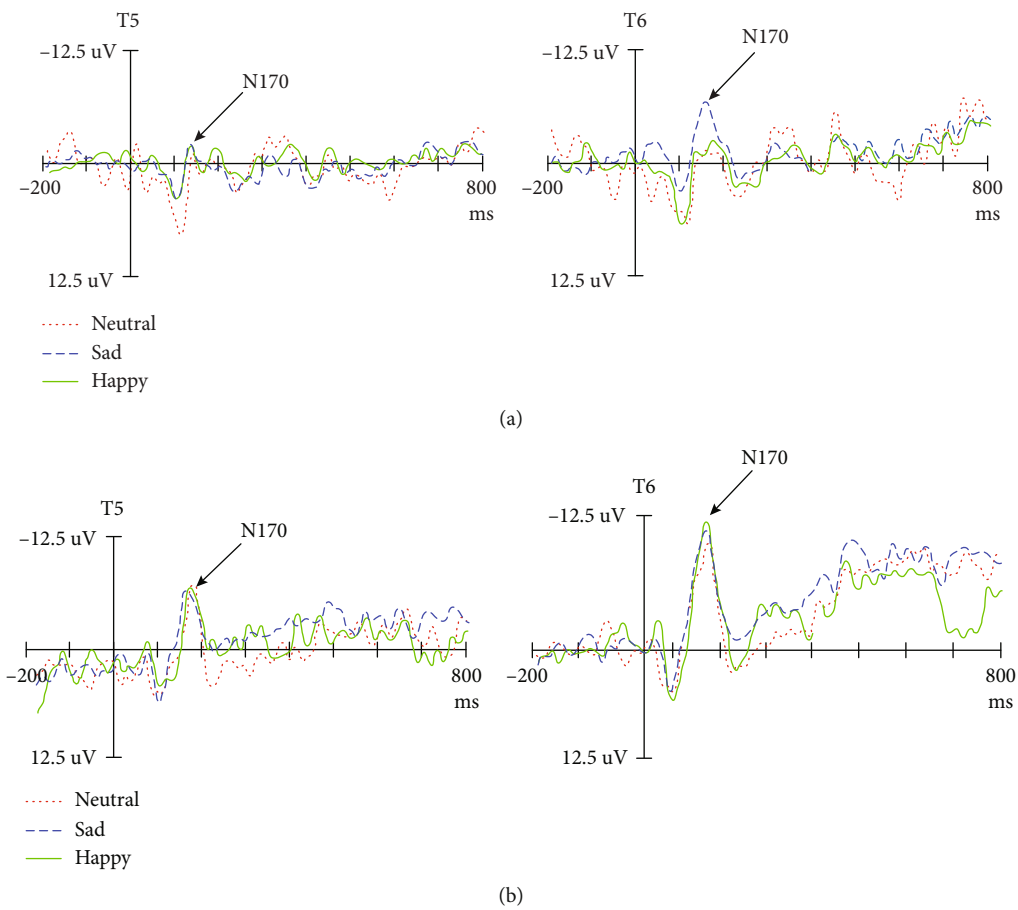

Figure 2: The wave of ERPs for facial expression category between the depressed (a) and control groups (b).

amplitude of N170 between the depression and control groups when processing sad and neutral faces ($P > 0.05$). There was no significant difference in the amplitude of N170 of different facial expressions between the two groups ($F < 1$). In the control group, the amplitude of N170 induced by happy faces was the largest and significantly larger than that induced by neutral and sad faces ($F_{(2,57)} = 8.82$, $P < 0.05$, $\eta^2_p = 0.246$). There was no significant difference between the two groups ($P > 0.05$; Figure 3), and this finding indicates that the classification of facial expressions of depressive patients is impaired at this stage. There was no significant difference in the main hemispheric effect, hemisphere × group, hemisphere × facial expression, and hemisphere × facial expression × group ($P > 0.05$).

Analysis of N170 latency of the T5 and T6 electrodes demonstrated a significant difference between the two groups ($P < 0.05$), and the latency of the depression group was prolonged. There was no significant difference in the latency of N170 between the depression and control groups ($P > 0.05$; Figure 2) when classifying happy faces ($P > 0.05$). When classifying neutral and sad faces, the latency of the depression group was longer than that of the control group ($P < 0.05$).

The amplitude of N170 in A1 and A2 was analyzed. The results demonstrated no significant difference in the amplitude of N170 between the depression and control groups ($P > 0.05$). The main effect of facial expression was significant ($F_{(2,57)} = 5.35$, $P < 0.05$, $\eta^2_p = 0.165$). The interaction effect of the facial expression × group was significant ($F_{(2,57)} = 5.71$, $P < 0.05$, $\eta^2_p = 0.175$, and others). When classifying happy faces, there was a significant difference in the amplitude of N170 between the depression and control groups ($P < 0.05$), and the amplitude of N170 in the depression group decreased. For sad and neutral faces, there was no significant difference between the two groups ($P > 0.05$; Figure 3). There was a significant difference in the latency of different facial expressions between the depression and control groups ($F_{(2,57)} = 10.50$, $P < 0.05$, $\eta^2_p = 0.280$). Thus, the amplitude of N170 induced by happy faces in the control group was the smallest and significantly smaller than that induced by neutral and sad faces (Figure 3). There was no significant difference between the neutral and sad faces ($P > 0.05$), suggesting that the two groups had a different classification mechanism.

The latency of N170 in A1 and A2 was analyzed. The results demonstrated a significant difference in latency between the depression and control groups ($P < 0.05$). The main effect of facial expression was significant ($F_{(2,57)} = 3.54$, $P < 0.05$, $\eta^2_p = 0.114$). The latency of the depression group was prolonged. The interaction effect of the facial expression × group was significant ($P < 0.05$). When classifying different facial expressions, there was a significant difference in the N170 latency between the depression and control groups

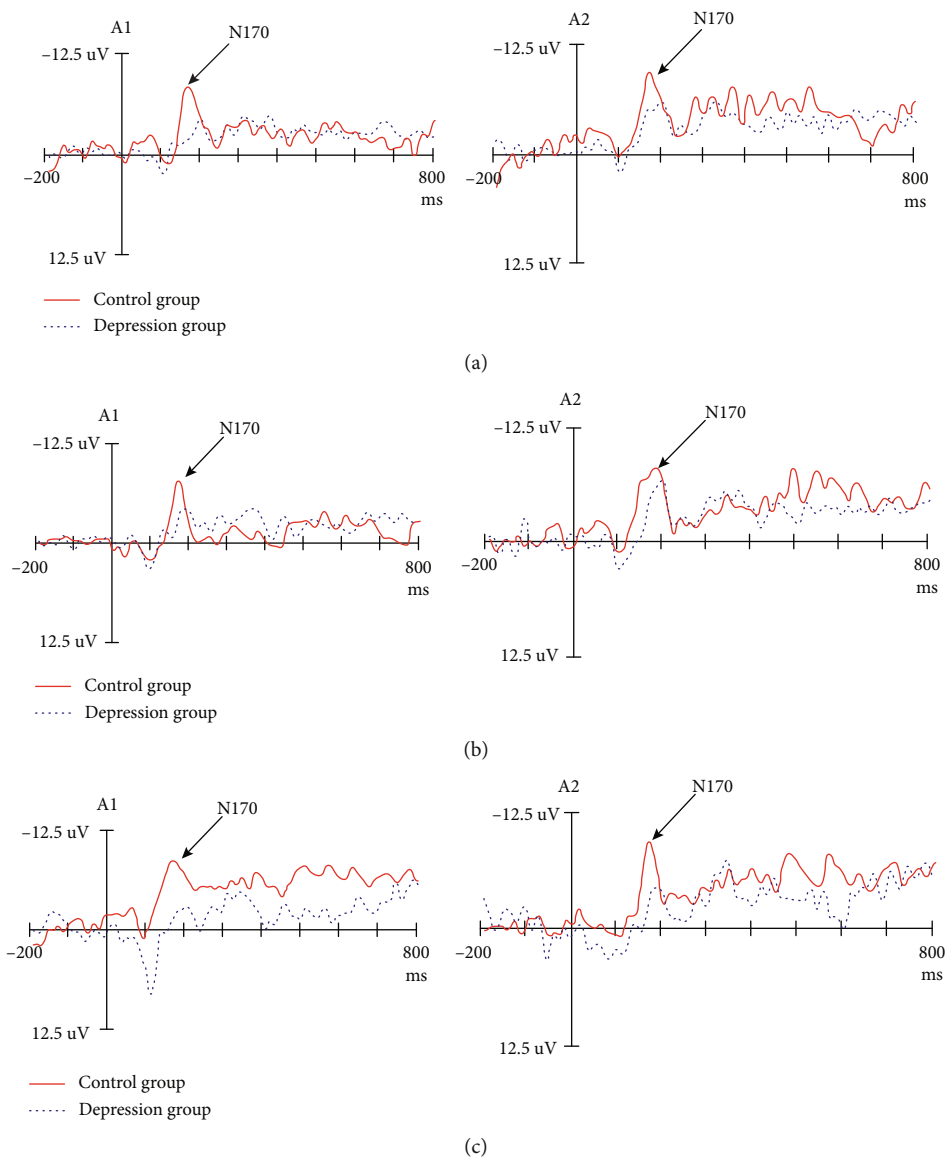

Figure 3: The amplitude and latency of facial expression ((a) happy face, (b) neutral face, and (c) sad face) between the depressed and control groups.

($P < 0.05$). The classification latency of different facial expressions in the depression group was prolonged. There was no significant difference in the N170 latency of different facial expression classifications in depression groups ($F < 1$). In the control group, the latency of happy faces was significantly shorter than that of neutral and sad faces; there was no significant difference between the two groups ($P > 0.05$).

4. Discussion

4.1. Behavioral Analysis of Expression Classification Patterns in the Depression and Control Groups. In this study, the accuracy and response time of facial expression classifications were obtained using the task of facial expression classification. The overall response time of depressed patients was longer than that of the control group, and there was an HFA effect. These findings indicate that for depressive patients in the face classification processing stage, the reaction speed decreased, resulting in a slowdown in processing speed. At this stage, depressed patients may have cognitive processing disorders.

In this study, the face classification effect of different expressions in patients with depression was studied, and the results demonstrated that this was inconsistent with the literature [6, 18, 28]. The main reasons may be as follows. First, the stimulus materials used in this study were different from those used in previous studies. The stimulus materials used in this study were real faces of Chinese people rather than cartoon or distorted faces. Second, this study was based on the speed of the facial expression classification, and this is also one of the innovative strengths of this research. The most likely reason is that depressed patients have cognitive dysfunction in face classification.

4.2. Physiologic Mechanisms of Classification Patterns in the Depression and Control Groups. In this study, we were the first to analyze the electrophysiologic changes of facial expression classification in depressed patients compared to the facial expression classification patterns of the control group and attempted to explain the mechanism of cognitive impairment in depressed patients. We found no difference in the N170 amplitude between the depression and control groups in face classification processing, and the latency of N170 was prolonged. When classifying happy faces, the depression group demonstrated a decrease in N170 amplitude and a prolongation of latency in some brain regions compared with the control group. In contrast, when classifying sad and neutral faces, no significant difference was observed in the N170 amplitude between the depression and control groups.

Compared with the control group, the pattern of facial expression classification processing was different in the depression group, and there was no difference in the latency and amplitude of facial expression classification processing in the depression group. The results showed that there was no significant difference in the processing of facial expression in the patients with depression at the EEG level, and the HFA effect of depression disappeared. That is, the processing advantage of positive faces disappeared.

This study directly compared the individual level of faces (happy, neutral, and sad) and induces significant N170 components, which supports conclusions in the literature [29]. ERP studies have shown that the response of depressed patients to negative information has not increased, unlike the positive information that decreased with impaired processing [13, 30]. The cognitive impairment of depressed patients was only caused by the "absence" or "avoidance" of positive faces. This study was the first to elaborate on the positive "avoidance" of depressed patients from the perspective of face classification. We further confirmed that the positive avoidance of depression may originate from the classification processing stage before the early structural coding and the processing stage after the classification processing. At this stage, the cognitive control disorder of the positive stimulus in depressed patients leads to the relative gain of the negative stimulus processing relative to the positive stimulus and in the stimulus-oriented processing. In the context of work, depression has an early inhibitory effect on negative information [31], which suggests that depressed patients may have a higher perceptual sensitivity to negative emotional information. This negative biased brain electrophysiologic mechanism revealed that the occurrence of depression was partly due to the failure of the cognitive control system to regulate the production and evaluation of positive emotions, which provides a basis for further revising the negative biased theory of depression.

A notable phenomenon was found in this study. Our study focused on first-episode, drug-naive patients. The behavioral results showed that the interaction between facial expressions and groups was not significant and that the response time of depressed patients decreased. This finding is inconsistent with other studies [20]. At the EEG level, there was a significant difference in the interaction effect of the facial expression and groups with respect to latency and amplitude. The HFA effect of patients with depression disappeared. Specifically, the processing advantage of positive faces disappeared, and the depression group had no difference in classification processing of different facial expressions. There was no difference in the amplitude and latency of neutral and sad faces between the symptomatic and control groups. These results suggest a cognitive information processing bias in depressed patients. Notably, the deviation of expression classification information, the abnormal positive emotional response, and the decrease of ERP amplitude induced by happy faces in the depression group indicated that patients with depression paid less attention to happy faces and increased avoidance. In the classification of happy facial expressions in depressed patients, the ERP amplitude was significantly lower than the control group, and the latency was significantly longer than the control group. The first-episode, drug-naïve, depressed patients cannot fully perceive the positive material stimulus in classification stages, their evaluation of the positive stimulus is too low, and they cannot eliminate depression through the induction of the positive material, which aggravates the negative cognitive bias of depression and makes it difficult for patients with depression to escape the negative mood.

5. Limitations of This Study

The current study was limited by the number of cases in the experimental group. The experimental group was not large; however, all of the subjects were diagnosed with first-time depressive disorder by clinical psychiatrists. It is really difficult to collect a large number of patients in accordance with the diagnostic standard. As clinical samples, the number of cases in this study were not less than the majority of similar published studies. We will consider doing a follow-up corollary study in the future to verify our conclusions. Because of the low spatial resolution of ERP technology, it is necessary to coordinate with other cognitive research methods in many studies involving cognitive brain areas.

Data Availability

The data used to support the findings of this study have not been made available because the data also form part of an ongoing study.

Conflicts of Interest

The authors declare that they have no conflicts of interest.

Acknowledgments

This research was supported by National Natural Science Foundation of China (81773536).

References

[1] M. Goyal, K. Goyal, M. Bathla, D. Kanimozhi, and D. Narkeesh, "Efficacy of myofascial unwinding and

myofascial release technique in a patient with somatic symptoms–a case report," *Indian Journal of Psychological Medicine*, vol. 39, no. 2, pp. 199–201, 2017.

[2] K. Mogg, K. E. Bradbury, and B. P. Bradley, "Interpretation of ambiguous information in clinical depression," *Behaviour Research and Therapy*, vol. 44, no. 10, pp. 1411–1419, 2006.

[3] J. L. Taylor and C. H. John, "Attentional and memory bias in persecutory delusions and depression," *Psychopathology*, vol. 37, no. 5, pp. 233–241, 2004.

[4] J. K. Gollan, H. T. Pane, M. S. McCloskey, and E. F. Coccaro, "Identifying differences in biased affective information processing in major depression," *Psychiatry Research*, vol. 159, no. 1-2, pp. 18–24, 2008.

[5] W. Heller, R. J. Davidson, G. A. Miller, and D. M. Tucker, "Neuropsychological mechanisms of individual differences in emotion, personality, and arousal," *Neuropsycholog*, vol. 7, no. 4, pp. 476–489, 1993.

[6] S. A. Surguladze, A. W. Young, C. Senior, G. Brébion, M. J. Travis, and M. L. Phillips, "Recognition accuracy and response bias to happy and sad facial expressions in patients with major depression," *Neuropsychology*, vol. 18, no. 2, pp. 212–218, 2004.

[7] S. C. Linden, M. C. Jackson, L. Subramanian, D. Healy, and D. E. J. Linden, "Sad benefit in face working memory: An emotional bias of melancholic depression," *Journal of Affective Disorders*, vol. 135, no. 1-3, pp. 251–257, 2011.

[8] Q. Dai and Z. Feng, "More excited for negative facial expressions in depression: evidence from an event-related potential study," *Clinical Neurophysiology*, vol. 123, no. 11, pp. 2172–2179, 2012.

[9] R. Maniglio, F. Gusciglio, V. Lofrese, M. B. Murri, A. Tamburello, and M. Innamorati, "Biased processing of neutral facial expressions is associated with depressive symptoms and suicide ideation in individuals at risk for major depression due to affective temperaments," *Comprehensive Psychiatry*, vol. 55, no. 3, pp. 518–525, 2014.

[10] J. M. Leppänen and J. K. Hietanen, "Positive facial expressions are recognized faster than negative facial expressions, but why?," *Psychological Research*, vol. 69, no. 1–2, pp. 22–29, 2004.

[11] M. Milders, S. Bell, J. Platt, R. Serrano, and O. Runcie, "Stable expression recognition abnormalities in unipolar depression," *Psychiatry Research*, vol. 179, no. 1, pp. 38–42, 2010.

[12] J. C. Zwick and L. Wolkenstein, "Facial emotion recognition, theory of mind and the role of facial mimicry in depression," *Journal of Affective Disorders*, vol. 210, pp. 90–99, 2017.

[13] C. M. Deveney and P. J. Deldin, "Memory of faces: a slow wave ERP study of major depression," *Emotion*, vol. 4, no. 3, pp. 295–304, 2004.

[14] J. L. Nandrino, V. Dodin, P. Martin, and M. Henniaux, "Emotional information processing in first and recurrent major depressive episodes," *Journal of Psychiatric Research*, vol. 38, no. 5, pp. 475–484, 2004.

[15] T. Kirita and M. Endo, "Happy face advantage in recognizing facial expressions," *Acta Psychologica*, vol. 89, no. 2, pp. 149–163, 1995.

[16] T. Suslow, K. Junghanns, and V. Arolt, "Detection of facial expressions of emotions in depression," *Perceptual and motor skills*, vol. 92, no. 3, pp. 857–868, 2001.

[17] Q. Dai, "Evaluation of depressed persons for emotional faces," *Chinese Journal of Applied Psychology*, vol. 13, no. 4, pp. 354–359, 2007.

[18] J. Joormann and I. H. Gotlib, "Is this happiness I see? Biases in the identification of emotional facial expressions in depression and social phobia," *Journal of Abnormal Psychology*, vol. 115, no. 4, pp. 705–714, 2006.

[19] S. Surguladze, M. J. Brammer, P. Keedwell et al., "A differential pattern of neural response toward sad versus happy facial expressions in major depressive disorder," *Biological Psychiatry*, vol. 57, no. 3, pp. 201–209, 2005.

[20] T. Suslow, U. Dannlowski, J. Lalee-Mentzel, U. S. Donges, V. Arolt, and A. Kersting, "Spatial processing of facial emotion in patients with unipolar depression: a longitudinal study," *Journal of Affective Disorders*, vol. 83, no. 1, pp. 59–63, 2004.

[21] B. T. Lee, J. H. Seok, B. C. Lee et al., "Neural correlates of affective processing in response to sad and angry facial stimuli in patients with major depressive disorder," *Progress in Neuro-Psychopharmacology and Biological Psychiatry*, vol. 32, no. 3, pp. 778–785, 2008.

[22] K. Mogg, N. Millar, and B. P. Brendan, "Biases in eye movements to threatening facial expressions in generalized anxiety disorder and depressive disorder," *Journal of Abnormal Psychology*, vol. 109, no. 4, pp. 695–704, 2000.

[23] E. Gilboa-schechtman, D. Erhard-weiss, and P. Jeczemien, "Interpersonal deficits meet cognitive biases: memory for facial expressions in depressed and anxious men and women," *Psychiatry Research*, vol. 113, no. 3, pp. 279–293, 2002.

[24] C. M. Zhu, "Assessment of the severity of depression," *Chinese journal of neurology and psychiatry*, vol. 18, no. 5, pp. 295–297, 1985.

[25] L. Bai, H. Ma, Y. X. Huang, and Y. J. Luo, "Development of Chinese emotional picture system," *Abstracts of Papers of the Tenth National Psychological Congress*, vol. 19, no. 11, pp. 4–7, 2005.

[26] S. Bintin, T. Allison, A. Puce, E. Perez, and G. McCarthy, "Electrophysiological studies of face perception in humans," *Journal of Cognitive Neuroscience*, vol. 8, no. 6, pp. 551–565, 1996.

[27] B. Rossion and C. Jacques, "Does physical interstimulus variance account for early electrophysiological face sensitive responses in the human brain? Ten lessons on the N170," *NeuroImage*, vol. 39, no. 4, pp. 1959–1979, 2008.

[28] K. L. Yoon, J. Joormann, and I. H. Gotlib, "Judging the intensity of facial expressions of emotion: depression-related biases in the processing of positive affect," *Journal of Abnormal Psychology*, vol. 118, no. 1, pp. 223–228, 2009.

[29] J. W. Tanaka and T. Curran, "A neural basis for expert object recognition," *Psychological Science*, vol. 12, no. 1, pp. 43–47, 2001.

[30] A. Y. Shestyuk, P. J. Deldin, J. E. Brand, and C. M. Deveney, "Reduced sustained brain activity during processing of positive emotional stimuli in major depression," *Biological Psychiatry*, vol. 57, no. 10, pp. 1089–1096, 2005.

[31] P. T. Michie, N. Solowij, J. M. Crawford, and L. C. Glue, "The effects of between-source discriminability on attended and unattended auditory ERPs," *Psychophysiology*, vol. 30, no. 2, pp. 131–221, 1993.

Hindawi
Neural Plasticity
Volume 2020, Article ID 8815195, 11 pages
https://doi.org/10.1155/2020/8815195

Research Article

Neuroprotective Effects of the Sonic Hedgehog Signaling Pathway in Ischemic Injury through Promotion of Synaptic and Neuronal Health

Sen Yin,[1,2] Xuemei Bai,[2] Danqing Xin,[2] Tingting Li,[2] Xili Chu,[2] Hongfei Ke,[2] Min Han,[2] Wenqiang Chen,[1] Xingang Li,[1] and Zhen Wang[2]

[1]*Qilu Hospital, Cheeloo College of Medicine, Shandong University, Jinan, Shandong, China*
[2]*Department of Physiology, School of Basic Medical Sciences, Cheeloo College of Medicine, Shandong University, Jinan, Shandong 250012, China*

Correspondence should be addressed to Xingang Li; lixg@sdu.edu.cn and Zhen Wang; wangzhen@sdu.edu.cn

Sen Yin and Xuemei Bai contributed equally to this work.

Received 24 April 2020; Revised 5 June 2020; Accepted 29 June 2020; Published 1 August 2020

Academic Editor: Jason H. Huang

Cerebral ischemia is a common cerebrovascular condition which often induces neuronal apoptosis, leading to brain damage. The sonic hedgehog (Shh) signaling pathway has been reported to be involved in ischemic stroke, but the underlying mechanisms have not been fully elucidated. In the present study, we demonstrated that expressions of Shh, Ptch, and Gli-1 were significantly downregulated at 24 h following oxygen-glucose deprivation (OGD) injury in neurons *in vitro*, effects which were associated with increasing numbers of apoptotic cells and reactive oxygen species generation. In addition, expressions of synaptic proteins (neuroligin and neurexin) were significantly downregulated at 8 h following OGD, also associated with concomitant neuronal apoptosis. Treatment with purmorphamine, a Shh agonist, increased Gli-1 in the nucleus of neurons and protected against OGD injury, whereas the Shh inhibitor, cyclopamine, produced the opposite effects. Activation of Shh signals promoted CREB and Akt phosphorylation; upregulated the expressions of BDNF, neuroligin, and neurexin; and decreased NF-κB phosphorylation following OGD. Notably, this activation of Shh signals was accompanied by improved neurobehavioral responses along with attenuations in edema and apoptosis at 48 h postischemic insult in rats. Taken together, these results demonstrate that activation of the Shh signaling pathway played a neuroprotective role in response to ischemic exposure via promotion of synaptic and neuronal health.

1. Introduction

Ischemic strokes are one of the leading causes of long-lasting disability in humans [1]. Cell death quickly results in neurons starved of oxygen and nutrients, and the subsequent excitotoxicity, oxidative stress, neuroinflammation, and apoptosis produce loss of structural and functional integrity of the brain [2]. Accordingly, novel therapeutic strategies for the restoration of central nervous system (CNS) integrity and promotion of functional recovery for patients with cerebral ischemia are urgently needed.

The sonic hedgehog (Shh) signaling pathway plays an important role in neurogenesis and neural patterning during development of the CNS [3]. When Shh binds to its receptor, Patched (Ptch), it depresses the G protein-coupled receptor Smoothened (Smo), leading to the activation of glioma-associated oncogene homolog 1 (Gli-1). Activated Gli-1 meditates the expression of many target genes that regulate cell growth, survival, and differentiation of cells, including neurons [4]. The Shh signaling pathway has been reported to be involved in ischemic stroke [5], as Shh expression was found to be upregulated in neurons during ischemia/hypoxia

[6]. Moreover, inhibition of the Shh pathway exacerbated ischemic damage in rats, effects which were correlated with a downregulation in the expressions of Gli1 and Ptch [7]. Purmorphamine (PUR), a small molecular agonist of the Shh coreceptor, Smo, exerted protective effects in the middle cerebral artery occlusion (MCAO) model [8]. PUR, which has also been shown to promote blood-brain barrier formation, plays a crucial role in activation of the endogenous anti-inflammatory system within the CNS [9], and recent findings have indicated that PUR protects cortical neurons and restores neurological deficits after ischemic stroke in rats [10]. It has been reported by us that PUR exerted neuroprotection against subarachnoid hemorrhage-induced injury in adult rats [11] and hypoxia-ischemia in neonatal mice [12].

Despite this relatively substantial survey of information on Shh, details regarding the role of Shh signaling in ischemic stroke have not been fully elucidated. As one attempts to rectify this deficit, in this report, we focused on expression levels and effects of the Shh signaling pathway following oxygen-glucose deprivation (OGD) injury. In this way, it will be possible to examine some of the underlying neuroprotective mechanisms of the Shh signaling pathway in ischemic injury.

2. Materials and Methods

2.1. Reagents and Antibodies. The antibodies used for Western blot included anti-p-Akt (9271S, Cell Signaling Technology, USA), anti-Akt (9272S, Cell Signaling Technology, USA), anti-Shh (20697-1-AP, Proteintech Group, USA), anti-Gli-1 (ab151796, Abcam, USA), anti-Patch (ab53715, Abcam, USA), anti-NF-κB (10745-1-AP, Proteintech Group, USA), anti-p-NF-κB (3033S, Cell Signaling Technology, USA), anti-p-CREB (9198S, Cell Signaling Technology, USA), anti-CREB (9197S, Cell Signaling Technology, USA), anti-BDNF (17465-1-AP, Proteintech Group, USA), anti-neuroligin (ab186279, Abcam, USA), anti-neurexin (ab222806, Abcam, USA), and anti-β-actin (TA-09, Zhongshan Golden Bridge Biotechnology, China). The antibody for immunofluorescence was anti-Gli-1 (ab151796, Abcam, USA). PUR and cyclopamine (Cyc, a smoothened inhibitor) were purchased from Selleck Chemicals (Houston, TX, USA). Thread embolus was purchased from Guangzhou Jialing Biotechnology Co., Ltd. (L3800, Guangzhou, China). Annexin V-FITC/PI Double Labeling Apoptosis Detection Kit was purchased from BestBio Science (Shanghai, China). Terminal deoxynucleotidyl transferase-mediated dUTP-biotin nick end labeling (TUNEL) kit was purchased from KeyGen Biotech (KGA7073, Beyotime, Shanghai, China).

2.2. Cell Culture, Treatments, and Oxygen-Glucose Deprivation (OGD)

2.2.1. Primary Neurons. Primary cortical neurons of mice were cultured as previously described [13]. Briefly, PND1 mice were used to harvest cortical neurons which were then cultured in serum-free neurobasal medium with 2% B27 and 1% penicillin-streptomycin. Cells were cultured in poly-D-lysine-coated twelve-well plates for 7 days and then treated with PUR (20 μM) with/without Cyc (10 μM).

To mimic the ischemic condition *in vitro*, cells were subjected to OGD. Briefly, cells were cultured at 37°C under 95% nitrogen and 5% CO_2 for 6 h in glucose-free DMEM (125 mM NaCl, 2.8 mM KCl, 1.5 mM $MgCl_2$, 0.05 mM $MgSO_4$, 2 mM $CaCl_2$, 0.83 mM NaH_2PO_4, 24 mM $NaHCO_3$, and 2 mM HEPES). After OGD, primary neurons were placed in the original neurobasal medium with PUR (20 μM) with/-without Cyc (10 μM) and returned to the incubator under normoxic conditions for the times indicated. Control cells were maintained under normal conditions without OGD. Cell apoptosis was assessed by TUNEL staining according to the manufacturer's protocol.

2.2.2. PC12 Cells. PC12 cells were cultured in DMEM containing 5% FBS and 1% penicillin/streptomycin. For MSC-exosome treatment, PC12 cells were seeded with FBS-free culture medium in 12-well plates and treated with exosomes (100 μg/mL) from transfected and untransfected MSCs at the times indicated.

To mimic ischemic condition *in vitro*, PC12 cells were exposed to OGD for 6 h. PC12 cells were then placed in the original medium with or without PUR (20 μM) and with/-without Cyc (10 μM) and returned to the incubator under normoxic conditions for the times indicated.

2.3. Determination of Apoptosis by Flow Cytometric Analysis. Apoptosis of PC12 cells was assessed with use of the annexin V-FITC/PI Double Labeling Apoptosis Detection Kit as previously described. The percent of annexin V-positive cells determined over 10,000 acquired events was analyzed with use of a FACS flow cytometer C6 (BD Biosciences, San Jose, CA, USA). All assays were performed in triplicate, and each experiment was repeated three times.

2.4. TUNEL Staining. Cellular death was determined with use of TUNEL staining according to the instructions provided and counterstained with DAPI. The number of TUNEL-positive cells was measured in six randomly selected microscopic fields at 200x magnification within the lesion area of each group as described above ($N = 4$ mice/group).

2.5. DHE Analysis. For determinations of ROS production in primary neurons, cells were stained with 10 μM DHE for 30 min. After rinsing and mounting, images were captured with the use of fluorescent microscopy (BX51; Olympus, Tokyo, Japan). DHE-staining results were pixilated and quantified with the use of the Image-Pro Plus image analysis system.

2.6. Western Blot. Tissues were homogenized with RIPA containing PMSF and protease/phosphatase inhibitors following centrifugation at 4°C at 13,800 × g for 10 min. Then, 5× loading buffer was added to the protein supernatant and total protein was quantified using a BCA assay kit CWBIO (Haimen, Jiangsu, China). Equal amounts of protein were separated by SDS-PAGE and then transferred to PVDF membranes. After blocking in 5% nonfat milk for 2 h, blots were probed using the following primary antibodies: Shh, Gli-1, Patch, p-CREB, CREB, BDNF, p-Akt, Akt, NF-κB, p-NF-κB, and β-actin at 4°C overnight. Secondary antibodies

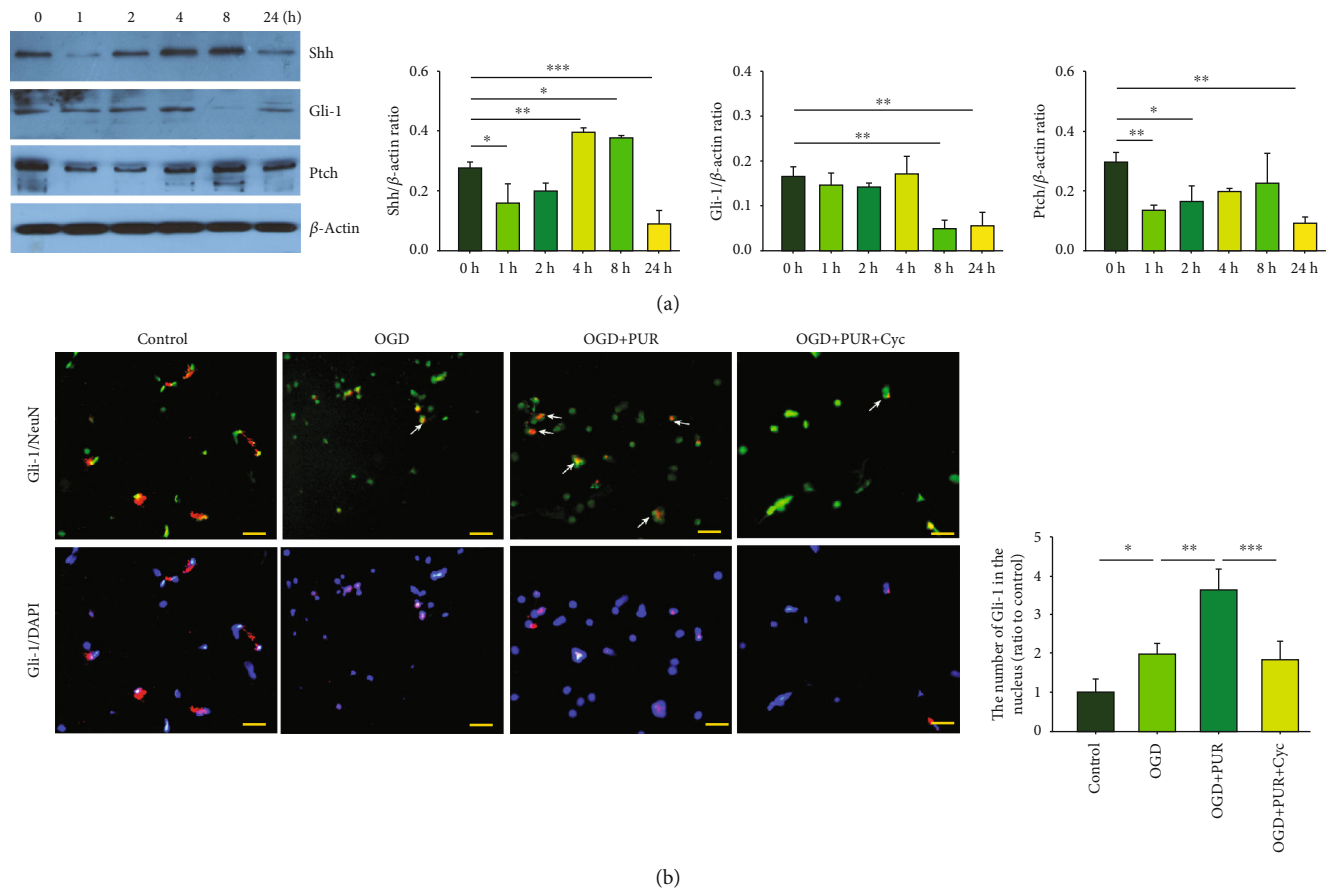

Figure 1: Effects of OGD exposure on the Shh signaling pathway: (a) protein levels of Shh, Gli-1, and patch at 1, 2, 4, 8, and 24 h after OGD exposure as determined by Western blot ($N = 3$/group); (b) nuclear translocation of Gli-1 at 24 h after OGD was observed with the use of immunofluorescent staining (scale bar = 50 μm). Quantification of Gli-1 nuclear translocation ($N = 4$/group). Values represent the mean ± SD; $^{*}p < 0.05$, $^{**}p < 0.01$, and $^{***}p < 0.001$ according to ANOVA according to ANOVA with Dunnett test in (a) and Tukey's post hoc comparisons in (b).

were then incubated with the membranes at 37°C for 60 min. The chemiluminescent signal was developed with use of ECL kit reagents (MILLIPORE, USA) and then detected with the use of the Tanon Imaging System (Tanon-4600). Densities of protein bands were semiquantified using ImageJ (National Institutes of Health, Bethesda, MD, USA).

2.7. Reverse Transcriptase Quantitative Real-Time PCR (qRT-PCR). Total RNA of tissue was isolated using TRIzol reagent CWBIO (Haimen, Jiangsu, China) according to the instructions of the manufacturer. Total RNA of EVs and H_2S-EVs were extracted using the Sera Mir EV RNA Extraction Kit (System Biosciences, USA) after isolation of EVs using ExoQuick-TC™ (System Biosciences, USA). Complementary DNA (cDNA) was synthesized using a reverse transcription system with the ReverTra Ace qPCR RT Kit (TOYOBO, Tokyo, Japan). Quantitative real-time PCR was performed using SYBR green PCR master mix (TOYOBO, Tokyo, Japan) on the Bio-Rad IQ5 Real-Time PCR System (Bio-Rad, USA). The specific primers for BDNF were purchased from RiboBio Co., Ltd. (Guangzhou, China): forward, 5′-AGC TGA GCG TGT GTG ACA GT-3′; reverse, 5′-ACC CAT GGG ATT ACA CTT GG-3′. Results were normalized with U6/actin according to the $2 - \Delta\Delta Ct$ method.

2.8. Immunofluorescent Staining. For immunofluorescent staining, cells were incubated with the primary antibody (Gli-1, 1 : 100) overnight at 4°C and with the secondary antibody at 37°C for 30 min on the following day. The nucleus was stained with DAPI for 10 min. Images were obtained with fluorescent microscopy (OLYMPUS-BX51, Olympus Corporation, Japan), and analyses of these images were performed using the Image-Pro Plus 6.0 software (Media Cybernetics, MD, USA).

2.9. Animal Model and Treatment. Animal experiments were performed according to the International Guiding Principles for Animal Research provided by the Council for International Organizations of Medical Sciences (CIOMS), and all procedures were approved by the Animal Ethical and Welfare Committee of Shandong University. Participants who worked with the animal models were trained according to procedures within the Institutional Animal Care and Use Committee Guidebook (IACUC). All procedures were

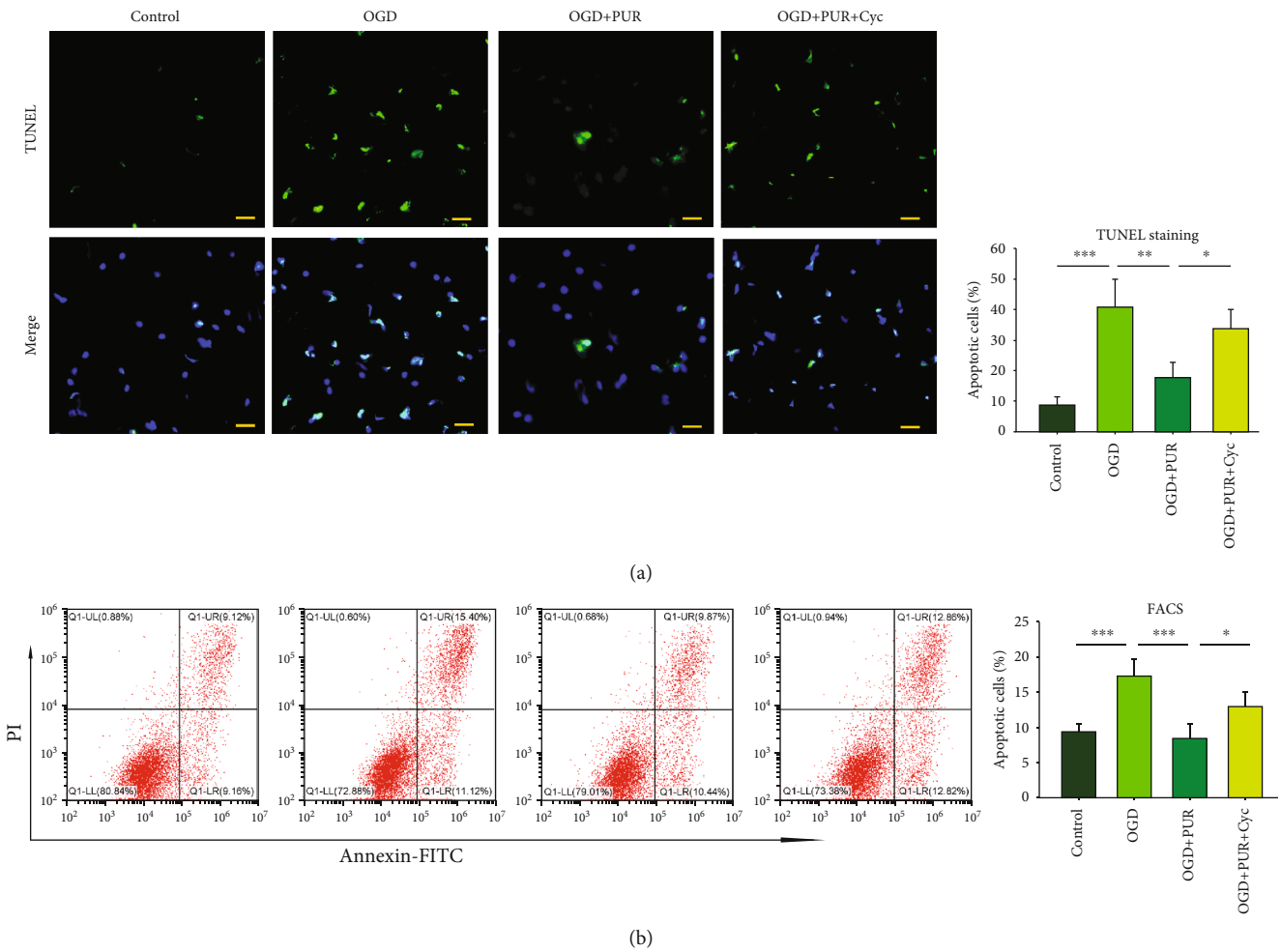

Figure 2: PUR activation of OGD-induced apoptosis: (a) apoptosis as determined by TUNEL staining at 24 h after OGD ($N = 4$/group; scale bar = 50 μm); (b) apoptosis as determined by FACS at 24 h after OGD ($N = 4$/group). Values represent the mean ± SD; $^{*}p < 0.05$, $^{**}p < 0.01$, and $^{***}p < 0.001$ according to ANOVA with Tukey's post hoc comparisons.

executed to minimize the pain experienced by the animals in these protocols.

The middle cerebral artery occlusion (MCAO) procedure was used to generate ischemic injury. Adult male Sprague-Dawley (SD) rats (280-320 g) were randomly divided into four groups ($N = 14$/group): (1) sham, (2) MCAO, (3) MCAO+PUR, and (4) MCAO+PUR+Cyc. Rats were treated with saline, PUR (5 mg/kg), or Cyc (1 mg/kg) and received intraperitoneal injections once per day for 2 days after MCAO. The MACO+PUR+Cyc group were pretreated with Cyc (1 mg/kg) at 30 min before PUR.

MCAO was based on the modified Longa method as previously described [14]. Briefly, for MACO model, rats were anesthetized with isoflurane. The right common carotid artery (CCA), external carotid artery (ECA), and internal carotid artery (ICA) were isolated followed by clamping of the ICA and CCA with microartery clips. The proximal portion of the ECA was ligated using a 5-0 polyester suture and severed at 3.0 mm from the bifurcation of the CCA. The ICA was then completely dissociated, and microsurgical scissors were used to incise a small opening in the arterial wall at 3 mm from the arterial bifurcation at the proximal end of the ECA. A thread embolus was inserted into the ECA parallel with that of the ICA, and the clamp on the ICA was then removed. After achieving microresistance, advancement of the embolus was stopped and the ECA was then tightened with a 5-0 polyester suture. The sham group animals underwent similar surgical procedures without applying the occlusion.

The brain infarct was assessed with use of 2,3,5,-triphenyltetrazolium chloride (TTC) staining at 2 days following injury. Neurological functions and brain water content were assessed at 2 days following injury.

2.10. Brain Tissue Water Content Determination. Brain tissues were quickly removed and weighed on an analytical balance with an accuracy of 0.01 mg (wet weight). The hemispheres were then dried in an oven at 105°C for 24 h to obtain the dry weight content [15]. The formula for brain water content was brain water content (%) = [(wet weight − dry weight)/wet weight] × 100%.

2.11. Neurobehavioral Tests. Behavior was assessed in a single-blinded manner using the modified Longa method and rated on a scale from 0–4 [14]: 0, no neurological deficit;

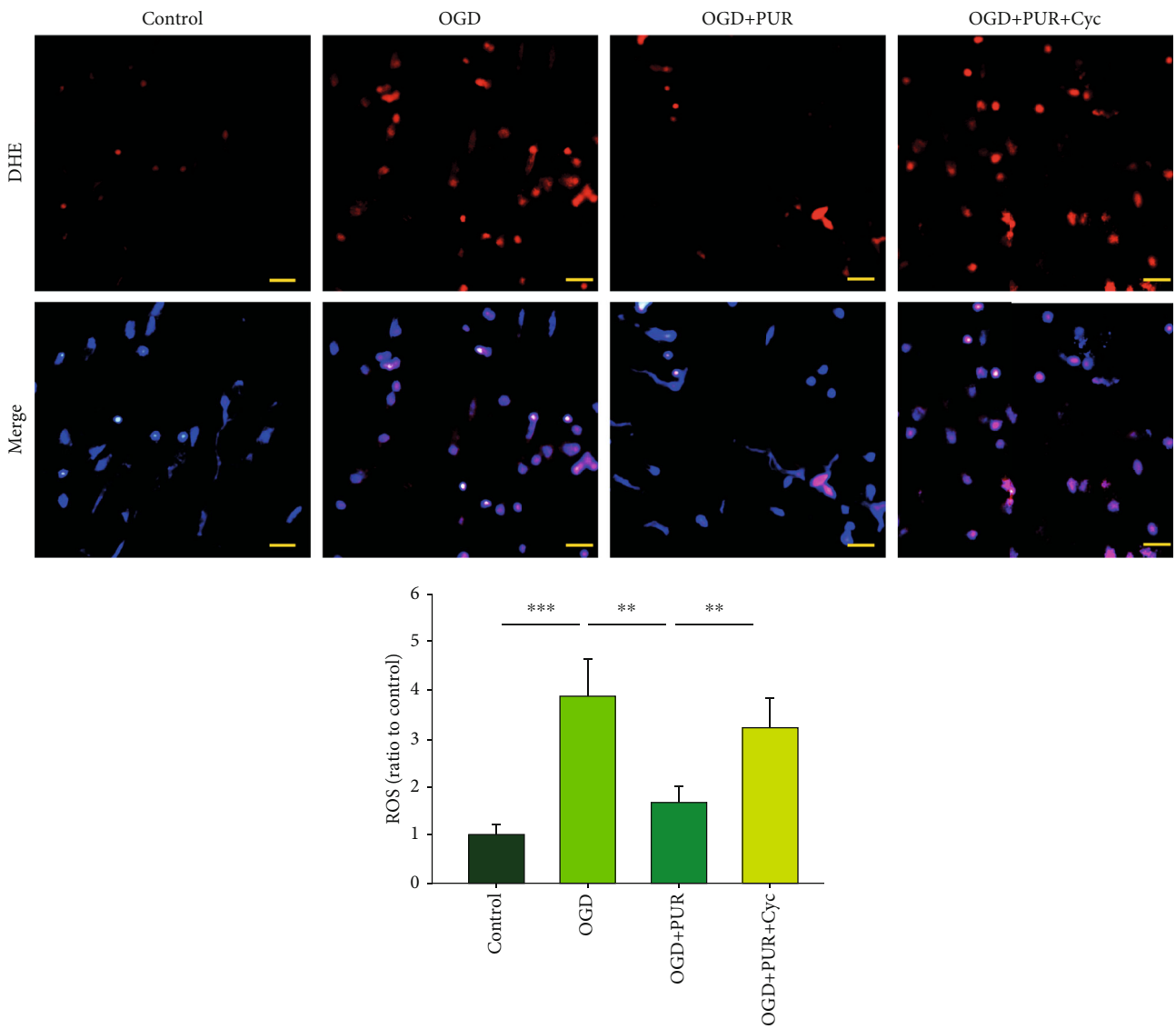

Figure 3: PUR activation of Shh on OGD-induced ROS generation. ROS levels were determined by DHE staining at 24 h after OGD ($N = 4$ /group; scale bar = 50 μm). Values represent the mean ± SD; $^{**}p < 0.01$ and $^{***}p < 0.001$ according to ANOVA with Tukey's post hoc comparisons.

1, unable to extend the contralateral forelimb and failure to straighten limb; 2, contralateral forelimb flexion and walking in a circle; 3, leans slightly to the contralateral side and walking in a circle toward the contralateral side; and 4, walking in a circle toward the contralateral side. Animals with scores of 1, 2, or 3 points were selected for the experiment.

2.12. TUNEL Analyses. TUNEL analyses of the brain section were determined as described above. Then, the brain sections were performed using the Image-Pro Plus 6.0 software by an investigator blinded as to experimental group assignments. The brain slices in the region containing the infarct lesion (between -1.60 and -2.00 mm from the bregma) were chosen to undergo TUNEL staining. All the slices of each group used in every independent experiment have the similar anatomical positions. The positive cells were counted within randomly selected peri-infarct areas which limited within 300 μm to the infarct.

2.13. Statistical Analyses. Results are expressed as mean ± SD. Correlation analysis between the expressions of neuroligin/-neurexin and TUNEL counts *in vitro* was performed with Pearson correlation test. Unless otherwise indicated, other data were analyzed using one-way ANOVAs followed by Tukey's test or Dunnett's test for post hoc comparisons using Prism software. A p value < 0.05 was required for results to be considered statistically significant.

3. Results

3.1. OGD Exposure Affects the Shh Signaling Pathway. Results from Western blots showed that compared with the control group, OGD exposure produced increased expressions of Shh

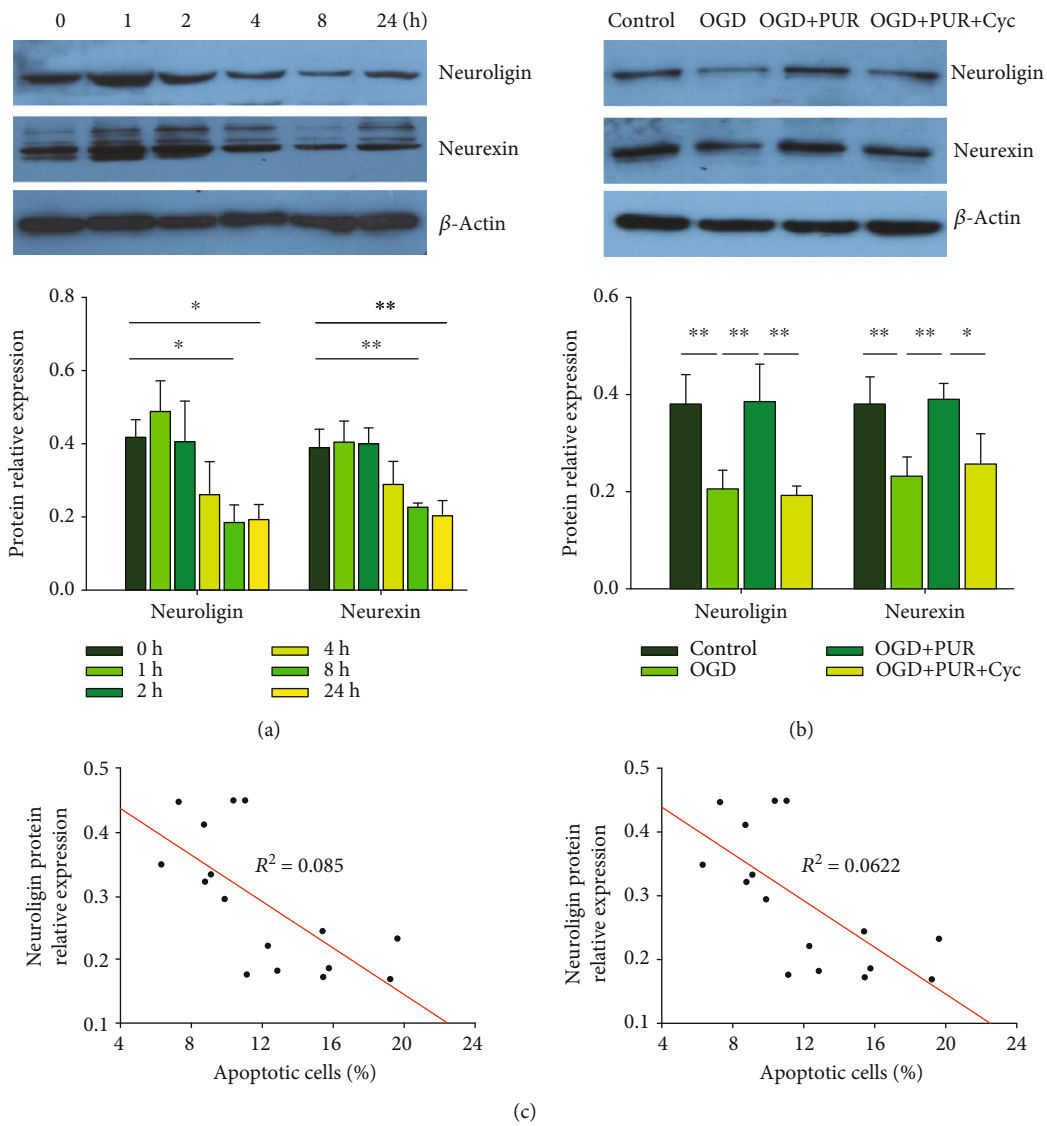

Figure 4: PUR activation of Shh on OGD-induced neuroligin and neurexin: (a) protein levels of neuroligin and neurexin at 1, 2, 4, 8, and 24 h after OGD as determined by Western blot ($N = 3$/group); (b) protein levels of neuroligin and neurexin at 24 h after OGD as determined by Western blot ($N = 4$/group); (c) Pearson correlation coefficients obtained between neuroligin/neurexin expressions and apoptosis following PUR treatment. Values represent the mean ± SD; $^{*}p < 0.05$ and $^{**}p < 0.01$ according to ANOVA with Dunnett test in (a) and Tukey's post hoc comparisons in (b).

at 4 h ([$F(5, 12 = 35.277, p < 0.001$], post hoc $p < 0.01$) and 8 h (post hoc $p < 0.05$) and decreased expressions at 1 h (post hoc $p < 0.01$) and 24 h (post hoc $p < 0.001$) (Figure 1(a)). Moreover, OGD exposure downregulated the expressions of Gli-1 ([$F(5, 12 = 12.486, p > 0.001$], post hoc $p < 0.01$) and Ptch ([$F(5, 12 = 5.959, p > 0.01$], post hoc $p < 0.01$) at 24 h. With immunofluorescent staining, PUR treatment was found to promote Gli-1 nuclear translocation ([$F(3, 12 = 27.524, p < 0.001$], post hoc $p < 0.01$) (Figure 1(b)). These effects of PUR on the Shh pathway following OGD exposure were blocked by Cyc pretreatment (Figure 1).

3.2. Activation of Shh Signals with PUR Attenuates Apoptosis Induced by OGD. Next, we examined whether PUR affected OGD-induced apoptosis in primary neurons using TUNEL staining. OGD significantly increased the percent of apoptotic/-total cells (40.6 ± 9.12%) compared with that of the control group (8.6 ± 2.90%) [$F(3, 12 = 22.202, p < 0.001$], post hoc $p < 0.001$), while treatment with 20 μM PUR significantly reduced the proportion of TUNEL-positive cells (17.84 ± 4.91%) as compared with the OGD group (post hoc $p < 0.01$). This effect of PUR on the number of TUNEL-positive cells was blocked by Cyc (33.84 ± 6.20%; post hoc $p < 0.05$) (Figure 2(a)).

Results of FACS showed that OGD exposure increased apoptosis in PC12 cells/total (17.4 ± 2.32%) as compared with the control group (9.41 ± 1.09%) [$F(3, 12 = 18.403, p < 0.001$], post hoc $p < 0.001$). Treatment with 20 μM PUR significantly reduced the proportion of TUNEL-positive cells (8.46% ± 1.97) as compared with the OGD group (post

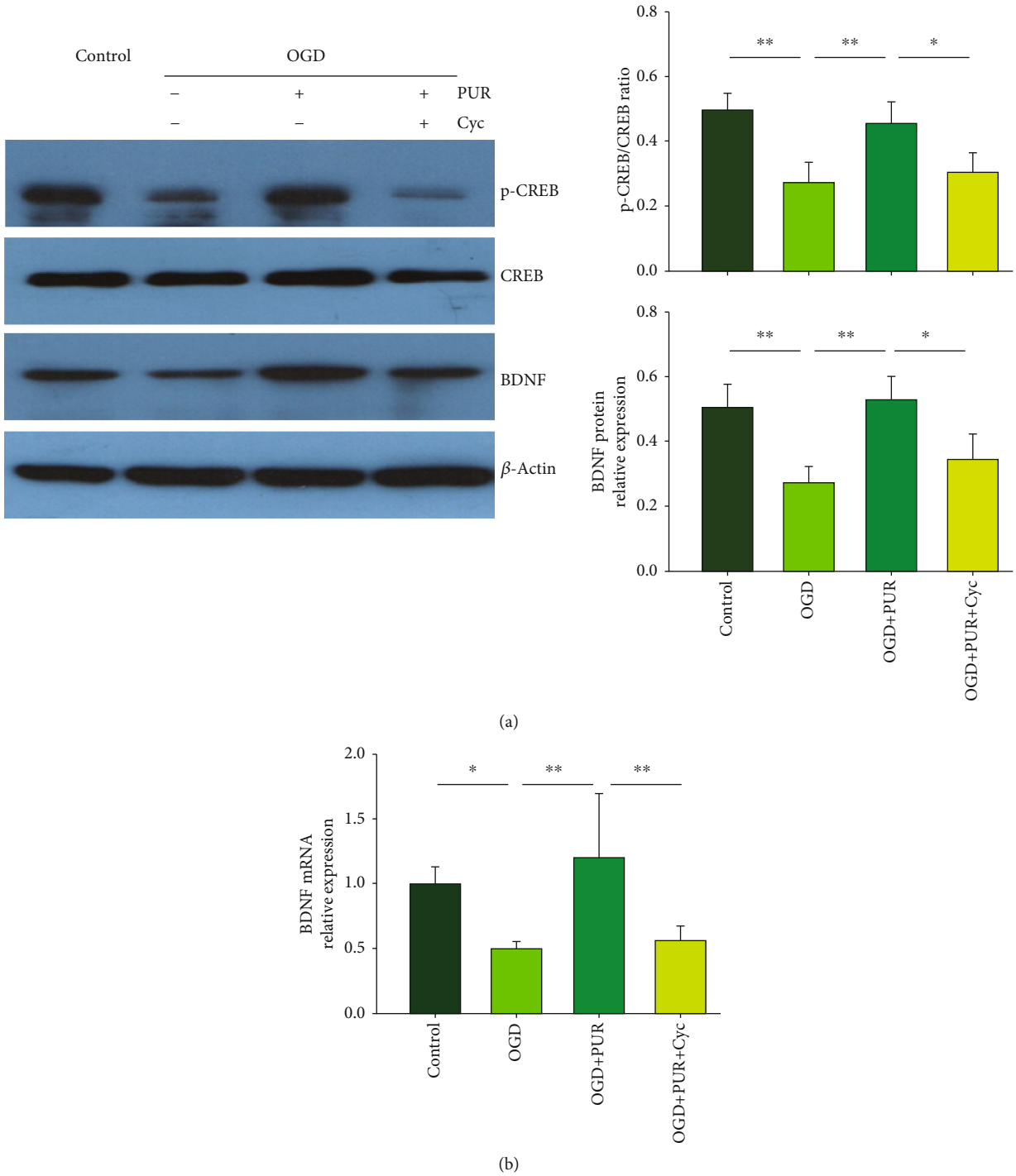

Figure 5: PUR activation of Shh on OGD-induced CREB and BDNF expressions: (a) protein levels of p-CREB, CREB, and BDNF at 4 h after OGD as determined with the use of Western blot ($N = 3$/group); (b) the level of BDNF mRNA at 4 h after OGD as determined with the use of qRT-PCR ($N = 3$/group). Values represent the mean ± SD, $^{*}p < 0.05$, and $^{**}p < 0.01$ according to ANOVA with Tukey's post hoc comparisons.

hoc $p < 0.001$). This effect of PUR on the number of TUNEL-positive cells was blocked by Cyc (13.03 ± 1.97%; post hoc $p < 0.05$) (Figure 2(b)).

3.3. Activation of Shh Signals Reduces OGD-Induced ROS Generation. Compared to the control group, OGD significantly increased ROS levels as determined at 24 h following OGD ([$F(3, 12 = 7.248$, $p < 0.001$], post hoc $p < 0.001$), while PUR treatment significantly attenuated this OGD-induced increase in ROS levels (post hoc $p < 0.01$). This effect of PUR on ROS generation was blocked by Cyc (post hoc $p < 0.01$) (Figure 3).

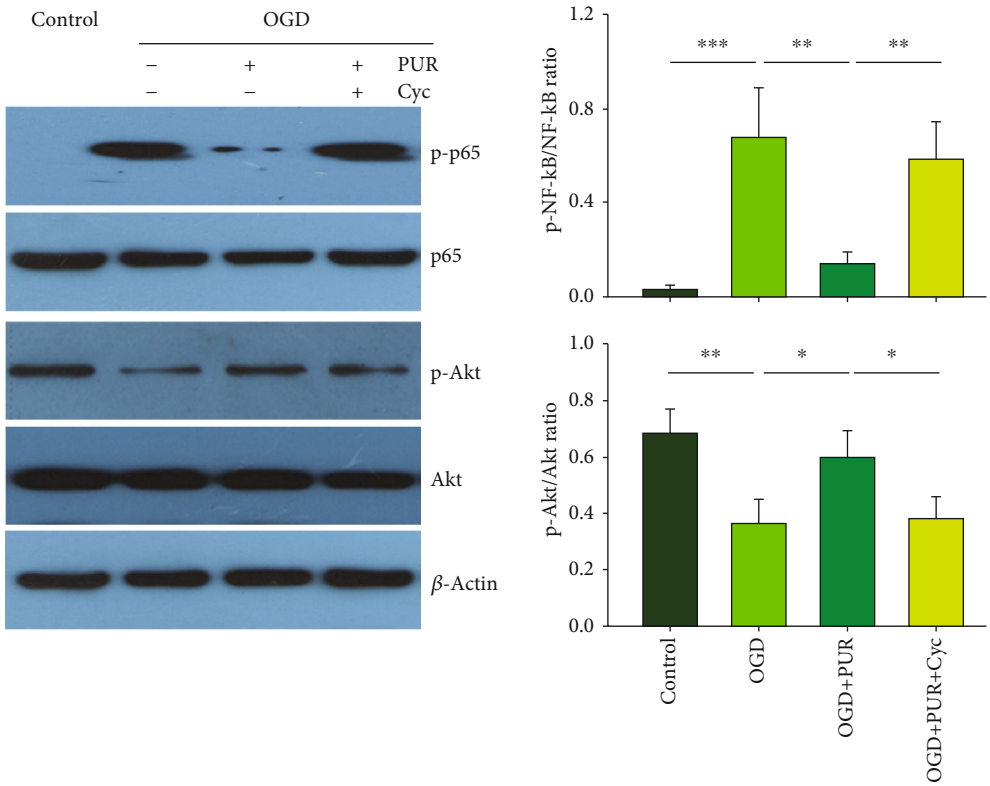

Figure 6: PUR activation of Shh on OGD-induced p-Akt and p-NF-κB. Protein levels of p-Akt, Akt, p-NF-κB, and NF-κB at 4 h after OGD as determined with use of Western blot ($N = 4$/group). Values represent the mean ± SD; $^{*}p < 0.05$, $^{**}p < 0.01$, and $^{***}p < 0.001$ according to ANOVA with Tukey's post hoc comparisons.

3.4. Activation of Shh Signals with PUR Attenuates OGD-Induced Reductions in Neuroligin and Neurexin. As synaptic proteins (neuroligin and neurexin) play a crucial role in stimulating synapse formation and reconstruction [16], we next examined the effects of OGD on the expressions of neuroligin and neurexin. Results from the Western blot assay demonstrated that neurons exposed to OGD showed a significant decrease in neuroligin expression at 8 h ([$F(5, 12 = 8.841$, $p < 0.01$], post hoc $p < 0.05$) and at 24 h (post hoc $p < 0.05$) post-OGD. Neurexin expression was also decreased at 8 h ([$F(5, 12 = 10.839$, $p < 0.001$], post hoc $p < 0.01$) and at 24 h (post hoc $p < 0.01$) after OGD exposure (Figure 4(a)). PUR treatment upregulated these OGD-induced reductions in neuroligin ([$F(3, 12 = 15.590$, $p < 0.001$], post hoc $p < 0.01$) and neurexin ([$F(3, 12 = 11.268$, $p < 0.01$], post hoc $p < 0.01$) at 8 h after OGD (Figure 4(b)). These effects of PUR on neuroligin and neurexin expression were blocked by Cyc (neuroligin, post hoc $p < 0.01$; neurexin, post hoc $p < 0.05$).

Moreover, increasing expressions of neuroligin and neurexin were found to be negatively correlated with attenuating levels of apoptosis following PUR treatment (neuroligin, Pearson $r = 0.686$, $p = 0.003$; neurexin, Pearson $r = 0.684$, $p = 0.004$) (Figure 4(c)).

3.5. Activation of Shh Signals Increases CREB and BDNF Expressions after OGD. Compared to the control group, OGD significantly decreased p-CREB expression at 4 h ([$F(3, 12 = 12.837$, $p < 0.001$], post hoc $p < 0.01$) and BDNF expression at 24 h ([$F(3, 12 = 13.288$, $p < 0.001$], post hoc $p < 0.01$) following OGD exposure. However, in response to PUR treatment, both p-CREB (post hoc $p < 0.01$) and BDNF (post hoc $p < 0.01$) expressions were significantly increased (Figure 5(a)). These effects of PUR on p-CREB and BDNF were blocked by Cyc (p-CREB, post hoc $p < 0.05$; BDNF, post hoc $p < 0.05$).

BDNF mRNA was also significantly decreased at 4 h after OGD exposure ([$F(3, 12 = 9.856$, $p < 0.001$], post hoc $p < 0.05$), while treatment with PUR increased this BDNF mRNA expression (post hoc $p < 0.01$) (Figure 5(b)).

3.6. Activation of Shh Signals with PUR Promotes p-Akt and Reduces p-NF-κB. Compared with the control group, the OGD exposure group showed a significantly decreased expression of p-Akt ([$F(3, 12 = 13.045$, $p < 0.001$], post hoc $p < 0.01$) and significantly increased expression of p-NF-κB ([$F(3, 12 = 22.439$, $p < 0.001$], post hoc $p < 0.001$) at 4 h post-OGD. PUR treatment increased both p-Akt (post hoc $p < 0.05$) and p-NF-κB (post hoc $p < 0.01$) expressions (Figure 6). These effects of PUR on p-Akt and p-NF-κB were blocked by Cyc (p-Akt, post hoc $p < 0.05$; p-NF-κB, post hoc $p < 0.01$) (Figure 6).

3.7. PUR Treatment Alleviates Neurologic Deficits, Edema, and Apoptosis after Ischemic Injury. Neurological deficit scores of the MCAO group were significantly lower than those of the sham group at 48 h ([$F(3, 20 = 24.512$, $p < 0.001$], post hoc $p < 0.01$), while PUR improved these deficits within the MCAO group at 24 h and 48 h after treatment

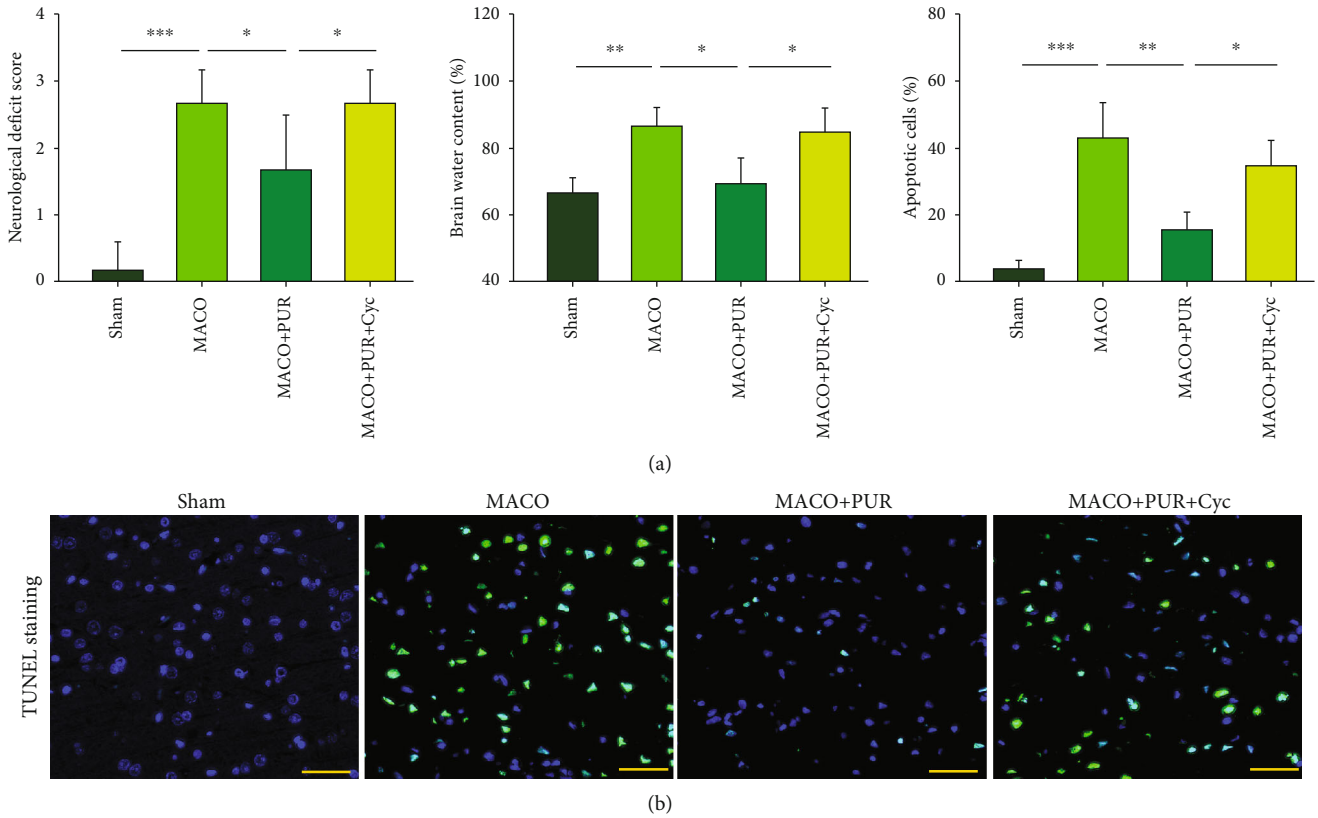

Figure 7: PUR activation of Shh on neurological recovery after MCAO. (a) Neurological function within each group was assessed at 48 h after MCAO ($N = 6$/group). Brain water content in rats from each group at 48 h ($N = 4$/group). (b) Apoptosis was determined with the use of TUNEL staining at 48 h after MACO injury ($N = 4$/group; scale bar = 50 μm). Values represent the mean ± SD, $^{*}p < 0.05$, $^{**}p < 0.01$, and $^{***}p < 0.001$ according to ANOVA with Tukey's post hoc comparisons.

(post hoc $p < 0.01$) (Figure 7(a)). Ischemic insult significantly increased the water content within the ipsilateral side of the brain ([$F(3, 12 = 10.797$, $p < 0.01$], post hoc $p < 0.01$), and PUR treatment markedly reduced this ischemic-induced brain edema as compared with that observed in the MACO group (post hoc $p < 0.05$) (Figure 7(b)).

In addition, this ischemic insult significantly increased the number of apoptotic cells within the ipsilateral side ([$F(3, 12 = 26.826$, $p < 0.001$], post hoc $p < 0.001$), an effect which was significantly reduced in response to PUR treatment (post hoc $p < 0.01$) (Figure 7(c)). These effects of PUR on neurological deficit scores, edema, and apoptosis were all blocked by Cyc (post hoc $p < 0.05$, for each) (Figure 7).

4. Discussion

In the present study, we demonstrate that activation of Shh signals was beneficial for neurological recovery after MCAO in rats. Moreover, we show that these beneficial effects of Shh signaling in response to ischemic exposure were associated with enhanced neuronal viability, increased neuroligin and neurexin expression along with activated Akt, and decreased NF-κB signaling.

Overall, alterations in Shh signaling have been shown to be related with a number of regenerative responses and post-injury pathophysiologies after trauma within diverse regions of the CNS [17]. For example, the Shh pathway is maximally activated at 72 h in response to brain injury followed by a return to baseline levels at 14 days [18] and cortical Shh protein levels are increased at 1 to 5 days after a cortical stab wound injury [19]. There is one report showing that expressions of Shh, Gli-1, and Ptch1 protein were all upregulated in cortical neurons at 6 h after MACO injury in rats [10], while others have reported that Gli1 and Ptch1 expressions were upregulated at 6, 12, 24, and 48 h postischemic injury [20]. However, a downregulation of Shh expression within the cortex has also been reported in the early stages after experimental subarachnoid hemorrhage [11, 21] and hypoxia-ischemia in neonatal mice [12]. In the present study, we found that neuronal expressions of Shh and Gli-1 were increased in the early stages of OGD insult, while the expressions of Shh, Gli-1, and Ptch were decreased at later time points following OGD. Activation of the Shh signaling pathway has been shown to increase Bcl-2, while suppressing Bax expression [22]. Moreover, exogenous Shh treatment reduces infarct volume along with promoting angiogenesis and neuronal survival after MACO injury [23]. Our current results demonstrate that restoring expression of the Shh signaling pathway with PUR played a protective role against neurotoxicity after ischemic exposure. That this neuroprotective effect

did involve a PUR-induced activation of the Shh signaling pathway was substantiated from results obtained with Cyc treatment, which reversed these beneficial effects of PUR upon ischemic exposure. Thus, we concluded that the upregulation of Shh signaling serves to resist ischemic injury in the early stages thereby exerting its beneficial therapeutic effects in cerebral ischemic stroke, while it is then decreased in the later stages due to the aggravation resulting from the injury.

Results from a previous study have demonstrated that PUR exhibits beneficial effects against stroke insult in rodent models and PUR does not alter the stroke-induced level of Shh signaling [10]. PUR plays an antiapoptotic role in the early stage by targeting neurons and also plays an anti-inflammatory role in late-stage inflammation by targeting astrocytes [10]. In addition, we found that PUR can reverse the expression of Shh signaling following OGD exposure in neurons *in vitro*. One explanation for this discrepancy likely comes from the different cell targets of PUR in the CNS following ischemic injury.

The CNS exhibits a substantial degree of plasticity after injury which then enables it to recover from functional deficits via processes involving neurogenesis, angiogenesis, axonal sprouting, and synaptic formation and remodeling. Activation of Shh receptors in the dendrites of hippocampal neurons has been shown to accelerate axonal elongation and synaptic plasticity after ischemic stroke [24]. The Shh pathway can mediate brain plasticity and functional recovery via plasminogen activator which, in part, explains the functional recovery observed after treatment of stroke with bone marrow stromal cells [25]. Moreover, exogenous Shh treatment increases the levels of BDNF and promotes nerve regeneration after cavernous nerve injury [26]. In line with these findings, our present results showed that activation of Shh signaling with PUR increased p-CREB and BDNF expression in response to OGD exposure, effects which were associated with an upregulation in the synaptic proteins, neuroligin and neurexin. The presynaptic neurexin and postsynaptic neuroligin are synaptic cell-adhesion molecules that connect neurons at synapses and regulate synaptic transmission [27]. Ischemia injury has been reported to increase neurexin-neuroligin1-PSD-95 interactions, which may represent an important target for therapeutic agents directed at the treatment of brain ischemia [28]. In the present study, restoring the expression of Shh signaling with PUR upregulated the expressions of neuroligin and neurexin, along with promoting cell survival and modulation of CREB/BDNF pathways. These data suggest that Shh signaling was able to mitigate ischemic injury via affects upon neurotrophic responses and synaptic plasticity.

Phosphorylated Akt is closely related to diverse cellular functions, such as cellular survival, apoptosis, and metabolism. The hedgehog signaling pathway component of Gli-1 can activate the PI3K-Akt pathway [29]. In line with this finding, we demonstrated that PUR activated Akt following OGD exposure in neurons. NF-κB induces the expressions of inflammation cytokines in astrocytes via the Shh signaling pathway [30]. The Shh ligand in the bone marrow microenvironment was involved in promoting NF-κB activity in multiple myeloma cells [31]. We found that PUR decreased OGD-induced phosphorylated NF-κB, associated with antiapoptotic effects. We speculated that the Akt and NF-κB pathways were responsible for PUR's neuroprotective activity, which needs further study.

Collectively, our data indicate that the Shh signaling pathway plays a significant neuroprotective role against ischemic injury by promoting synaptic and neuronal health.

Abbreviations

CNS: Central nervous system
CCA: Right common carotid artery
Cyc: Cyclopamine
ECA: External carotid artery
Gli-1: Glioma-associated oncogene homolog 1
ICA: Internal carotid artery
MCAO: Middle cerebral artery occlusion
OGD: Oxygen-glucose deprivation
PUR: Purmorphamine
Ptch: Patched
qRT-PCR: Reverse transcriptase quantitative real-time PCR
Smo: Smoothened
Shh: Sonic hedgehog
TUNEL: Terminal deoxynucleotidyl transferase-mediated dUTP-biotin nick end labeling.

Data Availability

The raw/processed data required to reproduce these findings cannot be shared at this time as the data also forms part of an ongoing study.

Conflicts of Interest

The authors declare that they have no conflict of interests.

Authors' Contributions

ZW contributed to the study design, data interpretation, writing, and revising of the final version of the manuscript; XGL contributed to the initial and final revision of the manuscript; SY and XMB contributed to the laboratory work and editing of the manuscript; DQX and TTL performed the flow cytometric analysis; MH and HFK implemented the MACO model; and SY, XLC, and WQC revised the manuscript. Sen Yin and Xuemei Bai contributed equally to this work.

Acknowledgments

The research funding support for this work was from the National Natural Science Foundation of China (Nos. 81873768 and 81671213 to Dr. Zhen Wang). The national key project of chronic non-communicable disease of China (No. 2016YFC1300403 to Dr. Wenqiang Chen), and National Natural Science Foundation of China (No. 81770436 to Dr. Wenqiang Chen).

References

[1] A. Moretti, F. Ferrari, and R. F. Villa, "Neuroprotection for ischaemic stroke: current status and challenges," *Pharmacology & Therapeutics*, vol. 146, pp. 23–34, 2015.

[2] R. Rodrigo, R. Fernandez-Gajardo, R. Gutierrez et al., "Oxidative stress and pathophysiology of ischemic stroke: novel therapeutic opportunities," *CNS & Neurological Disorders Drug Targets*, vol. 12, no. 5, pp. 698–714, 2013.

[3] N. H. Wilson and E. T. Stoeckli, "Sonic hedgehog regulates Wnt activity during neural circuit formation," *Vitamins and Hormones*, vol. 88, pp. 173–209, 2012.

[4] K. S. Ho and M. P. Scott, "Sonic hedgehog in the nervous system: functions, modifications and mechanisms," *Current Opinion in Neurobiology*, vol. 12, no. 1, pp. 57–63, 2002.

[5] L. Liu, B. Zhao, X. Xiong, and Z. Xia, "The neuroprotective roles of sonic hedgehog signaling pathway in ischemic stroke," *Neurochemical Research*, vol. 43, no. 12, pp. 2199–2211, 2018.

[6] J. R. Sims, S. W. Lee, K. Topalkara et al., "Sonic hedgehog regulates ischemia/hypoxia-induced neural progenitor proliferation," *Stroke*, vol. 40, no. 11, pp. 3618–3626, 2009.

[7] H. Ji, J. Miao, X. Zhang et al., "Inhibition of sonic hedgehog signaling aggravates brain damage associated with the down-regulation of Gli 1, Ptch 1 and SOD1 expression in acute ischemic stroke," *Neuroscience Letters*, vol. 506, no. 1, pp. 1–6, 2012.

[8] S. Sinha and J. K. Chen, "Purmorphamine activates the Hedgehog pathway by targeting Smoothened," *Nature Chemical Biology*, vol. 2, no. 1, pp. 29-30, 2006.

[9] J. I. Alvarez, A. Dodelet-Devillers, H. Kebir et al., "The Hedgehog pathway promotes blood-brain barrier integrity and CNS immune quiescence," *Science*, vol. 334, no. 6063, pp. 1727–1731, 2011.

[10] O. V. Chechneva, F. Mayrhofer, D. J. Daugherty et al., "A Smoothened receptor agonist is neuroprotective and promotes regeneration after ischemic brain injury," *Cell Death & Disease*, vol. 5, no. 10, p. e1481, 2014.

[11] Q. Hu, T. Li, L. Wang et al., "Neuroprotective effects of a Smoothened receptor agonist against early brain injury after experimental subarachnoid hemorrhage in rats," *Frontiers in Cellular Neuroscience*, vol. 10, 2017.

[12] D. Liu, X. Bai, W. Ma et al., "Purmorphamine attenuates neuro-inflammation and synaptic impairments after hypoxic-ischemic injury in neonatal mice via Shh signaling," *Frontiers in Pharmacology*, vol. 11, p. 204, 2020.

[13] Z. Wang, D. Liu, F. Wang et al., "Saturated fatty acids activate microglia via Toll-like receptor 4/NF-κB signalling," *The British Journal of Nutrition*, vol. 107, no. 2, pp. 229–241, 2012.

[14] E. Z. Longa, P. R. Weinstein, S. Carlson, and R. Cummins, "Reversible middle cerebral artery occlusion without craniectomy in rats," *Stroke*, vol. 20, no. 1, pp. 84–91, 1989.

[15] A. Shao, S. Guo, S. Tu et al., "Astragaloside IV alleviates early brain injury following experimental subarachnoid hemorrhage in rats," *International Journal of Medical Sciences*, vol. 11, no. 10, pp. 1073–1081, 2014.

[16] J. Elegheert, V. Cvetkovska, A. J. Clayton et al., "Structural mechanism for modulation of synaptic neuroligin-neurexin signaling by MDGA proteins," *Neuron*, vol. 96, no. 1, pp. 242–244, 2017.

[17] A. J. Mierzwa, G. M. Sullivan, L. A. Beer, S. Ahn, and R. C. Armstrong, "Comparison of cortical and white matter traumatic brain injury models reveals differential effects in the subventricular zone and divergent sonic hedgehog signaling pathways in neuroblasts and oligodendrocyte progenitors," *ASN Neuro*, vol. 6, no. 5, p. 175909141455178, 2014.

[18] N. M. Amankulor, D. Hambardzumyan, S. M. Pyonteck, O. J. Becher, J. A. Joyce, and E. C. Holland, "Sonic hedgehog pathway activation is induced by acute brain injury and regulated by injury-related inflammation," *The Journal of Neuroscience: The Official Journal of the Society for Neuroscience*, vol. 29, no. 33, pp. 10299–10308, 2009.

[19] S. Sirko, G. Behrendt, P. A. Johansson et al., "Reactive glia in the injured brain acquire stem cell properties in response to sonic hedgehog," *Cell Stem Cell*, vol. 12, no. 4, pp. 426–439, 2013.

[20] H. Ji, X. Zhang, Y. Du, H. Liu, S. Li, and L. Li, "Polydatin modulates inflammation by decreasing NF-κB activation and oxidative stress by increasing Gli1, Ptch1, SOD1 expression and ameliorates blood-brain barrier permeability for its neuroprotective effect in pMCAO rat brain," *Brain Research Bulletin*, vol. 87, no. 1, pp. 50–59, 2012.

[21] S. Zuo, W. Li, Q. Li et al., "Protective effects of Ephedra sinica extract on blood-brain barrier integrity and neurological function correlate with complement C3 reduction after subarachnoid hemorrhage in rats," *Neuroscience Letters*, vol. 609, pp. 216–222, 2015.

[22] R. L. Dai, S. Y. Zhu, Y. P. Xia et al., "Sonic hedgehog protects cortical neurons against oxidative stress," *Neurochemical Research*, vol. 36, no. 1, pp. 67–75, 2011.

[23] S. C. Chen, M. Huang, Q. W. He et al., "Administration of sonic hedgehog protein induces angiogenesis and has therapeutic effects after stroke in rats," *Neuroscience*, vol. 352, pp. 285–295, 2017.

[24] P. J. Yao, R. S. Petralia, and M. P. Mattson, "Sonic hedgehog signaling and hippocampal neuroplasticity," *Trends in Neurosciences*, vol. 39, no. 12, pp. 840–850, 2016.

[25] X. Ding, Y. Li, Z. Liu et al., "The sonic hedgehog pathway mediates brain plasticity and subsequent functional recovery after bone marrow stromal cell treatment of stroke in mice," *Journal of Cerebral Blood Flow and Metabolism*, vol. 33, no. 7, pp. 1015–1024, 2013.

[26] C. W. Bond, N. Angeloni, D. Harrington, S. Stupp, and C. A. Podlasek, "Sonic hedgehog regulates brain-derived neurotrophic factor in normal and regenerating cavernous nerves," *The Journal of Sexual Medicine*, vol. 10, no. 3, pp. 730–737, 2013.

[27] T. C. Sudhof, "Neuroligins and neurexins link synaptic function to cognitive disease," *Nature*, vol. 455, no. 7215, pp. 903–911, 2008.

[28] C. Li, D. Han, F. Zhang, C. Zhou, H. M. Yu, and G. Y. Zhang, "Preconditioning ischemia attenuates increased neurexin–neuroligin1–PSD-95 interaction after transient cerebral ischemia in rat hippocampus," *Neuroscience Letters*, vol. 426, no. 3, pp. 192–197, 2007.

[29] C. S. Kim, V. V. Vasko, Y. Kato et al., "AKT activation promotes metastasis in a mouse model of follicular thyroid carcinoma," *Endocrinology*, vol. 146, no. 10, pp. 4456–4463, 2005.

[30] K. Y. Chen and L. C. Wang, "Stimulation of IL-1β and IL-6 through NF-κB and sonic hedgehog-dependent pathways in mouse astrocytes by excretory/secretory products of fifth-stage larval Angiostrongylus cantonensis," *Parasites & Vectors*, vol. 10, no. 1, p. 445, 2017.

[31] K. Cai, W. Na, M. Guo et al., "Targeting the cross-talk between the hedgehog and NF-κB signaling pathways in multiple myeloma," *Leukemia & Lymphoma*, vol. 60, no. 3, pp. 772–781, 2019.

Hindawi
Neural Plasticity
Volume 2020, Article ID 8858415, 11 pages
https://doi.org/10.1155/2020/8858415

Review Article

GABAergic System in Stress: Implications of GABAergic Neuron Subpopulations and the Gut-Vagus-Brain Pathway

Xueqin Hou,[1] Cuiping Rong,[2] Fugang Wang,[1] Xiaoqian Liu,[1] Yi Sun,[1] and Han-Ting Zhang[3]

[1]*Institute of Pharmacology, Shandong First Medical University & Shandong Academy of Medical Sciences, Tai'an, Shandong 271016, China*
[2]*The Second Clinical Medical College, Guangzhou University of Chinese Medicine, Guangzhou, Guangdong 510006, China*
[3]*Departments of Neuroscience and Behavioral Medicine & Psychiatry, The Rockefeller Neurosciences Institute, West Virginia University Health Sciences Center, Morgantown, WV 26506, USA*

Correspondence should be addressed to Han-Ting Zhang; hzhang@hsc.wvu.edu

Received 15 May 2020; Revised 3 July 2020; Accepted 6 July 2020; Published 1 August 2020

Academic Editor: Fushun Wang

Stress can cause a variety of central nervous system disorders, which are critically mediated by the γ-aminobutyric acid (GABA) system in various brain structures. GABAergic neurons have different subsets, some of which coexpress certain neuropeptides that can be found in the digestive system. Accumulating evidence demonstrates that the gut-brain axis, which is primarily regulated by the vagus nerve, is involved in stress, suggesting a communication between the "gut-vagus-brain" pathway and the GABAergic neuronal system. Here, we first summarize the evidence that the GABAergic system plays an essential role in stress responses. In addition, we review the effects of stress on different brain regions and GABAergic neuron subpopulations, including somatostatin, parvalbumin, ionotropic serotonin receptor 5-HT3a, cholecystokinin, neuropeptide Y, and vasoactive intestinal peptide, with regard to signaling events, behavioral changes, and pathobiology of neuropsychiatric diseases. Finally, we discuss the gut-brain bidirectional communications and the connection of the GABAergic system and the gut-vagus-brain pathway.

1. Introduction

Stress is associated with various effects and mental disorders. Responses to stress vary from diet alteration to movement and sleep changes. Acute stress, such as trauma, can lead to rapid emotional changes and even result in long-term mental impairments. For instance, posttraumatic stress disorder (PTSD), a typical mental disorder, is often accompanied by depression and anxiety [1]. Chronic stress exposure, such as life stress (interpersonal loss, physical danger, humiliation, entrapment, role change/disruption, etc.), also increases depressive response and anxiety, and even triggers suicide in extreme cases [2–5]. Both acute and chronic stress-induced mental problems are associated with the γ-aminobutyric acid (GABA) system [6–9]. Gene polymorphism analysis of healthy subjects indicates that the GABA(A)α6 receptor subunit gene (GABRA6) polymorphism is responsive to psychological stress [10]. Therefore, agents targeting the GABAergic system are used to regulate depression, anxiety, or fear [11–13]. Interestingly, growing evidence has shown that gut-brain signals influence emotional behaviors [14–16], and the gut-brain axis may be a possible target for treating stress-related disorders [17]. A recent review has summarized the psychophysiological effects of prebiotics and discussed the important roles of bacteria-gut-brain signals in psychobiotic activity [18]. In addition to the gut microbiome, neurotransmitters and neuropeptides are also involved in the gut-brain communications [19–21]. Some neurotransmitters and neuropeptides in the central nervous system (CNS) are involved in regulating the function of the

digestive system [22–25]. Moreover, some neuropeptides are expressed in GABAergic neurons, which may be parts of the GABAergic system. In this review, we focus on how the GABAergic system impacts the gut-brain interaction in order to mediate stress-related disorders.

2. GABAergic Neuron Signaling and Stress

GABA is a major inhibitory neurotransmitter and is synthesized from the amino acid glutamate regulated by glutamate decarboxylases (GADs), including GAD1 and GAD2, whose genes encode GAD67 and GAD65 proteins, respectively [26]. GABAergic neurons are widely distributed in the CNS of mammals, and together with other GABA related factors, they compose the GABAergic system. The ventral medial prefrontal cortex (vmPFC) responds to the GABA reuptake inhibitor tiagabine [27] and is associated with fear responses and stress [28, 29], suggesting that the vmPFC GABAergic system plays a role in regulating stress-related emotion and responses. Additionally, many other GABAergic neuron-containing brain structures (such as the hippocampus and amygdala) and GABA-associated signaling are also involved in the stress regulation [30, 31].

GABAergic neurons coexpress various proteins or neuropeptides, such as somatostatin, parvalbumin, ionotropic serotonin receptor 5-HT3a (5-HT3aR), cholecystokinin, neuropeptide Y (NPY), vasoactive intestinal peptide, calbindin, and calretinin [32–34]. In addition, ~40% of GABAergic neurons are parvalbumin interneurons, ~30% are somatostatin interneurons, and ~30% are 5-HT3aR interneurons in the neocortex [35], which make up the three major subtypes of GABAergic neurons. Other proteins or neuropeptides are expressed in different subtypes of GABAergic neurons. For example, cholecystokinin and vasoactive intestinal peptide may express in 5HT3aR interneurons, and NPY is colocalized with somatostatin interneurons [35].

The changes in subpopulations of GABAergic neurons vary in different brain areas under stress [36, 37]. For example, long-term daily stress reduces the number of parvalbumin, calretinin, NPY, and somatostatin cells, but does not affect cholecystokinin and calbindin interneurons in the hippocampus [36]. Early life stress changes the structure and function of several brain regions, in addition to alterations of emotional behaviors and responses to stress in adults [38–40]. Exposure to long-term daily stress reduces calbindin neuron densities in the dorsolateral, medial, and ventral orbital cortex, but has no effect on cholecystokinin, NPY, parvalbumin, somatostatin, and calretinin neurons in any brain subregions in adult rats. Interestingly, enhanced density of cholecystokinin and NPY neurons in the ventral and lateral orbital cortices, respectively, is observed in stress-resilient rats, suggesting that cholecystokinin and NPY in the orbitofrontal cortex may be involved in stress resilience [41]. Taken together, these results suggest a complex GABAergic network change under stress. Also, it raises a question of how to control the GABAergic network in order to regulate stress-induced emotional behaviors. Of those coexpressing markers in GABAergic neurons, cholecystokinin, NPY, and vasoactive intestinal peptide are also known as gut-related modulators and involved in the regulation of energy. Subsequently, how do they connect to GABA signaling to play a role in the regulation of stress?

2.1. Somatostatin. Somatostatin is a chemical marker of GABAergic neurons [33]. Somatostatin deficit is a common pathological characteristic in neurological disorders with emotional changes. In patients with schizophrenia and bipolar disorder, somatostatin-immunoreactive neurons are decreased in the lateral amygdala, which may affect responses to fear and anxiety [42]. Mice deficient in somatostatin exhibits high behavioral emotionality, increased basal plasma corticosterone, and decreased GABA-synthesizing enzyme GAD67 gene expression [43], indicating that somatostatin influences the GABA signal and stress response. Upon 2 weeks of chronic mild stress in rats, somatostatin-2 receptors are significantly upregulated in the medial habenula, while the plasma somatostatin levels are also increased, suggesting that somatostatin and its receptors are involved in the stress response [44]. Longer duration (e.g., 7 weeks) of chronic mild stress in rats can cause decreases in consumption of sucrose solution and changes in somatostatin-2 receptors in response to antidepressant treatment [45]. Moreover, selective inactivation of the $\gamma 2$ subunit gene of GABAA receptors in somatostatin-positive GABAergic interneurons (SSTCre:$\gamma 2$(f/f) mice) mimic the behavioral effects of antidepressant and anxiolytic drugs, suggesting that sustained increases in GABAergic transmission produce antidepressant-like behavior by disinhibiting somatostatin-positive GABAergic interneurons [46].

2.2. Parvalbumin. Parvalbumin is another chemical marker of GABAergic neurons. Parvalbumin and somatostatin interneurons play distinct roles in the medial entorhinal cortex [47], a critical brain region associated with contextual memory [48]. Besides, parvalbumin- and somatostatin-expressing interneurons in the mPFC also have different activity patterns (weak and strong target-dependent delay-period activity), as well as distinct stimulation effects in spatial working memory. For instance, parvalbumin interneurons are strongly inhibited by reward, while only a subtype of somatostatin interneurons is inhibited [49]. Thus, parvalbumin and somatostatin interneurons may function in different ways. Selectively silencing parvalbumin, but not somatostatin, interneurons in the infralimbic cortex eliminates ventral hippocampal-mediated inhibition, while blocking infralimbic projectors reduces fear renewal [50], indicating that parvalbumin interneurons are involved in fear responses. Parvalbumin/GAD1 transgenic mice (silencing the GAD1) exhibit reduction of fear extinction, marked sensorimotor gating deficits, and elevated novelty-seeking [51]. Inhibition of parvalbumin interneurons disinhibits projection neurons from the prefrontal region and synchronizes their firing, resulting in fear [52]. After fear conditioning, parvalbumin interneurons show target- and region-selective plasticity in basolateral amygdala (BLA) subareas [53]. Together, parvalbumin interneurons regulate stress-

induced fear, and fear affects the parvalbumin interneurons in return.

2.3. HT3aR. Among the serotonin (5-HT) receptors in mammals, the 5-HT3R is the only ligand-gated ion channel receptor for 5-HT. The 5-HT3aRs are found in cholecystokinin positive and vasoactive intestinal peptide positive GABAergic interneurons, and these 5-HT3aR-expressing vasoactive intestinal peptide/cholecystokinin interneurons receive serotonergic and cholinergic fast synaptic transmission [54]. Furthermore, coexpression of 5-HT3aR and central calbindin 1 cannabinoid receptors have been detected in GABAergic neurons in the anterior olfactory nucleus, the cerebral cortex, hippocampus, dentate gyrus, subiculum, entorhinal cortex, and amygdala [55, 56]. Interestingly, the activation of 5-HT3 receptors by serotonin causes GABA release, whereas stimulation of calbindin 1 receptors by cannabinoids inhibits GABA release, indicating opposing effects on GABA neurotransmission [55]. The amygdala has been known to be involved in the regulation of emotion. A moderate density of 5-HT3aR neurons are found in the amygdalar basolateral nuclear complex, and almost all 5-HT3aR neurons are GABA positive. Therefore, serotonin may activate 5-HT3 receptors in the 5-HT3aR positive GABAergic neurons in the amygdala and lead to GABA release, resulting in emotional changes under stress.

2.4. Cholecystokinin. Cholecystokinin is a peptide hormone produced by enteroendocrine cells of the small intestine and released into the blood. Cholecystokinin is also widely distributed throughout the CNS, with high levels in the limbic system. The sulfated octapeptide, cholecystokinin-8S, is the major biologically active form of cholecystokinin in the CNS [57]. Intraperitoneal injections of cholecystokinin-8 enhance c-Fos (an immediate-early gene) expression in the dorsal CA3 and dentate gyrus of the hippocampus [58], indicating that cholecystokinin-8 activates neurons in the hippocampus. In the dentate gyrus, the activation of presynaptic 5-HT1B receptors in cholecystokinin interneurons inhibits GABA release and further disinhibits parvalbumin interneurons, leading to reduction of the granule cells activity. Furthermore, the inhibition of cholecystokinin neurons exhibits antidepressant-like effects on behavior, similar to selective serotonin reuptake inhibitors [59]. Thus, the activation of cholecystokinin neurons affects GABA release and depressant-like behavior.

Cholecystokinin-4, another form of cholecystokinin, has been known to induce panic attacks. In a double-blind, placebo-controlled study, 26 of 30 subjects exhibited obvious panic responses when they were challenged with cholecystokinin-4 [60]. Subjects who were treated with anxiolytics alprazolam prior to the rechallenge of cholecystokinin-4 showed a significant reduction of the panic-related scale scores and reported symptoms, as well as lower adrenocorticotropic-hormone and cortisol release. Because slow GABABR-mediated inhibitory postsynaptic currents were recorded in most cholecystokinin interneurons [61], it is possible that cholecystokinin interacts with the GABAergic system. Systemic activation of cholecystokinin-GABA neurons by clozapine-N-oxide in triple transgenic cholecystokinin-GABA/hM3Dq mice, in which about 22% of GABAergic neurons in the hippocampus and 19% in the prefrontal cortex are cholecystokinin-GABA neurons, not only enhanced contextual fear conditioning/discrimination, social/object recognition, and puzzle box performance, but also enhanced anxiety in the elevated plus maze [62].

2.5. NPY. NPY is a peptide derived from the brain and sympathetic nerves and involved in various functions in both the peripheral and central nervous systems. In the periphery, NPY is mainly released from the sympathetic nerves and serves as a regulator of fat growth [63]. In the brain, it is produced in various regions (such as the hypothalamus and amygdala) and is implicated in multiple functions, including energy homeostasis, food intake, metabolism, and stress response [64–67]. Stress can increase NPY expression in the brain [67]. Also, stress response and emotion can be affected by human NPY expression, as lower haplotype-driven NPY expression is related to higher emotion-induced activation of the amygdala [68]. Thus, NPY is thought to have stress-relieving and anxiolytic properties [69]. Chronic unpredictable stress for 5 weeks has been shown to reduce GAD67 protein levels in the prefrontal cortex and hippocampus in rats, without changing GAD65 protein expression. Additionally, the protein and RNA levels of somatostatin and NPY are also decreased following stress exposure, suggesting these subsets of GABAergic neurons may be sensitive to chronic stress [70]. NPY is colocalized with somatostatin interneurons in the brain [35]. In the BLA, somatostatin interneurons express NPY2-receptors, some of which coexpress NPY; stimulating BLA NPY2-receptors reduces tonic GABA release onto local principal neurons [30]. A combination of stress and high-fat diet activates central amygdala NPY neurons, resulting in increased feeding and reduced energy expenditure [67].

2.6. Vasoactive Intestinal Peptide. Vasoactive intestinal peptide, a gut hormone regulating energy metabolism [71, 72], is produced in many tissues, such as the gut and the hypothalamic suprachiasmatic nucleus in the brain [71, 73]. In the CNS, neocortical vasoactive intestinal peptide positive neurons are one subpopulation of GABAergic interneurons [74]. Vasoactive intestinal peptide increases GABA release in the hippocampus without changing glutamate release. Concerted synaptic action of vasoactive intestinal peptide causes disinhibition of pyramidal cell dendrites and enhances GABAergic transmission [75]. The connections between different types of GABAergic neurons result in disinhibitory effects. For example, in the primary somatosensory cortex, most of the parvalbumin cells are innervated by vasoactive intestinal peptide neurons [76]. Therefore, neocortical vasoactive intestinal peptide positive GABAergic neurons send outputs onto other interneurons or principal neurons and display a disinhibitory effect [74]. Vasoactive intestinal peptide modulates hippocampal synaptic GABAergic transmission via activation of two vasoactive intestinal peptide receptors, i.e., VPAC1 and VPAC2 receptors, which,

however, possess opposite effects on GABA release, as activation of VPAC1 or VPAC2 receptors inhibits or enhances GABA release, respectively [77]. Together, vasoactive intestinal peptide can affect GABAergic neurons, GABA level, and GAD expression [78, 79], which may further influence the stress-related behaviors.

3. Crosstalk between the GABAergic System and the Gut-Brain Pathway in Stress

3.1. The Vagus Nerve-Mediated Gut-Brain Pathway. The vagus nerve is an important neuronal component of the bidirectional communication of the gut-brain axis [80]. In addition to regulating the ingestive behavior, vagal afferent signaling has been implicated in the modulation of mood and affect, such as motivation and depression [81, 82]. Abdominal vagal afferents in rats display anhedonic behavior and increase behavioral despair [82]. It has been reported that disrupted vagal afferent signaling by subdiaphragmatic vagal deafferentation results in brain transcriptional changes in functional networks associated with schizophrenia, as well as dopamine alteration in the nucleus accumbens [83]. In another study, subdiaphragmatic vagal deafferentation rats exhibited a reduction in innate anxiety-like behavior assessed by open field test, elevated plus maze test, and food neophobia test, whereas their learning auditory-cued fear was increased [84]. Furthermore, these behavioral changes were related to the alterations of GABA and noradrenaline levels in the limbic system, without functional changes in the hypothalamus-pituitary-adrenal grand stress [84]. It suggests that vagal afferents may connect with the limbic system and affect the GABAergic system in the CNS. Selective ablation of gastrointestinal vagal sensory/afferent by saporin-based lesion impaired hippocampus-dependent behaviors in rats, indicating that vagus-mediated gut signaling, activates the hippocampus. Further monosynaptic and multisynaptic virus-based tracing investigation revealed a "medial nucleus tractus solitarius-medial septum-dorsal hippocampus glutamatergic neurons" connection, suggesting the existence of "gut-vagus-brainstem-septum-hippocampus" pathway [58]. Two types of vagal sensory neurons have been found to target the nucleus of the solitary tract (NTS) [85]. Moreover, various brain regions have been identified to be connected with the gut via the vagus nerve. Following the injection of pathological α-syn preformed fibrils into the duodenal and pyloric muscularis layer, pathologic α-syn could spread to the dorsal motor nucleus (DMN), caudal portions of the hindbrain (including the locus coeruleus), BLA, dorsal raphe nucleus (DRN), and the substantia nigra pars compacta (SNC). In addition, this gut-to-brain spread could be prevented by truncal vagotomy and α-syn deficiency [86]. This study supports the idea that the vagus nerve directly mediates the communication from the gut to the brain.

In the NTS, cholecystokinin-containing neurons, activation of which reduces appetite, are responsive to nutritional state and send projections to the paraventricular nucleus of the hypothalamus (PVH) [87]. The PVH also projects directly to the NTS [88], thereby establishing a connection from the brain to gut linked by the vagus nerve [80, 89]. Thus, the central autonomic network integrates the vagus nerve mediated visceral information and regulates the hypothalamic-pituitary-adrenal (HPA) axis [90], which is implicated in stress-related disorders [91, 92]. Moreover, cholecystokinin-4 administration could alter anxiety-like behavior and the HPA axis hormones such as corticosterone in rats exposed to early life stress [93].

To sum up, the vagus nerve-mediated gut-brain pathways at least involve "gut-vagus-NTS-septum-hippocampus" and "gut-vagus-DMN-hindbrain/BLA/DRN/SNC" pathways. The "NTS-PVH" loop might be a potential connection that regulates the "up-down" and "down-up" transmission. These complex neural pathways involve various stress-related brain regions, within which GABA signals play a crucial role. Alongside the gut-vagus-brain pathway, gut-associated factors, including cholecystokinin, NPY, and vasoactive intestinal peptide, act as modulators of GABA signaling, so as to regulate stress. Thus, we further discuss the crosstalk between the GABAergic system and the vagus mediated gut-brain pathway, especially the link with the hippocampus, amygdala, and hypothalamus, as well as related neural network.

3.2. The Crosstalk between the GABAergic System and the Vagus Nerve-Mediated Gut-Brain Pathways. The hippocampus is an important brain structure involved in various neural circuits and functions. Exposure to chronic stress has been shown to be accompanied by rising GABA levels in the dorsal hippocampus [94]. However, different stressors may cause distinct changes in hippocampal extracellular GABA levels; for instance, a novel environment increases GABA whereas forced swimming reduces GABA [7]. Interestingly, chronic stress affects specific GABAergic neuronal subpopulations in the hippocampus, including parvalbumin, calretinin, NPY, and somatostatin neurons, but not cholecystokinin and calbindin interneurons [8, 36]. The hippocampus receives inputs from the septum [95] and generates theta oscillations linked to multiple processes, including affect and locomotion [96, 97]. The septum receives inputs from the median raphe nucleus, in which inhibition of the GABAergic pathway affects theta oscillations and decreases anxiety [98]. Both the lateral and medial septum GABAA receptor signal can influence the hippocampal theta frequency, and the GABAA receptor agonist muscimol infused in the dorsal lateral septum reduces anxiety-like behavior [99]. Infusion of the GABAB receptor agonist baclofen into the lateral septum reduces stress-induced anorectic effect while increases sucrose intake [100]. It has been shown that early-life stress reduces GAD67 in the lateral septum [101]. These results suggest that the lateral septum GABAergic system is related to stress and food intake. Moreover, somatostatin interneurons in the dorsal lateral septum receive inputs from hippocampal CA3 directly [102], thereby forming a feedback loop between the hippocampus and the septum. The medial septum sends both GABAergic and glutamatergic outputs to the lateral habenula, which affects the aversion [103]. In addition, somatostatin interneurons in the hippocampus can be selectively inhibited by GABAergic neurons from the nucleus incertus, modulating of which

can shift the hippocampal network state and modify fear [31]. Overall, the median raphe nucleus projects to the septum, which projects to the hippocampus and lateral habenula, and the nucleus incertus projects to the hippocampus, thus forming a complex neural network associated with stress.

Amygdala is associated with stress and fear regulation [104–107]. In patients with schizophrenia and bipolar disorder, somatostatin positive neurons decreased in the amygdala [42]. Selective activation of NPY neurons in the central amygdala (CeA) leads to increased food intake and decreased energy expenditure under stress [67]. GABAergic serotonin receptor 2a-expressing neurons in the CeA modulate food consumption [108]. Furthermore, BLA to CeA neural circuit also mediates appetitive behaviors [109]. Thus, the BLA-CeA microcircuit within the amygdala plays a potential role in regulating stress and stress-induced appetitive behaviors. In the BLA, 5-HT3aR positive GABAergic neurons are found, and the main coexpressing marker is cholecystokinin, very few express calretinin, vasoactive intestinal peptide, or parvalbumin, and none expresses somatostatin or calbindin [110]. Another study also shows that vasoactive intestinal peptide interneurons are found in the mouse BLA [111]. Dopamine in the BLA selectively suppressed GABAergic transmission from parvalbumin interneurons to principal neurons but not to interneurons [112]. Activation of BLA NPY2-receptors reduces tonic GABA release onto BLA principal neurons and increases anxiety [30]. Selective activation of the BLA-mPFC input provides a safety-signaling mechanism whereby the mPFC taps into the microcircuitry of the amygdala to reduce fear [113]. In general, BLA neurons project to the CeA and mPFC, and the GABA pathways within these circuits are implicated in stress regulation through multiple mechanisms.

The mPFC is an important brain region involved in the emotional memories. By using a rat model for depression, researchers examined the effect of stress on GABAergic system changes in the mPFC [114]. Nine weeks of chronic mild stress exposure has been shown to decrease the amount of cholecystokinin, calretinin, and parvalbumin-positive GABAergic neurons in the mPFC. In contrast, NPY-positive neurons are increased in the entire mPFC in stress-resilient rats. Moreover, the object-place paired-associate learning is impaired in stress-susceptible rats, suggesting that fronto-limbic GABAergic dysfunctions may contribute to emotional changes in depression [114]. In addition, chronic stress increases presynaptic GABA release, which is accompanied by increased inhibition onto prefrontal glutamatergic output neurons, leading to a reduced effect on modulating stress-related behavior [115]. The frontal cortex subregion cingulate projects to the primary visual cortex and affects visual discrimination. These long-range projections induce synaptic disinhibition of pyramidal neurons through local GABAergic neurons microcircuit, including vasoactive intestinal peptide, somatostatin, and parvalbumin-positive GABAergic interneurons [116].

The hypothalamus is a component of the HPA axis. Neurons in the hypothalamus subarea PVH produce corticotropin-releasing hormone (CRH) involved in endocrine stress response. GABAergic neurons projecting to the PVH regulate the excitability of CRH neurons [117]. Following adrenalectomy in rats, the synthetic and secretory activities of CRH neurons are increased, and a higher number of GABA-CRH synaptic contacts are detected in the PVH [118], suggesting a connection between the GABAergic system and the HPA axis. Moreover, a population of CRH positive GABAergic long-range-projecting neurons in the extended amygdala innervates the ventral tegmental area, and the chronic lack of CRH from this type of neurons produces anxiety [119]. Therefore, the GABAergic system may regulate anxiety-like behavior through the HPA axis and related networks. As described previously, there is a "NTS-PVH" loop linking to the "gut-vagus-NTS-septum-hippocampus" pathway. Intraperitoneal injection of cholecystokinin-8S increases the amount of activated neurons in the NTS and PVH [120], while activating the NTS cholecystokinin axon terminals within the PVH affects appetite [87, 121], suggesting the effects on the gut pathway. The vagus nerve stimulation reduces the CRH/adrenocorticotropic hormone responses in the depressed subjects [122], suggesting the potential connection between the vagus and the HPA axis. Collectively, the gut and vagus pathways are related to the HPA axis, at least in part, through the "NTS-PVH".

3.3. Gut Microbiome in the GABAergic System and Vagal Communication. Growing evidence has shown that gut microbiome is involved in regulating stress-related behaviors and brain functions. Stress-associated anxiety- and depression-related behaviors are prevented by treatment with *Lactobacillus paracasei* Lpc-37, *Lactobacillus plantarum* LP12407, *Lactobacillus plantarum* LP12418, and *Lactobacillus plantarum* LP12151 [123]. *Lactobacillus plantarum* LP12418 can normalize the stress-induced reduction in adrenocorticotropic hormone [123]. Following probiotic bacterium *Lactobacillus rhamnosus* (JB-1) treatment, GABA levels are increased in the brain [124], and expression of GABA(B1β) and GABA(Aα2) is changed in several brain regions, including the hippocampus (lower GABA(B1β), higher GABA(Aα2)), amygdala (lower GABA(B1β) and GABA(Aα2)), and prefrontal cortex (lower GABA(Aα2)) [14]. One possible reason might be because many strains of Lactobacillus and Bifidobacterium are able to produce large quantities of GABA and activate GABA producing pathways [125, 126]. Moreover, *Lactobacillus rhamnosus* (JB-1) decreases stress-induced corticosterone and anxiety- and depression-related behavior, while no effects are found in vagotomized mice [14]. Similarly, *Lactobacillus plantarum* LP12418 also changes the expression of GABA(Aα2) and GABA(B1β) in the prefrontal cortex [123]. *Lactobacillus casei* strain Shirota not only suppresses stress-induced increases in glucocorticoids both in subjects and in rats but also stimulates vagal afferent activity and suppresses stress-induced activation of CRF cells in the PVH [127]. However, the effects of *Lactobacillus rhamnosus* (JB-1) were still unsatisfying in modifying stress-related measures and HPA response in male subjects in a clinical trial [128]. Overall, gut microbiome may play

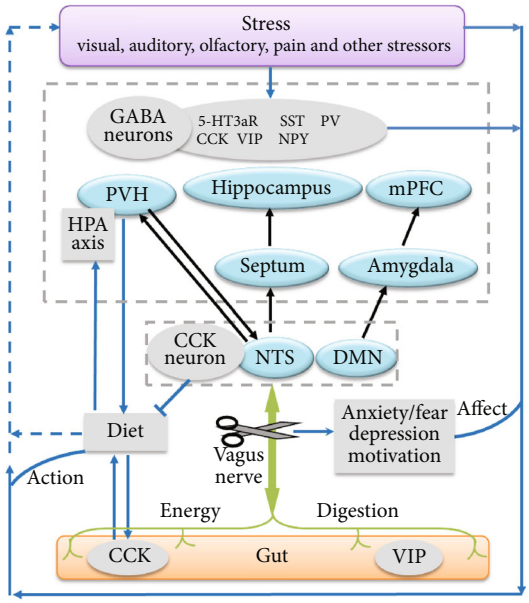

Figure 1: Potential role of crosstalk between the GABAergic system and the gut-vagus-brain pathway in stress. GABA, γ-aminobutyric acid; 5-HT3aR, serotonin receptor 5-HT3a; CCK, cholecystokinin; VIP, vasoactive intestinal peptide; SST, somatostatin; NPY, neuropeptide Y; PV, parvalbumin; mPFC, medial prefrontal cortex; PVH, paraventricular nucleus of the hypothalamus; NTS, nucleus of the solitary tract; DMN, dorsal motor nucleus; HPA, hypothalamic-pituitary-adrenal.

an important role in regulating stress-related behavior through the GABAergic system and the gut-vagus-brain pathway.

4. Conclusion and Future Perspectives

Stress can cause various mental changes and reactions, which may be attributed to multiple changes in the body, including the brain structure and related circuitry pathway. Several gut-related modulators, such as cholecystokinin, NPY, and vasoactive intestinal peptide, not only express in the digestive system but also exist in the CNS and colocalize with GABAergic neurons. In addition to regulating the diet, they are also implicated in stress, which involves various brain structures. Stress may alter gut-associated behavior, such as increased or decreased food intake [129, 130], which can further affect the gut hormone release [131]. The vagus nerve connects the gut with the brain bidirectionally, thereby establishing a gut-vagus-brain pathway. Thus, the crosstalk between the GABAergic system and the gut-vagus-brain pathway may play a potential role in stress (Figure 1).

Given that specific neuron types can be manipulated with chemogenetic and optogenetic approaches, the roles of different GABAergic neuron subgroups or relative cellular and molecular signals in stress can be further investigated. This may help find out more potential therapeutic targets for the treatment of stress-related CNS disorders, such as PTSD. It has been known that individuals with low plasma GABA levels are more susceptible to PTSD [132], which is commonly accompanied with functional gastrointestinal disorders [133]. Recent evidence indicates that gut microbiome is associated with stress-induced behaviors [134, 135]. Vagus nerve stimulation may improve PTSD-like symptoms [136]. Therefore, manipulation of the gut-vagus-brain pathway may have therapeutic potential for treating PTSD. However, the complex neuronal markers may lead to various functions of each GABAergic neuron subset in different brain regions or even in different subareas of the same region. In addition, the complicated connections between the GABAergic system and the gut-vagus-brain pathway may play a potential role in regulating stress. Further studies are needed to increase the target and region selectivity, which appears to be a challenge to the development of novel drugs or approaches for the treatment of stress-induced CNS disorders.

Conflicts of Interest

The authors declare no conflict of interest.

Acknowledgments

This work was supported by research grants from the Key Research and Development Project of Shandong Province (2019GSF108069), the National Natural Science Foundation of China (81703901), the Development Project of Traditional Chinese Medicine Science and Technology in Shandong Province (No. 2019-0361), the Academic Promotion Project of Shandong First Medical University (2019LJ003), and the Youth Innovation Team of Shandong Universities (2019KJK001).

References

[1] M. Başoğlu, M. Paker, E. Özmen, Ö. Taşdemir, and D. Şahin, "Factors related to long-term traumatic stress responses in survivors of torture in Turkey," *JAMA: The Journal of the American Medical Association*, vol. 272, no. 5, pp. 357–363, 1994.

[2] S. E. Mayer, N. L. Lopez-Duran, S. Sen, and J. L. Abelson, "Chronic stress, hair cortisol and depression: A prospective and longitudinal study of medical internship," *Psychoneuroendocrinology*, vol. 92, pp. 57–65, 2018.

[3] J. G. Stewart, G. S. Shields, E. C. Esposito et al., "Life Stress and Suicide in Adolescents," *Journal of Abnormal Child Psychology*, vol. 47, no. 10, pp. 1707–1722, 2019.

[4] J. L. Lukkes, S. Meda, B. S. Thompson, N. Freund, and S. L. Andersen, "Early life stress and later peer distress on depressive behavior in adolescent female rats: Effects of a novel intervention on GABA and D2 receptors," *Behavioural Brain Research*, vol. 330, pp. 37–45, 2017.

[5] D. M. Fergusson, L. J. Horwood, A. L. Miller, and M. A. Kennedy, "Life stress, 5-HTTLPR and mental disorder: findings from a 30-year longitudinal study," *The British Journal of Psychiatry*, vol. 198, no. 2, pp. 129–135, 2011.

[6] X. Gonda, P. Petschner, N. Eszlari et al., "Effects of Different Stressors Are Modulated by Different Neurobiological Systems: The Role of GABA-A Versus CB1 Receptor Gene

Variants in Anxiety and Depression," *Frontiers in Cellular Neuroscience*, vol. 13, 2019.

[7] L. de Groote and A. C. E. Linthorst, "Exposure to novelty and forced swimming evoke stressor-dependent changes in extracellular GABA in the rat hippocampus," *Neuroscience*, vol. 148, no. 3, pp. 794–805, 2007.

[8] W. Hu, M. Zhang, B. Czéh, G. Flügge, and W. Zhang, "Stress Impairs GABAergic Network Function in the Hippocampus by Activating Nongenomic Glucocorticoid Receptors and Affecting the Integrity of the Parvalbumin-Expressing Neuronal Network," *Neuropsychopharmacology*, vol. 35, no. 8, pp. 1693–1707, 2010.

[9] L. C. Houtepen, R. R. Schür, J. P. Wijnen et al., "Acute stress effects on GABA and glutamate levels in the prefrontal cortex: A 7T 1 H magnetic resonance spectroscopy study," *NeuroImage: Clinical*, vol. 14, pp. 195–200, 2017.

[10] M. Uhart, M. E. McCaul, L. M. Oswald, L. Choi, and G. S. Wand, "GABRA6 gene polymorphism and an attenuated stress response," *Molecular Psychiatry*, vol. 9, no. 11, pp. 998–1006, 2004.

[11] M. Bixo, K. Ekberg, I. S. Poromaa et al., "Treatment of premenstrual dysphoric disorder with the GABA A receptor modulating steroid antagonist Sepranolone (UC1010)-A randomized controlled trial," *Psychoneuroendocrinology*, vol. 80, pp. 46–55, 2017.

[12] G. M. Gafford, J. D. Guo, E. I. Flandreau, R. Hazra, D. G. Rainnie, and K. J. Ressler, "Cell-type specific deletion of GABA(A) 1 in corticotropin-releasing factor-containing neurons enhances anxiety and disrupts fear extinction," *Proceedings of the National Academy of Sciences*, vol. 109, no. 40, pp. 16330–16335, 2012.

[13] P. Zwanzger, D. Eser, C. Nothdurfter et al., "Effects of the GABA-reuptake inhibitor tiagabine on panic and anxiety in patients with panic disorder," *Pharmacopsychiatry*, vol. 42, no. 6, pp. 266–269, 2009.

[14] J. A. Bravo, P. Forsythe, M. V. Chew et al., "Ingestion of Lactobacillus strain regulates emotional behavior and central GABA receptor expression in a mouse via the vagus nerve," *Proceedings of the National Academy of Sciences*, vol. 108, no. 38, pp. 16050–16055, 2011.

[15] M. Soto, C. Herzog, J. A. Pacheco et al., "Gut microbiota modulate neurobehavior through changes in brain insulin sensitivity and metabolism," *Molecular Psychiatry*, vol. 23, no. 12, pp. 2287–2301, 2018.

[16] P. Zheng, B. Zeng, M. Liu et al., "The gut microbiome from patients with schizophrenia modulates the glutamate-glutamine-GABA cycle and schizophrenia-relevant behaviors in mice," *Science Advances*, vol. 5, no. 2, article eaau8317, 2019.

[17] L. V. Scott, G. Clarke, and T. G. Dinan, "The Brain-Gut Axis: A Target for Treating Stress-Related Disorders," *Inflammation in Psychiatry*, vol. 28, pp. 90–99, 2013.

[18] A. Sarkar, S. M. Lehto, S. Harty, T. G. Dinan, J. F. Cryan, and P. W. J. Burnet, "Psychobiotics and the Manipulation of Bacteria–Gut–Brain Signals," *Trends in Neurosciences*, vol. 39, no. 11, pp. 763–781, 2016.

[19] P. Holzer and A. Farzi, "Neuropeptides and the Microbiota-Gut-Brain Axis," *Microbial Endocrinology: The Microbiota-Gut-Brain Axis in Health and Disease*, pp. 195–219, 2014.

[20] R. Mittal, L. H. Debs, A. P. Patel et al., "Neurotransmitters: The Critical Modulators Regulating Gut-Brain Axis," *Journal of Cellular Physiology*, vol. 232, no. 9, pp. 2359–2372, 2017.

[21] K. G. Jameson and E. Y. Hsiao, "Linking the Gut Microbiota to a Brain Neurotransmitter," *Trends in Neurosciences*, vol. 41, no. 7, pp. 413-414, 2018.

[22] D. D. Lam and L. K. Heisler, "Serotonin and energy balance: molecular mechanisms and implications for type 2 diabetes," *Expert Reviews in Molecular Medicine*, vol. 9, no. 5, pp. 1–24, 2007.

[23] Q. Tong, C.-P. Ye, J. E. Jones, J. K. Elmquist, and B. B. Lowell, "Synaptic release of GABA by AgRP neurons is required for normal regulation of energy balance," *Nature Neuroscience*, vol. 11, no. 9, pp. 998–1000, 2008.

[24] H. Wang, G. Astarita, M. D. Taussig et al., "Deficiency of Lipoprotein Lipase in Neurons Modifies the Regulation of Energy Balance and Leads to Obesity," *Cell Metabolism*, vol. 13, no. 1, pp. 105–113, 2011.

[25] S. X. Luo, J. Huang, Q. Li et al., "Regulation of feeding by somatostatin neurons in the tuberal nucleus," *Science*, vol. 361, no. 6397, pp. 76–81, 2018.

[26] B. P. Grone and K. P. Maruska, "Three Distinct Glutamate Decarboxylase Genes in Vertebrates," *Scientific Reports*, vol. 6, no. 1, 2016.

[27] K. C. Evans, N. M. Simon, D. D. Dougherty et al., "A PET Study of Tiagabine Treatment Implicates Ventral Medial Prefrontal Cortex in Generalized Social Anxiety Disorder," *Neuropsychopharmacology*, vol. 34, no. 2, pp. 390–398, 2009.

[28] O. Bukalo, C. R. Pinard, S. Silverstein et al., "Prefrontal inputs to the amygdala instruct fear extinction memory formation," *Sci Adv*, vol. 1, no. 6, article e1500251, 2015.

[29] R. R. Rozeske, A. Der-Avakian, S. T. Bland, J. T. Beckley, L. R. Watkins, and S. F. Maier, "The Medial Prefrontal Cortex Regulates the Differential Expression of Morphine-Conditioned Place Preference Following a Single Exposure to Controllable or Uncontrollable Stress," *Neuropsychopharmacology*, vol. 34, no. 4, pp. 834–843, 2009.

[30] J. P. Mackay, M. Bompolaki, M. R. DeJoseph, S. D. Michaelson, J. H. Urban, and W. F. Colmers, "NPY2Receptors Reduce Tonic Action Potential-Independent GABABCurrents in the Basolateral Amygdala," *Journal of Neuroscience*, vol. 39, no. 25, pp. 4909–4930, 2019.

[31] A. Szőnyi, K. E. Sos, R. Nyilas et al., "Brainstem nucleus incertus controls contextual memory formation," *Science*, vol. 364, no. 6442, article eaaw0445, 2019.

[32] R. S. Duman, G. Sanacora, and J. H. Krystal, "Altered Connectivity in Depression: GABA and Glutamate Neurotransmitter Deficits and Reversal by Novel Treatments," *Neuron*, vol. 102, no. 1, pp. 75–90, 2019.

[33] Y. Kubota, N. Shigematsu, F. Karube et al., "Selective coexpression of multiple chemical markers defines discrete populations of neocortical GABAergic neurons," *Cerebral Cortex*, vol. 21, no. 8, pp. 1803–1817, 2011.

[34] S. H. Hendry, E. G. Jones, J. DeFelipe, D. Schmechel, C. Brandon, and P. C. Emson, "Neuropeptide-containing neurons of the cerebral cortex are also GABAergic," *Proceedings of the National Academy of Sciences of the United States of America*, vol. 81, no. 20, pp. 6526–6530, 1984.

[35] R. Tremblay, S. Lee, and B. Rudy, "GABAergic Interneurons in the Neocortex: From Cellular Properties to Circuits," *Neuron*, vol. 91, no. 2, pp. 260–292, 2016.

[36] B. Czéh, Z. K. Kalangyáné Varga, K. Henningsen, G. L. Kovács, A. Miseta, and O. Wiborg, "Chronic stress reduces the number of GABAergic interneurons in the adult rat

hippocampus, dorsal-ventral and region-specific differences," *Hippocampus*, vol. 25, no. 3, pp. 393–405, 2015.

[37] C. Giachino, N. Canalia, F. Capone et al., "Maternal deprivation and early handling affect density of calcium binding protein-containing neurons in selected brain regions and emotional behavior in periadolescent rats," *Neuroscience*, vol. 145, no. 2, pp. 568–578, 2007.

[38] H. J. Krugers and M. Joels, "Long-lasting Consequences of Early Life Stress on Brain Structure, Emotion and Cognition," vol. 18 of Current Topics in Behavioral Neurosciences, pp. 81–92, 2014.

[39] T. A. Kosten, H. J. Lee, and J. J. Kim, "Early life stress impairs fear conditioning in adult male and female rats," *Brain Research*, vol. 1087, no. 1, pp. 142–150, 2006.

[40] H. González-Pardo, J. L. Arias, G. Vallejo, and N. M. Conejo, "Influence of environmental enrichment on the volume of brain regions sensitive to early life stress by maternal separation in rats," *Psicothema*, vol. 31, no. 1, pp. 46–52, 2019.

[41] Z. Varga, D. Csabai, A. Miseta, O. Wiborg, and B. Czéh, "Chronic stress affects the number of GABAergic neurons in the orbitofrontal cortex of rats," *Behavioural Brain Research*, vol. 316, pp. 104–114, 2017.

[42] H. Pantazopoulos, J. T. Wiseman, M. Markota, L. Ehrenfeld, and S. Berretta, "Decreased Numbers of Somatostatin-Expressing Neurons in the Amygdala of Subjects With Bipolar Disorder or Schizophrenia: Relationship to Circadian Rhythms," *Biological Psychiatry*, vol. 81, no. 6, pp. 536–547, 2017.

[43] L. C. Lin and E. Sibille, "Somatostatin, neuronal vulnerability and behavioral emotionality," *Molecular Psychiatry*, vol. 20, no. 3, pp. 377–387, 2015.

[44] A. Faron-Górecka, M. Kuśmider, M. Kolasa et al., "Chronic mild stress alters the somatostatin receptors in the rat brain," *Psychopharmacology*, vol. 233, no. 2, pp. 255–266, 2016.

[45] A. Faron-Górecka, M. Kuśmider, J. Solich et al., "Regulation of somatostatin receptor 2 in the context of antidepressant treatment response in chronic mild stress in rat," *Psychopharmacology*, vol. 235, no. 7, pp. 2137–2149, 2018.

[46] T. Fuchs, S. J. Jefferson, A. Hooper, P. H. P. Yee, J. Maguire, and B. Luscher, "Disinhibition of somatostatin-positive GABAergic interneurons results in an anxiolytic and antidepressant-like brain state," *Molecular Psychiatry*, vol. 22, no. 6, pp. 920–930, 2017.

[47] C. Miao, Q. Cao, M. B. Moser, and E. I. Moser, "Parvalbumin and Somatostatin Interneurons Control Different Space-Coding Networks in the Medial Entorhinal Cortex," *Cell*, vol. 171, no. 3, pp. 507–521.e17, 2017.

[48] K. L. Wahlstrom, M. L. Huff, E. B. Emmons et al., "Basolateral Amygdala Inputs to the Medial Entorhinal Cortex Selectively Modulate the Consolidation of Spatial and Contextual Learning," *The Journal of Neuroscience*, vol. 38, no. 11, pp. 2698–2712, 2018.

[49] D. Kim, H. Jeong, J. Lee et al., "Distinct Roles of Parvalbumin- and Somatostatin-Expressing Interneurons in Working Memory," *Neuron*, vol. 92, no. 4, pp. 902–915, 2016.

[50] R. Marek, J. Jin, T. D. Goode et al., "Hippocampus-driven feed-forward inhibition of the prefrontal cortex mediates relapse of extinguished fear," *Nature Neuroscience*, vol. 21, no. 3, pp. 384–392, 2018.

[51] J. A. Brown, T. S. Ramikie, M. J. Schmidt et al., "Inhibition of parvalbumin-expressing interneurons results in complex behavioral changes," *Molecular Psychiatry*, vol. 20, no. 12, pp. 1499–1507, 2015.

[52] J. Courtin, F. Chaudun, R. R. Rozeske et al., "Prefrontal parvalbumin interneurons shape neuronal activity to drive fear expression," *Nature*, vol. 505, no. 7481, pp. 92–96, 2014.

[53] E. K. Lucas, A. M. Jegarl, H. Morishita, and R. L. Clem, "Multimodal and Site-Specific Plasticity of Amygdala Parvalbumin Interneurons after Fear Learning," *Neuron*, vol. 91, no. 3, pp. 629–643, 2016.

[54] I. Férézou, B. Cauli, E. L. Hill, J. Rossier, E. Hamel, and B. Lambolez, "5-HT3Receptors Mediate Serotonergic Fast Synaptic Excitation of Neocortical Vasoactive Intestinal Peptide/Cholecystokinin Interneurons," *The Journal of Neuroscience*, vol. 22, no. 17, pp. 7389–7397, 2002.

[55] M. Morales and C. Backman, "Coexistence of serotonin 3 (5-HT3) and CB1 cannabinoid receptors in interneurons of hippocampus and dentate gyrus," *Hippocampus*, vol. 12, no. 6, pp. 756–764, 2002.

[56] M. Morales, S. D. Wang, O. Diaz-Ruiz, and D. Hyun-Jin Jho, "Cannabinoid CB1 receptor and serotonin 3 receptor subunit A (5-HT3A) are co-expressed in GABA neurons in the rat telencephalon," *The Journal of Comparative Neurology*, vol. 468, no. 2, pp. 205–216, 2004.

[57] M. E. Bowers, D. C. Choi, and K. J. Ressler, "Neuropeptide regulation of fear and anxiety: implications of cholecystokinin, endogenous opioids, and neuropeptide Y," *Physiology & Behavior*, vol. 107, no. 5, pp. 699–710, 2012.

[58] A. N. Suarez, T. M. Hsu, C. M. Liu et al., "Gut vagal sensory signaling regulates hippocampus function through multi-order pathways," *Nature Communications*, vol. 9, no. 1, p. 2181, 2018.

[59] L. Medrihan, Y. Sagi, Z. Inde et al., "Initiation of Behavioral Response to Antidepressants by Cholecystokinin Neurons of the Dentate Gyrus," *Neuron*, vol. 95, no. 3, pp. 564–576.e4, 2017.

[60] P. Zwanzger, D. Eser, S. Aicher et al., "Effects of Alprazolam on Cholecystokinin-Tetrapeptide-Induced Panic and Hypothalamic–Pituitary–Adrenal-Axis Activity: A Placebo-Controlled Study," *Neuropsychopharmacology*, vol. 28, no. 5, pp. 979–984, 2003.

[61] S. A. Booker, D. Althof, A. Gross et al., "KCTD12 Auxiliary Proteins Modulate Kinetics of GABABReceptor-Mediated Inhibition in Cholecystokinin-Containing Interneurons," *Cerebral Cortex*, vol. 27, no. 3, pp. 2318–2334, 2017.

[62] P. D. Whissell, J. Y. Bang, I. Khan et al., "Selective Activation of Cholecystokinin-Expressing GABA (CCK-GABA) Neurons Enhances Memory and Cognition," *eNeuro*, vol. 6, no. 1, 2019.

[63] L. E. Kuo, J. B. Kitlinska, J. U. Tilan et al., "Neuropeptide Y acts directly in the periphery on fat tissue and mediates stress-induced obesity and metabolic syndrome," *Nature Medicine*, vol. 13, no. 7, pp. 803–811, 2007.

[64] X. Zhang and A. N. van den Pol, "Hypothalamic arcuate nucleus tyrosine hydroxylase neurons play orexigenic role in energy homeostasis," *Nature Neuroscience*, vol. 19, no. 10, pp. 1341–1347, 2016.

[65] Y. Nakamura, Y. Yanagawa, S. F. Morrison, and K. Nakamura, "Medullary Reticular Neurons Mediate Neuropeptide Y-Induced Metabolic Inhibition and Mastication," *Cell Metabolism*, vol. 25, no. 2, pp. 322–334, 2017.

[66] Q. Wu, Z. Zhao, and P. Shen, "Regulation of aversion to noxious food by Drosophila neuropeptide Y- and insulin-like systems," *Nature Neuroscience*, vol. 8, no. 10, pp. 1350–1355, 2005.

[67] C. K. Ip, L. Zhang, A. Farzi et al., "Amygdala NPY Circuits Promote the Development of Accelerated Obesity under Chronic Stress Conditions," *Cell Metabolism*, vol. 30, no. 1, pp. 111–128.e6, 2019.

[68] Z. Zhou, G. Zhu, A. R. Hariri et al., "Genetic variation in human NPY expression affects stress response and emotion," *Nature*, vol. 452, no. 7190, pp. 997–1001, 2008.

[69] F. Reichmann and P. Holzer, "Neuropeptide Y: A stressful review," *Neuropeptides*, vol. 55, pp. 99–109, 2016.

[70] M. Banasr, A. Lepack, C. Fee et al., "Characterization of GABAergic marker expression in the chronic unpredictable stress model of depression," *Chronic Stress*, vol. 1, article 247054701772045, no. 1, 2017.

[71] W. H. Rostene, "Neurobiological and neuroendocrine functions of the vasoactive intestinal peptide (VIP)," *Progress in Neurobiology*, vol. 22, no. 2, pp. 103–129, 1984.

[72] P. J. Magistretti, J. H. Morrison, W. J. Shoemaker, V. Sapin, and F. E. Bloom, "Vasoactive intestinal polypeptide induces glycogenolysis in mouse cortical slices: a possible regulatory mechanism for the local control of energy metabolism," *Proceedings of the National Academy of Sciences of the United States of America*, vol. 78, no. 10, pp. 6535–6539, 1981.

[73] M. L. H. J. Hermes, M. Kolaj, P. Doroshenko, E. Coderre, and L. P. Renaud, "Effects of VPAC2 Receptor Activation on Membrane Excitability and GABAergic Transmission in Subparaventricular Zone Neurons Targeted by Suprachiasmatic Nucleus," *Journal of Neurophysiology*, vol. 102, no. 3, pp. 1834–1842, 2009.

[74] X. Zhou, M. Rickmann, G. Hafner, and J. F. Staiger, "Subcellular Targeting of VIP Boutons in Mouse Barrel Cortex is Layer-Dependent and not Restricted to Interneurons," *Cerebral Cortex*, vol. 27, no. 11, pp. 5353–5368, 2017.

[75] D. Cunha-Reis, A. M. Sebastião, K. Wirkner, P. Illes, and J. A. Ribeiro, "VIP enhances both pre- and postsynaptic GABAergic transmission to hippocampal interneurones leading to increased excitatory synaptic transmission to CA1 pyramidal cells," *British Journal of Pharmacology*, vol. 143, no. 6, pp. 733–744, 2004.

[76] C. Dávid, A. Schleicher, W. Zuschratter, and J. F. Staiger, "The innervation of parvalbumin-containing interneurons by VIP-immunopositive interneurons in the primary somatosensory cortex of the adult rat," *The European Journal of Neuroscience*, vol. 25, no. 8, pp. 2329–2340, 2007.

[77] D. Cunha-Reis, J. A. Ribeiro, R. F. M. de Almeida, and A. M. Sebastião, "VPAC1and VPAC2receptor activation on GABA release from hippocampal nerve terminals involve several different signalling pathways," *British Journal of Pharmacology*, vol. 174, no. 24, pp. 4725–4737, 2017.

[78] O. T. Korkmaz, N. Tunçel, M. Tunçel, E. M. Öncü, V. Şahintürk, and M. Çelik, "Vasoactive Intestinal Peptide (VIP) Treatment of Parkinsonian Rats Increases Thalamic Gamma-Aminobutyric Acid (GABA) Levels and Alters the Release of Nerve Growth Factor (NGF) by Mast Cells," *Journal of Molecular Neuroscience*, vol. 41, no. 2, pp. 278–287, 2010.

[79] I. H. Yelkenli, E. Ulupinar, O. T. Korkmaz et al., "Modulation of Corpus Striatal Neurochemistry by Astrocytes and Vasoactive Intestinal Peptide (VIP) in Parkinsonian Rats," *Journal of Molecular Neuroscience*, vol. 59, no. 2, pp. 280–289, 2016.

[80] B. Bonaz, T. Bazin, and S. Pellissier, "The Vagus Nerve at the Interface of the Microbiota-Gut-Brain Axis," *Frontiers in Neuroscience*, vol. 12, 2018.

[81] J. W. Maniscalco and L. Rinaman, "Vagal Interoceptive Modulation of Motivated Behavior," *Physiology*, vol. 33, no. 2, pp. 151–167, 2018.

[82] M. Klarer, U. Weber-Stadlbauer, M. Arnold, W. Langhans, and U. Meyer, "Abdominal vagal deafferentation alters affective behaviors in rats," *Journal of Affective Disorders*, vol. 252, pp. 404–412, 2019.

[83] M. Klarer, J. P. Krieger, J. Richetto et al., "Abdominal Vagal Afferents Modulate the Brain Transcriptome and Behaviors Relevant to Schizophrenia," *The Journal of Neuroscience*, vol. 38, no. 7, pp. 1634–1647, 2018.

[84] M. Klarer, M. Arnold, L. Gunther, C. Winter, W. Langhans, and U. Meyer, "Gut Vagal Afferents Differentially Modulate Innate Anxiety and Learned Fear," *Journal of Neuroscience*, vol. 34, no. 21, pp. 7067–7076, 2014.

[85] E. K. Williams, R. B. Chang, D. E. Strochlic, B. D. Umans, B. B. Lowell, and S. D. Liberles, "Sensory Neurons that Detect Stretch and Nutrients in the Digestive System," *Cell*, vol. 166, no. 1, pp. 209–221, 2016.

[86] S. Kim, S. H. Kwon, T. I. Kam et al., "Transneuronal Propagation of Pathologic α-Synuclein from the Gut to the Brain Models Parkinson's Disease," *Neuron*, vol. 103, no. 4, pp. 627–641.e7, 2019.

[87] G. D'Agostino, D. J. Lyons, C. Cristiano et al., "Appetite controlled by a cholecystokinin nucleus of the solitary tract to hypothalamus neurocircuit," *Elife*, vol. 5, 2016.

[88] L. C. Conrad and D. W. Pfaff, "Efferents from medial basal forebrain and hypothalamus in the rat. II. An autoradiographic study of the anterior hypothalamus," *The Journal of Comparative Neurology*, vol. 169, no. 2, pp. 221–261, 1976.

[89] S. Breit, A. Kupferberg, G. Rogler, and G. Hasler, "Vagus Nerve as Modulator of the Brain–Gut Axis in Psychiatric and Inflammatory Disorders," *Frontiers in Psychiatry*, vol. 9, 2018.

[90] B. Bonaz, V. Sinniger, and S. Pellissier, "Vagus nerve stimulation: a new promising therapeutic tool in inflammatory bowel disease," *Journal of Internal Medicine*, vol. 282, no. 1, pp. 46–63, 2017.

[91] C. M. Pariante and S. L. Lightman, "The HPA axis in major depression: classical theories and new developments," *Trends in Neurosciences*, vol. 31, no. 9, pp. 464–468, 2008.

[92] A. Shea, C. Walsh, H. MacMillan, and M. Steiner, "Child maltreatment and HPA axis dysregulation: relationship to major depressive disorder and post traumatic stress disorder in females," *Psychoneuroendocrinology*, vol. 30, no. 2, pp. 162–178, 2005.

[93] M. H. Greisen, T. G. Bolwig, and G. Wortwein, "Cholecystokinin tetrapeptide effects on HPA axis function and elevated plus maze behaviour in maternally separated and handled rats," *Behavioural Brain Research*, vol. 161, no. 2, pp. 204–212, 2005.

[94] R. Magalhães, A. Novais, D. A. Barrière et al., "A Resting-State Functional MR Imaging and Spectroscopy Study of the Dorsal Hippocampus in the Chronic Unpredictable Stress Rat Model," *The Journal of Neuroscience*, vol. 39, no. 19, pp. 3640–3650, 2019.

[95] J. M. Staib, R. Della Valle, and D. K. Knox, "Disruption of medial septum and diagonal bands of Broca cholinergic projections to the ventral hippocampus disrupt auditory fear memory," *Neurobiology of Learning and Memory*, vol. 152, pp. 71–79, 2018.

[96] T. Korotkova, A. Ponomarenko, C. K. Monaghan et al., "Reconciling the different faces of hippocampal theta: The role of theta oscillations in cognitive, emotional and innate behaviors," *Neuroscience and Biobehavioral Reviews*, vol. 85, pp. 65–80, 2018.

[97] S. S. Chee, J. L. Menard, and H. C. Dringenberg, "Behavioral anxiolysis without reduction of hippocampal theta frequency after histamine application in the lateral septum of rats," *Hippocampus*, vol. 24, no. 6, pp. 615–627, 2014.

[98] Y. T. Hsiao, P. L. Yi, C. H. Cheng, and F. C. Chang, "Disruption of footshock-induced theta rhythms by stimulating median raphe nucleus reduces anxiety in rats," *Behavioural Brain Research*, vol. 247, pp. 193–200, 2013.

[99] S. S. Chee, J. L. Menard, and H. C. Dringenberg, "The lateral septum as a regulator of hippocampal theta oscillations and defensive behavior in rats," *Journal of Neurophysiology*, vol. 113, no. 6, pp. 1831–1841, 2015.

[100] A. Mitra, C. Lenglos, and E. Timofeeva, "Inhibition in the lateral septum increases sucrose intake and decreases anorectic effects of stress," *The European Journal of Neuroscience*, vol. 41, no. 4, pp. 420–433, 2015.

[101] M. I. Cordero, N. Just, G. L. Poirier, and C. Sandi, "Effects of paternal and peripubertal stress on aggression, anxiety, and metabolic alterations in the lateral septum," *European Neuropsychopharmacology*, vol. 26, no. 2, pp. 357–367, 2016.

[102] A. Besnard, Y. Gao, M. TaeWoo Kim et al., "Dorsolateral septum somatostatin interneurons gate mobility to calibrate context-specific behavioral fear responses," *Nature Neuroscience*, vol. 22, no. 3, pp. 436–446, 2019.

[103] G.-W. Zhang, L. Shen, W. Zhong, Y. Xiong, L. I. Zhang, and H. W. Tao, "Transforming Sensory Cues into Aversive Emotion via Septal-Habenular Pathway," *Neuron*, vol. 99, no. 5, pp. 1016–1028.e5, 2018.

[104] B. G. Dias, J. V. Goodman, R. Ahluwalia, A. E. Easton, R. Andero, and K. J. Ressler, "Amygdala-dependent fear memory consolidation via miR-34a and Notch signaling," *Neuron*, vol. 83, no. 4, pp. 906–918, 2014.

[105] H. S. Knobloch, A. Charlet, L. C. Hoffmann et al., "Evoked axonal oxytocin release in the central amygdala attenuates fear response," *Neuron*, vol. 73, no. 3, pp. 553–566, 2012.

[106] J. Waddell, D. A. Bangasser, and T. J. Shors, "The basolateral nucleus of the amygdala is necessary to induce the opposing effects of stressful experience on learning in males and females," *Journal of Neuroscience*, vol. 28, no. 20, pp. 5290–5294, 2008.

[107] W. B. Kim and J. H. Cho, "Encoding of Discriminative Fear Memory by Input-Specific LTP in the Amygdala," *Neuron*, vol. 95, no. 5, pp. 1129–1146.e5, 2017.

[108] A. M. Douglass, H. Kucukdereli, M. Ponserre et al., "Central amygdala circuits modulate food consumption through a positive-valence mechanism," *Nature Neuroscience*, vol. 20, no. 10, pp. 1384–1394, 2017.

[109] J. Kim, X. Zhang, S. Muralidhar, S. A. LeBlanc, and S. Tonegawa, "Basolateral to Central Amygdala Neural Circuits for Appetitive Behaviors," *Neuron*, vol. 93, no. 6, pp. 1464–1479.e5, 2017.

[110] F. Mascagni and A. J. McDonald, "A novel subpopulation of 5-HT type 3A receptor subunit immunoreactive interneurons in the rat basolateral amygdala," *Neuroscience*, vol. 144, no. 3, pp. 1015–1024, 2007.

[111] T. Rhomberg, L. Rovira-Esteban, A. Vikór et al., "Vasoactive Intestinal Polypeptide-Immunoreactive Interneurons within Circuits of the Mouse Basolateral Amygdala," *The Journal of Neuroscience*, vol. 38, no. 31, pp. 6983–7003, 2018.

[112] H. Y. Chu, W. Ito, J. Li, and A. Morozov, "Target-specific suppression of GABA release from parvalbumin interneurons in the basolateral amygdala by dopamine," *Journal of Neuroscience*, vol. 32, no. 42, pp. 14815–14820, 2012.

[113] E. Likhtik, J. M. Stujenske, M. A. Topiwala, A. Z. Harris, and J. A. Gordon, "Prefrontal entrainment of amygdala activity signals safety in learned fear and innate anxiety," *Nature Neuroscience*, vol. 17, no. 1, pp. 106–113, 2014.

[114] B. Czéh, I. Vardya, Z. Varga et al., "Long-Term Stress Disrupts the Structural and Functional Integrity of GABAergic Neuronal Networks in the Medial Prefrontal Cortex of Rats," *Frontiers in Cellular Neuroscience*, vol. 12, 2018.

[115] J. M. McKlveen, R. L. Morano, M. Fitzgerald et al., "Chronic Stress Increases Prefrontal Inhibition: A Mechanism for Stress-Induced Prefrontal Dysfunction," *Biological Psychiatry*, vol. 80, no. 10, pp. 754–764, 2016.

[116] S. Zhang, M. Xu, T. Kamigaki et al., "Selective attention. Long-range and local circuits for top-down modulation of visual cortex processing," *Science*, vol. 345, no. 6197, pp. 660–665, 2014.

[117] K. Kakizawa, M. Watanabe, H. Mutoh et al., "A novel GABA-mediated corticotropin-releasing hormone secretory mechanism in the median eminence," *Science Advances*, vol. 2, no. 8, article e1501723, 2016.

[118] I. H. Miklos and K. J. Kovacs, "GABAergic innervation of corticotropin-releasing hormone (CRH)-secreting parvocellular neurons and its plasticity as demonstrated by quantitative immunoelectron microscopy," *Neuroscience*, vol. 113, no. 3, pp. 581–592, 2002.

[119] N. Dedic, C. Kühne, M. Jakovcevski et al., "Chronic CRH depletion from GABAergic, long-range projection neurons in the extended amygdala reduces dopamine release and increases anxiety," *Nature Neuroscience*, vol. 21, no. 6, pp. 803–807, 2018.

[120] K. M. Engster, L. Frommelt, T. Hofmann et al., "Peripheral injected cholecystokinin-8S modulates the concentration of serotonin in nerve fibers of the rat brainstem," *Peptides*, vol. 59, pp. 25–33, 2014.

[121] C. W. Roman, S. R. Sloat, and R. D. Palmiter, "A tale of two circuits: CCK(NTS) neuron stimulation controls appetite and induces opposing motivational states by projections to distinct brain regions," *Neuroscience*, vol. 358, pp. 316–324, 2017.

[122] V. O'Keane, T. G. Dinan, L. Scott, and C. Corcoran, "Changes in Hypothalamic–Pituitary–Adrenal Axis Measures After Vagus Nerve Stimulation Therapy in Chronic Depression," *Biological Psychiatry*, vol. 58, no. 12, pp. 963–968, 2005.

[123] L. K. Stenman, E. Patterson, J. Meunier, F. J. Roman, and M. J. Lehtinen, "Strain specific stress-modulating effects of candidate probiotics: A systematic screening in a mouse model of chronic restraint stress," *Behavioural Brain Research*, vol. 379, article 112376, 2020.

[124] R. Janik, L. A. M. Thomason, A. M. Stanisz, P. Forsythe, J. Bienenstock, and G. J. Stanisz, "Magnetic resonance spectroscopy reveals oral Lactobacillus promotion of increases in brain GABA, N-acetyl aspartate and glutamate," *NeuroImage*, vol. 125, pp. 988–995, 2016.

[125] R. A. Yunes, E. U. Poluektova, M. S. Dyachkova et al., "GABA production and structure of gadB/gadC genes in Lactobacillus and Bifidobacterium strains from human microbiota," *Anaerobe*, vol. 42, pp. 197–204, 2016.

[126] P. Strandwitz, K. H. Kim, D. Terekhova et al., "GABA-modulating bacteria of the human gut microbiota," *Nature Microbiology*, vol. 4, no. 3, pp. 396–403, 2019.

[127] M. Takada, K. Nishida, A. Kataoka-Kato et al., "Probiotic Lactobacillus casei strain Shirota relieves stress-associated symptoms by modulating the gut-brain interaction in human and animal models," *Neurogastroenterology and Motility*, vol. 28, no. 7, pp. 1027–1036, 2016.

[128] J. R. Kelly, A. P. Allen, A. Temko et al., "Lost in translation? The potential psychobiotic Lactobacillus rhamnosus (JB-1) fails to modulate stress or cognitive performance in healthy male subjects," *Brain, Behavior, and Immunity*, vol. 61, pp. 50–59, 2017.

[129] Y. M. Ulrich-Lai, S. Fulton, M. Wilson, G. Petrovich, and L. Rinaman, "Stress exposure, food intake and emotional state," *Stress*, vol. 18, no. 4, pp. 381–399, 2015.

[130] T. Onaka and Y. Takayanagi, "Role of oxytocin in the control of stress and food intake," *Journal of Neuroendocrinology*, vol. 31, no. 3, article e12700, 2019.

[131] R. Chandra, Y. Wang, R. A. Shahid, S. R. Vigna, N. J. Freedman, and R. A. Liddle, "Immunoglobulin-like domain containing receptor 1 mediates fat-stimulated cholecystokinin secretion," *The Journal of Clinical Investigation*, vol. 123, no. 8, pp. 3343–3352, 2013.

[132] G. Vaiva, P. Thomas, F. Ducrocq et al., "Low posttrauma GABA plasma levels as a predictive factor in the development of acute posttraumatic stress disorder," *Biological Psychiatry*, vol. 55, no. 3, pp. 250–254, 2004.

[133] R. Stam, L. M. A. Akkermans, and V. M. Wiegant, "Trauma and the gut: interactions between stressful experience and intestinal function," *Gut*, vol. 40, no. 6, pp. 704–709, 1997.

[134] A. Gautam, R. Kumar, N. Chakraborty et al., "Altered fecal microbiota composition in all male aggressor-exposed rodent model simulating features of post-traumatic stress disorder," *Journal of Neuroscience Research*, vol. 96, no. 7, pp. 1311–1323, 2018.

[135] J. Pearson-Leary, C. Zhao, K. Bittinger et al., "The gut microbiome regulates the increases in depressive-type behaviors and in inflammatory processes in the ventral hippocampus of stress vulnerable rats," *Molecular Psychiatry*, vol. 25, no. 5, pp. 1068–1079, 2020.

[136] L. J. Noble, I. J. Gonzalez, V. B. Meruva et al., "Effects of vagus nerve stimulation on extinction of conditioned fear and post-traumatic stress disorder symptoms in rats," *Translational Psychiatry*, vol. 7, no. 8, article e1217, 2017.